Kathrin Heckenbichler BSc MSc

Reductive C-C Bond Formations Using Engineered Ene-Reductases

DISSERTATION

zur Erlangung des akademischen Grades

Doktorin der technischen Wissenschaften

eingereicht an der

Technischen Universität Graz

Betreuer

Univ.-Prof. Dipl.-Ing. Dr. rer. nat. Rolf Breinbauer

Institut für Organische Chemie
Technische Universität Graz

Graz, Dezember 2017

EIDESSTATTLICHE ERKLÄRUNG

Ich erkläre an Eides statt, dass ich die vorliegende Arbeit selbstständig verfasst, andere als die angegebenen Quellen/Hilfsmittel nicht benutzt, und die den benutzten Quellen wörtlich und inhaltlich entnommenen Stellen als solche kenntlich gemacht habe. Das in TUGRAZonline hochgeladene Textdokument ist mit der vorliegenden Dissertation identisch.

Datum

Unterschrift

Meiner Familie

Kurzzusammenfassung

Modifizierte Enzyme dienen als leistungsfähige Katalysatoren für die Konstruktion von Kohlenstoffgerüsten in natürlichen sowie künstlichen Molekülen. Durch sie kann die Bandbreite von industriell gefertigten Molekülen, die durch Biokatalyse synthetisiert werden, vergrößert werden. Enoat-Reduktasen, die üblicherweise als "alte gelbe Fermente" bezeichnet werden, katalysieren die chemo-, regio- und stereoselektive Reduktion einer aktivierten Doppelbindung durch einen FMN-Cofaktor. Es sollte die Hypothese geprüft werden, dass eine Enoat-Reduktase so zu modifizieren, dass sie eine reduktive Zyklisierung katalysieren kann. Das Enolat-Intermediat, das aus dem Hydridtransfer des $FMNH_2$-Cofaktors resultiert, soll ein internes Elektrophil des Substrates angreifen, wodurch ein zyklisches Produkt entsteht.

Diese neue katalytische Promiskuität von En-Reduktasen wurde beobachtet. In Proof-of-Concept-Experimenten konnten wir zeigen, dass bestimmte Enoat-Reduktasen in der Lage sind, die reduktive C-C Bindungsknüpfung von ungesättigten Aldehyden und Ketonen mit einem internen Elektrophil unter Bildung eines zyklischen Produkts durchzuführen. Durch die Mutation einer katalytisch aktiven Aminosäure innerhalb von Opr3 und YqjM, wird die natürliche Funktion, die asymmetrische Reduktion einer aktivierten C=C Doppelbindung, unterdrückt. In dieser biokatalytischen Umwandlung werden zwei neue stereogene Zentren in einem Schritt gebildet. Es wurde gezeigt, dass durch die Umsetzung von Substraten mit einem sterisch anspruchsvollen Substituenten, zyklische Produkte in hoher Enantiomerenreinheit gebildet werden.

Abstract

Modified enzymes serve as powerful tools for the construction of carbon skeletons in natural and non-natural molecules and will increase the range of industrially important molecules that can be synthesized through biocatalysis. Enoate reductases, commonly denoted as “old yellow enzymes”, catalyze the reduction of an activated double bond in a highly chemo-, regio-, and stereoselctive manner using an FMN cofactor. We envisioned that an enoate reductase can be redesigned to function as an enzyme catalyzing a reductive cyclization, if the enolate intermediate resulting from the hydride transfer from the $FMNH_2$-cofactor is trapped by an internal electrophile of the substrate.

A new catalytic promiscuity of ene-reductases was observed. In proof-of-concept experiments we could show that certain enoate reductases are able to perform the reductive C-C bond formation of unsaturated aldehydes and ketones with an internal electrophile yielding a cyclic product. By mutating one key active site residue of Opr3 and YqjM their natural function, the asymmetric reduction of activated C=C double bonds, is suppressed. Moreover, this biocatalytic transformation represents a reductive C-C bond formation where two new stereogenic centers are formed in one step. We could show by offering substrates with a sterically demanding substituent, that cyclic products were formed in high enantiomeric purity.

1 Introduction

Carbon-carbon bond formations are essential for the construction of structurally complex molecules. A common feature of complex molecules found in nature is a carbon atom to which four distinct carbon substituents are attached, a so called quaternary stereogenic center. For the construction of such stereogenic centers, several catalytic and enantioselective transformations have been developed including DIELS-ALDER reactions, intramolecular HECK-reactions, or Pd-catalyzed allylic alkylations.[1]

Many of these reactions do not possess a biological counterpart, although nature is capable of constructing a diverse set of organic compounds including simple metabolites as well as complex natural products. Enzymes, which are the catalysts used by nature, are composed of only 20 canonical amino acids, but can accelerate a range of different reactions. However, for carbon-carbon bond formations only a limited repertoire of enzymes is available, i.e. aldolases, hydroxynitrile lyases, thiamine diphosphate dependent enzymes, and terpene cyclases.[2-4]

The development of enzymes which are able to perform non-biological reactions is a growing field at the interface between chemistry and biology. Catalytic antibodies, *de novo* designed enzymes, and the introduction of artificial cofactors into proteins brought access to biocatalysts which are able to catalyze non-natural C-C bond formations to expand the biocatalytic toolbox.[2,5-12] Over the last few years, it was recognized that one single active site can catalyze different chemical transformations, which in combination with protein engineering makes new chemical reactions accessible.[13,14]

2 Theoretical Background

2.1 Biocatalytic reduction of C=C double bonds

Old yellow enzymes (OYE) from yeast, plants, fungi, and bacteria have already been studied for a long time. In 1932, OYE from brewer's bottom yeast was the first enzyme of this family which was described.[15,16] Soon after that, THEORELL realized that a small organic molecule was responsible for the catalytic function of OYE1, namely flavin mononucleotide (FMN), which is associated with the protein in a 1:1 stochiometry.[17,18] Proteins from the OYE-family are known to perform the reduction of an activated C=C double bond in α,β-unsaturated compounds. The reduction of the electron-deficient double bond takes place through the transfer of a hydride, derived from a reduced flavin cofactor ($FMNH_2$), to the β-carbon of an α,β-unsaturated carbonyl compound (Scheme 1). A proton uptake occurs from the other side at the α-carbon hence this reaction occurs in a *trans*-specific fashion.[19] Groups which are able to activate the double bond are ketones, aldehydes, nitroolefins, esters, and carboxylic acids. A pair of residues, typically His/His, Asn/His or Asn/Asn, depending on the enzyme, act as H-bonding donors to the electron withdrawing group to further activate the double bond.[20]

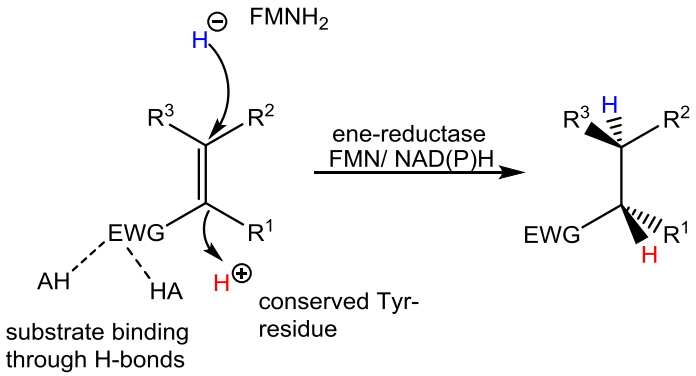

Scheme 1: *trans*-Specific hydrogenation in ene-reductases.

The catalytic cycle consists of two so called 'half-reactions', the addition of [H_2] to the substrate is generally denoted as the 'oxidative half reaction' while the 'reductive half reaction' is denoted as the reduction of the oxidized flavin cofactor at the expense of NAD(P)H.[21] Before the substrate is bound in the active site of ene-reductases, the FMN cofactor is reduced by NAD(P)H and then the hydride is transferred to C-β (Scheme 2). FMN functions as a temporary electron-sink of electrons, which are then passed on to an electron accepting species, i.e. an electron accepting protein or a substrate. Usually NADH and NADPH are both accepted as cofactors by ene-reductases, albeit exceptions are known.[22,23]

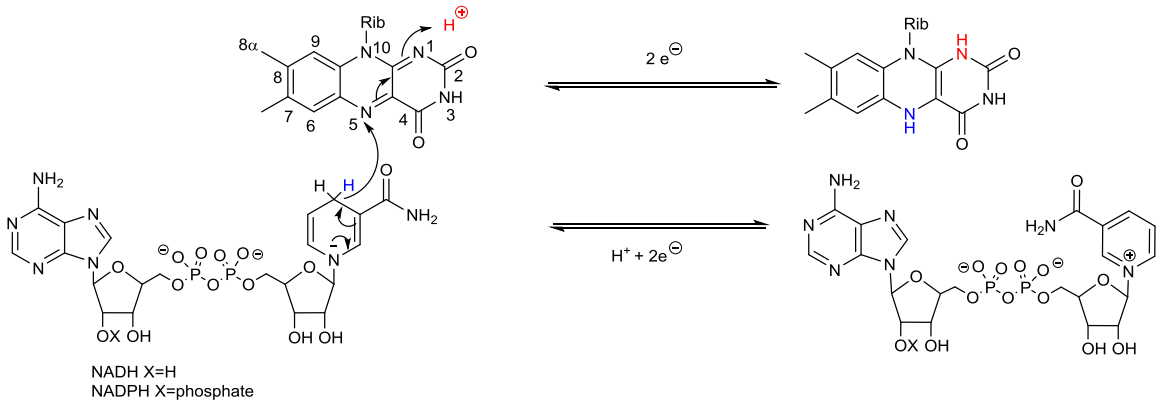

Scheme 2: Electron transfer reaction between NADH resp. NADPH and flavin.

2.2 Mechanistic insights in Old yellow enzyme (OYE1)

The search for the natural substrate of OYE1 has been of great interest for many years. Starting in 1976, ABRAMOVITZ and MASSEY observed that upon binding of a phenolate anion to OYE1, charge-transfer complexes are formed. However, phenolic compounds were not converted by OYEs.[24,25] In 1993, reasonable turnovers of compounds containing an α,β-unsaturated carbonyl moiety were reported by MASSEY and co-workers for the first time.[19] Only one year later, FOX and KARPLUS solved the crystal structure of OYE1 and relevant active side residues were identified.[26] Considerable research effort was invested to elucidate how this enzyme class functions and which active site residues are responsible for the catalytic turnover. Figure 1 illustrates relevant active site residues in OYE1. FMN is shown in yellow and Thr-37 is shown in deep red. The two hydrogen bonding donors which activate the double bond are displayed in blue (His-191) and in purple (Asn-194). The proton donor Tyr-196 is shown in pink.[20,27]

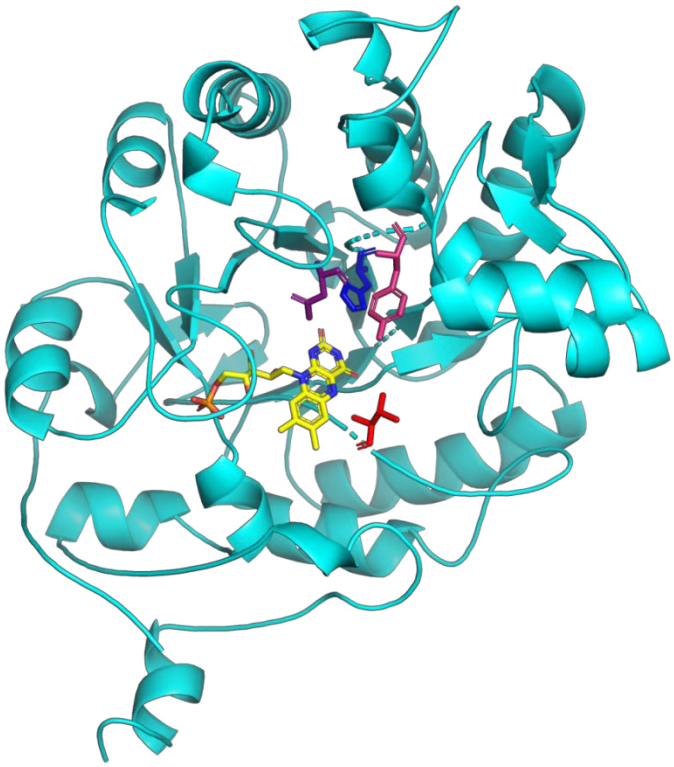

Figure 1: Relevant amino acid residues in the active site of OYE1. Figure prepared with: The PyMol Molecular Graphics System, DeLano Scientific, San Carlos, CA.

α,β-Unsaturated aldehydes and ketones are efficient substrates for the turnover reaction with NADPH (see Scheme 3). In the reductive half reaction enzyme bound FMN gets reduced at the expense of NADPH. The pro-*R* hydrogen of the reduced pyridine ring is transferred to the flavin.[28] In the oxidative half-reaction the FMN hydride gets delivered to the C-β of the

carbonyl function while the enzyme bound flavin gets oxidized. Then a proton is added at α-position of the carbonyl function from the opposite side. It has been suggested by SCRUTTON and co-workers that the hydride and the proton get transferred simultaneously to the electron deficient double bond of a substrate (i.e. 2-cyclohexenone).[29]

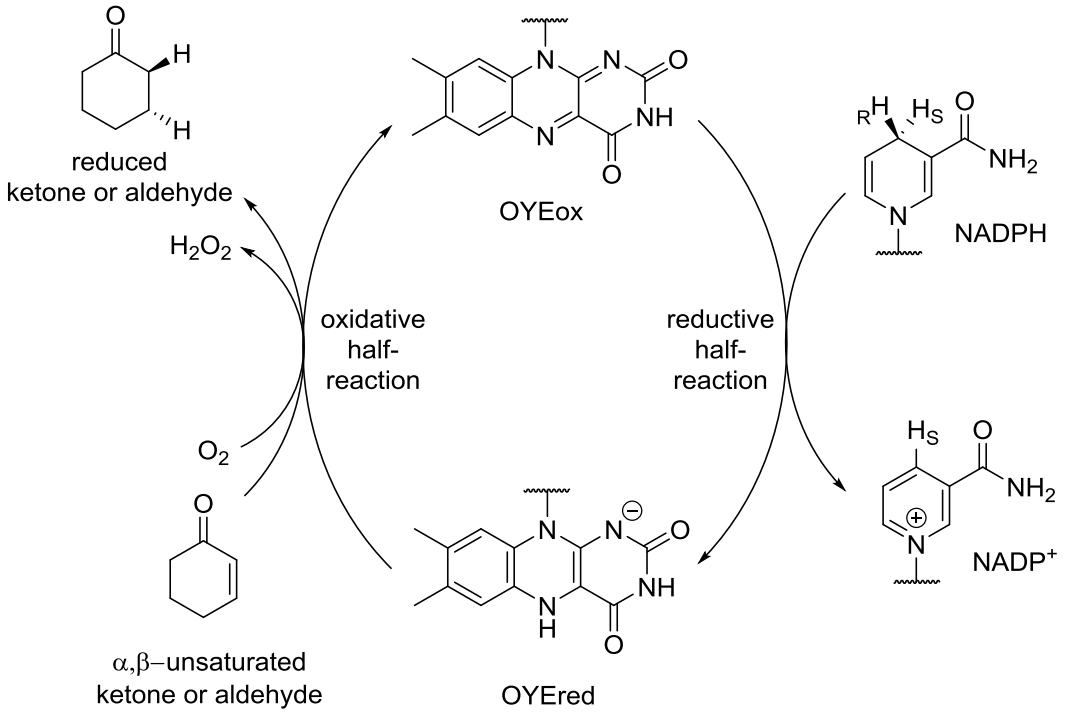

Scheme 3: Catalytic cycle for OYEs.

To elucidate how the overall addition of H_2 takes place, the reduction of *trans*-3-phenyl-2-propenal (**1**) with [4-pro-*R*-$^2H_1$]NADPD in H_2O or D_2O has been studied by MASSEY and co-workers (shown in Scheme 4).[30]

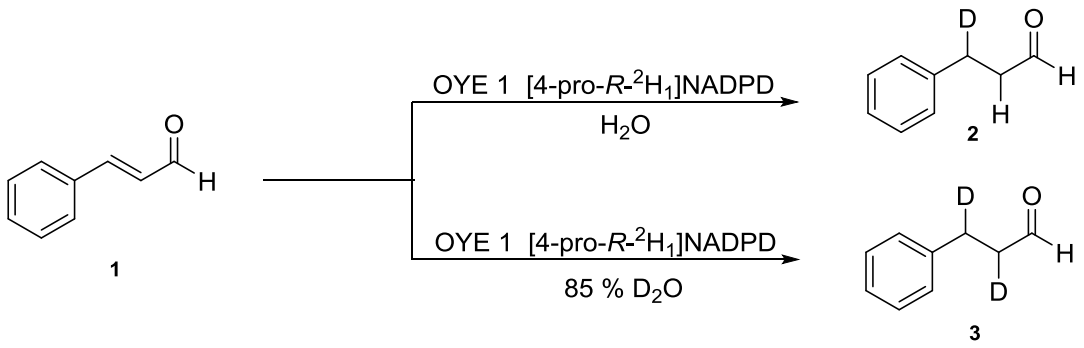

Scheme 4: Incorporation of deuterium in the reduction of cinnamaldehyde (**1**). Data taken from [30].

When *trans*-3-phenyl-2-propenal (**1**) was reduced with [4-pro-*R*-$^2H_1$]NADPD in H_2O, the mass spectrum of the reduction product indicated the incorporation of a single deuterium atom. FMN was reduced by [4-pro-*R*-$^2H_1$]NADPD and the transfer of the deuterium atom to C-β of the α,β-unsaturated aldehyde was confirmed by the observation of a fragment ion that indicates that the deuterium was incorporated at the benzylic methylene carbon. When *trans*-3-phenyl-2-propenal (**1**) was reduced with [4-pro-*R*-$^2H_1$]NADPD in 85 % D_2O, two deuterium atoms were incorporated according to mass spectrometry, which indicates that the reprotonation of C-α occurs via the solvent.[30] When crystal structure analysis showed that Tyr-196 is ideally suited to serve as an active site acid, which can deliver a proton to the α-position, a Tyr to Phe (Y196F) mutation was constructed by KOHLI and MASSEY.[26,27] To obtain the full kinetics of the catalytic cycle and to determine the effect of the Y196F mutagenesis on catalysis, the reductive and the oxidative half-reactions were studied by stopped-flow spectrophotometric measurements, in which 2-cyclohexenone was used as a substrate (see Scheme 3). The reductive half-reaction was not affected by the mutation of Tyr-196 to Phe when compared to the wild type OYE1, but the rate of the oxidative half–reaction was slower by nearly 6 orders of magnitude when compared to wild type OYE1. KOHLI and MASSEY concluded that for the successful reduction of the α,β-unsaturated double bond the hydride transfer from flavin to C-β and the proton uptake from Tyr-196 is required.[26,27] However, the proton transfer step seems to be under discussion since the details of this reaction step were not conclusively determined. It is not known if the proton comes directly from Tyr-196 or whether a water molecule held in position by Tyr-196 donates the proton. LONSDALE and REETZ gained mechanistic insights in the hydride/proton transfer reactions by the application of quantum mechanics/molecular mechanics calculations.[31] The oxidative half reaction of YqjM WT (an OYE which will be described in chapter 2.4 in more detail) and 2-cyclohexenone was calculated. In Scheme 5 dotted lines which represent the reaction coordinates used during reaction modeling are shown: r_{H^-} is the hydride transfer reaction coordinate, r_{PY} refers to direct proton transfer from Y169 and r_{PW} refers to the proton transfer from Y169 via a bridging water molecule.[31]

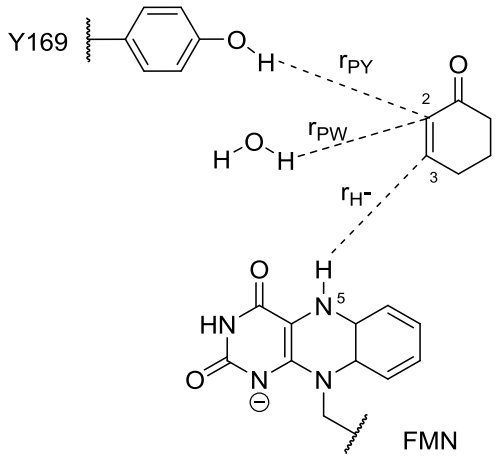

Scheme 5: Possible reaction coordinates of the reduction of 2-cyclohexenone with YqjM WT.

According to LONSDALE and REETZ energy pathways across 2D potential energy surfaces suggested, that it is energetically most favourable when the hydride transfer and the proton transfer occur as separate steps, which is in contrast to calculations from SCRUTTON and coworkers which had been mentioned before.[29,31] However, calculations by LONSDALE and REETZ indicate that the hydride transfer to the C-β of the substrate is the rate-determining step and that the resulting enolate intermediate is stabilized by two histidine side chains (His-164 and His-167 in YqjM). Moreover, the stabilizing histidines prevent the O-atom of the enolate from protonation of Tyr-169, enabling the proton instead to transfer to C-α of the ketone function. Until today there is no experimental evidence for an isolated enolate intermediate. Furthermore the calculated reaction pathways by LONSDALE and REETZ indicate that Y-169 is more likely to protonate the substrate directly, instead of the protonation via a bridged water molecule.[31] The crystal structure of OYE1 was solved with *p*-hydroxybenzaldehyde bound to the enzyme by FOX and KARPLUS as illustrated in Figure 2.[26]

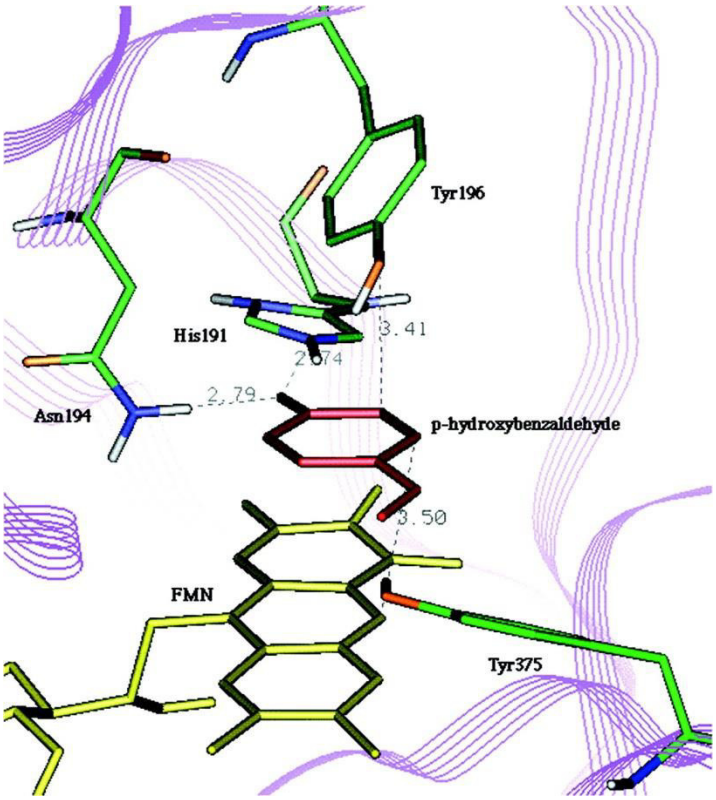

Figure 2: The active site of OYE1 with *p*-hydroxybenzaldehyde bound. FMN is shown in yellow, *p*-hydroxybenzaldehyde is shown in red. Hydrogen bonding distances are given between donor and acceptor atoms, the assumed location of the hydrogen atoms is ignored. Figure taken from reference [20].

The phenolic anion is hydrogen-bonded to His-191 and Asn-194 indicating that these two residues are involved in substrate binding.[26] To evaluate the effects of His-191 and Asn-194 on catalysis, mutants were generated by MASSEY and co-workers.[20] Asn-194 was exchanged to His and a double mutant H191N/N194H of OYE1 was made. The oxidative half-reaction of OYE1 and mutants was studied. When O_2 is offered as a substrate for OYE1 it gets reduced to H_2O_2 as shown in Scheme 3. The kinetics of oxidation of OYE1, N194H, and H191N/N194H were determined using stopped flow spectrophotometry. According to MASSEY the rate constants were not remarkable affected by the mutations since the rate constants were similar in magnitude when compared to OYE1. However, when 2-cyclohexenone was offered as a substrate, the oxidation by the N194H and H191N/N194H was dramatically less efficient than the oxidation reaction with OYE1. MASSEY and co-workers concluded that a proper alignment of 2-cyclohexenone is only achieved when it interacts with His-191 and Asn-194. If this hydrogen bonding interaction is not available, the β-position of 2-cyclohexenone does not receive the hydride from the N-5 of the flavin and the overall function of the mutants is diminished.[20] Mutation at Tyr-196, His-191, and Asn-194 affected the oxidative half reaction and decreased the overall enzyme activity tremendously. In contrast, when Thr-37 was exchanged against alanine, the reductive half reaction was affected when compared to wild

type OYE1.[32] When oxidized T37A was reduced by NADPH under anaerobic conditions, the rate constant was only 8 % compared to that of the wild type OYE1. This indicated that Thr-37 and its hydrogen bonding with the C-4 oxygen of FMN (Figure 1, Thr-37 is shown in red, C-4 oxygen is shown in red) seem to play an important role in controlling the redox properties of flavin.[32]

2.3 12-Oxophytodienoate reductase 3 from *Lycopersicon esculentum*

12-Oxophytodienoate reductase 3 (Opr3) from *Lycopersicon esculentum* belongs to the family of old yellow enzymes. This enzyme participates in the biosynthesis of jasmonic acid where it catalyzes the reduction of the cyclopentenone moiety in (9*S*,13*S*)-OPDA to 8-((1*S*,2*S*)-3-oxo-2-((*Z*)-pent-2-en-1-yl)cyclopentyl)octanoic acid (1*S*,2*S*)-OPC, as it is illustrated in Scheme 6.[33]

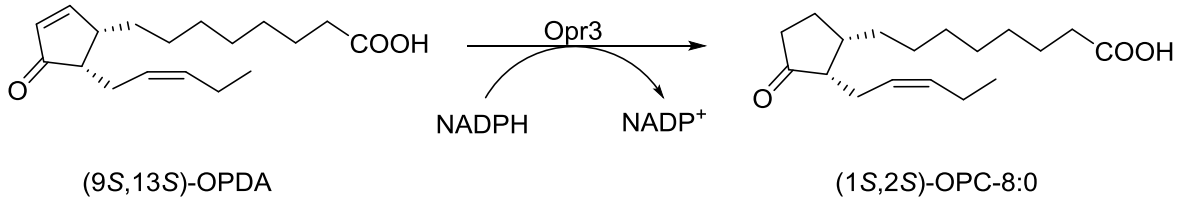

Scheme 6: Opr3 catalyzes the reduction of (9*S*,13*S*)-OPDA to (1*S*,2*S*)-OPC.

Opr3 has several isozymes which have been identified from plants, including three isoforms in *Lycopersicon esculentum*, five in *Arabidopsis thaliana*, and thirteen in *Oryza sativa*. While Opr3 from *Lycopersicon esculentum* and Opr3 from *Arabidopsis thaliana* are able to catalyze the reduction of all four stereoisomers of OPDA, the large majority of Opr enzymes catalyze only the reduction of the (9*R*,13*R*)-OPDA stereoisomer and fail to react with the (*S*,*S*)-stereoisomer.[33] In Opr3 the FMN cofactor is bound noncovalently and the amino acids which perform side-chain interactions with the FMN cofactor are 100 % conserved within the OYE family. Figure 3a illustrates the key interactions which are involved in binding FMN in Opr3.[34]

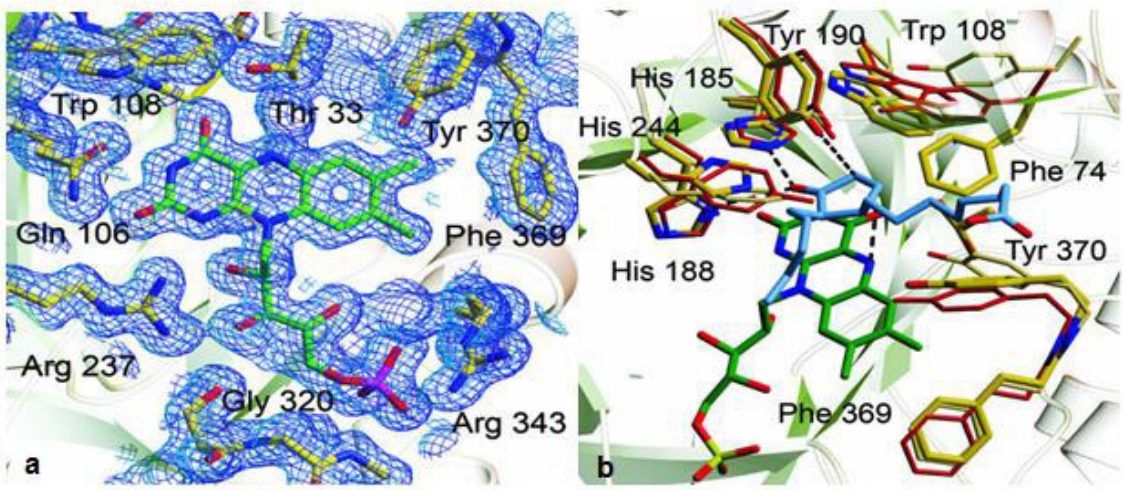

Figure 3: (a) FMN binding site of Opr3. FMN is shown in green, amino acids that contact FMN are shown in yellow; (b) Superposition of the substrate binding pockets of Opr3 (yellow), Opr1(red) and OYE1 (beige); FMN in Opr3 is shown in green and (9*R*,13*R*)-OPDA (substrate of Opr1) is shown in blue. Figure taken from reference [34].

The hydroxyl and amide group of Thr-33 are in hydrogen bonding distance to O(4) and N(5) of the FMN isoalloxazine ring. Arg-237 and Gln-106 form hydrogen bonds to N(3) and O(2) of the FMN. In Figure 3b, a superposition of the substrate binding pockets of Opr3 (yellow), Opr1 (red), and OYE1 (beige) is shown. For OYE1 it is shown that FMN (green), in particular the H of N(5), is positioned that it can be easily transferred to the substrates C-β (shown in blue). Tyr-190 is in ideal position to serve as a proton donor to reprotonate the C-α of the substrate. In the superposition of Opr1, Opr3, and OYE1 it can be seen that His-185, His-188, and Tyr-190 are positioned virtually identical, with the exception of His-188, which is in several enzymes replaced against Asn. The corresponding atoms responsible for substrate activation and positioning (Asn Nδ2 and His Nδ1) overlay perfectly.[22,26,35,36] However, it is observed that pronounced differences between Opr1 and Opr3 exist regarding the opening of the substrate binding cavity. In Opr3 His-244 and Phe-74 above the FMN turn away from the active site and therefore give rise to a wide entrance in the active site binding pocket (Figure 3b). In contrast, the entrance to the binding cavity in Opr1 is rather narrow since two large Tyr-residues (Tyr-246 and Tyr-78) are located above FMN (not shown in Figure 3b). This difference in Opr1 and Opr3 might be the reason for the broader substrate acceptance of Opr3 in contrast to Opr1. The structural comparison of Opr1, Opr3, and OYE1 reveals distinct structural conservation of catalytically important amino acids while the substrate specificity depends on the specific enzyme.[22,26,34]

2.4 YqjM from *Bacillus subtilis*

YqjM, which originates from *Bacillus subtilis*, shares many characteristics with other OYE homologs. It binds FMN tightly but not covalently and it is capable of reducing flavin in the reductive half reaction at the expense of NADPH. YqjM transfers electrons from the reduced flavin cofactor to a variety of α,β-unsaturated carbonyl functions (i.e. 2-cyclohexenone) in the oxidative half reaction, as other members in the OYE family do. Figure 4 shows an illustration of the flavin binding site in YqjM (hydrogen bonds are illustrated as thin red dots).[37]

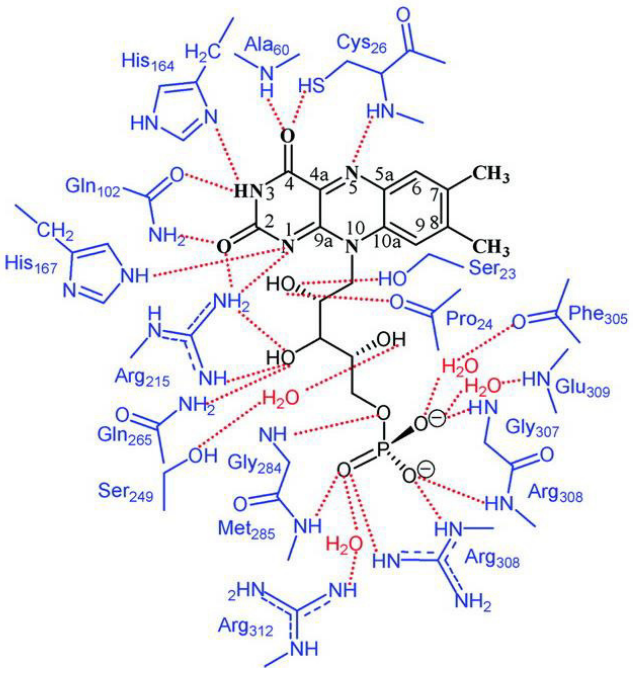

Figure 4: The schematic FMN-binding site in YqjM. Figure taken from reference [37].

Similar as in OYEs a glutamine (Gln-106) is in hydrogen bonding distance to N(3) and O(2) of the isoalloxazine ring of the FMN cofactor. CLAUSEN and co-workers described that phenolic inhibitors bind in the anionic phenolate state via two His-residues (His-164 and His-167) similar as in other OYEs. Besides these similarities, major differences in the active site of YqjM can be described. The O(4) is not hydrogen bonded to a Thr, as it is known for other OYEs, instead it interacts with a cysteine (Cys-26). Moreover, this cysteine can either form a hydrogen bond with O(4) or it can, upon adopting another conformation, form a hydrogen bond to N(5) of the isoalloxazine ring, which indicates that Cys-26 might act as a redox sensor that controls the redox potential of flavin depending on the presence of a substrate.[37] Another unique feature of YqjM is the so-called butterfly bending at the hypothetical N(5)-N(10) hinge of the FMN-cofactor since usually the FMN-cofactor is planar. His-164 and His-

167 are responsible for activating the C=C double bond of the carbonyl function of a substrate, while Tyr-169 can be considered as the acid catalyst protonating C-α.[38] This Tyr-residue superimposes perfectly with Y-196 in OYE1.[26] It was shown by MACHEROUX and co-workers that nitro compounds (2,4,6-trinitrotoluene and nitroglycerine) are reduced by YqjM and this led to the discovery that the expression of YqjM is strongly induced by nitro compounds. In fact, after incubation with TNT for 15 min high levels of protein were observed. This inducible YqjM expression led to the assumption that this enzyme might have a role in the detoxification of xenobiotics. However, nitroorganic compounds are rarely found in nature therefore the induction of the enzyme might be caused by a secondary induction mechanism. TNT is known to cause the production of H_2O_2 and the effect of H_2O_2 was investigated during YqjM expression. Upon incubation with H_2O_2 a similar inductive effect was observed as it was observed with incubation of TNT. It was concluded that YqjM might not have one single physiological substrate *in vivo*, but it is involved in a general stress response system and is responsible for the maintenance of the redox-state of the cell.[37]

2.5 Substrate scope and stereochemical investigations of Opr3 and YqjM

The substrate scope of Opr3 from *Lycopersicon esculentum* and YqjM from *Bacillus subtilis* was investigated by FABER and coworkers.[23] A variety of different substrates were selected to gain insight in the substrate-preferences of YqjM and Opr3. Substrates were selected for the (i) nature of activating group, (ii) chain length and ring size, (iii) relative position of substituents at the C=C double bond and the (iv) influence of the cofactors NADH and NADPH on activity and stereoselectivity. Scheme 7 shows the asymmetric bioreduction of citral (**4a**).

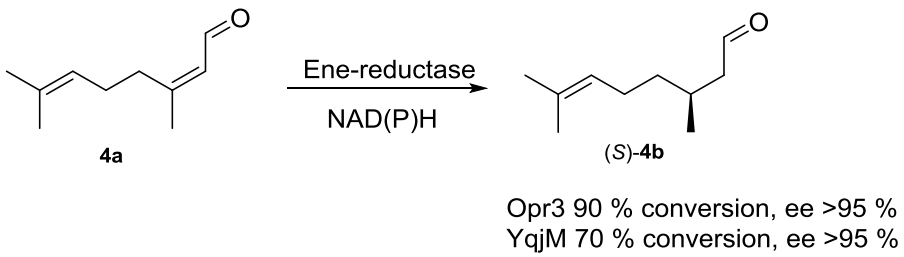

Scheme 7: Reduction of citral (**4a**) by ene-reductases. Data taken from [23].

The reduction of citral (**4a**) highlights the excellent chemoselectivity of ene-reductases. While the activated double bond is reduced by both enzymes, the isolated double bond is not converted at all by both enzymes. The substituent at C-β seems to be tolerated by both enzymes and very good stereoselctivities were obtained (>95 %). The reduction of a short-chain aldeyhde **5a** is displayed in Scheme 8.

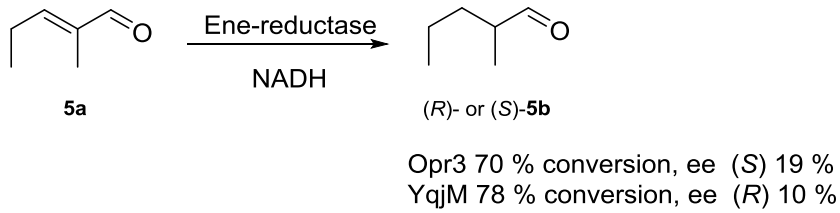

Scheme 8: Reduction of (*E*)-2-methylpent-enal (**5a**) by ene-reductases. Data taken from [23].

HALL *et al* showed that Opr3 and YqjM enzymes converted (*E*)-2-methylpent-enal (**5a**) in up to 78 % albeit poor stereoselctivities were obtained. While Opr3 slightly favours the (*S*)-stereoisomer, YqjM favours the (*R*)-stereoisomer. HALL *et al* hypothesized that the large differences in stereoselectivity observed in the conversion of **4a** and **5a**, might be due to the racemisation of compound **5b** catalyzed by ene-reductase, which had already been observed by OYEs from yeasts. Scheme 9 displays the asymmetric bioreduction of cyclic ketones **6a** and **7a** with a substituent at the α-position by ene-reductases.[23]

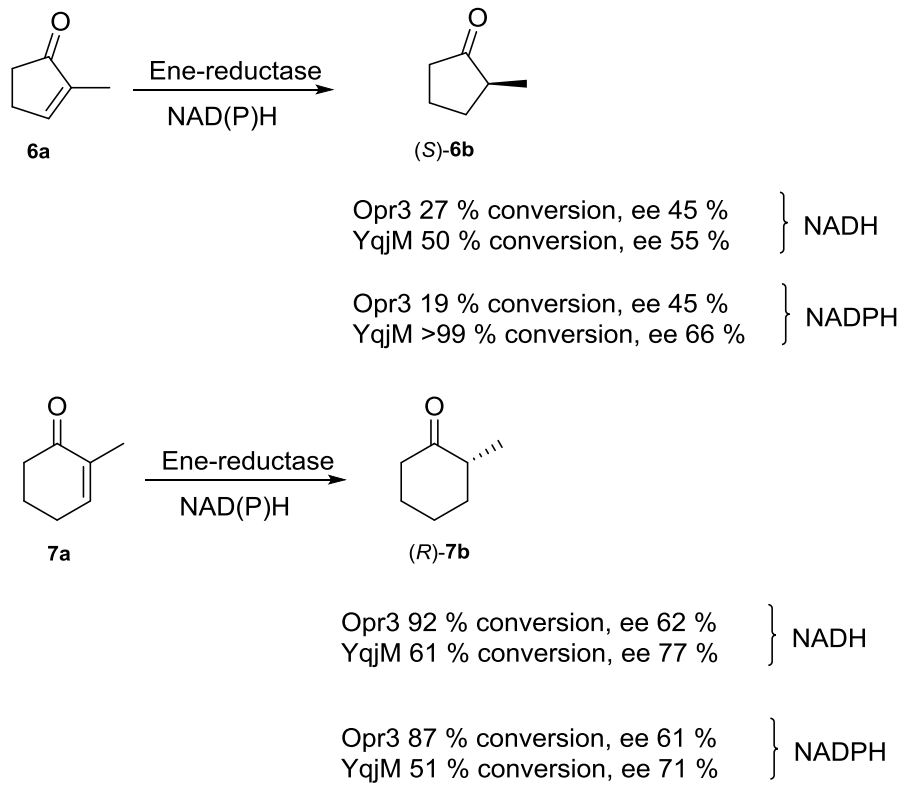

Scheme 9: Reduction of 2-methylcyclopentenone (**6a**) and 2-methylcyclohexenone (**7a**) by ene-reductases. Data taken from [23].

The reduction of 2-methylcyclopentenone (**6a**) was tested by FABER and co-workers. Substrate **6a** was converted in moderate conversions and ee's by both enzymes when NADH was applied. With NADPH as cofactor **6a** was fully converted by YqjM and an ee of 66 % was achieved. By the conversion of 2-methylcyclohexenone (**7a**) it was observed that the substrate is better accepted by Opr3 (conversion up to 92 %), albeit moderate stereoselectivities were obtained. The use of NADPH resulted in a lower conversion of the starting material. HALL *et al* did not provide an explanation for the cofactor dependency of both reactions. It was claimed that "allosteric effects" are responsible for the cofactor dependency of conversions. While both α-substituted cyclic ketones were reduced by Opr3 and YqjM, the corresponding β-substituted cyclic ketones (**8a** and **9a**) were not converted by both enzymes (Scheme 10).[23]

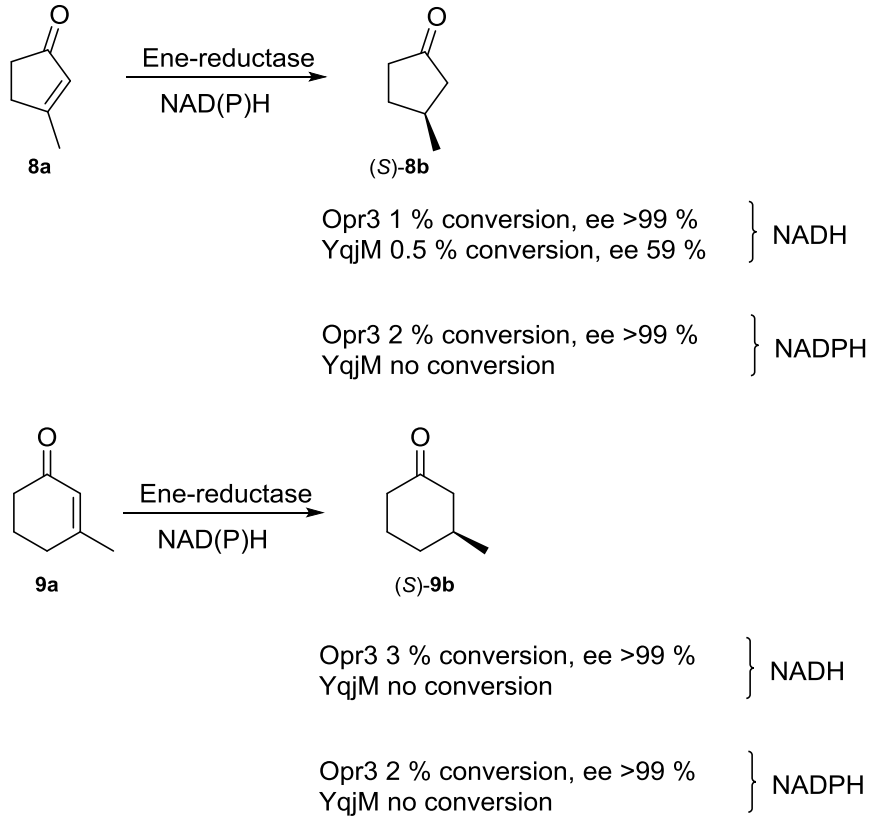

Scheme 10: Reduction of 3-methylcyclopentenone (**8a**) and 3-methylcyclohexenone (**9a**) by ene-reductases. Data taken from [23].

HALL *et al* showed that ketoisophorone (**10a**) was converted by Opr3 and YqjM in excellent conversions and stereoselectivities when a cofactor recycling system was used (Scheme 11). Again, the type of cofactor and the recycling system have a significant influence on the stereoselecetivity of this reaction.[23]

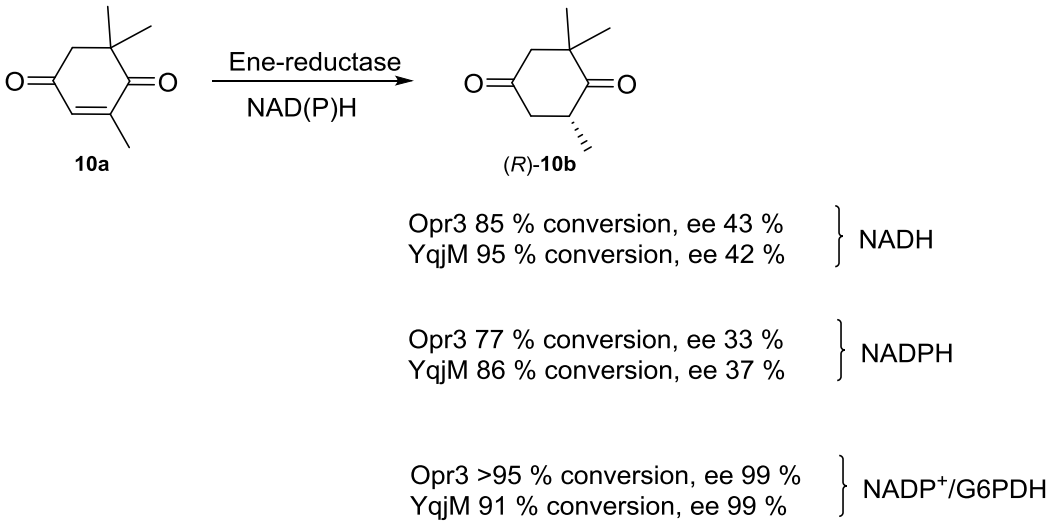

Scheme 11: Reduction of ketoisophorone (**10a**) by ene-reductases. Data taken from [23].

Scheme 12 displays the asymmetric bioreduction of α-methylmaleimides (**11a** and **12a**). The initial plan by HALL *et al* was to engineer the substrate **11a**, by offering a substrate with a much bulkier *N*-substituent in **12a**. The plan of engineering a substrate was unnecessary because both substrates were converted by both enzymes in excellent conversions (up to >99 %) and stereoselectivities (up to >99 %). A cofactor dependency in this case was not observed. NADH and NADPH gave comparable results.[23]

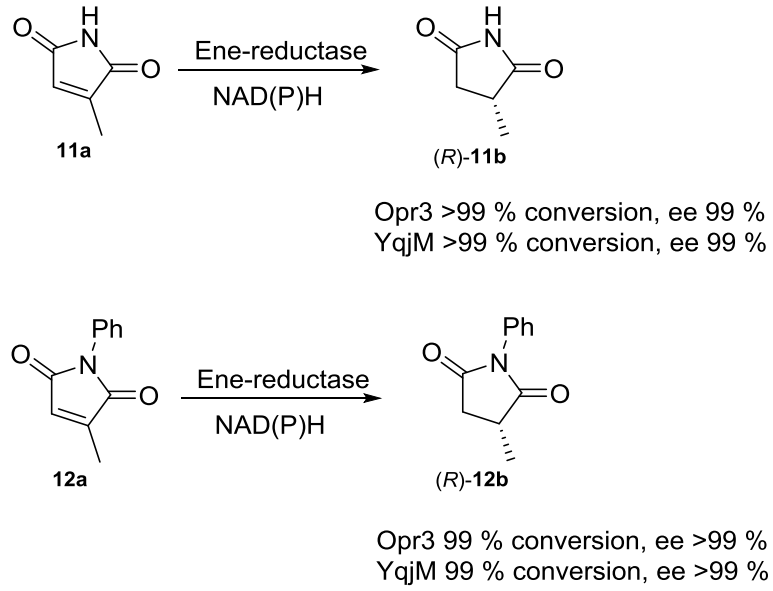

Scheme 12: Reduction of α-methylmaleimides (**11a** and **12a**) by ene-reductases. Data taken from [23].

In addition, the reduction of nitroalkenes was attempted by HALL *et al* (see Scheme 13). 1-Nitro-2-phenylpropene (**13a**) served as a model substrate. Both enzymes delivered the (*S*)-stereoisomer (**13b**) in ee's up to 92 %. Interestingly, when NADH served as a cofactor YqjM showed an enhanced conversion (up to 94 %) and stereoselectivity (92 %) in contrast to NADPH.[23]

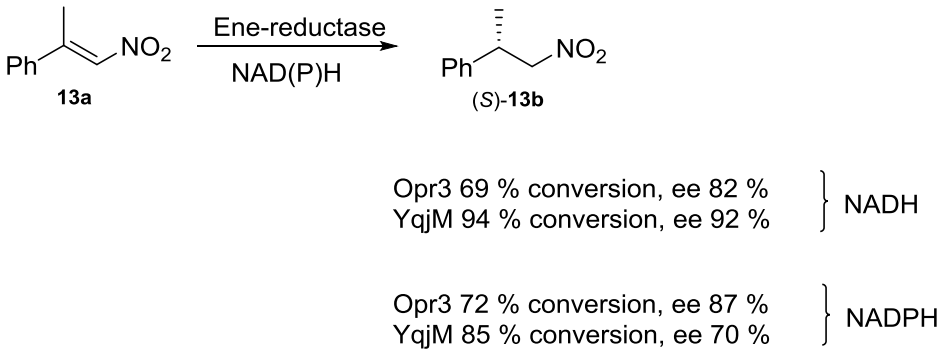

Scheme 13: Reduction of 1-nitro-2-phenylpropene (**13a**) by ene-reductases. Data taken from [23].

HALL *et al* tested the asymmetric reduction of α-methylmaleic acid (**14a**) (Scheme 14). This reduction of the C=C double bond failed with both enzymes. However, it is known that isozyme Opr1 is catalyzing this reduction in high conversions and high stereoselectivities.[39]

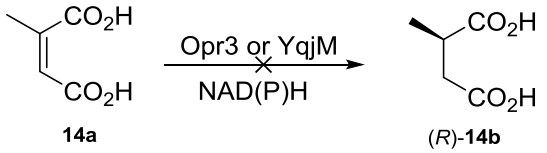

14a (*R*)-**14b**

Scheme 14: Reduction of α-methylmaleic acid (**14a**) by Opr3 and YqjM. Data taken from [39].

2.6 New enzyme activites

2.6.1 Protein engineering of members of the old yellow enzyme family

The enzymatic reduction of an activated double-bond goes in hand with the creation of new stereogenic centers. Native OYEs often display a very high stereoselectivity towards their natural substrate, but these enzymes have a very size-restricted active site which limits their substrate scope to small substrates. If chirality is introduced early in a synthetic sequence it has to be carried through the whole synthesis with numerous opportunities for racemization and epimerization. Thus, it would be more desirable to synthesize a late stage prochiral alkene and then reduce it with high enantioselectivity. However, late stage intermediates are typically larger and the application of an ene-reductase is not possible anymore. In addition, the stereoselectivities of OYEs are very often the same. For synthetic applications it would be ideal to have pairs of enantiocomplementary OYEs. Wild type OYEs are limited by these two key deficiencies. Firstly, their size restricted active site goes in hand with their limited substrate scope and secondly, their lack of the counterpart OYE make it difficult to form the opposite stereoisomer. The logical choice for overcoming these deficiencies is protein engineering.[40] In this chapter one example of the REETZ-group is discussed where directed evolution, in particular iterative saturation mutagenesis (ISM), has been used to broaden the substrate scope and to control the enantioselectivity of YqjM from *Bacillus subtilis*. The asymmetric reduction of 3-methylcyclohexenone was used as a model reaction in which YqjM reduces the double bond of **15a** to 3-methylcyclohexanone **16** (Scheme 15).[41]

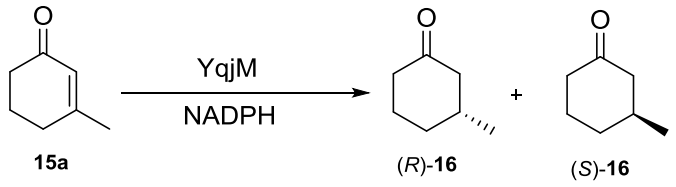

Scheme 15: Reduction of 3-methylcyclohexenone (**15**) by YqjM WT.

Since the YqjM WT was hardly reducing substrate **15a** (3 % conversion) with a moderate ee of 76 % in favour of the (*R*)-stereoisomer, the enzyme catalyst was optimized. In fact, the goal was to find enzyme catalysts which were able to convert substrate **15a** in excellent conversions and to deliver the (*R*)-stereoisomer as well as the (*S*)-stereoisomer in excellent stereoselectivities. Residues aligning the active site or residues which are near the binding pocket were chosen as randomization sites. This process was named CASTing (combinatorial active-site saturation test).[42-45] The X-ray structure of YqjM with *p*-hydroxybenzaldehyde

bound as inhibitor was used by REETZ to choose appropriate randomization sites (Figure 5).[38,41]

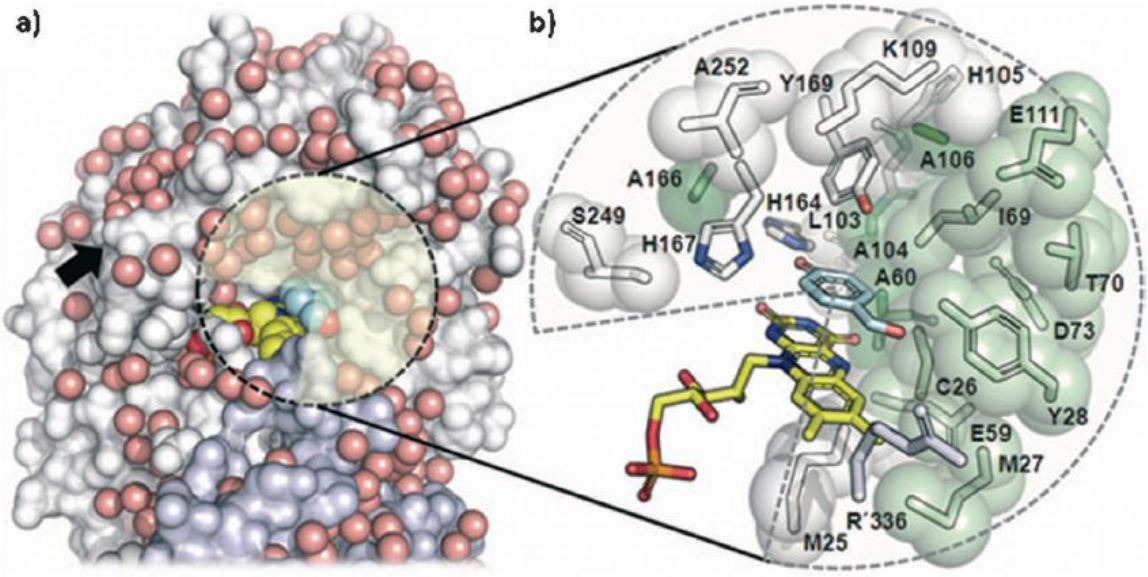

Figure 5: a) Space filling model of YqjM (Chain A, light gray; Chain B, light blue; red spheres, water molecules; yellow spheres, FMN; blue spheres, *p*-hydroxybenzaldehyde as inhibitor); b) Close up view of the catalytic active site displays amino acids which were selected for saturation mutagenesis. Figure taken from [41].

Based on the distance to the inhibitor *p*-hydroxybenzaldehyde, twenty amino acid residues were chosen for saturation mutagenesis. The triad His-164, His-167, and Tyr-169 was excluded from mutagenesis since these residues participate in the catalytic process. The selection of amino acids was separated into three groups: (i) a so called "hot zone" composed of Cys-26, Tyr-28, Ile-69, Asp-73, Thr-70, Met-25, Met-27, and Glu-111, these amino acid residues are located close to the C-β of the substrate, (ii) a so called "soft zone" composed of Ala-60, Ala-104, Ala-106, and Lys-109, these amino acids pointing to C-α of the substrate, (iii) a so called "indifferent zone" composed of Leu-103, His-105, Ala-166, Ser-249, Gly-251, Ala-258, Arg-336. Twenty libraries were formed out of the first round of saturation mutagenesis. According to BOUGIOUKOU *et al* not all libraries contained hits, which means that the chosen amino acid position was either no hot spot or the amino acid position requires at least one further point mutation to exhibit a cooperative effect. In all libraries, (*S*)- and (*R*)-selective active mutants were found and already notably ee's were obtained, i.e. Ala104Tyr (24 % conversion, ee= 91 % (*R*)) and Thr70His (9 % conversion, ee= 84 % (*S*)). The second round of amino acids to be randomized was chosen from the best hits from round one concerning their impact on conversion and enantioselectivity. Best variants from round one and round two are shown in Figure 6.[41]

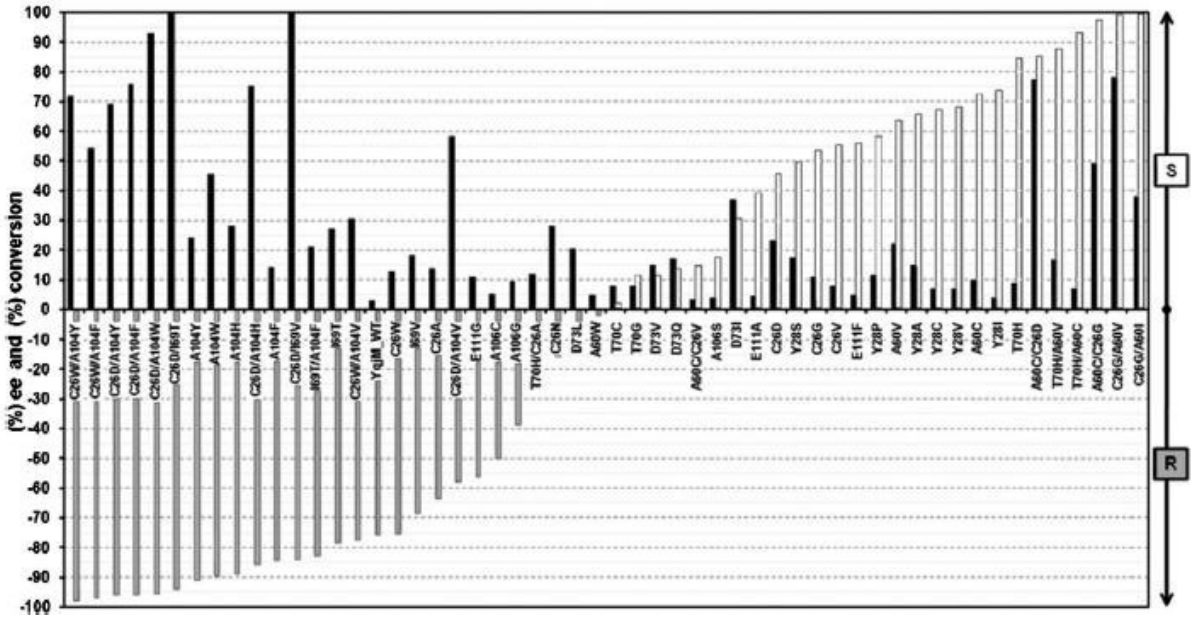

Figure 6: Best variants from round one and round two of saturation mutagenesis from reduction of 3-methylcyclohexenone (**14**). Variants are arranged according to their respective enantioselectivity. Gray bars represent (*R*)-selectivity, open bars represent (*S*)-selectivity, black bars represent conversion. Figure taken from [41].

REETZ and co-workers observed that highly selective (*R*)-variants also achieve high ee-values, e.i. Cys26Asp/Ile69Thr ee= 94 %, 130 fold-improvement in activity. This trend is not observed within the (*S*)-selective variants. Although Cys26Gly/Ala60Val showed excellent stereoselectivity and good activity (data not shown) other variants did only display high enantioselectivity Cys26Gly/Ala60Ile ee= >99% accompanied by low activity. With highly active and highly enantioselective variants in hands, BOUGIOUKOU *et al* expanded the substrate scope of YqjM (Scheme 16) and substrates bearing sterically more demanding substituents were offered to YqjM WT and variants.[41]

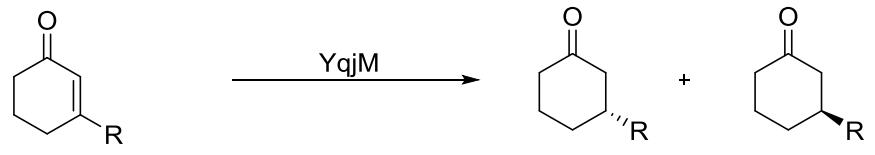

15b R = ethyl
15c R = isopropyl
15d R = *n*-butyl
15e R = CO_2Me

(*R*)-**16** (*S*)-**16**

Scheme 16: Bioreduction of additional substrates for YqjM variants which showed best results in the model reaction.

REETZ and co-workers observed that substrates **15b**-**15d** were not converted at all by the YqjM WT enzyme (Table 1, Entries 1,4 and 7). Both enantiomers of products **16b** and **16c**

were accessible, when the best variants from two saturation mutagenesis rounds were used (Table 1, Entries 2, 3, 5 and 6). The (*S*)-selective variants showed only low conversions, although excellent stereoselectivities were obtained (Table 1, Entries 3 and 6). The already high conversion of the YqjM WT in the reduction of substrate **15e** could be further improved by applying directed evolution (Table 1, Entries 9, 10 and 11).

Table 1: Expansion of the substrate scope of YqjM variants. Data taken from [41].

Entry	YqjM	Substrate	Product **16** conversion [%]/ ee [%]
1	WT	**15b**	-/-
2	C26D/I69T	**15b**	100/99 (*R*)
3	C26G/A60V	**15b**	9/96 (*S*)
4	WT	**15c**	-/-
5	C26D/I69T	**15c**	33/99 (*R*)
6	C26G/A60V	**15c**	2/91 (*S*)
7	WT	**15d**	-/-
8	C26D/I69T	**15d**	92/99 (*R*)
9	WT	**15e**	85/99 (*R*)
10	C26D/A60V	**15e**	92/99 (*R*)
11	C26G	**15e**	100/98 (*R*)

With the knowledge of the X-ray structure of an ene-reductase it was possible to elucidate active site residues which are located near the bound inhibitor *p*-hydroxybenzaldehyde.[38] Through the selection of a set of amino acids for randomization it was possible to create active variants within two rounds of iterative saturation mutagenesis. The active variants were able to deliver both enantiomers of 3-methylcyclohexanone (**16**). Moreover, REETZ and co-workers showed that variants selected against one substrate often show similar properties towards a range of substrates.[41]

2.6.2 Identification of promiscuous ene-reductase activity by the use of 'catalophores'

A structural bioinformatics method for the prediction of catalytic promiscuity in enzymes was developed by STEINKELLNER and GRUBER. As a proof of concept a database search motif was obtained through the analysis of active site constellations in available OYE structures. As already mentioned earlier in this chapter, the three key active site residues in OYEs are two hydrogen bonding donors which activate the double bond (His/His, His/Asn, or Asn/Asn) and the proton donating tyrosine. Four distances (Figure 7a, d_1, d_2, d_3 and d_4) for the relative position of required functional groups were defined. Distance d_1 ranges from the center of the imidazole ring of His to the N(5) position of the flavin isoalloxazine ring. Distance d_2 was defined as the distance between the center of the imidazole ring of histidine and the second hydrogen donor (Asn or His, depending on OYE). Distance d_3 ranges from the second hydrogen bonding donor to the N(5) position of the flavin isoalloxazine ring. Distance d_4 was defined as the distance between the N(5) position of the flavin isoalloxazine ring and the oxygen of the hydroxyl function of tyrosine.[46]

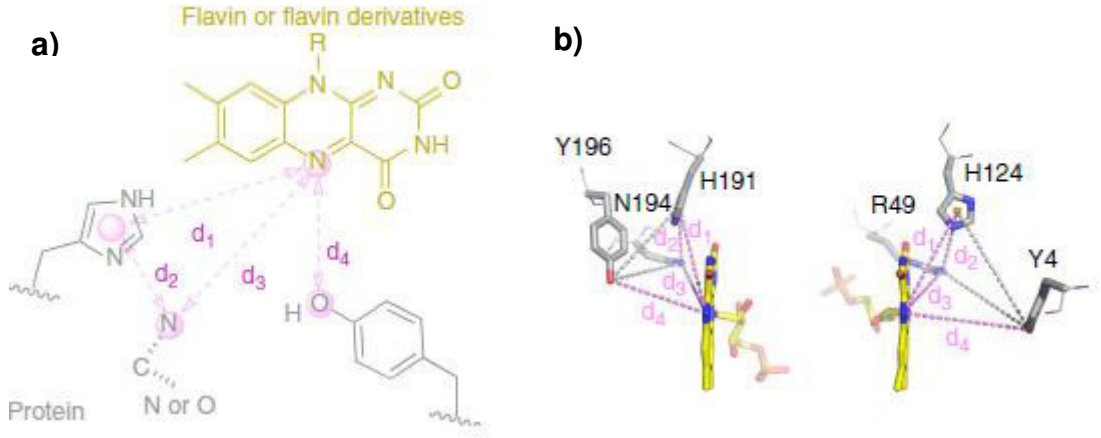

Figure 7: a) Search template with distance descriptors d_1, d_2, d_3, and d_4. b) Comparision of the positions of catalytic active site residues of OYE1 (left) and *Ph*ENR (right). Figure taken from [46].

This motif was used as a search template in two commercial databases. After numerous hits were obtained, the majority of hits was excluded since most of the structures found were OYE structures with high sequence similarity. However, two hits remained annotated as 'putative styrene monooxygenase reductase component' from *Thermus thermophiles* (*Tt*ENR) and 'FMN-binding protein' from *Pyrococcus horikoshii* (*Ph*ENR). Although these two enzymes displayed a different fold, different protein size, and an overall low sequence identity (<10 %) to typical OYEs, *Ph*ENR and *Tt*ENR exhibit very similar arrangements of active site functional groups. Even more interesting was, that the active site constellations in *Ph*ENR and

*Tt*ENR show the mirror symmetry to typical OYE structures. The *re*-face of the isoalloxazine ring is accessible to the substrate, in contrast to OYEs were the *si*-face is accessible (Figure 7b). When crystals structures of *Ph*ENR and *Tt*ENR bound to *p*-hydroxybenzaldehyde were obtained, it was observed that the phenolate oxygen is hydrogen bonded to His-124 and Arg-49 in *Ph*ENR and to His-131 and Arg-58 in *Tt*ENR. These residues correspond to His-191 and Asn-194 in OYE1. Furthermore, the residues Tyr-4 in *Ph*ENR and Tyr-14 in *Tt*ENR correspond to Tyr-196 in OYE1.[26] Alternate binding modes were observed when crystals of *Ph*ENR and *Tt*ENR bound to 2-cyclohexenone were obtained. Although the carbonyl function was hydrogen bonding to the above mentioned His and Arg-residues, the relative positions of the protons donors (Tyr-4 and Tyr-14) are less optimal to donate a proton to the C-α of the substrate. Biochemical characterizations elucidated crucial differences when compared to OYE1, i.e. a different kinetic mechanism and a drastically more negative redox-potential. Both enzymes were tested in biocatalytic transformations by offering typical OYE substrates. 2-Cyclohexenone was not reduced at all by both enzymes, which was expected in terms of the alternate binding mode observed in crystal structures. Also in the reduction of 2-methylcyclopentenone (**6a**) and 2-methylcyclohexenone (**6b**), which are typically very well accepted by members of OYEs, no conversion was observed. In contrast, the reduction of α-methylmaleimide (**12a**) by *Ph*ENR and *Tt*ENR (Scheme 17) delivered the opposite stereoisomer, when compared to Opr3 and YqjM, in good stereoselectivities (chapter 2.5). The reversed stereoselectivity of *Ph*ENR and *Tt*ENR can be explained by the mirror symmetry of the active site constellation, since the *re*-face (instead of the *si*-face) of the isoalloxazine ring is accessible to the substrate.[23,46]

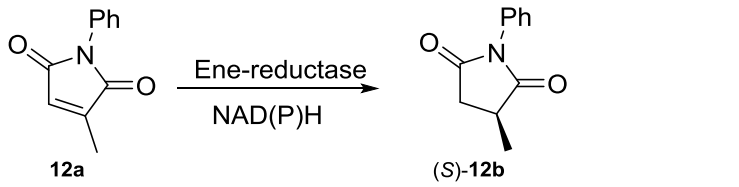

Scheme 17: Reduction of α-methylmaleimide (**12a**) by *Ph*ENR and *Tt*ENR. Data taken from [46].

GRUBER and co-workers demonstrated how a promiscuous enzyme activity can be identified starting from mechanistic and structural considerations. Moreover, if the search for a promiscuous enzyme leads to a hit in a PDB data bank, this promiscuous enzyme has already been expressed and has been stable enough for purification and crystallization. This method describes a valuable tool for the identification and development of novel biocatalysts.[46]

2.6.3 Non-natural C-C-bond formations from engineered cofactor-depending enyzmes

The development of new bioctalaysts for non-natural reactions will expand the tool box of biocatalyis and facilitates the construction of biocatalytic routes for the synthesis of chemical products *in vitro* and *in vivo*.[47,48] Through directed evolution it was possible to develop enzymes for challenging transformations that have no biological counterparts (Scheme 18). Reactions from organic chemistry (Scheme 18, shown in red letters) served as template for the introduction of new enzyme activities in existing co-factor dependent enzymes (Scheme 18, shown in green letters).

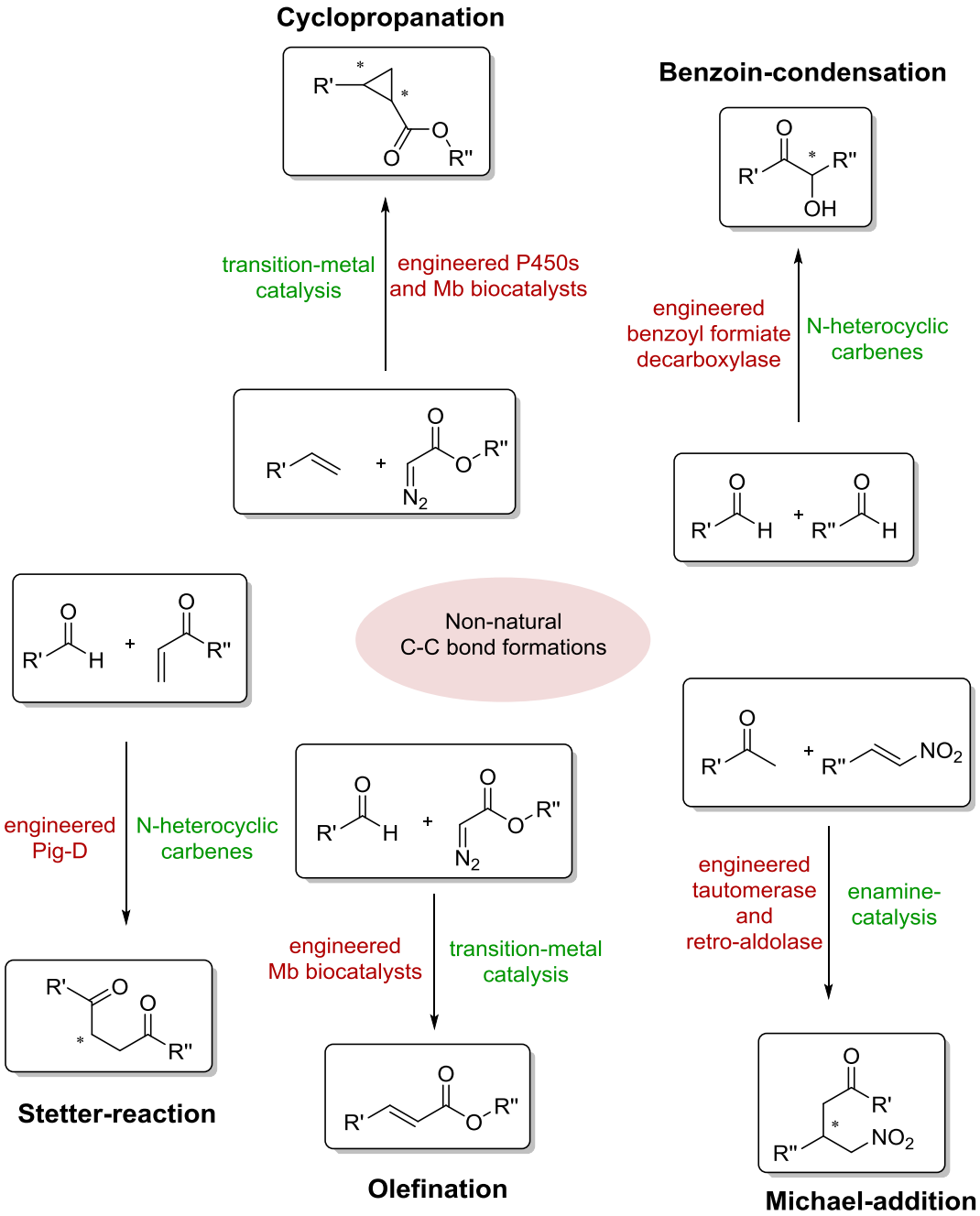

Scheme 18: Unnatural C-C bond formations by engineered enzymes.

In organic synthesis the asymmetric cyclopropanation of olefins is accomplished through the use of high energy carbene precursors (i.e. diazoesters) and transition metal catalysts (Fe, Cu, Ir, Ru, Co, Rh).[49-53] This transformation does not possess a biological counterpart. Inspired by cytochrome P450s, which are able to insert oxygen atoms into C-H bonds and C=C double bonds, ARNOLD and co-workers demonstrated that engineered P450s are able to insert carbenes into C=C double bonds. Styrenes were cyclopropanated via diazoester reagents under anaerobic conditions yielding cyclopropanes in good yields and very good diastereoselectivities and enantioselectivities.[54-57] Two years later, it was shown by the group of FASAN, that also engineered myoglobin catalysts enable the cyclopropanation of styrene with ethyl diazoacetate in excellent conversions (up to >99 %) and excellent de's and ee's (up to >99 %).[58] An engineered myoglobin catalyst was also used for WITTIG-olefinations using diazo-precursors.[59] A coupling reaction between two aldehydes, a so called benzoin condensation, is catalyzed by N-heterocyclic carbenes. The coupling of two very similar aldehydes is a challenging task for small molecule NHC catalysts, since high amounts of homo-coupling products are formed.[60] A thiamine dependent enzyme, which is known for catalyzing a decarboxylation reaction, possesses the ability to perform a benzoin condensation. The so called BRESLOW-intermediate, which is also formed in NHC-catalysis, results from reaction of the thiamine cofactor of the enzyme with the aldehyde substrate. It was possible to obtain excellent chemoselectivity when structurally similar aldehydes were used by applying benzoyl formiate decarboxylase.[61] The BRESLOW-intermediate can also add in a 1,4-conjugate fashion to α,β-unsaturated ketones, in a reaction called STETTER-reaction.[62] The decarboxylase PigD, a thiamine-dependent enzyme, displayed "Stetterase" activity.[63] In the field of organocatalysis enamine and iminium catalysis have been used for asymmetric MICHAEL-reactions.[64-66] It was shown by POELARENDS and co-workers that an engineered tautomerase is able to perform an asymmetric MICHAEL-reaction.[67] The group of HILVERT recently illustrated how an engineered carbo-ligase performs a MICHAEL-reaction.[68] Other approaches, i.e. catalytic antibodies, *de novo* designed enzymes, and artificial metalloenzymes, have also delivered biocatalysts that catalyze reactions not known from nature, but the description of these is beyond the scope of this thesis.

2.6.4 Hydrogen-mediated reductive aldolcyclizations

In 2002, the reductive generation of transition metal enolates using elemental hydrogen as terminal reductant was published by KRISCHE and co-workers. The generated transition metal enolates were trapped by an intramolecular or exogenous electrophile, enabling C-C bond formation.[69] The catalytic hydrogenation of enones and enals in the presence of an electrophile **17** results either in the formation of an aldol product **18** or in the formation of a simple 1,4-reduction product **19** (Scheme 19).[69]

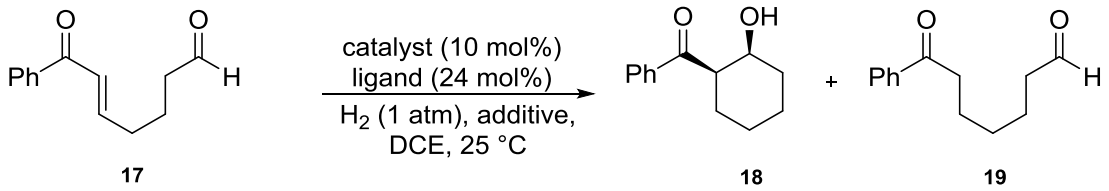

Scheme 19: Catalytic hydrogenation to yield the product of aldolization **18** or the 1,4-reduction product **19**.

It was shown by the group of KRISCHE that catalytic hydrogenation with the neutral rhodium complex [$Rh(PPh_3)_3Cl$] (WILKINSON-catalyst) led to 1,4-reduction products and only to trace quantities of the aldol product (Table 2, Entry 1). It was observed that by the use of Rh catalysts with a more cationic character [$Rh^I(COD)_2OTf$], a nearly equal yield of 1,4-reduction product **19** and aldol product **18** was obtained (Table 2, Entry 2). By the addition of substoichiometric amounts of KOAc, which serves as a mild basic additive, the formation of the aldol product **18** is increased and the 1,4-reduction product **19** is almost completely suppressed (Table 2, Entry 5).[70]

Table 2: Reaction optimization of aldolization products **18**. Data taken from [70].

Entry	Catalyst	Ligand	Additive (mol%)	Yield aldol (*syn/anti*)	Yield 1,4-reduction
1	$Rh(PPh_3)_3Cl$	-	-	1 % (99:1)	95 %
2	$Rh(COD)_2OTf$	Ph_3P	-	21 % (99:1)	25 %
3	$Rh(COD)_2OTf$	Ph_3P	KOAc (30 %)	59 % (58:1)	21 %
4	$Rh(COD)_2OTf$	$(p\text{-}F_3CC_6H_4)_3P$	-	57 % (14:1)	22 %
5	$Rh(COD)_2OTf$	$(p\text{-}F_3CC_6H_4)_3P$	KOAc (30 %)	89 % (10:1)	0.1 %

This effect shows that upon the application of a basic additive, the catalytic cycle switches from a di-hydride catalytic cycle to a mono-hydride catalytic cycle (Scheme 20) as it was postulated by SCHROCK and OSBORN. In the di-hydride catalytic cycle [$LnXRh^{III}(H)_2$] complex is responsible for the 1,4-reduction of the substrate. In the mono-hydride catalytic

cycle, the [LnXRh^{III}(H)$_2$] complex gets deprotonated by KOAc yielding a Rh^{I}-complex, which delivers a hydride to the β-carbon of the substrate and forms an enolate complex. Then the enolate gets trapped by the internal electrophile and upon binding of H_2, the product gets released from the catalytic cycle (Scheme 20).[71-73]

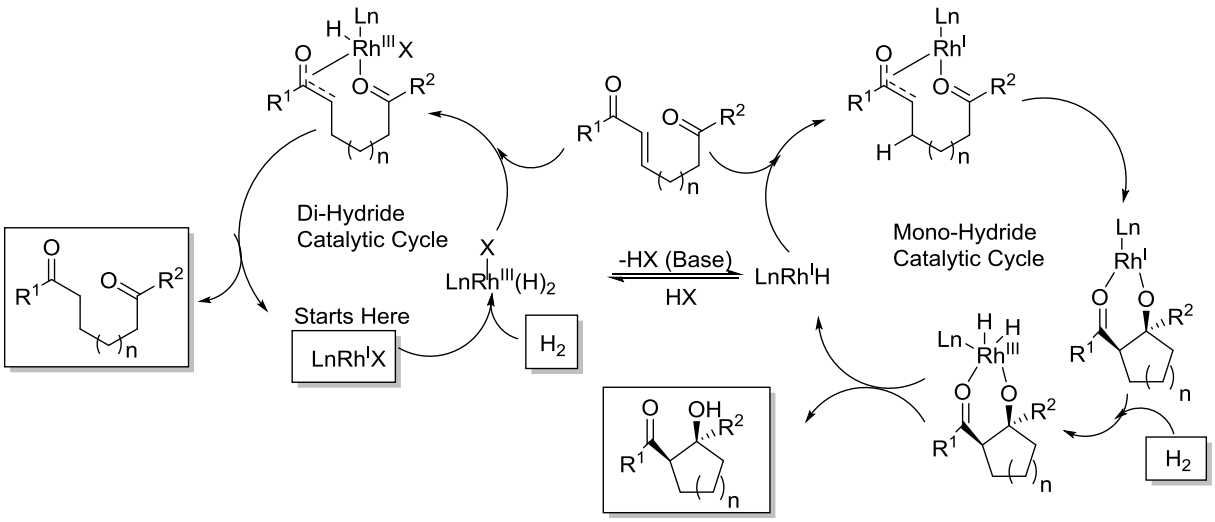

Scheme 20. Use of elemental hydrogen as terminal reductant for catalytic aldol cycloreductions. Picture adapted from [74].

In 2003 KRISCHE probed the viability of ketones as electrophilic partners for trapping the metal enolate. Various keto-enones and dione-enones successfully formed 5- and 6-membered ring products with excellent de's (>95).[75] A few months later the group of KRISCHE illustrated the reductive aldolcyclization using Rh(I) with arylboronic acids, water and various phosphine ligands. As substrates various aromatic and aliphatic mono-enone-mono-ketones were used.[76] In 2004 the catalytic hydrogenation-aldolization of enals was reported, which yielded various bicyclic products.[77] Earlier literature by the group of KRISCHE describes the use of cobalt-complexes (Co(dpm)$_2$) and $PhSiH_3$ as the reductant for the reductive aldolization.[78,79]

3 Aim of Work

Ene-reductases perform the reduction of the activated C=C double bond in α,β-unsaturated carbonyl compounds. The reduction of the electron-deficient double bond takes place through the transfer of a hydride, derived from a reduced flavin cofactor ($FMNH_2$), to the β-carbon of an α,β-unsaturated carbonyl compound. Upon the addition of the hydride, an enolate intermediate is formed. In the next step, a proton derived from a conserved Tyr-residue, is added from the opposite site to the α-carbon of the substrate (Scheme 21). In this valuable transformation two stereogenic centers are formed in one step.[19,20,26,27]

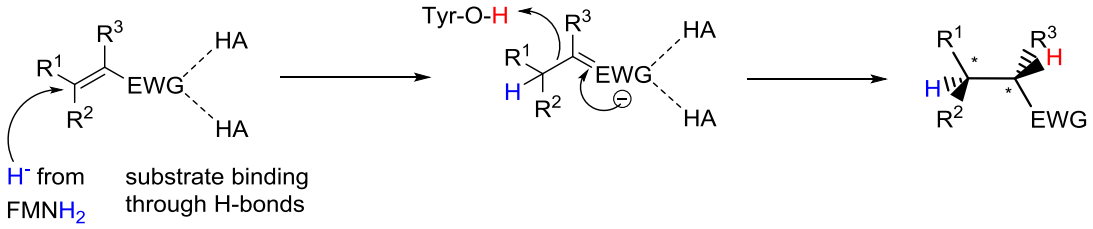

Scheme 21: Hydride and proton transfer in the reduction of α,β-unsaturated carbonyl compounds catalyzed by ene-reductases.

Groups which are able to activate the double bond are ketones, aldehydes, nitro groups, esters, and carboxylic acids. A pair of residues, typically His/His, Asn/His, or Asn/Asn, act as H-bonding donors to the electron withdrawing group further activating the double bond.[20,26]

We envision that one can engineer this enzyme class for reductive carbocyclizations by offering substrates which exhibit an internal electrophile and can react intramolecularly with the generated enolate to produce cyclized products. Alkylhalides could function as such an internal electrophile. The reaction should follow the proposed mechanism shown in Scheme 22. The FMN-hydride should attack at the C-β atom but the reprotonation step should be prevented. Instead of the reprotonation step (Scheme 22, red arrow) the enolate should alternatively attack the internal electrophile which would lead to a cyclization product (Scheme 22, blue arrow). We hypothesize that the reactive Tyr-residue in ene-reductases, which is responsible for the reprotonation of C-α, could be exchanged against an amino acid which cannot act as a proton donor to disable the reprotonation step (i.e.: Phe).

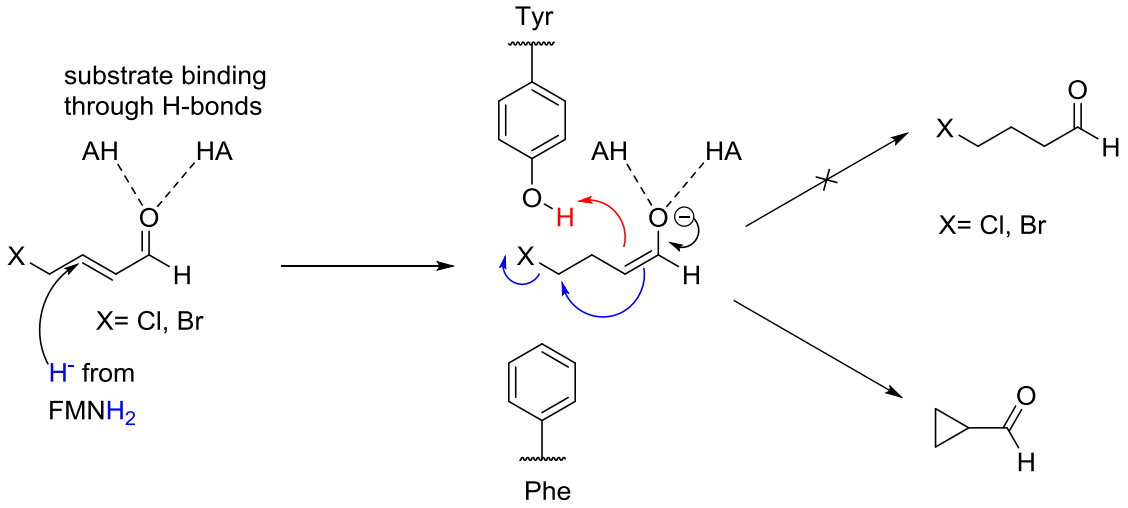

Scheme 22: Proposed mechanism for the reductive cyclization using engineered ene-reductases. Blue arrows indicate the reductive cyclization pathway, red arrows indicate the natural reduction pathway of ene-reductases.

One of the main aims of this thesis was to find variants from two different ene-reductases, namely Opr3 and YqjM, which would be able to perform a reductive carbocyclization reaction. The variants should be obtained by single site directed mutagenesis. Since we wanted to avoid any side reactions which are known from whole cell systems, we decided to use purified enzymes. Additionally we wanted to express and purify the wild type enzymes of Opr3 and YqjM. Another aim of this thesis was to synthesize a range of different α,β-unsaturated aldehydes, ketones, and esters bearing a halogen in γ-position (Scheme 23). We wanted to investigate the scope and limitations of this reaction concerning the EWG-moiety present in α,β-unsaturated substrates (compounds **20**-**23**). The influence of the leaving group on the reductive cyclization reaction by comparing substrates with different leaving groups (compounds **20** and **24**, **25** and **26**, **27** and **28**, **29** and **30**, **31** and **32**) should also be investigated. Moreover, we wanted to explore if a substituent at the α- or β-position of the double bond is accepted by ene-reductases and how this substitution pattern is influencing the reductive cyclization (compounds **25**-**34**).

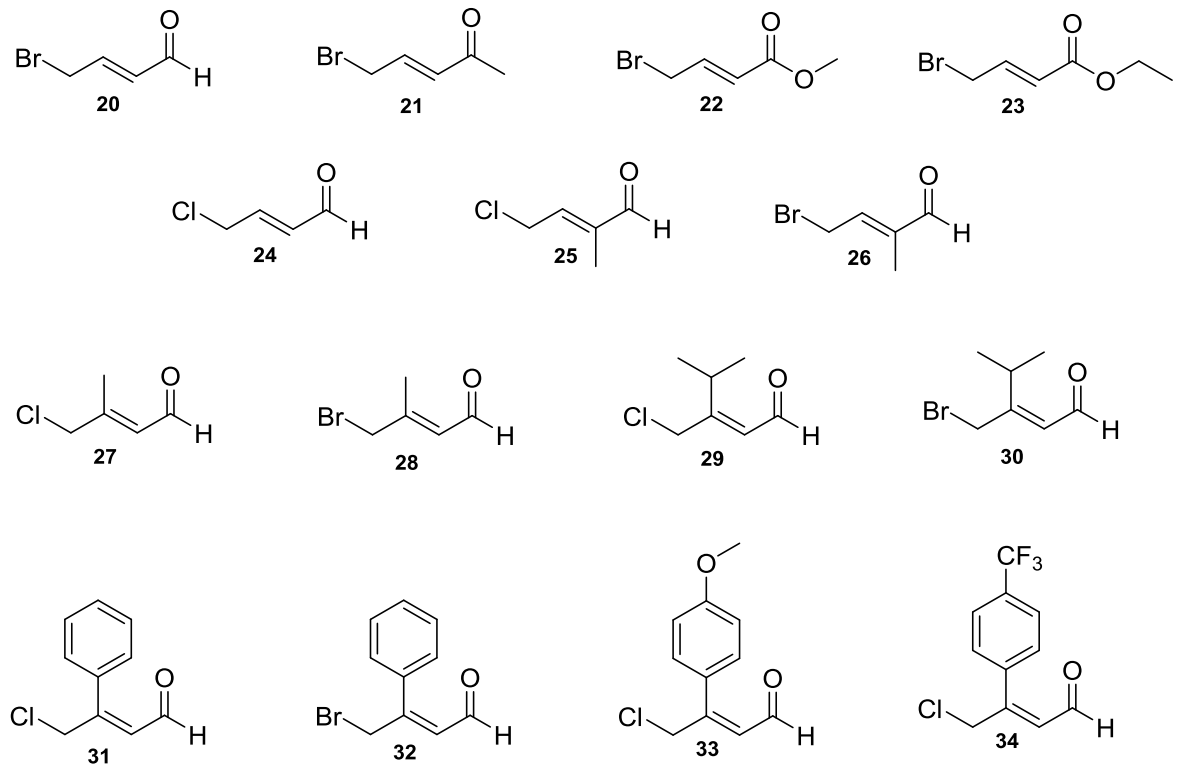

Scheme 23: Substrates for reductive cyclization experiments with ene-reductase variants.

Since ene-reductases display a strong stereoinduction in their natural reduction reaction it would be interesting to examine their capability of performing stereoselective reductive carbocyclizations.[23,39] Upon the conversion of substrates bearing a substituent at the β-position of the double bond (compounds **27**-**34**) a cyclopropane with two stereogenic centers could be formed (Scheme 24).

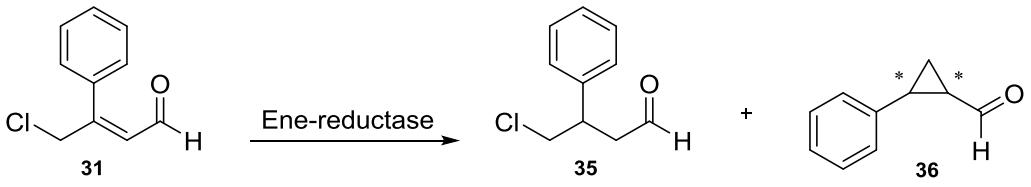

Scheme 24: Conversion of substrate **31** by ene-reductase variants.

4 Results and Discussion

4.1 Substrate scope

In preliminary studies by HECKENBICHLER the formation of five and six-membered ring systems via the ene-reductase enabled carbocycliaztaion had been inverstigated. Unfortunately, the formation of a five and six-membered ring was not observed.[95] During the MSc-thesis of Anna SCHWEIGER complex substrates for the formation of five-membered rings were synthesized. The ring closure reaction should be facilitated by alteration of the conformational angle (THORPE-INGOLD-effect), or by the restriction of the molecules flexibility through the attachment to a ring system.[80,81] However, the formation of a five-membered ring by the ene-reductase enabled carbocyclization could not be accomplished yet.

The substrate scope in this thesis focuses on the formation of three-membered ring systems. For the investigation of the ene-reductase enabled reductive carbocyclization we envisioned to synthesize a broad range of diverse substrates to gain insight into this new biocatalytic transformation. First of all we wanted to investigate the scope and limitations of this interesting reaction concerning the EWG-moiety present in α,β-unsaturated MICHAEL-acceptors. α,β-Unsaturated aldehydes and ketones are known substrates of ene-reductases, the reduction of the double bond occurs quickly and in a clean fashion.[82-85] In contrast, the reduction of α,β-unsaturated esters by ene-reductases proceeds very slowly.[86,87] Scheme 25 illustrates substrates with different electron-withdrawing groups as MICHAEL-acceptors and their expected cyclization products.

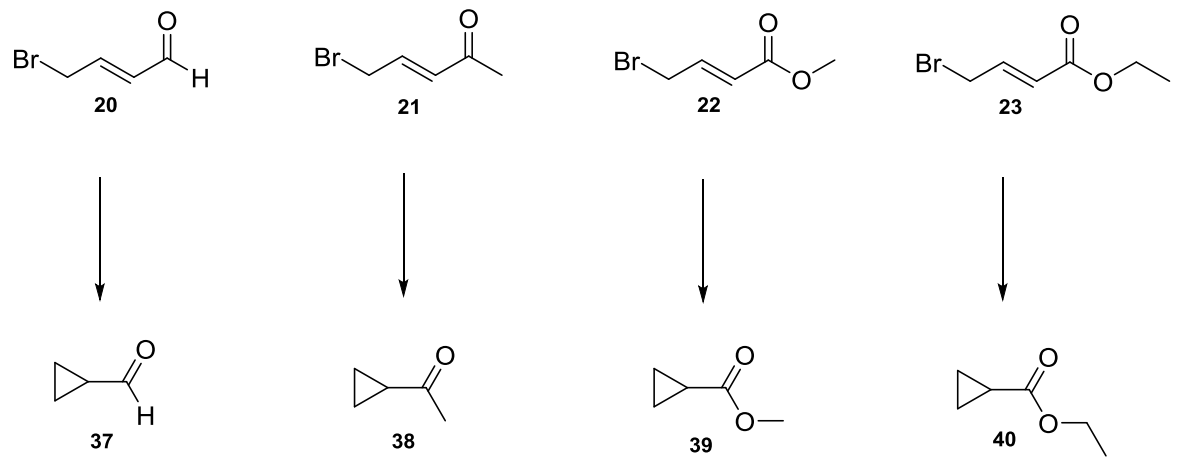

Scheme 25: Diverse set of MICHAEL-acceptors in substrates **20**-**23** and expected cyclization products **37**-**40**.

Next, we wanted to investigate the influence of the electrophilicity of the γ-carbon on the reductive cyclization reaction. Therefore allylic chlorides and bromides were synthesized and their ring formation activities were compared (Scheme 26). We expected that the substrate which carries bromine as leaving group might give better conversions to a cyclic product since the bromine renders the γ-carbon more electrophilic than the chlorine does.

Scheme 26: Influence of the electrophilicity of the γ-carbon in substrates **20** and **24**.

As ene-reductases do tolerate substitution at the double bond in the α-position, we were interested how the substitution in α-position is influencing the ene-reductase enabled reductive carbocyclization.[39] Scheme 27 displays substrates bearing a methyl-substituent at C-α and their expected cyclization products.

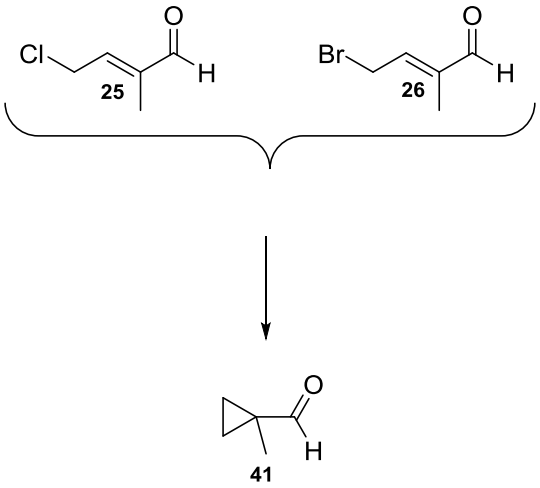

Scheme 27: Substrates **25** and **26** bearing an α-methyl-substituent and their expect cyclization product **41**.

Even more interesting is the conversion of substrates with a β-substitutent at the double bond since the ene-reductase enabled carbocyclization would lead to the formation of a cyclopropane with two newly established stereogenic centers. As ene-reductases are known to possess a strong stereoinduction in their natural reduction reaction it would be interesting to examine their capability of performing stereoselective reductive carbocyclizations.[23,39] Scheme 28 displays substrates bearing a β-methyl-substituent and their expected cyclization product.

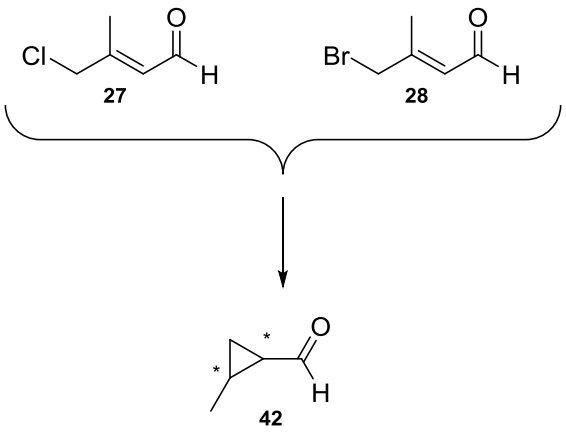

Scheme 28: Substrates **27** and **28** bearing a β-methyl-substituent and expected cyclization product **42**.

Moreover, we wanted to investigate if ene-reductases accept substrates with sterically more demanding substituents at C-β and whether the enantioselectivities and diastereoselectivities of the cyclopropane products can be influenced by steric effects. Scheme 29 illustrates substrates bearing an isopropyl- or phenyl-substituent at C-β.

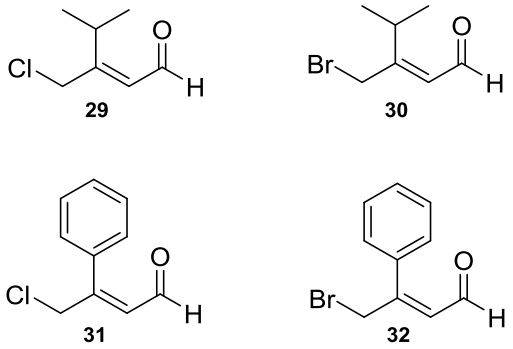

Scheme 29: Substrates with sterically demanding β-substituents.

Besides the investigation of the influence of steric effects on the substrate, we decided to include inductive and resonance effects as well. Two substrates, one bearing an electron-rich β-phenyl-substituent and the other one bearing an electron-deficient β-phenyl-substituent, were synthesized and tested as substrates for ene-reductases (Scheme 30).

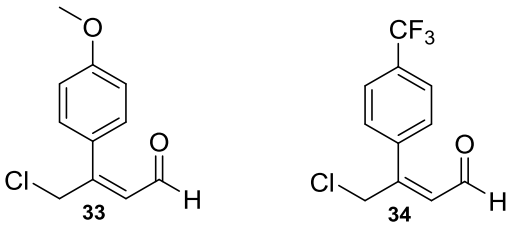

Scheme 30: Substrates bearing either electron-deficient or electron-rich β-phenyl-substituents.

4.2 Synthesis of compounds

4.2.1 Synthesis of (*E*)-4-bromobut-2-enal (20) and reference compounds

(*E*)-4-Bromobut-2-enal (**20**) was synthesized in two steps according to the sequence shown in Scheme 31.

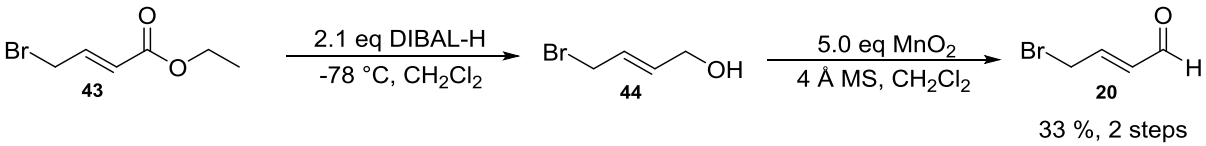

Scheme 31: Synthesis of (*E*)-4-bromobut-2-enal (**20**).

Commercially available ethyl 4-bromocrotonate (**43**) (technical grade, 75 %) was purified via flash chromatography prior to use. The ester moiety was then reduced using 2.1 eq DIBAL-H at -78 °C, as TLC indicated complete consumption of starting materials (10 min) the reaction solution was quenched at -78 °C using excess Rochelle salt solution. The work up procedure proved to be challenging since it was crucial to maintain the temperature at -78 °C during quenching, otherwise allylic alcohol **44** decomposed upon the exothermic release of heat. After quenching with excess Rochelle salt solution, a cloudy emulsion formed and the formation of two clear phases needed several hours of vigorous stirring at 22 °C. When the reaction mixture was quenched at -78° C using excess 1 M aq. HCl the phase separation occurred within 1 h of stirring and was therefore the preferred method. In this step it was not possible to evaporate the solvent since upon evaporation decomposition of allylic alcohol **44** occurred. Therefore, the organic phase was dried over Na_2SO_4 and used subsequently in the next reaction step in which the alcohol was oxidized by allylic oxidation using activated MnO_2. To avoid overoxidation to the carboxylic acid upon formation of the aldehyde hydrate (see Scheme 32) 4 Å molecular sieves were added to the reaction solution.

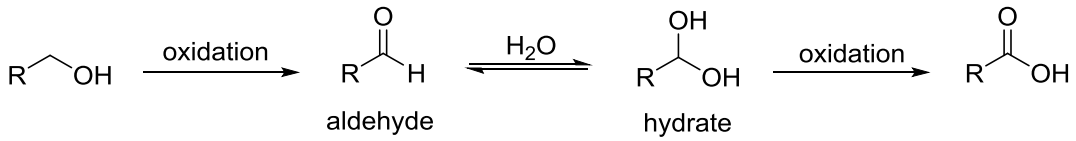

Scheme 32: Overoxidation of aldehyde to the carboxylic acid via the aldehyde hydrate.

After full conversion of starting material was detected, MnO_2 was removed via filtration through a pad of silica and the solvent had to be evaporated very carefully at 35 °C bath temperature. Substrate **20** was obtained in a rather low yield of 33 %, which might be due to the high volatility of compound **20**.

The reduction of 4-bromocrotonate with DIBAL-H and the subsequent allylic oxidation with MnO_2 had to be performed under the complete exclusion of light. (*E*)-4-bromobut-2-enal (**20**) was stored under a slight stream of N_2, in a flask covered by aluminum foil and had to be used immediately in the biocatalytic experiments. The biocatalytic experiments had to be performed under the exclusion of light as well.

When substrate **20** is converted by ene-reductases the formation of two products can be expected, as shown in Scheme 33.

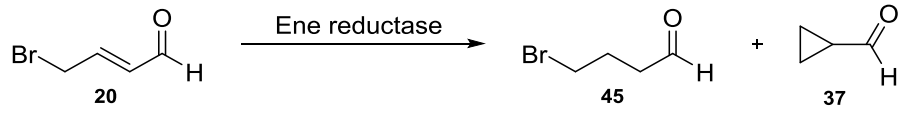

Scheme 33: Conversion of substrate **20** by ene-reductases.

Besides the formation of the desired cyclopropanecarbaldehyde **37** it could be possible, that the product of the natural ene-reductase reaction, compound **45**, is formed. Therefore, 4-bromobutanal was synthesized as a reference compound (Scheme 34).

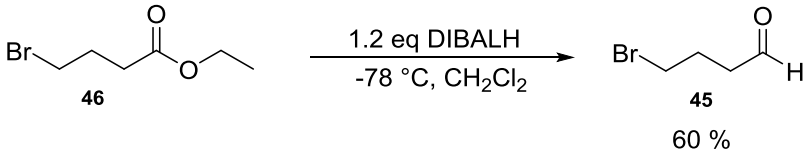

Scheme 34: Synthesis of 4-bromobutanal (**45**).

Starting from commercially available ethyl 4-bromobutanoate (**46**) compound **45** was synthesized in one step according to a procedure by BROWN *et al.*[112] It was possible to reduce the ester directly to the aldehyde using DIBAL-H by taking care to maintain the reaction temperature at -78 °C. After the formation of a LEWIS acid-base complex DIBAL-H reduces the carbonyl compound via a tetrahedral intermediate, which is stable at -78 °C, until it collapses upon aqueous work up to the aldehyde and further reduction is not possible (see Scheme 35).

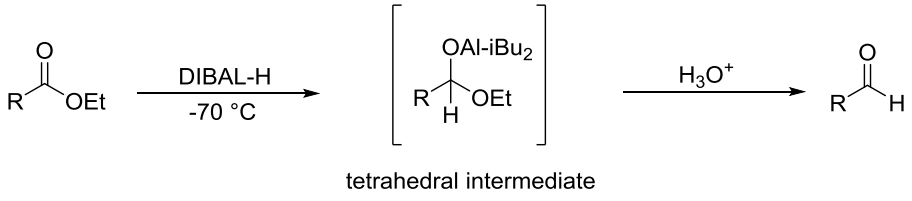

Scheme 35: Reduction of an ester to the corresponding aldehyde via the tetrahedral intermediate.

After aqueous work up 4-bromobutanal (**45**) was isolated in 60 % yield.

4.2.2 Synthesis of (*E*)-5-bromopent-3-en-2-one (21) and reference compounds

The intended synthesis route to (*E*)-5-bromopent-3-en-2-one (**21**) is shown in Scheme 36. The synthesis of allylic alcohol **49** via a WITTIG-reaction between 1,4-dioxane-2,5-diol (**47**) and WITTIG-ylen **48** was not possible. The reaction mixture was stirred under reflux for several days, nevertheless a conversion of the starting material was not observed and this synthesis was abandoned.

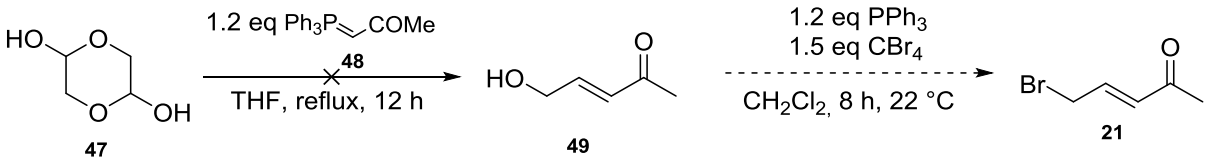

Scheme 36: Intended synthesis route to (*E*)-5-bromopent-3-en-2-one (**21**).

Scheme 37 shows an alternative synthesis of compound **21**. According to a procedure by LI *et al,* 2-bromo-1,1-diethoxyethane (**50**) was deprotected using 20.0 eq of trifluoroacetic acid.[88] After aqueous work up and extraction with CH_2Cl_2, the solvent was carefully evaporated under reduced pressure (35 °C bath temperature, 650 mbar). A GC-FID sample from the receiving flask indicated that 2-bromoacetaldehyde (**51**) was unfortunately co-evaporated. The content of the receiving flask and the round bottom flask were combined and subsequently used in the WITTIG-reaction with WITTIG-ylen **48**. After flash chromatography compound **21** was isolated in only 11 % yield. During ^{1}H-NMR experiments a vicinal coupling constant of $^3J_{HH}$ = 15.7 Hz was observed. This refers to an angle of 180° between the olefinic protons, thus the double bond was assigned as (*E*)-configurated.

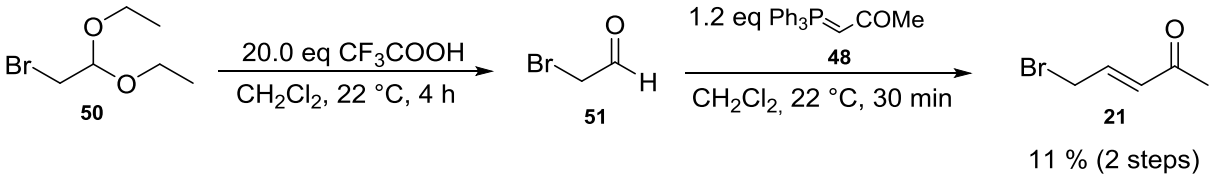

Scheme 37: Synthesis of (*E*)-5-bromopent-3-en-2-one (**21**).

For the conversion of (*E*)-5-bromopent-3-en-2-one (**21**) with ene-reductases we expected the formation of two different products (see Scheme 38). Besides the product of reductive cyclization 1-cyclopropylethan-1-one (**38**), the undesired byproduct 5-bromopentan-2-one (**52**), which is the result of the natural ene-reductase pathway, could be formed to some extent.

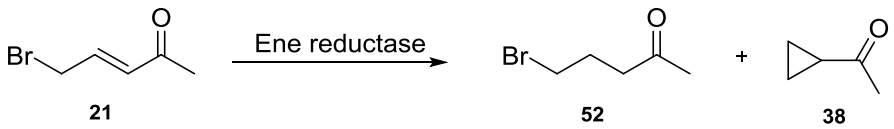

Scheme 38: Conversion of substrate **21** by ene-reductases.

5-Bromopentan-2-one (**52**) was synthesized in one step starting from 3-acetyldihydrofuran-2(3*H*)-one (**53**), as it is shown in Scheme 39, to assign GC-FID retention times with this reference compound.

Scheme 39: Synthesis of 5-bromopentan-2-one (**52**).

Following a procedure by MILLER *et al* lactone **53** was cleaved by 1.5 eq HBr and after flash chromatography compound **52** was isolated in 52 % yield.[114]

4.2.3 Synthesis of (*E*)-4-chlorobut-2-enal (24) and reference compounds

(*E*)-4-Chlorobut-2-enal (**24**) was synthesized in four steps starting from 1,4-dioxane-2,5-diol (**47**) according to the sequence shown in Scheme 40.

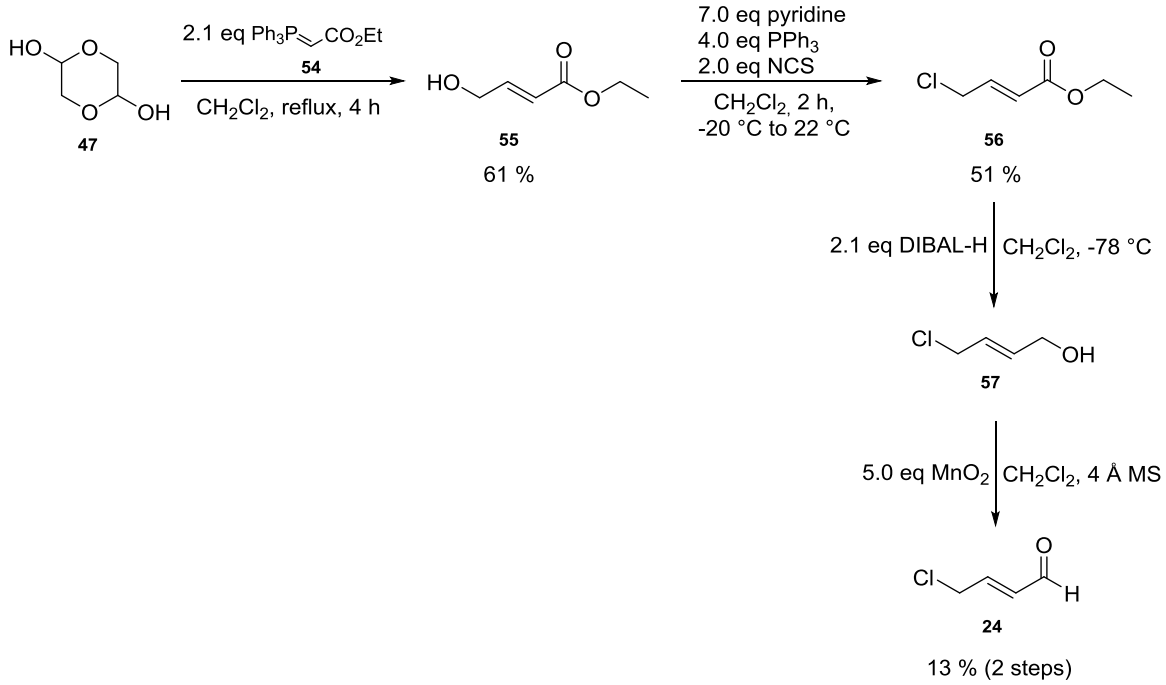

Scheme 40: Synthesis of (*E*)-4-chlorobut-2-enal (**24**).

Synthesis of compound **55** followed a slightly modified procedure by Sadhukhan *et al.*[99] A simple WITTIG-reaction was performed by the addition of an already deprotonated WITTIG-ylen **54** to a solution of commercially available 1,4-dioxane-2,5-diol (**47**) in CH_2Cl_2. Purification via flash chromatography furnished allylic alcohol **55** in a moderate yield of 61 %. In the next reaction step the hydroxyl function was substituted against chlorine in an APPEL-reaction. *N*-Chlorosuccinimide had to be added as a solid since it exhibits only poor solubility in CH_2Cl_2. It turned out to be crucial for this reaction to maintain the reaction temperature at -20 °C until the portionwise addition of solid *N*-chlorosuccinimide was completed. The work up of the APPEL-reaction turned out to be difficult, since after quenching the reaction mixture by addition of 5 % aqueous HCl, a phase separation was only achieved, when centrifugation was used. After the aqueous phase was separated, the organic phase was washed with 10 w% $CuSO_4$-solution to remove excess pyridine. For purification of allylic chloride **56** it is mandatory to apply flash chromatography with a 100-fold excess of SiO_2 in order to guarantee separation of excess triphenylphosphine and triphenylphosphine oxide. Compound **56** was isolated in a moderate yield of 51 %. The vicinal coupling constant $^3J_{HH}$ of 15.4 Hz, which was observed during ^{1}H-NMR experiments, corresponds to an angle of 180°

between the protons of the olefin, which supports the assumption that the (*E*)-isomer was isolated. In the last reaction sequence the ester was first reduced to the corresponding allylic alcohol **57** and then oxidized in a subsequent reaction using activated MnO_2. After MnO_2 was removed through filtration through a pad of silica, the allylic aldehyde **24** was obtained in very low yield of 13 %. The last two reaction steps had to be performed under the complete exclusion of light. (*E*)-4-Chlorobut-2-enal (**24**) was stored under a slight stream of N_2, in a flask covered by aluminum foil and had to be used immediately in the biocatalytic experiments.

When substrate **24** is converted with ene-reductases and variants it might be possible, that besides the formation of cyclopropanecarbaldehyde **37**, the product of the natural reduction reaction, compound **58**, is formed (see Scheme 41).

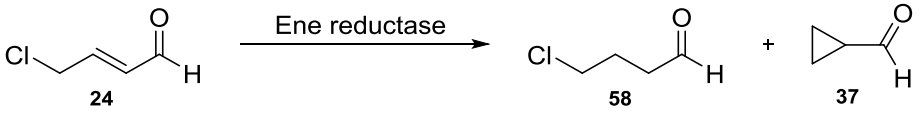

Scheme 41: Conversion of substrate **24** by ene-reductases.

Compound **58** was synthesized as shown in Scheme 42. Staring from commercially available 4-chloro-1-butanol (**59**), oxidation was executed with 1.5 eq PCC. PCC was removed via filtration through a pad of silica and 4-chlorobutanal (**58**) was isolated in 66 % yield.

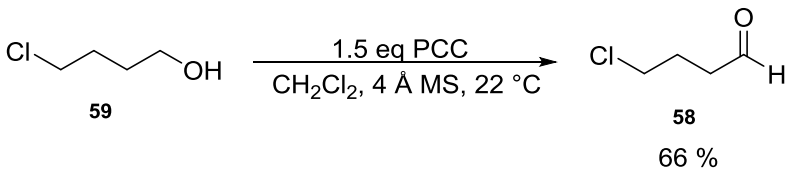

Scheme 42: Synthesis of 4-chlorobutanal (**58**).

4.2.4 Synthesis of (*E*)-4-chloro-2-methylbut-2-enal (25) and reference compounds

(*E*)-4-Chloro-2-methylbut-2-enal (**25**) was synthesized in 4 steps according to the synthesis route depicted in Scheme 43.

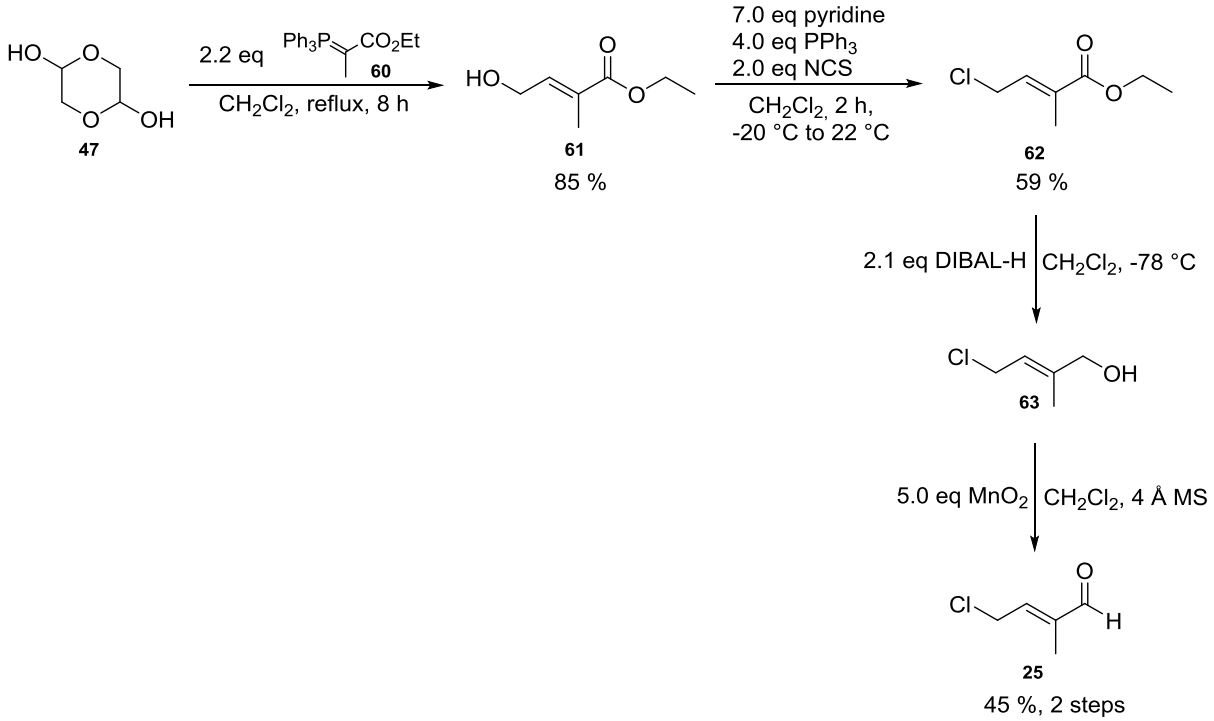

Scheme 43: Synthesis of (*E*)-4-chloro-2-methylbut-2-enal (**25**).

Following the WITTIG-reaction described in 4.2.3 1,4-dioxane-2,5-diol (**47**) was converted with WITTIG-ylen **60**. The allylic alcohol **61** was furnished in very good yield of 85 % and in the subsequent reaction step, the hydroxyl function was substituted against chlorine in order to create a much more electrophilic γ-carbon. The (*E*)-configuration of the allylic chloride **62** was determined via the observation of an NOE-Effect between protons of the methylene group at C-α and protons at C-γ which indicates that these protons are located at the same side of the double bond. The last two steps in this synthesis sequence, reduction of the ester to the alcohol **63** and subsequent allylic oxidation to (*E*)-4-chloro-2-methylbut-2-enal (**25**), were performed under the exclusion of light since otherwise an isomerization of the double bond was observed. (*E*)-4-Chloro-2-methylbut-2-enal (**25**) was obtained in a yield of 45 % over 2 steps. The last two reaction steps had to be performed under the complete exclusion of light. Compound **25** was stored under a slight stream of N_2, in a flask covered by aluminum foil and had to be used immediately in the biocatalytic experiments.

When substrate **25** is converted by ene-reductases, we hypothesized that the formation of two different products is imaginable. 4-Chloro-2-methylbutanal (**64**) is the product of the natural

reduction reaction and 1-methylcyclopropane-1-carbaldehyde (**41**) is the desired product of the C-C bond formation (Scheme 44).

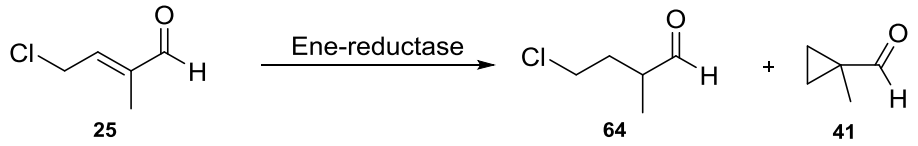

Scheme 44: Conversion of substrate **25** by ene-reductases.

Scheme 45 illustrates the synthesis of 4-chloro-2-methylbutanal (**64**) starting from compound **61**. The double bond in allylic alcohol **61** was reduced following a procedure by BRENNA *et al.*[89] The formation of a byproduct was observed, which we speculated to result from lactonization. However, we did not isolate the byproduct and performed the APPEL-reaction to compound **66** subsequently. In the last two steps, the ester of **66** was reduced to alcohol **67**, which was subsequently oxidized using 1.5 eq PCC. 4-Chloro-2-methylbutanal (**64**) was obtained in a very low yield of 7 %.

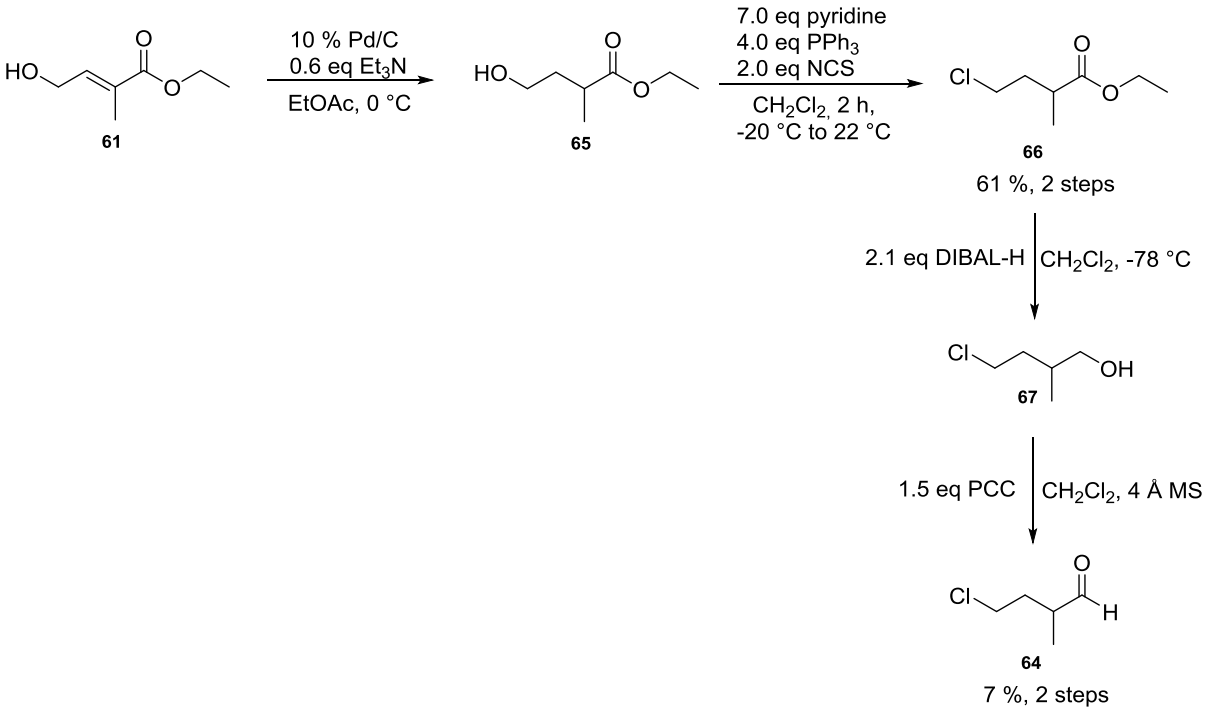

Scheme 45: Synthesis of 4-chloro-2-methylbutanal (**64**).

Staring from commercially available (1-methylcyclopropyl)methanol (**68**), 1-methylcyclopropane-1-carbaldehyde (**41**) was synthesized in one step, as depicted in Scheme 46. Oxidation of the primary alcohol afforded compound **41** in only 25 % yield, which might be due to the high volatility of this compound.

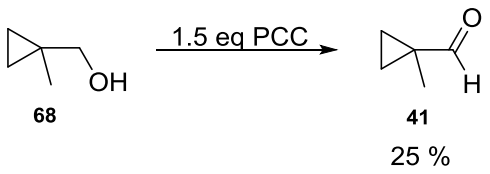

68 **41**

25 %

Scheme 46: Synthesis of 1-methylcyclopropane-1-carbaldehyde (**41**).

4.2.5 Synthesis of (*E*)-4-bromo-2-methylbut-2-enal (26)

(*E*)-4-Bromo-2-methylbut-2-enal (**26**) was synthesized in 3 steps starting from compound **61** as shown in Scheme 47.

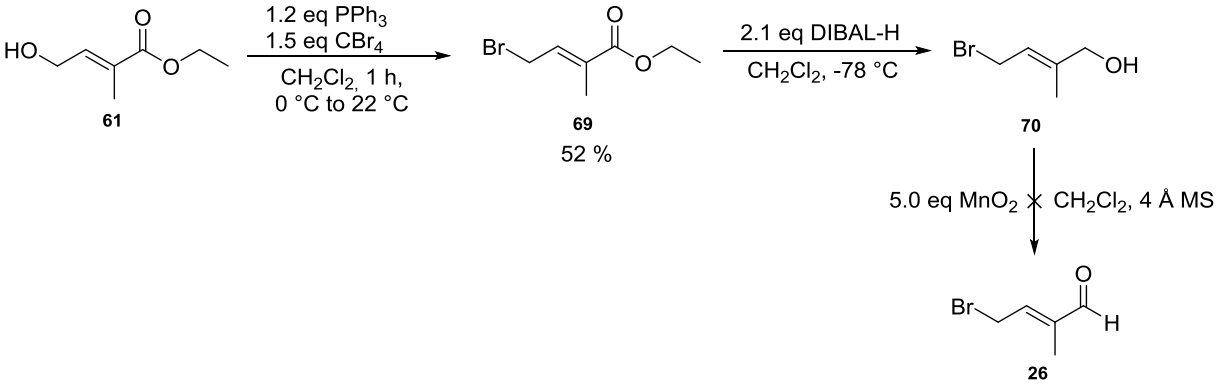

Scheme 47: Synthesis of (*E*)-4-bromo-2-methylbut-2-enal (**26**).

An APPEL-reaction furnished allylic bromide **69** in 52 % yield. By the observation of an NOE-effect between protons of the methylene group at C-α and protons at C-γ, it is assumed that these protons are located at the same side of the double bond, indicating that compound **69** is (*E*)-configurated. In the next step, the ester moiety was reduced using 2.1 eq of DIBAL-H and further oxidized to the corresponding aldehyde **26** using 5.0 eq activated MnO_2. Although this synthesis sequence was performed under the exclusion of light it was not possible to isolate compound (*E*)-4-bromo-2-methylbut-2-enal (**26**). This experiment was repeated three times, in none of the experiments it was possible to conduct NMR-spectra which would indicate the presence of compound **26** due to the intrinsic instability of this compound.

4.2.6 Synthesis of (*E*)-4-chloro-3-methylbut-2-enal (27) and reference compounds

Scheme 48 displays the synthesis of (*E*)-4-chloro-3-methylbut-2-enal (**27**) in 3 steps.

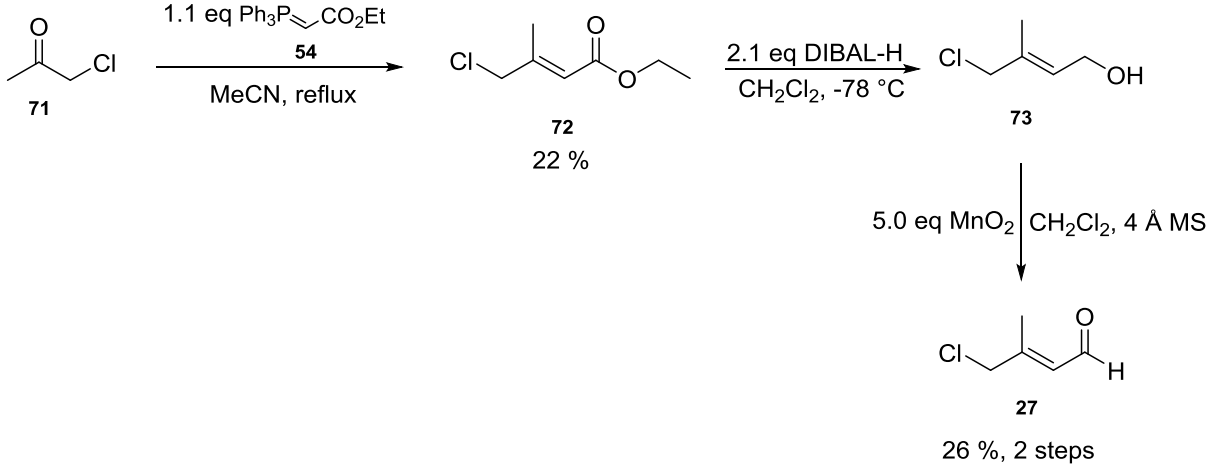

Scheme 48: Synthesis of (*E*)-4-chloro-3-methylbut-2-enal (**27**).

Starting from 1-chloropropan-2-one (**71**) a WITTIG-reaction was executed by the use of already deprotonated WITTIG-ylen **54**. Ethyl (*E*)-4-chloro-3-methylbut-2-enoate (**72**) was isolated in only 22 % yield, which might be due to the fact that we had to apply flash chromatography two times. After the first flash chromatography it was not possible to completely remove the (*Z*)-isomer of compound **72**, therefore, flash chromatography had to be applied a second time. NMR experiments showed an NOE-effect between the olefinic proton at C-α and protons at C-γ, which indicates that these protons are at the same side of the double bond, confirming the (*E*)-configuration of the isolated product. The last two steps were again a reduction of the ester moiety of compound **72** to the corresponding allylic alcohol **73** and susbsequent allylic oxidation using 5.0 eq MnO_2. (*E*)-4-Chloro-3-methylbut-2-enal (**27**) was isolated in 26 % yield. The last two reaction steps had to be performed under complete exclusion of light. Compound **27** was stored under a slight stream of N_2, in a flask covered by aluminum foil and had to be used immediately in the biocatalytic experiments.

As illustrated in Scheme 49, conversion of substrate **27** by ene-reductases can lead to the formation of a cyclopropane with two newly formed stereogenic centers **42**. We decided to analyze the chiral cyclopropanes as the corresponding alcohols **76**, since aldehydes exhibit only short time stability. It might also be possible that the unwanted natural reduction reaction is occurring. Additionally compound **74** had to be synthesized for reference purposes.

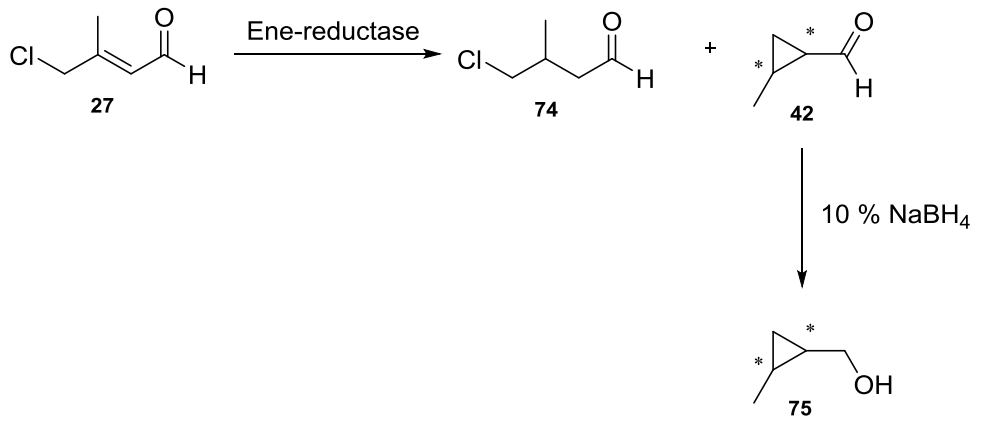

Scheme 49: Conversion of substrate **27** by ene-reductases.

For the determination of the diastereomeric excess and the enantiomeric excess, *cis*-**75** (*rac*) and *trans*-**75** (*rac*) were synthesized. The synthesis of racemic cyclopropane *cis*-**75** is displayed in Scheme 50.

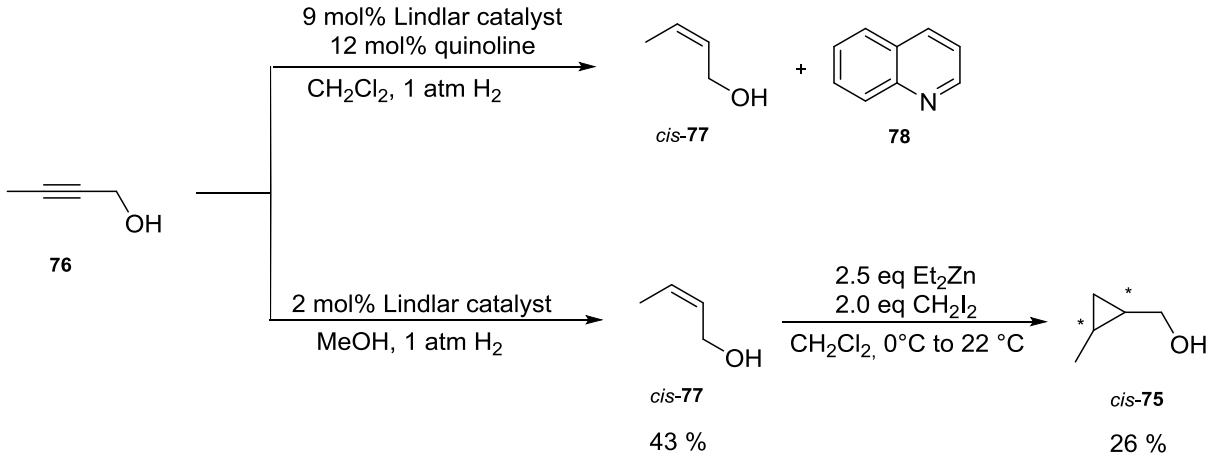

Scheme 50: Synthesis of racemic cyclopropane *cis*-**75**.

The hydrogenation of an alkyne to the corresponding *cis*-alkene is accomplished by the use of LINDLAR catalyst. The heterogeneous catalyst adds H_2 in a *syn*-fashion thus only the *cis*-alkene is formed. Starting from but-2-yn-1-ol (**76**) a procedure published by Fox *et al* was used.[90] The hydrogenation was accomplished by the use of 9 mol% LINDLAR catalyst and 12 mol% quinoline (**78**) as catalyst poison. After 48 h complete conversion of but-2-yn-1-ol (**76**) was detected via GC-FID, the catalyst was removed by filtration and the product was purified via distillation. Unfortunately, quinoline was still detected via GC-FID after distillation. We reasoned that by the use of a lower catalyst loading it would be possible to perform this hydrogenation without any catalyst poison. Following a procedure by WHITE *et al* but-2-yn-1-ol (**76**) was hydrogenated using 2 mol% LINDLAR catalyst in MeOH.[124] Within 5 d the starting material was consumed and the product was purified via distillation, which

finally furnished but-2-en-1-ol (*cis*-**77**) in 43 % yield. In the next step, a SIMMONS-SMITH reaction was used to perform a stereospecific cylopropanation reaction. Following a procedure by PIETRUSZKA *et al,* 2.5 eq Et_2Zn and 2.0 eq CH_2I_2 were used, but reaction conversion stopped at ~ 50 %.[118] This reaction was performed several times with increased amounts of Et_2Zn and CH_2I_2, however, this did not enhance the conversion of but-2-en-1-ol. Fortunately, it was possible to purify (2-methylcyclopropyl)methanol (*cis*-**75**) via flash chromatography. Diethylether and n-pentane were chosen as eluents for column chromatography to avoid product losses due to evaporation of high boiling solvents. (2-Methylcyclopropyl)methanol (*cis*-**75**) was obtained in a low yield of 26 %.

The synthesis of racemic (2-methylcyclopropyl)methanol (*trans*-**75**) is displayed in Scheme 51.

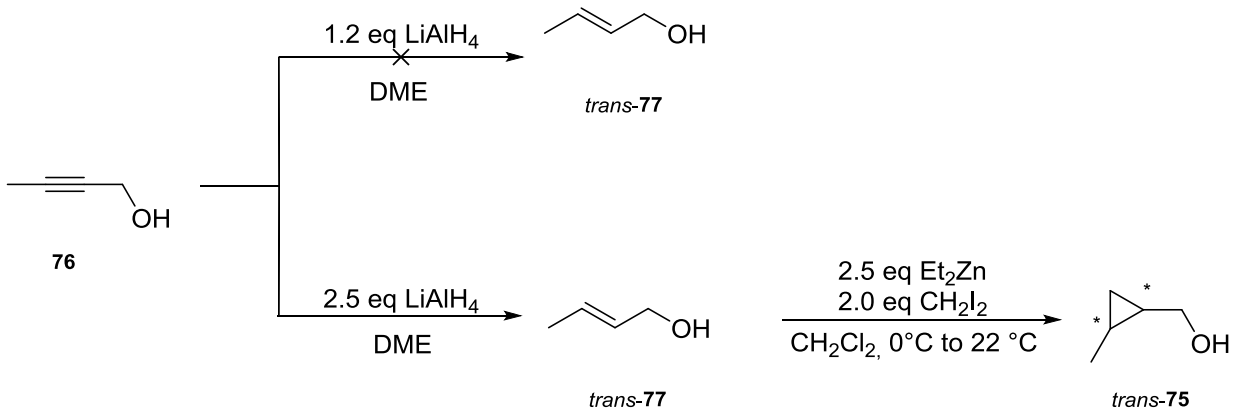

Scheme 51: Synthesis of racemic cyclopropane *trans*-**75**.

The reduction of an alkyne by $LiAlH_4$ delivers the corresponding *trans*-alkene. The complementary stereochemistry in this alkyne reduction is presumably achieved by the coordination of the hydroxyl group at aluminum and the formation of a cyclic intermediate followed by an intramolecular Al-H addition. Upon quenching with water the second hydrogen is added from the opposite side and the addition of [H_2] is overall *anti*. Following a procedure by FISTRUP *et al*, but-2-yn-1-ol (**76**) was reduced by 1.2 eq $LiAlH_4$ in 1,2-DME.[91] After the reaction conversion stopped at around 50 %, we decided to follow another procedure published by REHBEIN *et al* where 2.1 eq $LiAlH_4$ were used.[123] After complete consumption of but-2-yn-1-ol (**76**) within 8 h, the product was purified by distillation and (*E*)-but-2-en-1-ol (**77**) was obtained in a moderate yield of 62 %. Again the procedure by PIETRUSZKA *et al* was followed for the stereospecific cyclopropanation reaction and it was possible to furnish *trans* (2-methylcyclopropyl)methanol (*trans*-**75**) in 28 % yield.[118]

For the assignment of the absolute configuration, we decided to synthesize one single enantiomer of *cis*-(2-methylcyclopropyl)methanol and one single enantiomer of *trans*-(2-methylcyclopropyl)methanol (see Scheme 52).

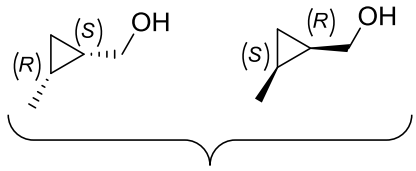

cis-(2-methylcyclopropyl)methanol

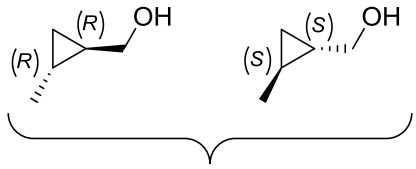

trans-(2-methylcyclopropyl)methanol

Scheme 52: Enantiomers and diastereomers of **75**.

The enantioselective cyclopropanation of (*E*)-but-2-en-1-ol (*trans*-**77**) and (*Z*)-but-2-en-1-ol (*cis*-**77**) has already been described. The chiral controller in this SIMMONS-SMITH reaction is a dioxaborolane ligand which is easily accessible in a one step synthesis (Scheme 53).[92] Starting from (2*S*,3*S*)-2,3-dihydroxy-N^1,N^1,N^4,N^4-tetramethylsuccinamide (-)-**79** and n-butylboronic acid (**80**), dioxaborolane ligand (4*S*,5*S*)-**81** was afforded in 97 % yield. The asymmetric SIMMONS-SMITH reaction was executed according to a procedure by CARNEIRO *et al* and ((1*S*,2*R*)-2-methylcyclopropyl)methanol (1*S*,2*R*)-**76** was obtained in 9 % yield and 78 % ee.[126]

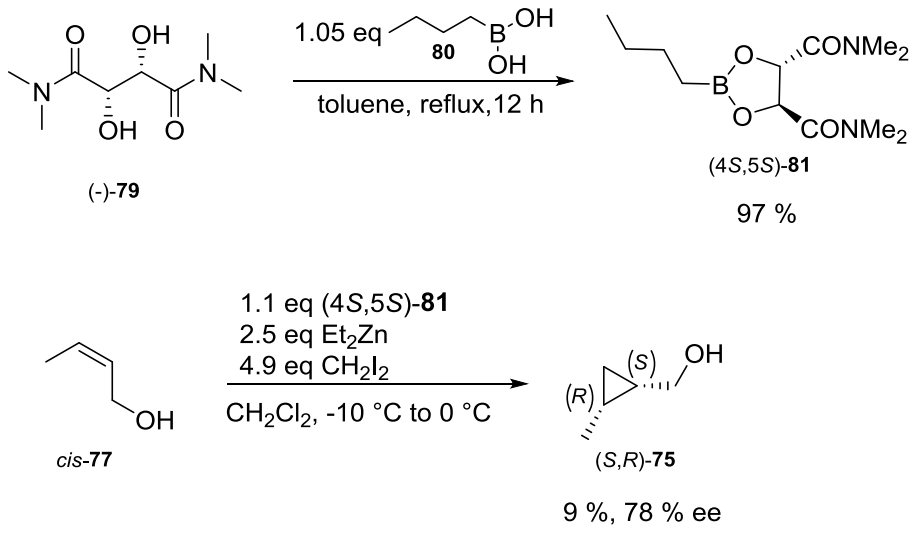

Scheme 53: Asymmetric synthesis of ((1*S*,2*R*)-2-methylcyclopropyl)methanol (*S*,*R*)-**75**.

(4*R*,5*R*)-2-Butyl-N^4,N^4,N^5,N^5-tetramethyl-1,3,2-dioxaborolane-4,5-dicarboxamide (4*R*,5*R*)-**81** was prepared as described above, starting from (+)-**79**, and was obtained in 94 % yield (Scheme 54). ((1*S*,2*S*)-2-Methylcyclopropyl)methanol (*S*,*S*)-**75** was prepared according to a procedure by WHITE *et al* and obtained in 38 % yield and 88 % ee.[124]

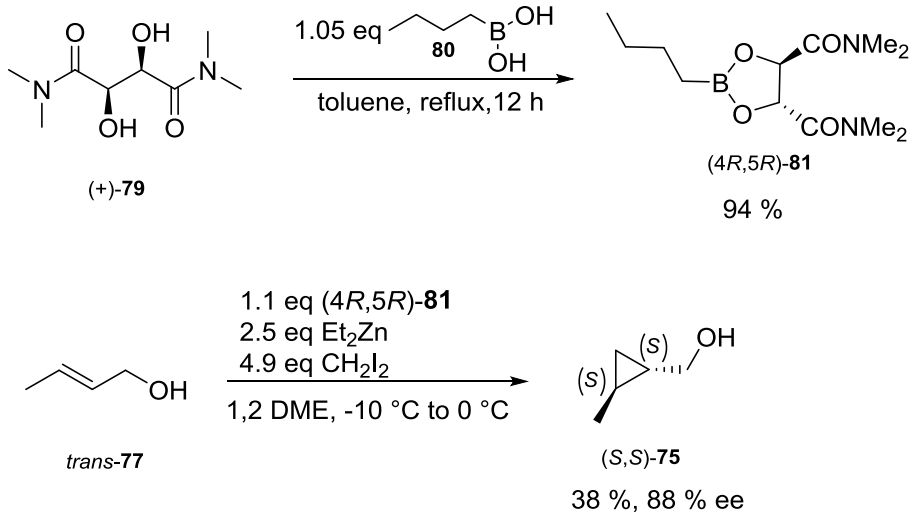

Scheme 54: Synthesis of ((1*S*,2*S*)-2-methylcyclopropyl)methanol (*S*,*S*)-**75**.

As mentioned earlier in this chapter compound **74**, the product of the natural ene-reductase reaction, was synthesized in five steps as depicted in Scheme 55. A WITTIG-reaction between deprotonated WITTIG-ylen **54** and 1-hydroxypropan-2-one (**82**) was executed which afforded compound **83** in 55 % yield. The last four reaction steps were performed as already discussed in chapter 4.2.4. 4-Chloro-3-methylbutanal (**74**) was obtained in 27 % yield over 5 steps.

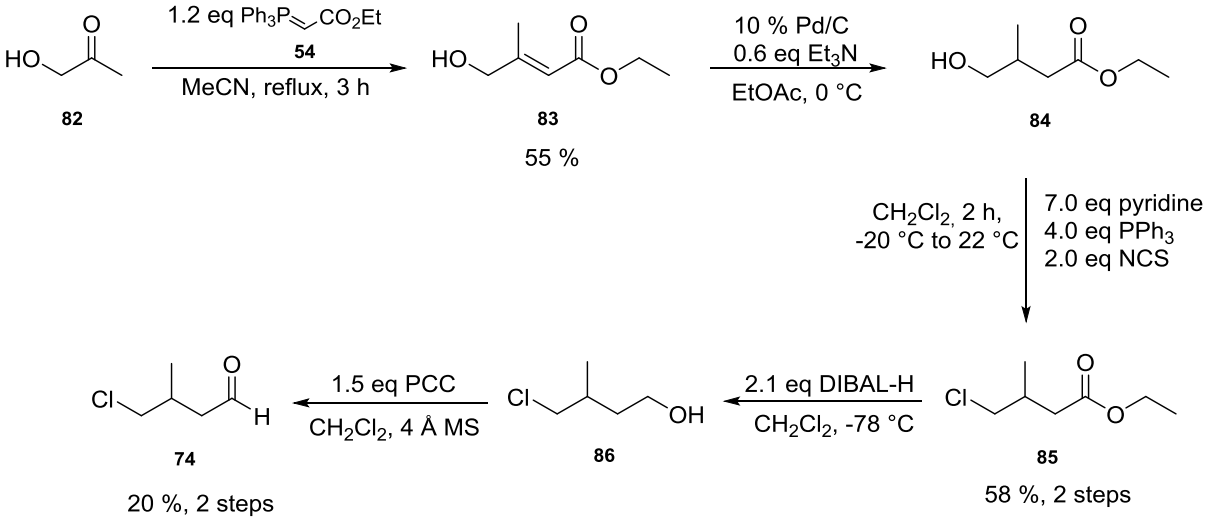

Scheme 55: Synthesis of 4-chloro-3-methylbutanal (**74**).

4.2.7 Synthesis of (*E*)-4-bromo-3-methylbut-2-enal (28) and reference compounds

The preparation of ethyl (*E*)-4-hydroxy-3-methylbut-2-enoate (**83**) has already been described in chapter 4.2.6. The hydroxyl function of **83** was substituted against bromine in an APPEL-reaction which allowed the formation of **87** in 51 % yield (see Scheme 56). The observation of an NOE-effect between the olefinic proton at C-α and protons at C-γ indicates that these protons are at the same side of the double bond confirming (*E*)-configuration. For the formation of (*E*)-4-bromo-3-methylbut-2-enal (**28**) the ester-functionality of **87** was reduced to the corresponding allylic alcohol **88** by 2.1 eq DIBAL-H. Allylic oxidation using 5.0 eq MnO_2 furnished (*E*)-4-bromo-3-methylbut-2-enal (**28**) in 34 % yield. The transformation of the ethyl (*E*)-4-bromo-3-methylbut-2-enoate (**87**) to the allylic aldehyde **28** proved to be challenging because of the light sensitivity of compound **28**. This experiment had to be performed under the complete exclusion of light. (*E*)-4-Bromo-3-methylbut-2-enal (**28**) was stored under a slight stream of N_2, in a flask covered by aluminum foil and had to be used immediately in the biocatalytic experiments.

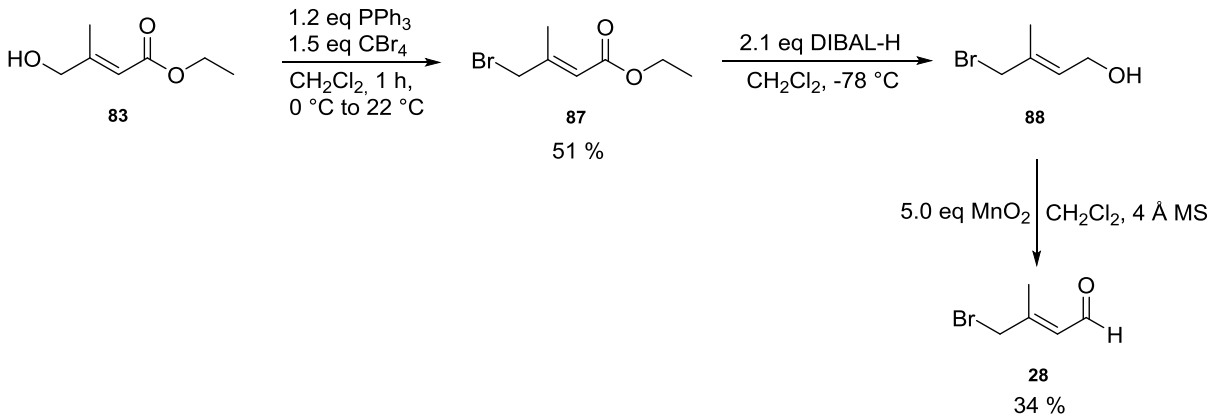

Scheme 56: Synthesis of (*E*)-4-bromo-3-methylbut-2-enal (**28**).

The biocatalytic conversion of (*E*)-4-bromo-3-methylbut-2-enal (**28**) would result in the formation of a cyclopropane with two newly established stereogenic centers **42** (Scheme 57). For the identification of possible side products 4-bromo-3-methylbutanal (**89**) had to be synthesized (Scheme 58).

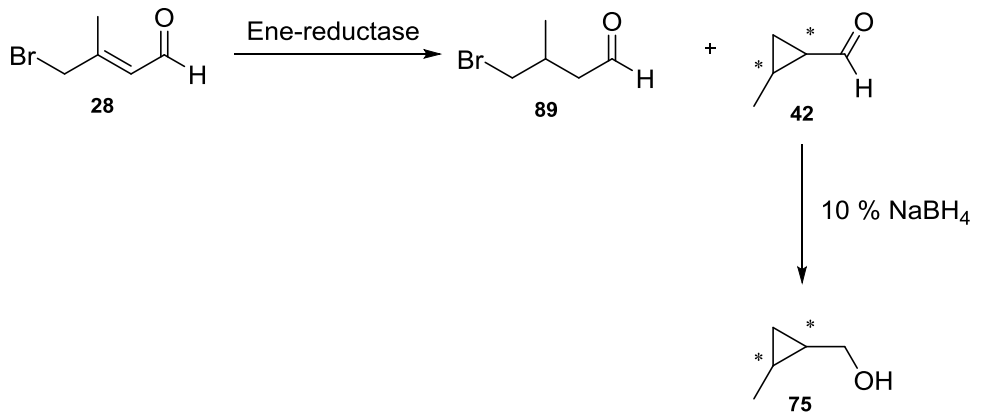

Scheme 57: Conversion of substrate **28** by ene-reductases.

The double bond of compound **83** was reduced with 10 % Pd/C and H_2 at 0 °C. Again the formation of a byproduct was observed, and therefore the APPEL-reaction was applied subsequently. Ethyl 4-bromo-3-methylbutanoate (**91**) was obtained in a yield of 67 % over 2 steps. The last two reaction steps were performed as already discussed in chapter 4.2.4. 4-Bromo-3-methylbutanal (**89**) was obtained in 74 % yield over 2 steps.

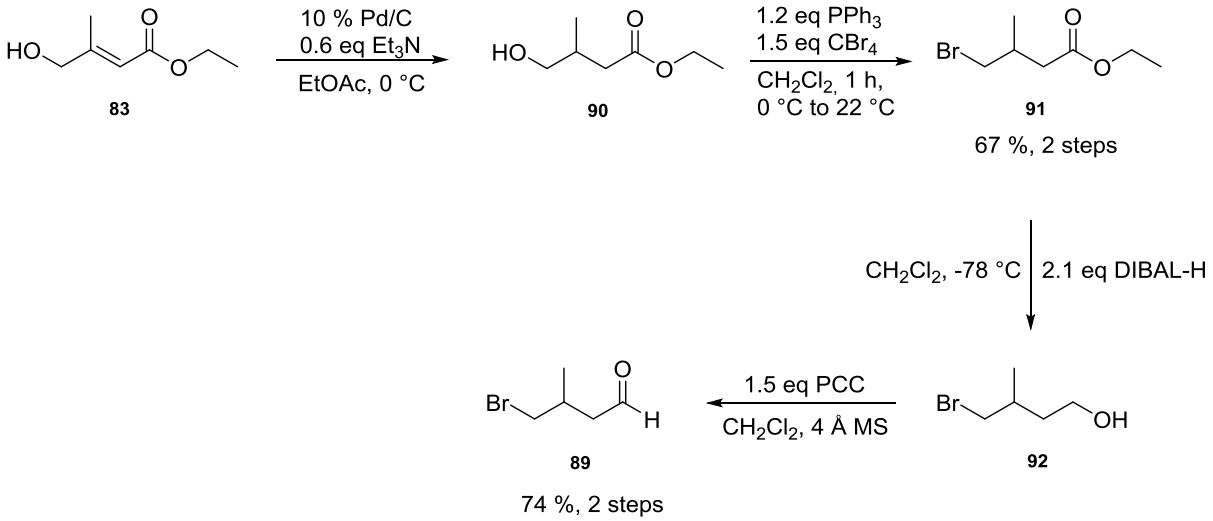

Scheme 58: Synthesis of 4-bromo-3-methylbutanal (**89**).

4.2.8 Synthesis of (*E*)-3-(chloromethyl)-4-methylpent-2-enal (29) and (*E*)-3-(bromomethyl)-4-methylpent-2-enal (30)

Compounds **29** and **30** proved to be the most challenging substrates synthesized in this thesis. Three different synthetic sequences were attempted, nevertheless it was not possible to synthesize substrates **29** or **30**. Scheme 59 illustrates synthesis route #1. In 1984, the nucleophilic addition of GRIGNARD-reagents at acetylenic diols was described by ISHINO *et al.*[93] The addition of a variety of GRIGNARD-reagents was successfully examined. Although it was described that GRIGNARD-reagents obtained from primary bromides are the most reactive ones, we followed that protocol to test if it would be possible to alkylate but-2-yne-1,4-diol (**93**) with a GRIGNARD-reagent, which had been obtained from a secondary bromide (**94**). Unfortunately, the formation of the alkylated diol **95** was never observed. In a second attempt we decided to change the electronic properties of the triple bond and protected selectively one hydroxyl function of but-2-yne-1,4-diol (**93**) with a silyl protecting group. Following again ISHINO's protocol, the formation of (*E*)-4-((tert-butyldiphenylsilyl)oxy)-2-isopropylbut-2-en-1-ol (**97**) was not observed, in fact compound **96** was not converted at all. Starting from compound **97**, substrates **29** and **30** could have been synthesized in three steps. After a APPEL-reaction to the bromide or chloride of **98**, a deprotection step and an allylic oxidation using MnO_2 could lead to substrates **29** and **30**.

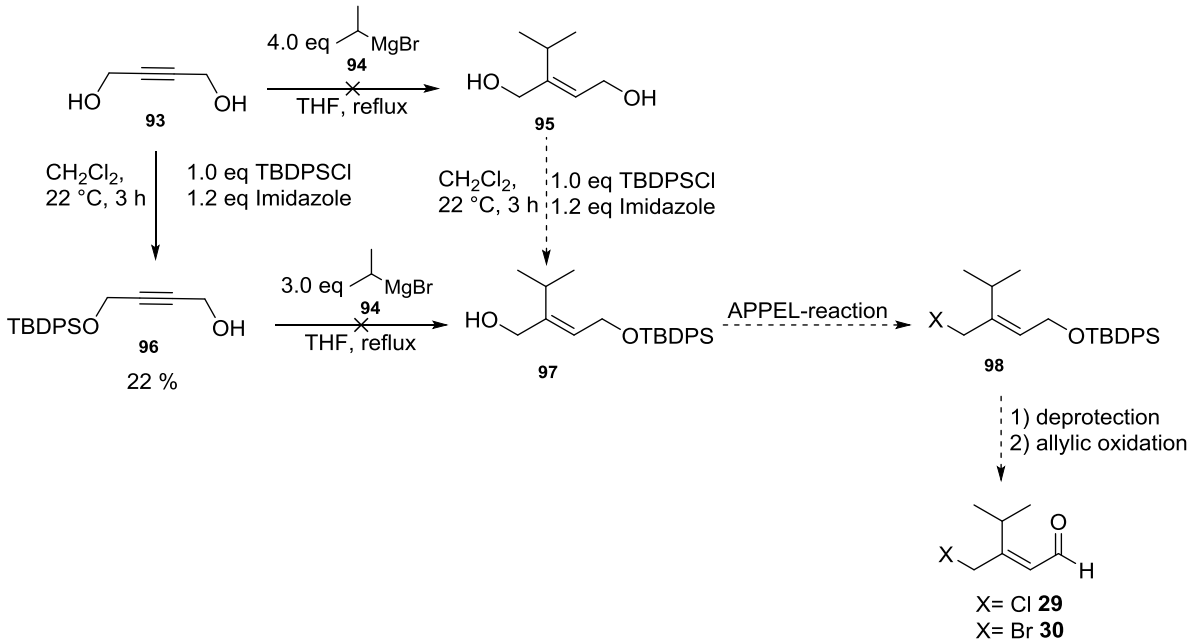

Scheme 59: Synthesis route #1 to (*E*)-3-(chloromethyl)-4-methylpent-2-enal (**29**) or (*E*)-3-(bromomethyl)-4-methylpent-2-enal (**30**).

However, the introduction of an isopropyl substituent at C-β could also be achieved by the use of reagent **100** as it was published by SENTER *et al* (Scheme 60).[107] Ethyl 2-(diethoxyphosphoryl)acetate (**99**) was deprotonated with KOtBu and then alkylated by 2-iodopropane yielding ethyl 2-(diethoxyphosphoryl)-3-methylbutanoate (**100**) in 95 % yield. In the next step, a HORNER-WADSWORTH-EMMONS olefination was examined. Compound **100** was deprotonated with LHMDS and further converted with 1,4-dioxane-2,5-diol (**47**). Unfortunately, no conversion of the starting material was observed. Starting from **101** we wanted to protect the hydroxyl function, reduce the ester moiety to the alcohol with DIBAL-H. Then we wanted to perform an APPEL-reaction to the corresponding bromide or chloride and after deprotection and oxidation substrates **29** and **30** could have been obtained. In order to make sure that the handling of LHMDS and HORNER-WADSWORTH-EMMONS-reagent **100** was correct, the original protocol by SENTER *et al* was followed.[107] As an electrophile, acetaldehyde (**102**) was used in this olefination reaction and ethyl 2-isopropylbut-2-enoate (**103**) (*Z*/*E* ratio 1/4) was obtained in 43 % yield. Starting from compound **103** numerous different procedures for the SeO_2 mediated allylic oxidation were tested, nevertheless compound **101** could not be obtained by any of the procedures which were used.

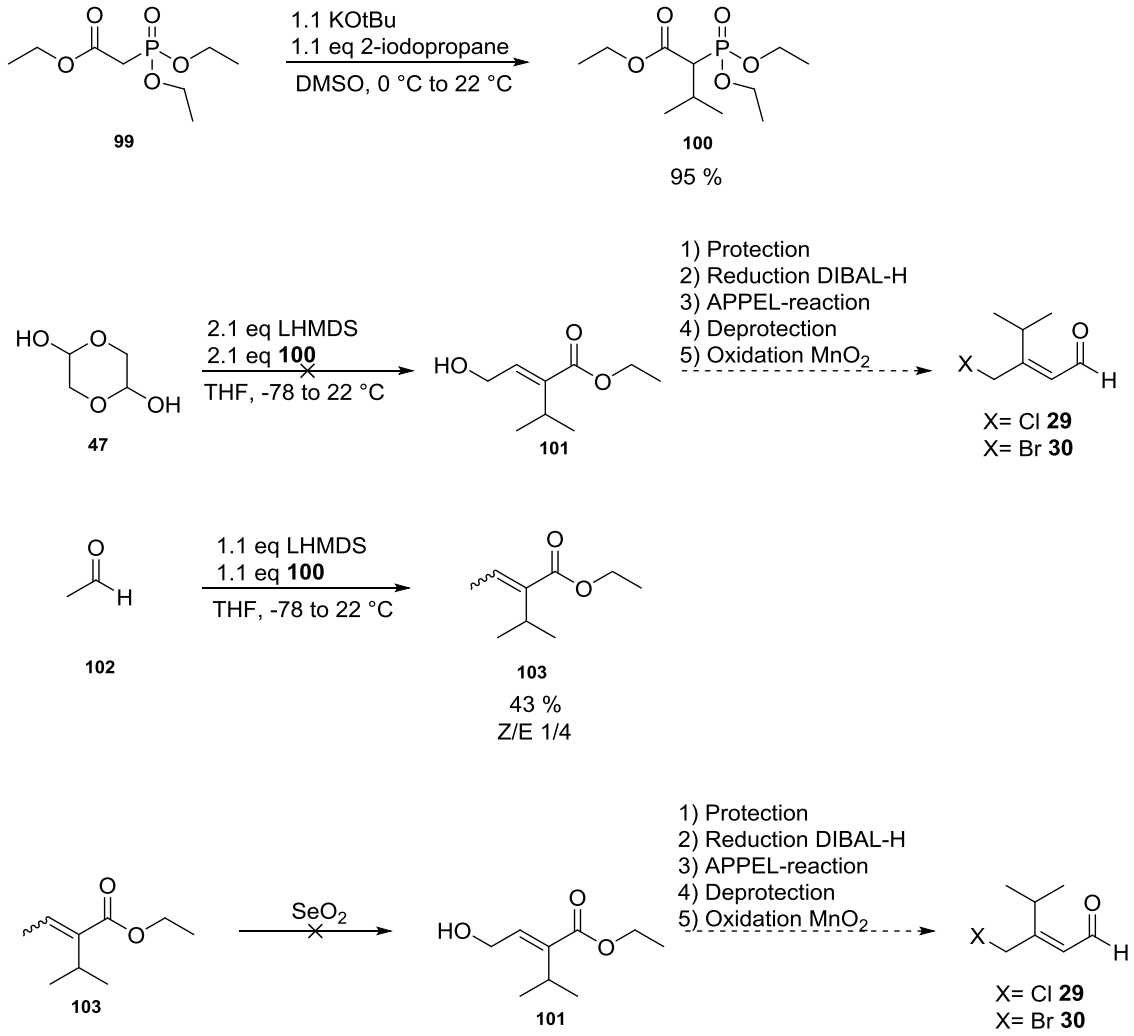

Scheme 60: Synthesis route #2 to (*E*)-3-(chloromethyl)-4-methylpent-2-enal (**29**) or (*E*)-3-(bromomethyl)-4-methylpent-2-enal (**30**).

In synthesis route #3 we wanted to test whether it is possible to perform the previously described HORNER-WADSWORTH-EMMONS-reaction with an already protected small aldehyde (Scheme 61). A SWERN-oxidation of 2-((tert-butyldimethylsilyl)oxy)ethan-1-ol (**104**) furnished protected aldehyde **105** in 39 % yield. Compound **105** was immediately used in the HORNER-WADSWORTH-EMMONS-reaction, but formation of compound **106** was not observed. Until now, the synthesis of (*E*)-3-(chloromethyl)-4-methylpent-2-enal (**29**) and (*E*)-3-(bromomethyl)-4-methylpent-2-enal (**30**) has not yet been accomplished.

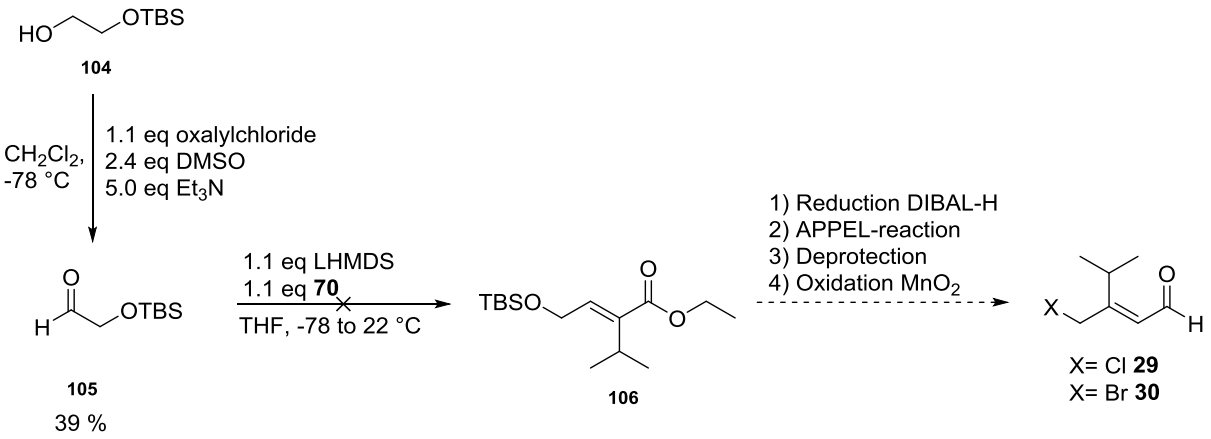

Scheme 61: Synthesis route #3 to (*E*)-3-(chloromethyl)-4-methylpent-2-enal (**29**) or (*E*)-3-(bromomethyl)-4-methylpent-2-enal (**30**).

4.2.9 Synthesis of (*E*)-4-chloro-3-phenylbut-2-enal (31) and reference compounds

The synthesis of (*E*)-4-chloro-3-phenylbut-2-enal (**31**) is illustrated in Scheme 62.

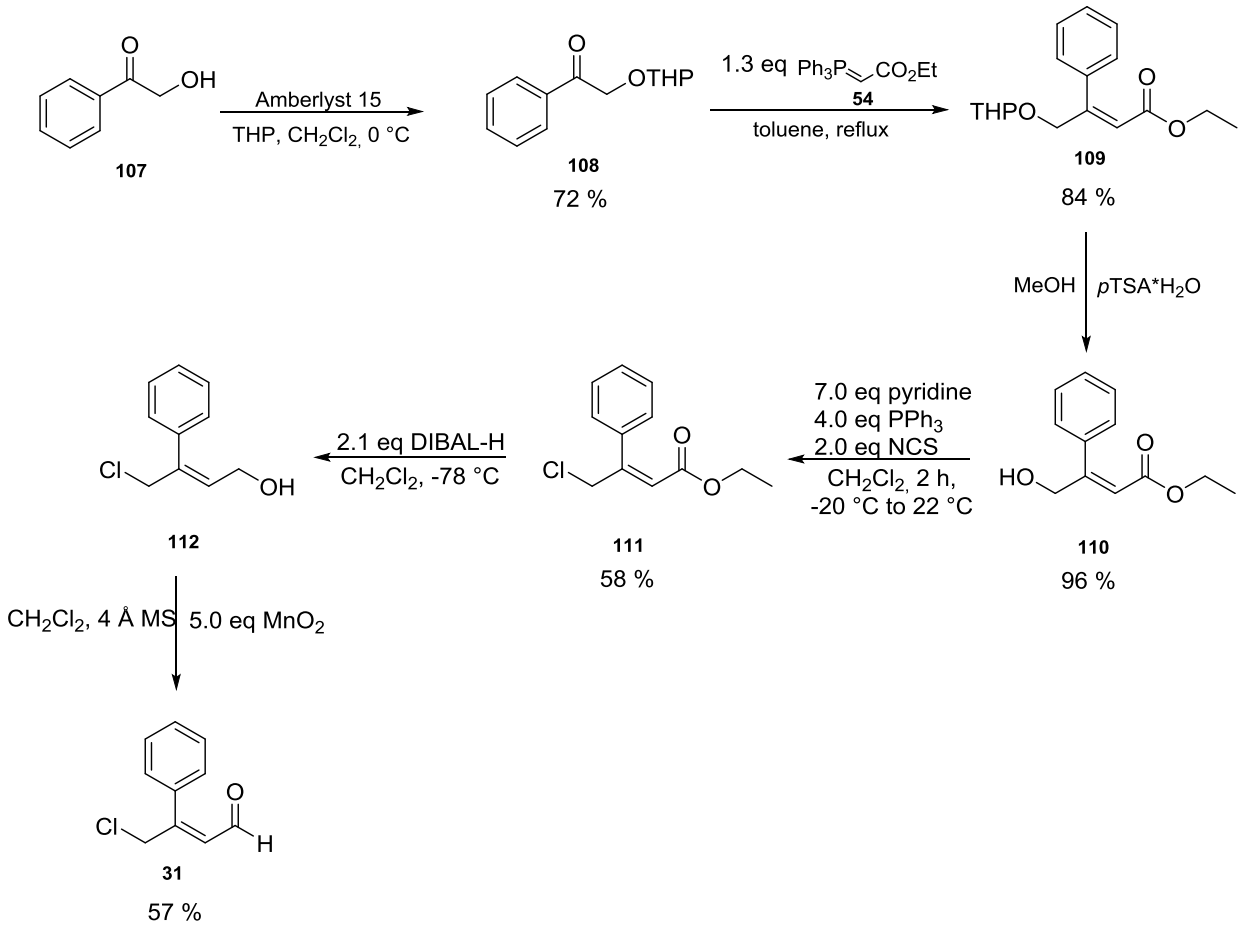

Scheme 62: Synthesis of (*E*)-4-chloro-3-phenylbut-2-enal (**31**).

Steps 1 to 3 have been described by LU *et al* previously, so following these procedures the α-hydroxyketone **107** was protected to give compound **108** in 72 % yield.[111] In the next step a WITTIG-reaction employing deprotonated WITTIG-ylen **57** was carried out. The literature procedure was slightly modified. In the original protocol by LU *et al* acetonitrile served as a solvent in the WITTIG-reaction. By applying the original protocol the yield of compound **109** was only moderate (51 %). When toluene was used as a solvent, the oil bath temperature was increased to 135 °C, which resulted in a shorter reaction time (3 d) and ethyl (*E*)-3-phenyl-4-((tetrahydro-2*H*-pyran-2-yl)oxy)but-2-enoate was isolated in 84 % yield. Compound **109** was deprotected and the hydroxyl function was substituted against chlorine in an APPEL-reaction which furnished ethyl (*E*)-4-chloro-3-phenylbut-2-enoate (**111**) in 58 % yield. NMR experiments displayed an NOE-effect of the olefinic proton at C-α and the protons of C-γ which indicates that these protons are located at the same side of the double bond, which confirms that the (*E*)-isomer of **111** was isolated. Reduction of the ester-moiety and

subsequent allylic oxidation of (*E*)-4-chloro-3-phenylbut-2-en-1-ol (**112**) afforded substrate **31** in 57 % yield after purification via column chromatography. The last two reaction steps had to be performed under the complete exclusion of light. (*E*)-4-Chloro-3-phenylbut-2-enal (**31**) was stored under a slight stream of N_2, in a flask covered by aluminum foil and had to be used immediately in the biocatalytic experiments.

To circumvent the protection and deprotection steps before and after the WITTIG-reaction, it was tested if direct conversion of 2-hydroxy-1-phenylethan-1-one (**107**) to ethyl (*E*)-4-hydroxy-3-phenylbut-2-enoate (**110**) would be possible. Unfortunately, a conversion of the starting material **107** was not observed in this reaction.

When substrate **31** is converted by ene-reductase wild types and variants (Scheme 63), the ene-reductase mediated reductive cyclization reaction would lead to the formation of a cyclopropane with two newly established stereogenic centers **114**. For the reasons discussed above, the enantiomeric excess of **114** was determined after the reduction using $NaBH_4$ to the corresponding alcohol **115**. To identify the undesired byproduct of the natural ene-reductase pathway compound **113** was synthesized.

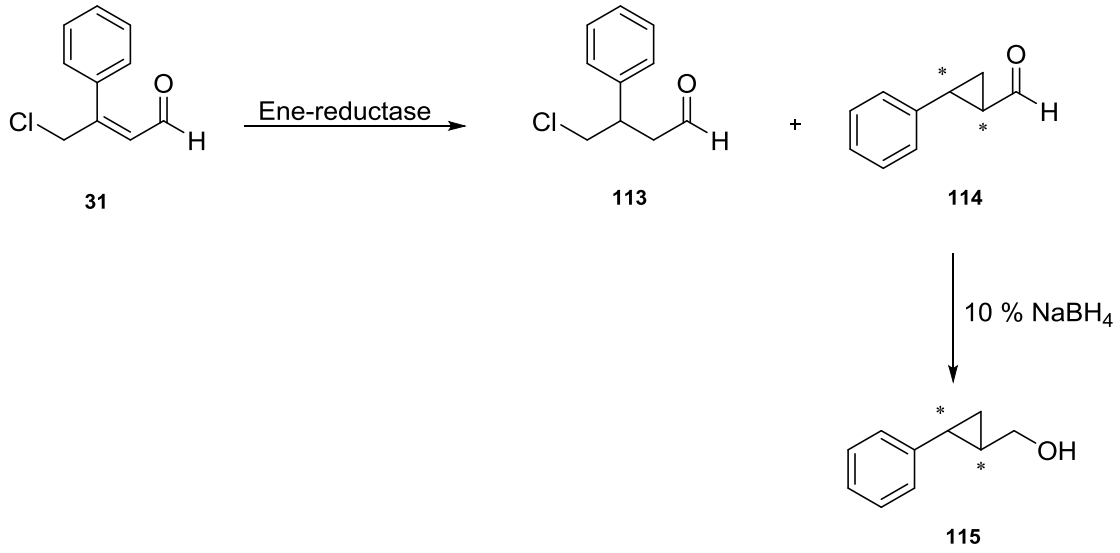

31 **113** **114** **115**

Scheme 63: Conversion of substrate **31** by ene-reductases.

Racemic (2-phenylcyclopropyl)methanol (*trans*-**115**) was synthesized in one step starting from (*E*)-3-phenyl-2-propen-1-ol (*trans*-**116**) (Scheme 64). In a stereospecific SIMMONS-SMITH-reaction, the *trans*-configurated double bond of **116** is converted to a *trans*-cyclopropane (*trans*-**115**).

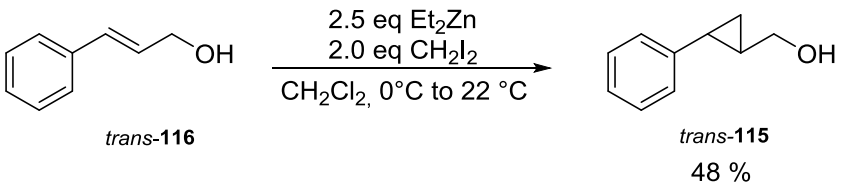

Scheme 64: Synthesis of (2-phenylcyclopropyl)methanol (*trans*-**115**).

Racemic (2-phenylcyclopropyl)methanol (*cis*-**115**) was synthesized starting from 3-phenylprop-2-yn-1-ol (**117**) (see Scheme 65). Following a procedure by KIM *et al* alkyne **117** was reduced using 5 mol% Lindlar catalyst and 7 mol% quinoline.[94] Within 4 h the starting material was fully converted, but only the product of overreduction of the double bond, compound **118**, was isolated. We decided to examine a procedure by FAN *et al* in which an increased amount of catalyst poison (44 mol% quinoline) was used.[120] (*Z*)-3-Phenyl-2-propen-1-ol was furnished in 69 % yield. Racemic (2-phenylcyclopropyl)methanol (*cis*-**115**) was then obtained via SIMMONS-SMITH-cyclopropanation, as it was already described before, in a good yield of 70 %.

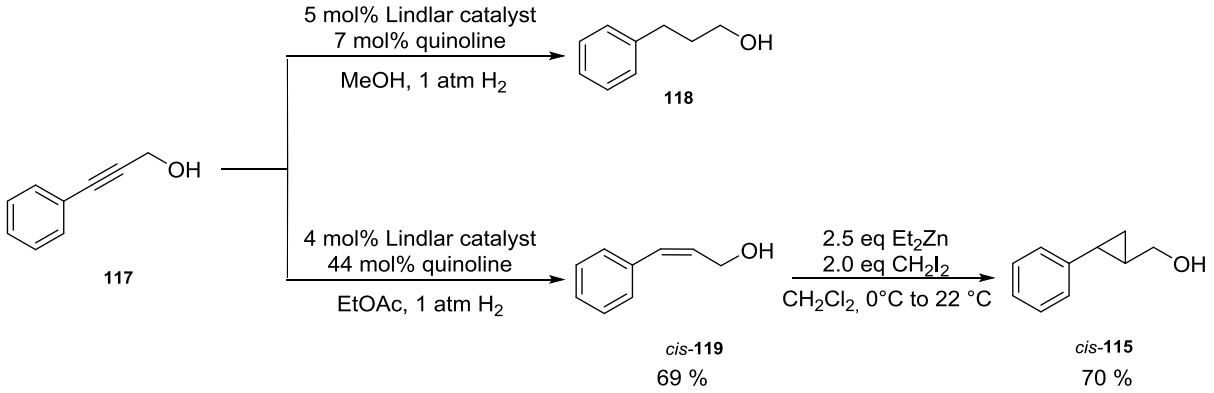

Scheme 65: Synthesis of (2-phenylcyclopropyl)methanol (*cis*-**115**).

As depicted in Scheme 66, 4-chloro-3-phenylbutanal (**113**) was synthesized in 4 steps starting from ethyl (*E*)-4-hydroxy-3-phenylbut-2-enoate (**110**). Hydrogenation of the double bond using a continuous flow reactor (H-Cube™) afforded compound **120** in 67 % yield. Following an APPEL-reaction to compound **121**, reduction of the ester moiety to the alcohol **122** and subsequent oxidation using 1.5 eq PCC, 4-chloro-3-phenylbutanal (**113**) was obtained in 42 % yield.

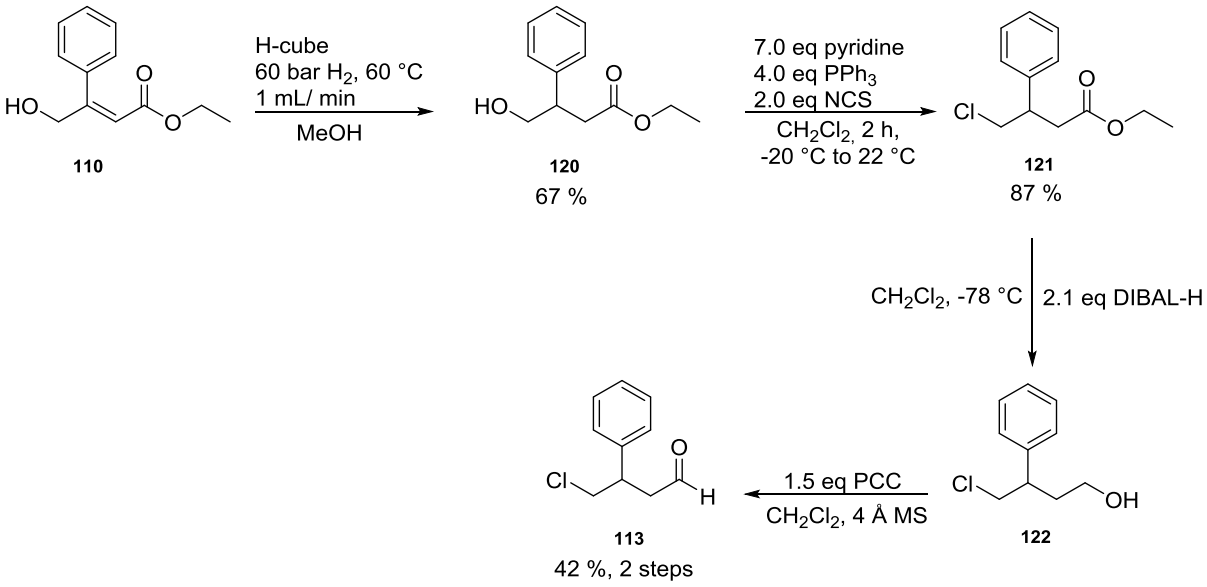

Scheme 66: Synthesis of 4-chloro-3-phenylbutanal (**113**).

4.2.10 Synthesis of (*E*)-4-bromo-3-phenylbut-2-enal (32)

It would be highly desirable to easily obtain substrates for ene-reductase mediated carbocyclization reactions via a short-step synthesis. Thus we tested if it would be possible to directly convert commercially available 2-bromo-1-phenylethan-1-one (**123**) to ethyl (*E*)-4-bromo-3-phenylbut-2-enoate (**124**) in a WITTIG-reaction (Scheme 67). Two already successfully used solvents from previous WITTIG-reactions were examined. The reaction mixtures were heated under reflux for several days, nevertheless the sterically congested ketone proved to be unreactive under harsh conditions and starting material was not converted at all.

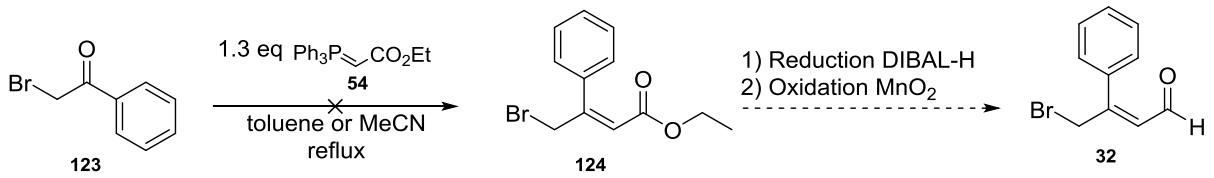

Scheme 67: Synthesis route #1 to (*E*)-4-bromo-3-phenylbut-2-enal (**32**).

Scheme 68 illustrates the synthesis of (*E*)-4-bromo-3-phenylbut-2-enal (**32**) starting from ethyl (*E*)-4-hydroxy-3-phenylbut-2-enoate (**110**). The hydroxyl function of **110** was substituted against bromine in an APPEL-reaction producing **124** in 77 % yield. An NOE-effect between the olefinic proton at C-α and protons at C-γ is observed, which indicates that these protons are at the same side of the double bond thus, indicating (*E*)-configuration. In the next step the ester functionality was reduced to the corresponding allylic alcohol **125**. This reaction proceeded in a spot-to-spot reaction according to TLC. But after the oxidation of the allylic alcohol **125** using MnO_2, (*E*)-4-bromo-3-phenylbut-2-enal (**32**) was not successfully isolated. We hypothesized that the bromine in allylic position might cause tremendous light sensitivity.

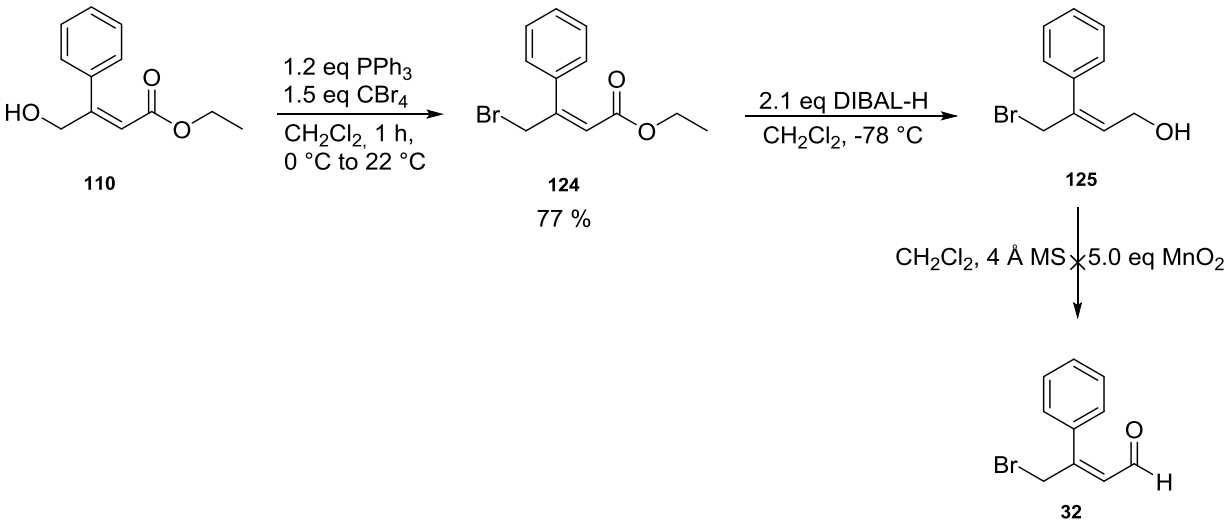

Scheme 68: Synthesis of (*E*)-4-bromo-3-phenylbut-2-enal (**32**).

4.2.11 Synthesis of (*E*)-4-chloro-3-(4-methoxyphenyl)but-2-enal (33)

For the synthesis of (*E*)-4-chloro-3-(4-methoxyphenyl)but-2-enal (**33**) the synthesis strategy described in 4.2.9 was used (Scheme 69). Substitution of bromine in compound **126** furnished 2-hydroxy-1-(4-methoxyphenyl)ethan-1-one (**127**) in quantitative yield. In the next step, the hydroxyl-function was protected, which furnished compound **128** in 83 % yield. After the WITTIG-reaction, the hydroxyl function of ethyl (*E*)-3-(4-methoxyphenyl)-4-((tetrahydro-2*H*-pyran-2-yl)oxy)but-2-enoate (**129**) was deprotected to yield ethyl (*E*)-4-hydroxy-3-(4-methoxyphenyl)but-2-enoate (**130**) in 90 % yield. The hydroxyl function was substituted against chlorine in an APPEL-reaction and ethyl (*E*)-4-chloro-3-(4-methoxyphenyl)but-2-enoate (**131**) was furnished in 55 % yield. As it is was already discussed in 4.2.9, the observation of an NOE-effect between the olefinic proton at C-α and protons at C-γ indicates that these protons are located at the same side of the double bond, which confirms that the (*E*)-isomer of **131** was isolated.

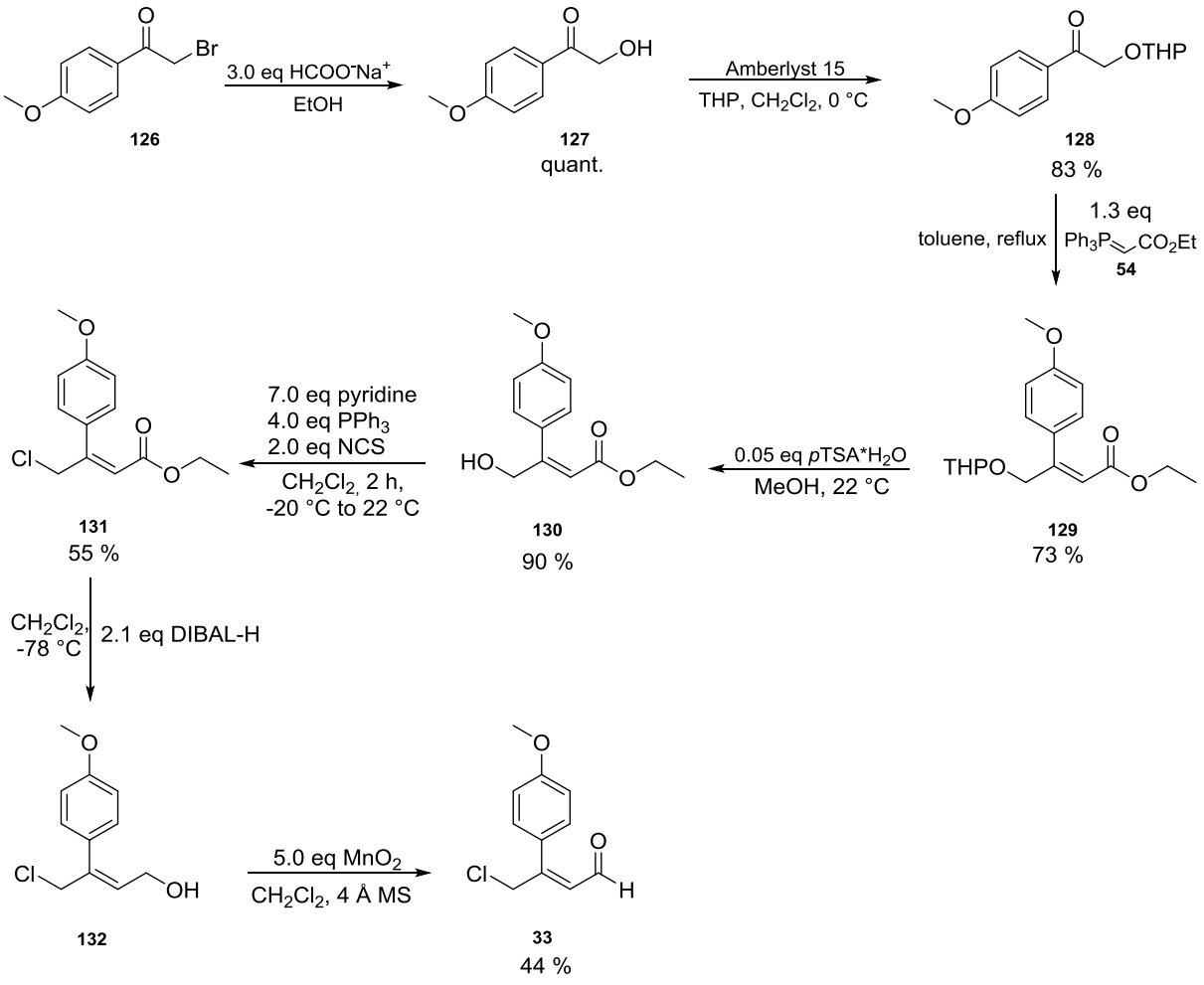

Scheme 69: Synthesis of (E)-4-chloro-3-(4-methoxyphenyl)but-2-enal (**33**).

The ester moiety in compound **131** was reduced with 2.1 eq DIBAL-H and subsequent allylic oxidation of (*E*)-4-chloro-3-phenylbut-2-en-1-ol (**132**) afforded substrate **33** in 44 % yield after purification via column chromatography. The last two reaction steps had to be performed under the complete exclusion of light. (*E*)-4-Chloro-3-(4-methoxyphenyl)but-2-enal (**33**) was stored under a slight stream of N_2, in a flask covered by aluminum foil, and had to be used immediately in the biocatalytic experiments.

4.2.12 Synthesis of (*E*)-4-chloro-3-(4-(trifluoromethyl)phenyl)but-2-enal (34)

Once more, the synthesis strategy which had already been described in 4.2.9 was applied to synthesize (*E*)-4-chloro-3-(4-(trifluoromethyl)phenyl)but-2-enal (**34**) (Scheme 70). Starting from commercially available 2-bromo-1-(4-(trifluoromethyl)phenyl)ethan-1-one (**133**) the bromide was substituted, which furnished α-hydroxyketone **134** in quantitative yield. For the WITTIG-reaction the hydroxyl function of **134** was protected and 2-((tetrahydro-2*H*-pyran-2-yl)oxy)-1-(4-(trifluoromethyl)phenyl)ethan-1-one (**135**) was isolated in 57 % yield. After WITTIG-reaction and deprotection of the hydroxyl function using 0.05 eq *p*TSA*monohydrate allylic alcohol **137** was obtained in 60 % yield. Via an APPEL-reaction the hydroxyl function was substituted against chlorine, which accomplished the formation of ethyl (*E*)-4-chloro-3-(4-(trifluoromethyl)phenyl)but-2-enoate (**138**) in 66 % yield. The observation of an NOE-effect between the olefinic proton of C-α and protons of C-γ confirmed the (*E*)-configuration of the double bond. Reduction of the ester in compound **138** and subsequent allylic oxidation using MnO_2 of (*E*)-4-chloro-3-(4-(trifluoromethyl)phenyl)but-2-en-1-ol (**139**) afforded substrate **34** in 51 % yield after purification via column chromatography. The last two reaction steps had to be performed under the complete exclusion of light. (*E*)-4-Chloro-3-(4-(trifluoromethyl)phenyl)but-2-enal (**34**) was stored under a slight stream of N_2 in a flask covered by aluminum foil and had to be used immediately in the biocatalytic experiments.

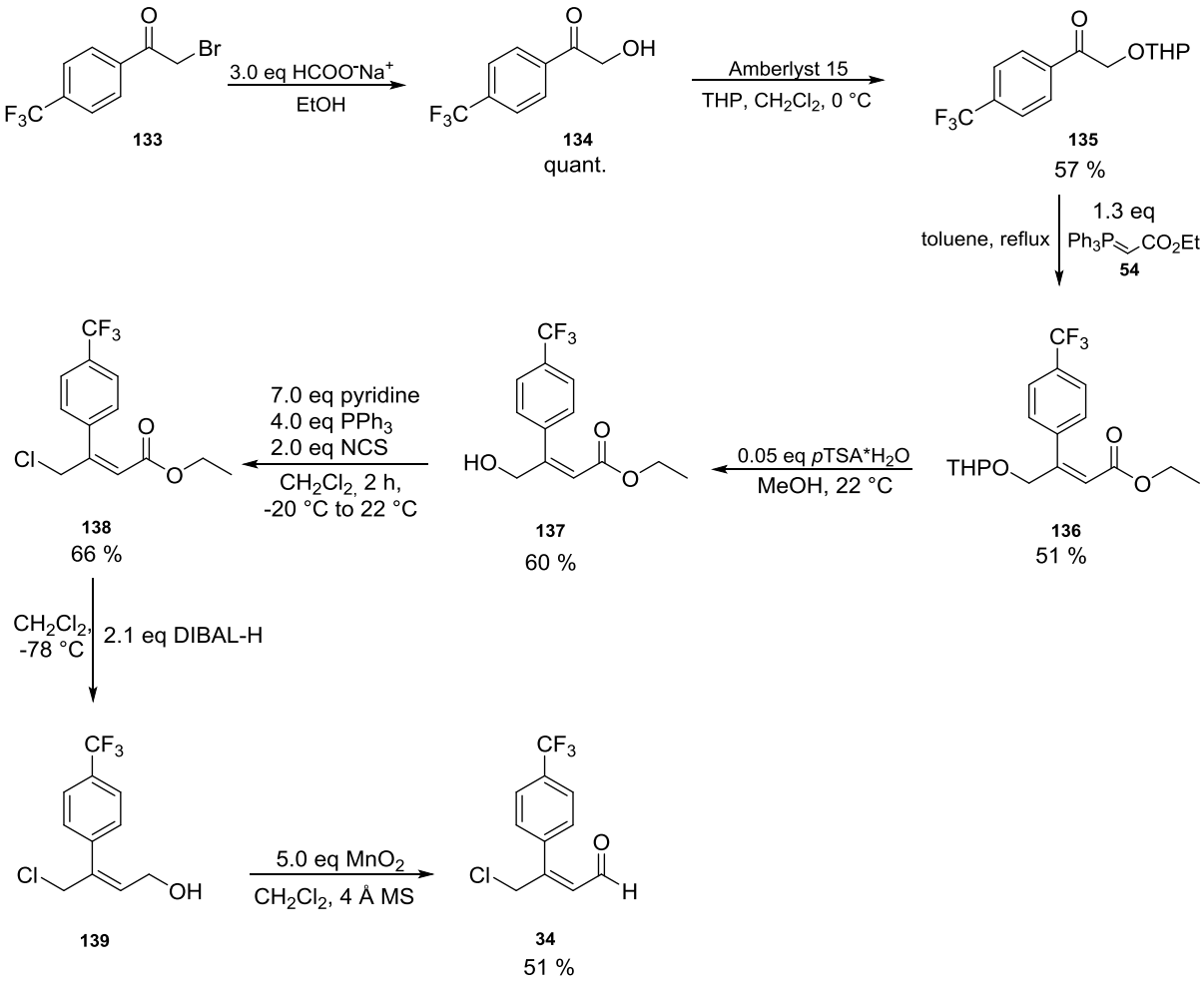

Scheme 70: Synthesis of (*E*)-4-chloro-3-(4-(trifluoromethyl)phenyl)but-2-enal (**34**).

4.3 Generation of enzyme variants

As it was already outlined in chapter 3, the generation of suitable enzyme variants is crucial for the ene-reductase mediated reductive carbocyclization reaction. The major objective in this study is to favour the reductive cyclization reaction over the natural ene-reductase pathway. The design of enzyme variants, in particular the design of the catalyst, represents the centerpiece of this thesis. Figure 8 displays the active site of Opr3 WT, the reactive Tyr at position 190 is shown in pink. This Tyr is responsible for the reprotonation of the enolate and represents the working point in single site directed mutagenesis.

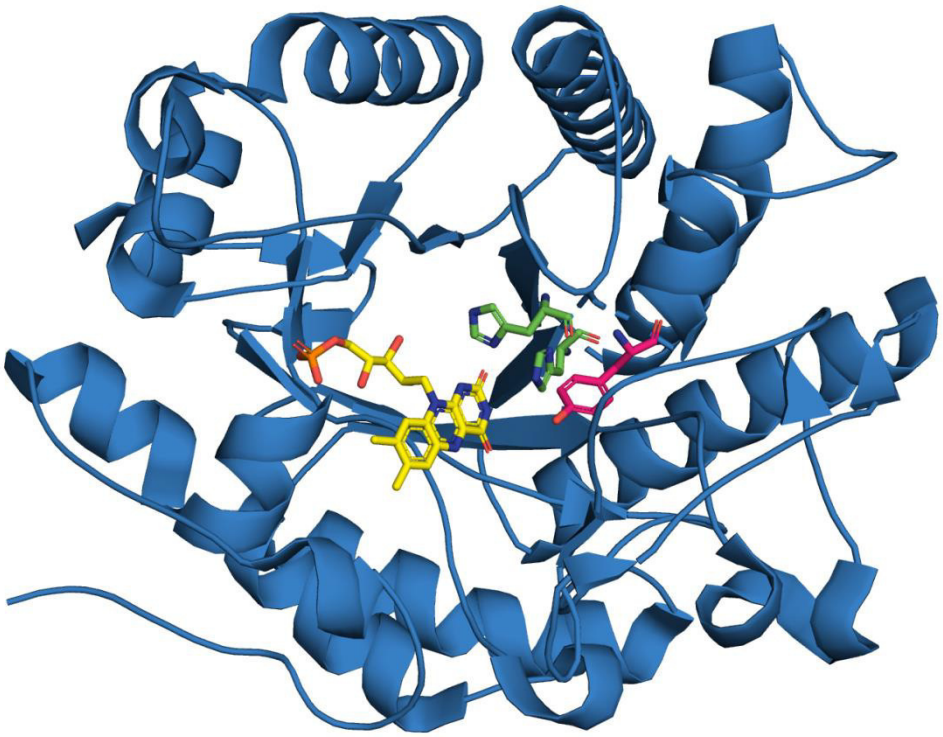

Figure 8: Active site of Opr3 WT, FMN is shown in yellow, His-185 and His-188 are shown in green and Tyr-190 is shown in pink. Picture prepared with: The PyMol Molecular Graphics System, DeLano Scientific, San Carlos, CA.

In preliminary studies by HECKENBICHLER the reactive Tyr-residue in the active site of Opr3 and YqjM was exchanged against Asn, Cys, and Ser (Scheme 71).[95]

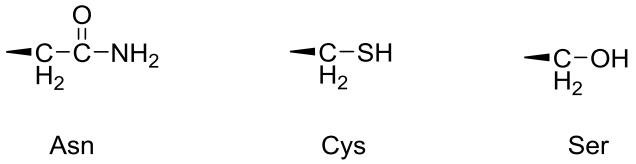

Scheme 71: Amino acid side chains of aspargine, cysteine, and serine.

We formerly assumed that by stabilizing the enolate intermediate through polar amino acids, the formation of a cyclic product is facilitated. Moreover, we hoped that Asn, Cys, and Ser were not able to act as proton donors in this reductive carbocyclization reaction. However, this hypothesis was rejected since only the formation of the product of the natural ene-reductase pathway was observed. Thus, we assumed that by the incorporation of apolar and aliphatic amino acids (Ala, Leu), which are not able to act as proton donors, water is excluded from the active site and hence a reprotonation of the enolate is less likely (Scheme 72). Through single-site directed mutagenesis Tyr-190 in Opr3 was replaced against Ala and Leu. However, when Opr3 Y190A and Opr3 Y190L were tested, the formation of a cyclic product was not observed.

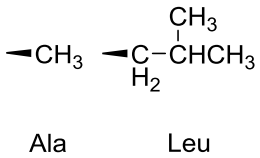

Scheme 72: Amino acid side chains of alanine and leucine.

Nevertheless, these negative results led to a new idea. Instead of exchanging the reactive Tyr-residue in Opr3 and YqjM against a polar or a small aliphatic amino acid we assumed, that the exchange to a hydrophobic and sterically demanding amino acid could favour the reductive cyclization reaction over the natural ene-reductase reduction. We further hypothesized that an apolar and sterically demanding amino acid would effectively displace water molecules from the active site, hence making a reprotonation of the enolate less favoured. Therefore, the Tyr-residue at position 190 in Opr3 was exchanged against Phe. As preliminary results indicated that the Phe variant was promising, the Trp variant of Opr3 was also expressed (Scheme 73).

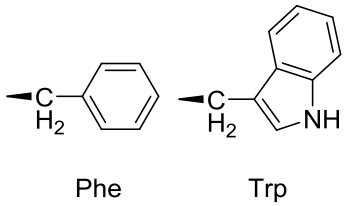

Scheme 73: Amino acid side chains of phenylalanine and tryptophan.

Encouraged by the results which were obtained by Opr3 Y190F and Opr3 Y190W, we decided to expand our enzyme repertoire. The Tyr-residue which was responsible for reprotonation in YqjM, namely Tyr-169, was exchanged against Phe and Trp through single site directed mutagenesis. With our enzyme set in hands we started the investigation of this biocatalytic C-C bond forming reaction.

4.4 Assay development and proof of concept

In the early stages of this project the main focus of attention was dedicated to the development of a biocatalytic assay and a suitable method for the quantification of results. For the optimization of the reaction conditions and the quantification of results we used the reaction displayed in Scheme 74 as a model reaction. The conversion of (*E*)-4-bromobut-2-enal (**20**) leads either to the desired product of reductive cyclization **37** or to the product of the natural reduction reaction **45**.

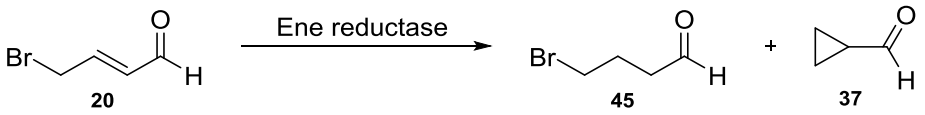

Scheme 74: Model reaction for ene-reductase mediated reductive cyclization.

In the beginning, the reproducibility of conversions turned out to be a serious problem, Table 3 shows triplicates of each enzyme when monitoring the model reaction (Scheme 74). The decrease of starting material was measured after 180 min reaction time. For the quantification we decided to use nonane as an internal standard. Within every triplicate major deviations were observed, hence these results were not trustworthy. For example, the overall conversion of compound **20**, when incubating with Opr3 Y190W, ranged from no conversion to 85 % conversion (Table 3, Entries 7, 8 and 9).

Table 3: Triplicates of model reaction #1.

Entry	Enzyme	Conversion [%]*
1	Opr3 WT	72
2	Opr3 WT	63
3	Opr3 WT	33
4	Opr3 Y190F	84
5	Opr3 Y190F	48
6	Opr3 Y190F	34
7	Opr3 Y190W	85
8	Opr3 Y190W	45
9	Opr3 Y190W	nc
10	YqjM Y169F	71
11	YqjM Y169F	62
12	YqjM Y169F	26

*Reaction conditions: 300 µL stock solution (10 mM substrate, 1 vol% DMF, $V_{substrate}=V_{nonane}$ and 10 mM NADH in 50 mM sodium phosphate-buffer at pH 7.5 and 150 mM NaCl) and enzyme (5 µM) in 300 µL sodium phosphate-buffer (50 mM, pH 7.5, 150 mM NaCl) per tube, 180 min and 25 °C at 300 rpm; nc = no conversion.

From these observations we concluded that the internal standard we used might be responsible for the observed deviations. We hypothesized that upon the extraction of analytes from the aqueous buffer phase into an organic solvent varying amounts of internal standard were extracted, which might be the reason for the major deviations within every triplicate. As a result, we decided to change the internal standard and instead of nonane 1,2-DME was used (Table 4).

Table 4: Triplicates of model reaction #2.

Entry	Enzyme	Conversion [%]*
1	Opr3 WT	46
2	Opr3 WT	48
3	Opr3 WT	46
4	Opr3 Y190F	55
5	Opr3 Y190F	53
6	Opr3 Y190F	54
7	Opr3 Y190W	25
8	Opr3 Y190W	25
9	Opr3 Y190W	23
10	YqjM Y169F	39
11	YqjM Y169F	43
12	YqjM Y169F	43

*Reaction conditions: 300 µL stock solution (10 mM substrate, 1 vol% DMF, $V_{substrate}=V_{1,2\text{-DME}}$ and 10 mM NADH in 50 mM sodium phosphate-buffer at pH 7.5 and 150 mM NaCl) and enzyme (5 µM) in 300 µL sodium phosphate-buffer (50 mM, pH 7.5, 150 mM NaCl) per tube, 180 min and 25 °C at 300 rpm.

The results obtained from the approach using 1,2-DME as internal standard were within 5 % of each other in every triplicate. For example, when monitoring the conversion of (*E*)-4-bromobut-2-enal (**20**) by YqjM Y169F (Table 4, Entries 10-12) conversions from 39 % to 43 % were obtained. In every enzyme triplicate, the starting material was not converted completely. We reasoned that the amount of NADH might responsible for that since we used NADH only in an equimolar amount (10 mM substrate and 10 mM NADH). By the use of 1.5 eq of NADH it should be possible to run reactions until completion.

After having established a suitable procedure for performing a biocatalytic assay and monitoring the reaction conversions with an internal standard all enzymes which showed cyclopropanation activity in previously obtained studies were compared (shown in Table 1).

Table 5: Conversion of (*E*)-4-bromobut-2-enal by ene-reductases.

Entry	Enzyme	Conversion [%]*	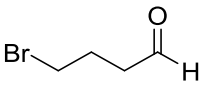 [%]	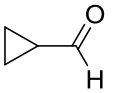 [%]
1	Opr3 WT	74	66	34
2	Opr3 Y190F	93	12	88
3	Opr3 Y190W	45	22	78
4	YqjM WT	>99	59	41
5	YqjM Y169F	>99	2	98
6	YqjM Y169W	3	50	50

*Reaction conditions: 300 µL stock solution (10 mM substrate, 1 vol% DMF, $V_{substrate}=V_{1,2\text{-}DME}$ and 15 mM NADH in 50 mM sodium phosphate-buffer at pH 7.5 and 150 mM NaCl) and enzyme (5 µM) in 300 µL sodium phosphate-buffer (50 mM, pH 7.5, 150 mM NaCl) per tube, 180 min and 25 °C at 300 rpm.

Wild type enzymes exhibited already measurable levels of reductive cyclization activity and formed the cyclopropane product **37** in 34 % conversion (Opr3 WT, Table 5, Entry 1) and 44 % conversion (YqjM WT, Table 5, Entry 4). This activity of ene-reductase wild types has not yet been described in literature. O'CONNOR and co-workers recently showed that a wild type enzyme from *Catharanthus roseus* is catalyzing a similar reductive cyclization reaction in the biosynthesis of iroids. After a hydride transfer from NADPH to C-β of an α,β-unsaturated aldehyde, an intramolecular cyclization delivers a five-membered ring.[96] In our system, an improvement in starting material consumption and cyclopropanation activity was achieved when Opr3 Y190F (Table 5, Entry 2) was incubated with substrate **20**. Although Opr3 Y190W (Table 5, Entry 3) displayed a moderate conversion of starting material (45 %), a 2-fold improvement of cyclopropanation activity could be detected. The exchange of the Tyr residue against Phe in YqjM seems to be the key for achieving high conversion and high selectivity in this C-C bond forming reaction. This mutation alone converted YqjM WT with moderate ring formation activity (41 %) into an active catalyst. The Phe variant of YqjM converted (*E*)-4-bromobut-2-enal (**20**) smoothly in >99 % conversion with a high preference for the cyclization reaction over the natural reduction reaction. However, the Trp variant of YqjM did not convert (*E*)-4-bromobut-2-enal (**20**) and we hypothesized that this bulky amino acid residue might block the entry to the active site. Therefore, this variant was not further investigated.

To verify retention times of starting material and products a blank reaction (containing all ingredients except enzyme, Figure 9), cyclopropanecarbaldehyde **37** (Figure 10), and 4-bromobutanal **45** (Figure 11) were co-injected in GC-FID.

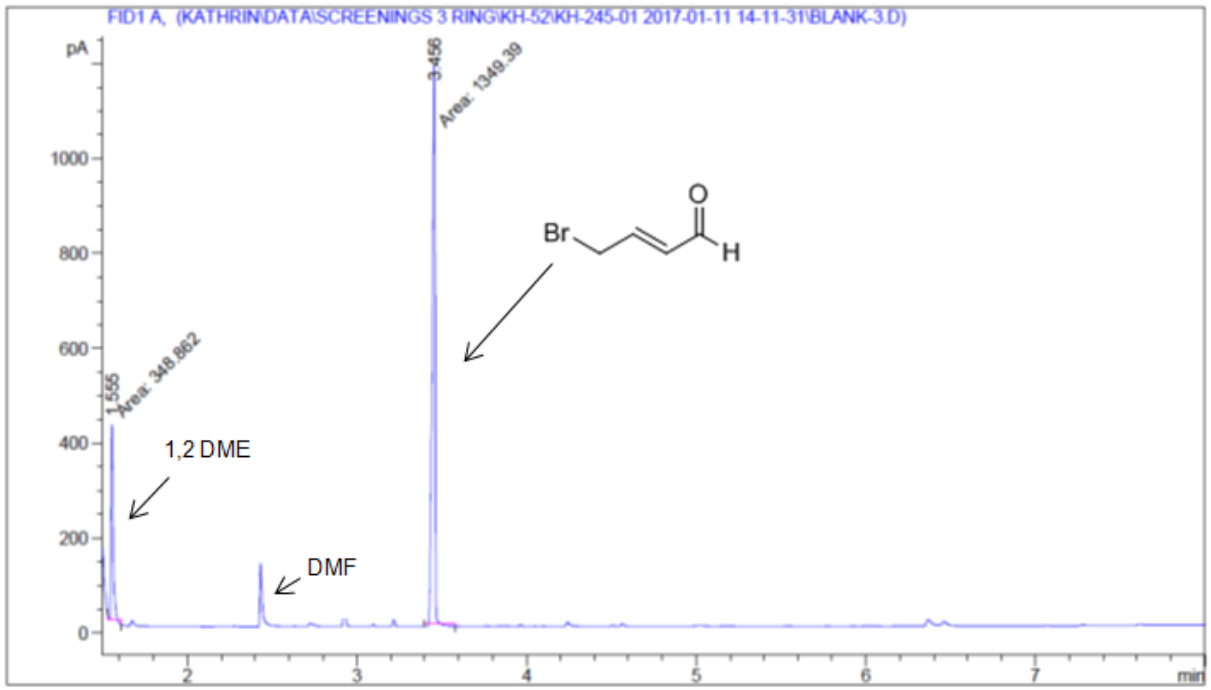

Figure 9: GC-FID chromatogram of blank reaction (method KH_80_30_280).

Figure 10: GC-FID chromatogram of commercially available cyclopropanecarbaldehyde (**37**) (method KH_80_30_280).

Figure 11: GC-FID chromatogram of reduction reference 4-bromobutanal (**45**) (method KH_80_30_280).

Figure 12 shows the GC-FID chromatogram after the conversion of (*E*)-4-bromobut-2-enal (**20**) with YqjM Y169F. It is clearly observed that the starting material at t_R= 3.5 min is consumed completely. The reduction by-product **45** is formed to a small extent (t_R= 3.1 min) and the main product **37** is observed at a t_R of 1.7 min.

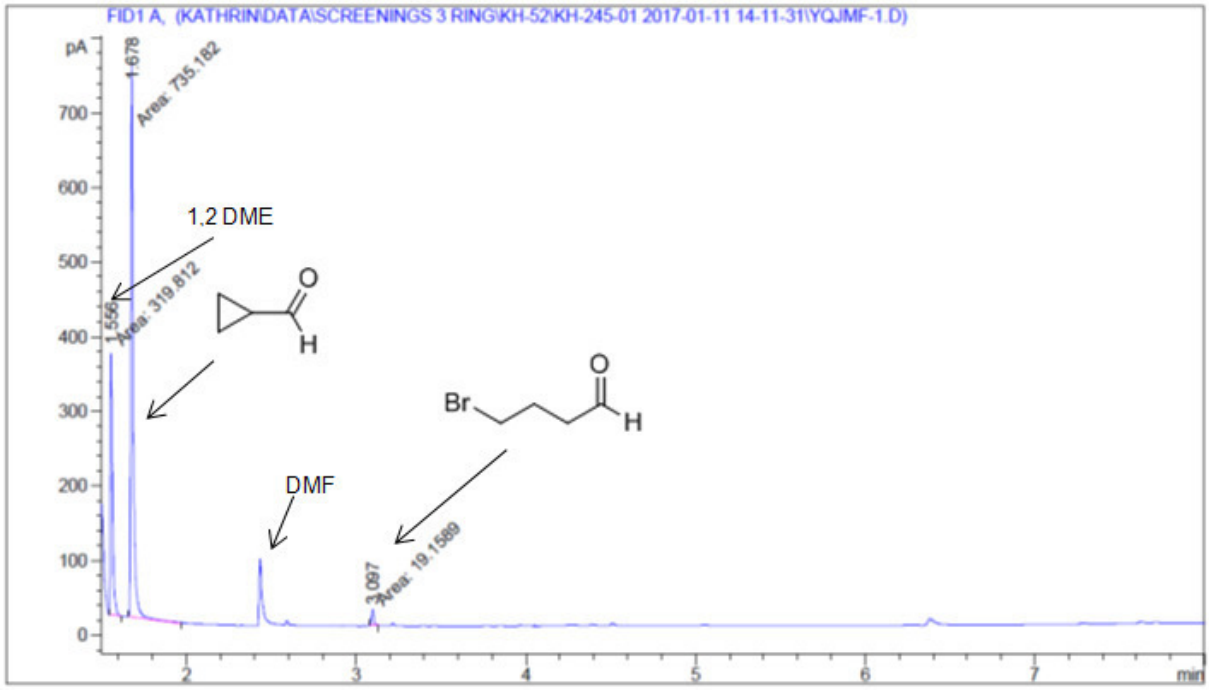

Figure 12: GC-FID chromatogram of crude YqjM Y169F preparation (method KH_80_30_280).

As a proof of concept experiment (*E*)-4-bromobut-2-enal (**20**) was converted with ene-reductase variants (OPR3 Y190F or YqjM Y169F) in a preparative scale reaction. Since it was not possible to isolate the very volatile cyclopropanecarbaldehyde (**37**), it was converted into the corresponding 2,4-dinitrophenylhydrazone in a subsequent chemical reaction (Scheme 75):

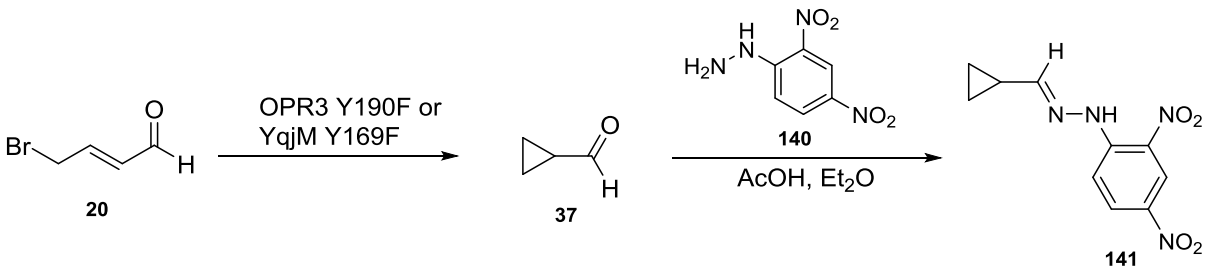

Scheme 75: Preparative scale reaction with (*E*)-4-bromobut-2-enal (**20**) and YqjM Y169F.

In the first preparative scale reaction, (*E*)-4-bromobut-2-enal (**20**) was converted with Opr3 Y190F. Reaction conditions were conducted as described in 7.8.1 (10 mM substrate, 15 mM NADH, and 5 µM Opr3 Y190F) but the internal standard (1,2 DME) and the cosolvent (DMF) were not used because an internal standard for quantification was not needed and we wanted to avoid purification problems afterwards caused by traces of DMF. After 180 min only 50 % of starting material was converted according to GC-FID, so additional enzyme was added and the reaction mixture was shaken at 25 °C for another 8 h. The overall enzyme concentration was then 10 µM, but conversion seemed to stop at 50 %. We hypothesized that the substrate (*E*)-4-bromobut-2-enal (**20**) was not properly dissolved in the buffer without DMF and 1,2-DME as cosolvents. In the next experiment we decided to use DMF (1 % final concentration) as well as 1,2-DME (0.1 % final concentration) to enhance the solubility of the substrate. Within 180 min full conversion was achieved. The reaction solution was extracted with diethylether and subsequently acetic acid and 1.1 eq 2,4-dinitrophenylhydrazine were added to trap cyclopropanecarbaldehyde as the corresponding 2,4-dinitrophenylhydrazone. The product was purified via flash chromatography, but it was not possible to remove excess 2,4-dinitrophenylhydrazine (**140**). Purification of compound **141** using preparative HPLC and preparative TLC resulted in a low product yield of 6 %.

Finally, (*E*)-4-bromobut-2-enal (**20**) was converted with YqjM Y169F, since the formation of the reduction byproduct **45** was neglible and under the already established reaction procedure for preparative scale reactions (10 mM substrate, 15 mM NADH, 5 µM YqjM Y169F, 1 % DMF and 0.1 % 1,2-DME) it was possible to fully convert the starting material. In the

subsequent hydrazone formation only 0.75 eq of 2,4-dinitrophenylhydrazine (**140**) were used to simplify purification of compound **141**. After column chromatography 1-(cyclopropylmethylene)-2-(2,4-dinitrophenyl)hydrazine (**141**) was isolated in 60 % yield (based on substrate **20**). As the trapping reagent **140** was used in substoichiometric amounts, a yield of 79 % was obtained for product **141**.

To confirm that this reductive cyclization reaction is enzyme-catalyzed, a time-conversion study was carried out. We followed the reaction conversions of 3 different samples, compositions of samples A-C are shown in Table 6.

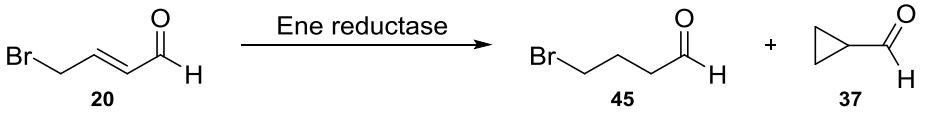

Scheme 76: Model reaction for ene-reductase mediated reductive cyclization.

Table 6: Sample composition for time-conversion study.

Entry	Sample	Enzyme [5 µM]	NADH [15 mM]	Substrate **1** [10 mM]
1	A	-	+	+
2	B	+	-	+
3	C	+	+	+

Sample A and B represent control experiments, in sample A substrate **20** and NADH are incubated without the active enzyme, hence a conversion of the starting material is not observed (Figure 13, Sample A). In sample B the substrate is incubated with the active enzyme but without the addition of NADH, therefore the FMN-cofactor is not reduced. As the hydride is not transferred to the C-β of the substrate, an enolate is not formed and the conversion of the starting material is not observed (Figure 13, Sample B). Sample C shows the successful enzyme catalyzed reaction, the substrate is incubated with enzyme and NADH, conversion of the starting material **20** was monitored over time and within 180 min of reaction time the starting material was completely consumed (Figure 13, Sample C).

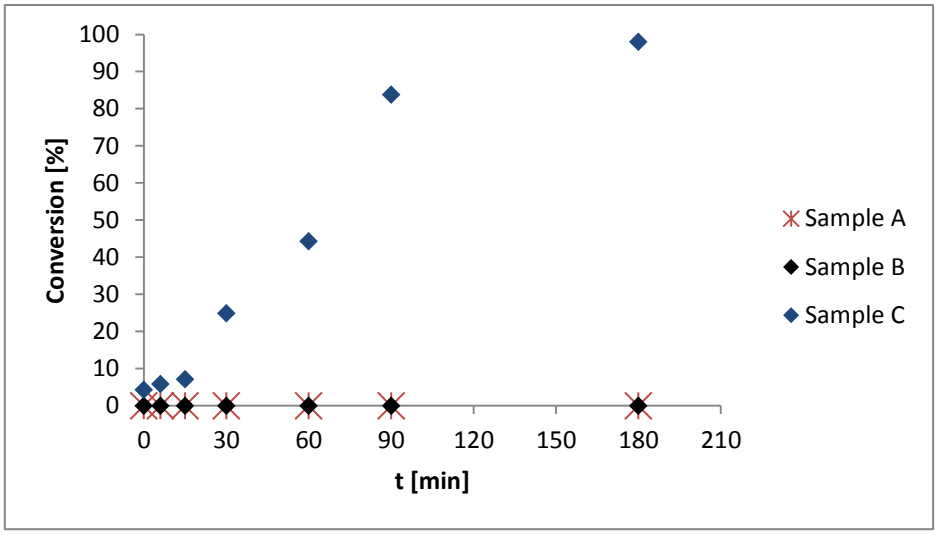

Figure 13: Time conversion study with samples A, B and C.

4.4.1 Influenece of electron withdrawing groups on biocatalytic reductive carbocyclizations

In this biocatalytic C-C bond forming reaction we wanted to investigate how the EWG-moiety is influencing the ring formation activity. Scheme 77 displays the conversion of (*E*)-4-bromobut-2-enal (**20**) and (*E*)-5-bromopent-3-en-2-one (**21**) with ene-reductase wild types and variants. The conversions of (*E*)-4-bromobut-2-enal (**20**) have already been discussed in 4.4.

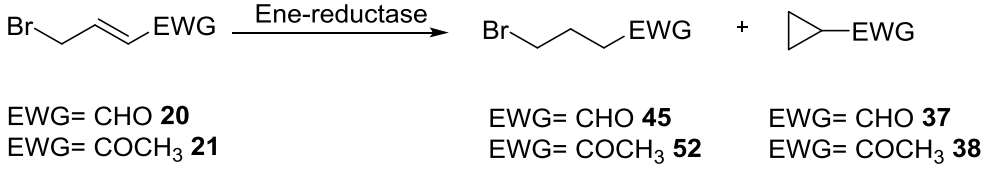

Scheme 77: Conversion of (*E*)-4-bromobut-2-enal (**20**) vs (*E*)-5-bromopent-3-en-2-one (**21**).

Overall the ketone substrate **21** is better accepted by ene-reductases since conversions are higher than those of the aldehyde substrate **20**. For example, Opr3 Y190W shows a moderate conversion of 45 % when (*E*)-4-bromobut-2-enal (**20**) was converted (Table 7, Entry 5). When this variant converts the ketone substrate **21** the overall conversion was increased to 85 % (Table 7, Entry 6). On the other hand YqjM WT and YqjM Y169F seemed to convert both substrates equally well (Table 7, Entries 7-10). In contrast with YqjM Y169W, (*E*)-4-bromobut-2-enal (**20**) was converted in only 3 % while (*E*)-5-bromopent-3-en-2-one (**21**) was converted in up to 28 % (Table 7, Entries 11-12). Regarding the reductive carbocylization reaction, enzymes of Opr show comparable results in the ring formation activity (Table 7, Entries 1-6) when ketone and aldehyde substrates were compared. As it was expected, Opr3 WT showed only a low ring formation activity (up to 34 %) in contrast to Opr3 variants (ring formation activity up to 88 %). Interestingly, a different result was observed when the wild type enzyme of YqjM converts (*E*)-4-bromobut-2-enal (**20**) and (*E*)-5-bromopent-3-en-2-one (**21**). In the conversion of the aldehyde substrate **20** the ring formation activity was drastically enhanced (Table 7, Entry 7) in contrast to the ketone substrate **21** (ring formation up to 7 %, Table 7, Entry 8). The key to achieve high conversions and high ring formation activity is YqjM Y169F, both substrates were converted in >99 % conversion with excellent selectivity for the reductive carbocyclization reaction (up to 98 %, Table 7, Entries 9 and 10).

Table 7: Conversion of (*E*)-4-bromobut-2-enal (**20**) vs (*E*)-5-bromopent-3-en-2-one (**21**).

Entry	Enzyme	EWG	Conversion [%]*	Br–EWG [%]	EWG [%]
1	Opr3 WT	CHO	74	66	34
2	Opr3 WT	$COCH_3$	97	72	28
3	Opr3 Y190F	CHO	93	12	88
4	Opr3 Y190F	$COCH_3$	97	14	86
5	Opr3 Y190W	CHO	45	22	78
6	Opr3 Y190W	$COCH_3$	85	16	84
7	YqjM WT	CHO	>99	59	41
8	YqjM WT	$COCH_3$	>99	93	7
9	YqjM Y169F	CHO	>99	2	98
10	YqjM Y169F	$COCH_3$	>99	2	98
11	YqjM Y169W	CHO	3	50	50
12	YqjM Y169W	$COCH_3$	28	25	75

*Reaction conditions: 300 µL stock solution (10 mM substrate, 1 vol% DMF, $V_{substrate}=V_{1,2\text{-}DME}$ and 15 mM NADH in 50 mM sodium phosphate-buffer at pH 7.5 and 150 mM NaCl) and enzyme (5 µM) in 300 µL sodium phosphate-buffer (50 mM, pH 7.5, 150 mM NaCl) per tube, 180 min and 25 °C at 300 rpm.

In Scheme 78 the conversion of two ester substrates with ene-reductase wild types and variants is displayed.

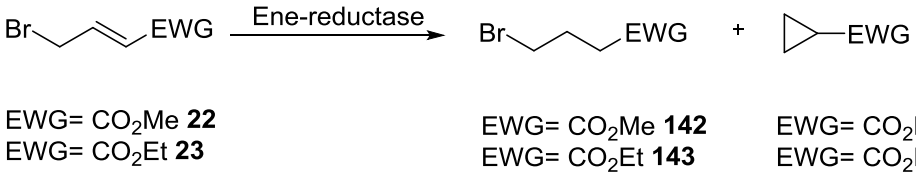

Scheme 78: Synthesis of ethyl (*E*)-4-bromobut-2-enoate (**22**) vs methyl (*E*)-4-bromobut-2-enoate (**23**).

As shown in Table 8, none of the enzymes converted ethyl (*E*)-4-bromobut-2-enoate (**23**) or methyl (*E*)-4-bromobut-2-enoate (**22**). It has already been shown by HALL *et al* that the conversion of simple monocarboxylic esters requires an additional activating group (second ester or a halogen substituent located at the double bond) to be accepted by ene-reductases.[97] Still we wanted to investigate this substrate class for the biocatalytic reductive C-C bond formation.

Table 8: Synthesis of ethyl (*E*)-4-bromobut-2-enoate (**22**) vs methyl (*E*)-4-bromobut-2-enoate (**23**).

Entry	Enzyme	EWG	Conversion [%]*	Br–EWG [%]	EWG [%]
1	Opr3 WT	CO_2Me	nc	nd	nd
2	Opr3 WT	CO_2Et	nc	nd	nd
3	Opr3 Y190F	CO_2Me	nc	nd	nd
4	Opr3 Y190F	CO_2Et	nc	nd	nd
5	Opr3 Y190W	CO_2Me	nc	nd	nd
6	Opr3 Y190W	CO_2Et	nc	nd	nd
7	YqjM WT	CO_2Me	nc	nd	nd
8	YqjM WT	CO_2Et	nc	nd	nd
9	YqjM Y169F	CO_2Me	nc	nd	nd
10	YqjM Y169F	CO_2Et	nc	nd	nd
11	YqjM Y169W	CO_2Me	nc	nd	nd
12	YqjM Y169W	CO_2Et	nc	nd	nd

*Reaction conditions: 300 µL stock solution (10 mM substrate, 1 vol% DMF, $V_{substrate}=V_{1,2\text{-}DME}$ and 15 mM NADH in 50 mM sodium phosphate-buffer at pH 7.5 and 150 mM NaCl) and enzyme (5 µM) in 300 µL sodium phosphate-buffer (50 mM, pH 7.5, 150 mM NaCl) per tube, 180 min and 25 °C at 300 rpm; nc = no conversion, nd = not determined.

4.4.2 Influence of leaving groups on biocatalytic reductive carbocyclizations

Next we wanted to study whether the electrophilicity of the γ-carbon influences the formation of a cyclic product in the ene-reductase enabled carbocyclization reaction. A substrate bearing bromine as leaving group (**20**) and a substrate which bears chlorine as leaving group (**24**) were compared (see Scheme 79).

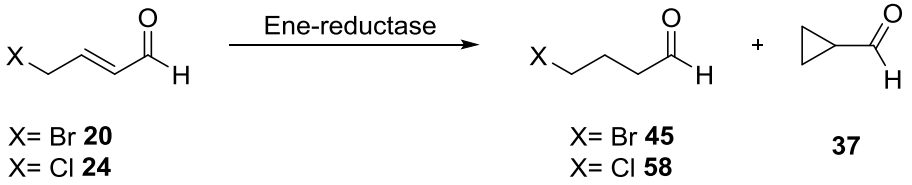

Scheme 79: Conversion of (*E*)-4-bromobut-2-enal (**20**) vs (*E*)-4-chlorobut-2-enal (**24**).

Both substrates were accepted by ene-reductase wild types and variants. Interestingly (*E*)-4-chlorobut-2-enal (**24**) was converted to a higher extent by Opr3 wild types and variants as compared to (*E*)-4-bromobut-2-enal (**20**) (Table 9, Entries 1 to 6). For example, when Opr3 Y190W converted both substrates, compound **24** was converted in up to 85 % (Table 9, Entry 6) whereas compound **20** was converted in only 45 % (Table 9, Entry 5). YqjM WT and YqjM Y169F converted both substrates in >99 % conversion (Table 9, Entries 7 to 10). In

terms of the ring formation activity it is clearly observed that an increase in electrophilicity of the γ-carbon is responsible for higher conversions to cyclopropanecarbaldehyde (**37**). Opr3 WT possesses a low ring formation activity when (*E*)-4-chlorobut-2-enal (**24**) was offered as a substrate. When (*E*)-4-bromobut-2-enal (**20**) was converted by Opr3 WT, a twofold improvement in cyclopropanation activity was observed (Table 9, Entries 1 and 2). A threefold improvement in ring formation activity was observed when Opr3 Y190F converted the bromine substrate **20** (up to 88 %, Table 9, Entry 3) in contrast to the chlorine substrate **24** (27 %, Table 9, Entry 4). Overall the ring formation activity is enhanced by offering a substrate which bears bromine in allylic position, since the γ-carbon renders more electrophilic in contrast to a chlorine in allylic position. However, in contrast to bromine substrates, the chlorine substrates exhibit better stability and are easier to handle.

Table 9: Conversion of (*E*)-4-bromobut-2-enal (**20**) vs (*E*)-4-chlorobut-2-enal (**24**).

Entry	Enzyme	X	Conversion [%]*	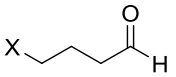	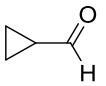
				[%]	[%]
1	Opr3 WT	Br	74	66	34
2	Opr3 WT	Cl	98	85	15
3	Opr3 Y190F	Br	93	12	88
4	Opr3 Y190F	Cl	>99	73	27
5	Opr3 Y190W	Br	45	22	78
6	Opr3 Y190W	Cl	85	82	18
7	YqjM WT	Br	>99	59	41
8	YqjM WT	Cl	>99	83	17
9	YqjM Y169F	Br	>99	2	98
10	YqjM Y169F	Cl	>99	66	34

*Reaction conditions: 300 µL stock solution (10 mM substrate, 1 vol% DMF, $V_{substrate}=V_{1,2\text{-}DME}$ and 15 mM NADH in 50 mM sodium phosphate-buffer at pH 7.5 and 150 mM NaCl) and enzyme (5 µM) in 300 µL sodium phosphate-buffer (50 mM, pH 7.5, 150 mM NaCl) per tube, 180 min and 25 °C at 300 rpm.

4.4.3 Influence of an α-substituent on biocatalytic reductive carbocyclizations

In the experiment discussed in this chapter we wanted to examine if a α-methyl-substituent is influencing the ring formation activity in the ene-reductase enabled reductive carbocyclization. The conversions of (*E*)-4-chlorobut-2-enal (**24**) and (*E*)-4-chloro-2-methylbut-2-enal (**25**) were compared (Scheme 80).

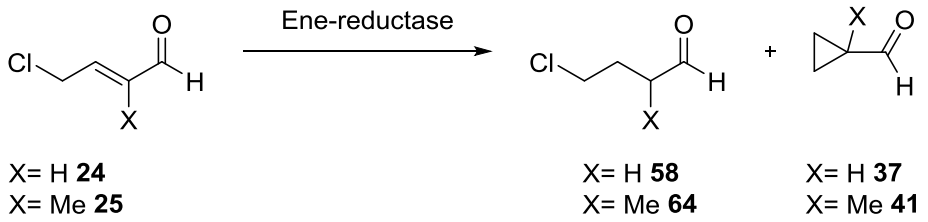

Scheme 80: Conversion of (*E*)-4-chlorobut-2-enal (**24**) vs (*E*)-4-chloro-2-methylbut-2-enal (**25**).

When (*E*)-4-chloro-2-methylbut-2-enal (**25**) was offered as a substrate for enzyme wild types and variants compound **25** was converted perfectly in >99 % conversion (Table 10, Entries 2, 4, 6, 8, 10). Wild type enzymes of Opr3 and YqjM did already display a threefold enhancement in cyclopropanation activity when the α-substituted substrate **25** was offered (Table 10, Entries 2 and 8). The same increase in reductive cyclization activity was observed when variants of Opr3 and YqjM were subjected to (*E*)-4-chloro-2-methylbut-2-enal (**25**) (Table 10, Entries 4, 6 and 10).

Table 10: Conversion of (*E*)-4-chlorobut-2-enal (**24**) vs (*E*)-4-chloro-2-methylbut-2-enal (**25**).

Entry	Enzyme	X	Conversion [%]*	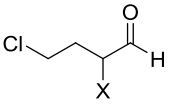 [%]	 [%]
1	Opr3 WT	H	98	85	15
2	Opr3 WT	Me	>99	54	46
3	Opr3 Y190F	H	>99	73	27
4	Opr3 Y190F	Me	>99	32	68
5	Opr3 Y190W	H	85	82	18
6	Opr3 Y190W	Me	>99	35	65
7	YqjM WT	H	>99	83	17
8	YqjM WT	Me	>99	44	56
9	YqjM Y169F	H	>99	66	34
10	YqjM Y169F	Me	>99	24	76

*Reaction conditions: 300 µL stock solution (10 mM substrate, 1 vol% DMF, $V_{substrate}=V_{1,2\text{-DME}}$ and 15 mM NADH in 50 mM sodium phosphate-buffer at pH 7.5 and 150 mM NaCl) and enzyme (5 µM) in 300 µL sodium phosphate-buffer (50 mM, pH 7.5, 150 mM NaCl) per tube, 180 min and 25 °C at 300 rpm.

We hypothesized that this increase in reductive cyclization activity might be the result of the electronic properties from the methyl function in α-position which destabilizes the enolate intermediate. The much more reactive enolate intermediate might be responsible for the enhanced cyclopropanation acitivity. Another possible explanation is that through the additional methyl function, water gets displaced from the active site and the ring-formation activity is therefore enhanced.

We envisioned that the conversion of (*E*)-4-bromo-2-methylbut-2-enal (**26**) with ene-reductase variants and wild types would result in even higher conversions to the cyclopropane product. Unfortunately it was not possible to successfully synthesize (*E*)-4-bromo-2-methylbut-2-enal (**26**).

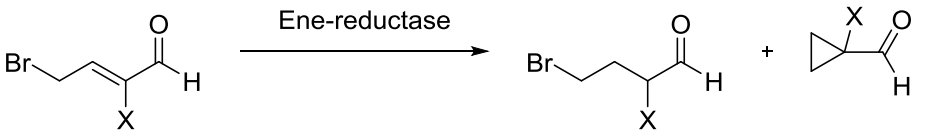

Scheme 81: Conversion of (*E*)-4-bromo-2-methylbut-2-enal (**20**) vs (*E*)-4-bromobut-2-enal (**26**).

4.4.4 Influence of a β-substituent on biocatalytic reductive carbocyclizations

In this chapter we discuss the influence of a substituent in β-position of the double bond on the ene-reductase enabled carbocyclization. This transformation is of great interest, since the conversion of such a substrate could lead to the formation of a cyclopropane with two newly established stereogenic centers (Scheme 82). Our investigation started with the comparison of substrate conversions of the unsubstituted (*E*)-4-chlorobut-2-enal (**24**) and the β-methyl substituted (*E*)-4-chloro-3-methylbut-2-enal (**27**).

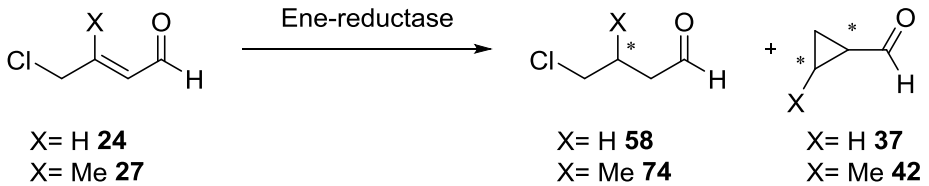

Scheme 82: Conversion of (*E*)-4-chlorobut-2-enal (**24**) vs (*E*)-4-chloro-3-methylbut-2-enal (**27**).

As shown in Table 11 the overall substrate conversion was not affected by a substituent in β-position of the double bond. Opr3 Y190W represents the only exception, since (*E*)-4-

chlorobut-2-enal (**24**) was converted in 85 % whereas (*E*)-4-chloro-3-methylbut-2-enal (**27**) was converted in >99 % (Table 11, Entries 5 and 7). However, wild type enzymes of Opr3 and YqjM did already show a two- to threefold increase in cyclopropanation activity when the methyl-substituted substrate **27** was offered (Table 11, Entries 2 and 8) in contrast to the unsubstituted substrate **24**. Opr3 Y190F and Y190W did convert (*E*)-4-chloro-3-methylbut-2-enal (**27**) to the desired product of reductive cyclization **42** in conversions up to 81 %, which represents a twofold increase in reductive cyclization activity compared to Opr3 WT (Table 11, Entries 4 and 6) . In comparison with the unsubstituted (*E*)-4-chlorobut-2-enal (**24**), Opr3 Y190F showed a threefold and Opr3 Y190W a fourfold improvement in the selectivity of this C-C bond forming reaction (Table 11, Entries 3-6). In summary, through a β-methyl-substituent the reductive cyclization is favoured over the natural ene-reductase reaction.

Table 11: Conversion of (*E*)-4-chlorobut-2-enal (**24**) vs (*E*)-4-chloro-3-methylbut-2-enal (**27**).

Entry	Enzyme	X	Conversion [%]*	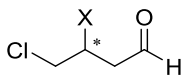 [%]	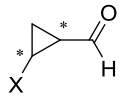 [%]
1	Opr3 WT	H	98	85	15
2	Opr3 WT	Me	>99	57	43
3	Opr3 Y190F	H	>99	73	27
4	Opr3 Y190F	Me	>99	19	81
5	Opr3 Y190W	H	85	82	18
6	Opr3 Y190W	Me	>99	22	78
7	YqjM WT	H	>99	83	17
8	YqjM WT	Me	95	69	31
9	YqjM Y169F	H	>99	66	34
10	YqjM Y169F	Me	>99	12	88

*Reaction conditions: 300 µL stock solution (10 mM substrate, 1 vol% DMF, $V_{substrate}$=$V_{1,2\text{-}DME}$ and 15 mM NADH in 50 mM sodium phosphate-buffer at pH 7.5 and 150 mM NaCl) and enzyme (5 µM) in 300 µL sodium phosphate-buffer (50 mM, pH 7.5, 150 mM NaCl) per tube, 180 min and 25 °C at 300 rpm.

As we have already discussed in 4.4.2 the selectivity of this reductive C-C bond formation increases when a substrate with bromine as leaving group is offered to ene-reductases. We investigated if cyclopropanation acitivity is further increased by offering (*E*)-4-bromo-3-methylbut-2-enal (**28**) as a substrate for ene-reductase mediated carbocyclization (Scheme 83).

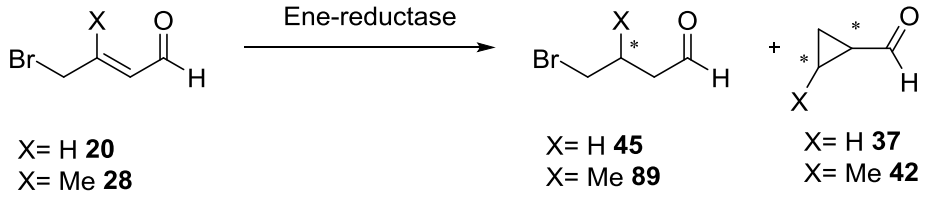

Scheme 83: Conversion of (*E*)-4-bromobut-2-enal (**20**) vs (*E*)-4-bromo-3-methylbut-2-enal (**28**).

Table 12 compares the conversions and selectivities of (*E*)-4-bromobut-2-enal (**20**) and (*E*)-4-bromo-3-methylbut-2-enal (**28**). When methyl substituted substrate **28** was incubated with enzymes of Opr3 an increase in the overall conversion was observed compared to unsubstituted substrate **20** (Table 12, Entries 1 to 6). The selectivity of Opr3 wild type enzyme was tremendously increased when a substrate bearing a β-methyl-substituent **28** was provided (Table 12, Entries 1 and 2). When the unsubstitued (*E*)-4-bromobut-2-enal (**20**) was converted, the formation of a cyclopropane product was observed in 34 % selectivity. When the β-methyl substituted substate **28** was offered to Opr3 WT then the formation of the cyclopropane product **42** was observed in 87 % selectivity, which represents a 2.5-fold increase in cyclopropanation activity. It is worth mentioning that Opr3 Y190F and YqjM Y169F transformed (*E*)-4-bromo-3-methylbut-2-enal in (**28**) >99 % conversion and with excellent selectivity for the reductive cyclization reaction (Table 12, Entries 4 and 10). Although Opr3 Y190W displayed a moderate conversion of both substrates (45 % and 70 %) the cyclopropanation activity is excellent when converting (*E*)-4-bromo-3-methylbut-2-enal (**28**) (Table 12, Entry 6).

Table 12: Conversion of (*E*)-4-bromobut-2-enal (**20**) vs (*E*)-4-bromo-3-methylbut-2-enal (**28**).

Entry	Enzyme	X	Conversion [%]*	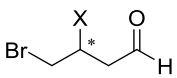 [%]	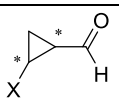 [%]
1	Opr3 WT	H	74	66	34
2	Opr3 WT	Me	>99	13	87
3	Opr3 Y190F	H	93	12	88
4	Opr3 Y190F	Me	>99	<1	>99
5	Opr3 Y190W	H	45	22	78
6	Opr3 Y190W	Me	70	<1	>99
7	YqjM WT	H	>99	59	41
8	YqjM WT	Me	>99	35	65
9	YqjM Y169F	H	>99	2	98
10	YqjM Y169F	Me	>99	<1	>99

*Reaction conditions: 300 µL stock solution (10 mM substrate, 1 vol% DMF, $V_{substrate}$=$V_{1,2\text{-}DME}$ and 15 mM NADH in 50 mM sodium phosphate-buffer at pH 7.5 and 150 mM NaCl) and enzyme (5 µM) in 300 µL sodium phosphate-buffer (50 mM, pH 7.5, 150 mM NaCl) per tube, 180 min and 25 °C at 300 rpm.

Once more, we wanted to investigate the influence of the leaving group on the ene-reductase mediated reductive carbocyclization (Scheme 84) when a substrate with a substitution in β-position is offered to ene-reductases.

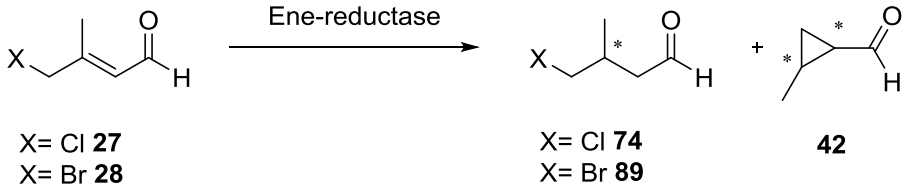

Scheme 84: Conversion of (*E*)-4-chloro-3-methylbut-2-enal (**27**) vs (*E*)-4-bromo-3-methylbut-2-enal (**28**).

As it was already discussed in 4.4.2 when a substrate which bears bromine in allylic position is offered to ene-reductases, the ring formation activity is tremendously enhanced since the γ-carbon renders more electrophilic in contrast to chlorine in allylic position. This trend is also reflected in Table 13. When the bromine substrate **28** was offered to all enzyme wild types and variants, the selectivity for the C-C bond forming reaction was clearly enhanced when compared to the chlorine substrate **27**.

Table 13: Conversion of (*E*)-4-chloro-3-methylbut-2-enal (**27**) vs (*E*)-4-bromo-3-methylbut-2-enal (**28**).

Entry	Enzyme	X	Conversion [%]*	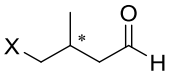 [%]	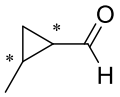 [%]
1	Opr3 WT	Cl	>99	57	43
2	Opr3 WT	Br	>99	13	87
3	Opr3 Y190F	Cl	>99	19	81
4	Opr3 Y190F	Br	>99	<1	>99
5	Opr3 Y190W	Cl	>99	22	78
6	Opr3 Y190W	Br	70	<1	>99
7	YqjM WT	Cl	95	69	31
8	YqjM WT	Br	>99	35	65
9	YqjM Y169F	Cl	>99	12	88
10	YqjM Y169F	Br	>99	<1	>99

*Reaction conditions: 300 µL stock solution (10 mM substrate, 1 vol% DMF, $V_{substrate}$=$V_{1,2\text{-DME}}$ and 15 mM NADH in 50 mM sodium phosphate-buffer at pH 7.5 and 150 mM NaCl) and enzyme (5 µM) in 300 µL sodium phosphate-buffer (50 mM, pH 7.5, 150 mM NaCl) per tube, 180 min and 25 °C at 300 rpm.

As already mentioned before, the conversion of a substrate with a β-substituent leads to the formation of a cyclopropane with two newly established stereogenic centers. As ene-reductases possess a known potential for the asymmetric reduction of activated double bonds,

we wanted to examine if ene-reductases are capable of performing an asymmetric reductive carbocyclization reaction.

Table 14 displays the diastereomeric and enantiomeric excess of (2-methylcyclopropyl)methanol products (**75**) obtained from the conversion of (*E*)-4-chloro-3-methylbut-2-enal (**27**) with ene-reductase variants.

Table 14: Determination of the diastereomeric and enantiomeric excess of (2-methylcyclopropyl)methanol (**75**).

Entry	Enzyme	*de trans*/*cis* [%]	*ee* [%] 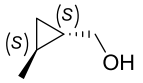	*ee* [%] 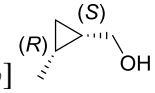
1	Opr3 WT	68	87	>99
2	Opr3 Y190F	57	61	54
3	Opr3 Y190W	64	31	24
4	YqjM WT	67	52	56
5	YqjM Y169F	72	-80	-55

When (*E*)-4-chloro-3-methylbut-2-enal (**27**) served as a substrate for Opr3 and YqjM wild types good de's up to 68 % were obtained (Table 14, Entries 1 and 4). The mutation of the tyrosine residue in YqjM and Opr3 did not seem to affect the diastereoselectivities (Table 14, Entries 2, 3 and 6). We observed that Opr3 WT has a strong preference for the (*R*,*S*)-**75** stereoisomer, which was obtained in >99 % ee (Table 14, Entry 1). In contrast, Opr3 Y190F and Opr3 Y190W showed only moderate stereoinduction (Table 14, Entries 2 and 3). The YqjM WT showed a slight preference for the (*S*,*S*)-**75** stereoisomer (Table 14, Entry 4). Interestingly the Phe variant showed a reversed as well as enhanced enantioselectivity, indicating that subtle changes in the binding site might have large consequences in substrate recognition (Table 14, Entry 5).

Table 15 summarizes the diastereomeric and enantiomeric excess of (2-methylcyclopropyl)methanol products (**75**) obtained from the conversion of (*E*)-4-bromo-3-methylbut-2-enal (**28**) with ene-reductase variants. Unfortunately, the ee of the *cis*-product could not be determined as a by-product of the reduction of **28** was overlaying with the product peaks.

Table 15: Determination of the diastereomeric and enantiomeric excess of (2-methylcyclopropyl)methanol (**75**).

Entry	Enzyme	*de trans/cis* [%]	*ee* [%] 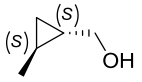	*ee* [%] 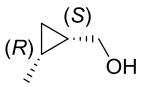
1	Opr3 WT	14	92	nd
2	Opr3 Y190F	58	22	nd
3	Opr3 Y190W	13	39	nd
4	YqjM WT	-54	81	nd
5	YqjM Y169F	-30	-67	nd

nd = not determined.

When (*E*)-4-bromo-3-methylbut-2-enal (**28**) was provided as a substrate to Opr3 Y190F *trans*-**75** (de 58 %) was favoured, which represents a 4-fold improvement over Opr3 WT and Opr3 Y190W (Table 15, Entries 1 to 3). YqjM WT and its Phe variant showed a reversed diastereoselectivity, however only moderate de's were obtained (Table 15, Entries 4 and 5). We observed that Opr3 WT has a strong preference for the (*S*,*S*)-**75** stereoisomer, which was obtained in 92 % ee (Table 15, Entry 1). In contrast, Opr3 Y190F and Opr3 Y190W showed only slight stereoinduction (Table 15, Entries 2 and 3). The Yqjm WT showed a strong preference for the (*S*,*S*)-**75** stereoisomer (Table 15, Entry 4). Interestingly, the Phe variant showed again reversed enantioselectivity (Table 15, Entry 5).

To elucidate if the leaving group has an influence on the diastereoselctivities and enantioselectivities of (2-methylcyclopropyl)methanol products, we compared de's and ee's of reductive cyclization products obtained by the conversions of (*E*)-4-chloro-3-methylbut-2-enal (**27**) and (*E*)-4-bromo-3-methylbut-2-enal (**28**) (Scheme 85, Table 16).

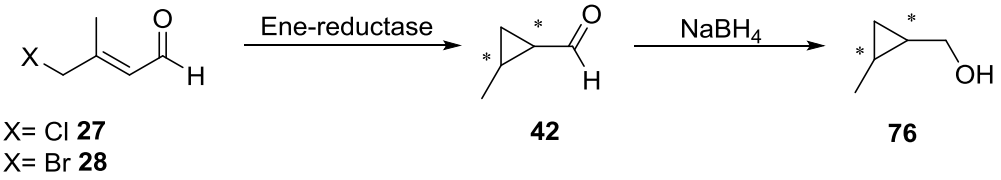

Scheme 85: Comparison of the diastereomeric and enantiomeric excess of the conversions of (*E*)-4-chloro-3-methylbut-2-enal (**27**) vs (*E*)-4-bromo-3-methylbut-2-enal (**28**).

When (*E*)-4-chloro-3-methylbut-2-enal (**27**) was offered as a substrate for Opr3 enzymes promising de's (up to 68 %) were obtained (Table 16, Entries 1, 3 and 5). Low diastereoselectivities were observed when (*E*)-4-bromo-3-methylbut-2-enal (**28**) was incubated with Opr3 WT and Opr3 Y190W indicating that various binding modes of the substrate in the active site are possible. Surprisingly, when (*E*)-4-bromo-3-methylbut-2-enal

(**28**) served as a substrate for YqjM WT and YqjM Y169F, a reversed diastereoselectivity was observed compared to the conversion of the chlorine substrate **27** (Table 16, Entries 8 and 10). The conversion of the bromine **28** or the chlorine substrate **27** in Opr3 WT, Opr3 Y190W and YqjM Y169F did not seem to affect the entioselectivity of (*S,S*)-**75** since comparable ee's were obtained (Table 16, Entries 1, 2, 5, 6, 9, and 10). In contrast, Opr3 Y190F conversion of chlorine substrate **27** delivered (*S*,*S*)-**76** in up to 61 % ee while the bromine substrate delivered the (*S*,*S*)-stereoisomer in only 22 % ee. A different result was observed in YqjM WT, the chlorine substrate **27** delivered the (*S*,*S*)-stereoisomer in 52 % ee, while the bromine substrate **28** produced (*S*,*S*)-**75** in a good ee of 81 %.

Table 16: Comparision of the diastereomeric and enantiomeric excess of the conversions of (*E*)-4-chloro-3-methylbut-2-enal (**27**) vs (*E*)-4-bromo-3-methylbut-2-enal (**28**).

Entry	Enzyme	X	*de trans*/*cis* [%]	*ee* [%] 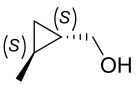	*ee* [%] 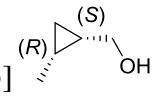
1	Opr3 WT	Cl	68	87	>99
2	Opr3 WT	Br	14	92	nd
3	Opr3 Y190F	Cl	57	61	54
4	Opr3 Y190F	Br	58	22	nd
5	Opr3 Y190W	Cl	64	31	24
6	Opr3 Y190W	Br	13	39	nd
7	YqjM WT	Cl	67	52	56
8	YqjM WT	Br	-54	81	nd
9	YqjM Y169F	Cl	72	-80	-55
10	YqjM Y169F	Br	-30	-67	nd

nd = not determined.

The biocatalytic reductive C-C bond formation, so far presented in this chapter, achieved synthetically useful conversions, albeit the stereoselectivity of ene-reductases was moderate. We assume that by offering substrates with sterically demanding substituents to ene-reductases, we could further increase the diastereoselectivities and enantioselectivities. As already discussed in 4.2.8 it was not possible to synthesize a substrate with an isopropyl group at the β-position of the double bond so far. Nevertheless, we wanted to further investigate the ene-reductase enabled reductive carbocyclization and we were interested in engineering a substrate to enhance the enantiodiscrimination and the selectivity of this biocatalytic C-C bond forming reaction. We hypothesized that a sterically demanding and apolar phenyl-substituent at β-position would on the one hand be potentially highly enantiodiscriminating and on the other hand further enhance the selectivity of the reductive cyclization reaction over the natural reduction reaction. This apolar substituent could further increase the activity for

the ring forming reaction since water molecules might be displaced from the active site effectively.

So we provided (*E*)-4-chloro-3-phenylbut-2-enal (**31**) as a substrate for the ene-reductase enabled carbocyclization reaction and compared conversions and selectivities with substrates bearing a hydrogen, substrate **24**, or a methyl-group, substrate **27**, at β-position of the double bond (Scheme 86).

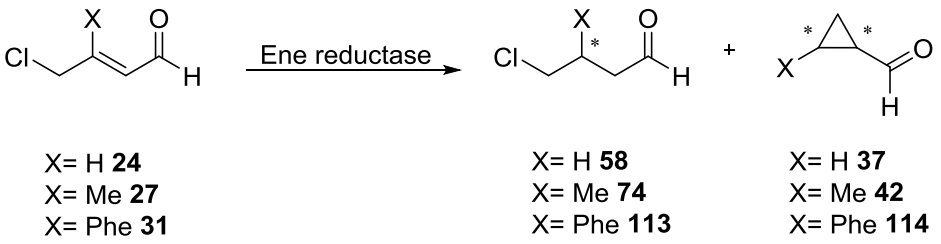

Scheme 86: Conversion of substrate **24**, **27,** and **31** by ene-reductases.

Table 17: Conversion of (*E*)-4-chlorobut-2-enal (**24**) vs (*E*)-4-chloro-3-methylbut-2-enal (**27**) vs (*E*)-4-chloro-3-phenylbut-2-enal (**31**).

Entry	Enzyme	X	Conversion [%]*	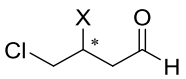 [%]	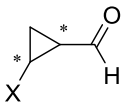 [%]
1	Opr3 WT	H	98	85	15
2	Opr3 WT	Me	>99	57	43
3	Opr3 WT	Ph	>99	52	48
4	Opr3 Y190F	H	>99	73	27
5	Opr3 Y190F	Me	>99	19	81
6	Opr3 Y190F	Ph	>99	25	75
7	Opr3 Y190W	H	85	82	18
8	Opr3 Y190W	Me	>99	22	78
9	Opr3 Y190W	Ph	94	29	71
10	YqjM WT	H	>99	83	17
11	YqjM WT	Me	95	69	31
12	YqjM WT	Ph	81	28	72
13	YqjM Y169F	H	>99	66	34
14	YqjM Y169F	Me	>99	12	88
15	YqjM Y169F	Ph	89	5	95

*Reaction conditions: 300 µL stock solution (10 mM substrate, 1 vol% DMF, $V_{substrate}=V_{1,2\text{-DME}}$ and 15 mM NADH in 50 mM sodium phosphate-buffer at pH 7.5 and 150 mM NaCl) and enzyme (5 µM) in 300 µL sodium phosphate-buffer (50 mM, pH 7.5, 150 mM NaCl) per tube, 180 min and 25 °C at 300 rpm.

Opr3 WT and Opr3 Y190F converted (*E*)-4-chloro-3-phenylbut-2-enal (**31**) in excellent conversions (up to >99 %, Table 17, Entries 3 and 6). An influence of the sterically demanding phenyl group at C-β did not seem to have any effect on conversions when compared to substrates which carry either no substituent (**24**) or a methyl-group at β-position (**27**) (Table 17, Entries 1, 2, 4 and 5). When Opr3 Y190W, YqjM WT and YqjM Y169F were incubated with (*E*)-4-chloro-3-phenylbut-2-enal (**31**), the conversion decreased to a small extent when compared to the conversions obtained by the incubation with (*E*)-4-chloro-3-methylbut-2-enal (**27**) (Table 17, Entries 9, 12 and 15). For all Opr3 enzymes the selectivity of the C-C bond formation was still higher in conversion of (*E*)-4-chloro-3-phenylbut-2-enal (**31**) (Table 17, Entries 6 and 9). Interestingly, in YqjM WT and YqjM Y169F the conversion of a phenyl substituted substrate **31** increased the selectivity of the C-C bond forming reaction in comparison to the methyl substituted substrate **27** (Table 17, Entries 12 and 15). In particular, when YqjM WT converted (*E*)-4-chloro-3-phenylbut-2-enal (**31**) a twofold enhancement in the reductive cyclization selectivity was obtained (up to 72 %).

Another interesting aspect of the conversion of (*E*)-4-chloro-3-phenylbut-2-enal (**31**) by ene-reductases is the effect of the phenyl-substituent on the diastereosectivities of (2-phenylcyclopropyl)methanol (**115**) products. Table 18 summarizes the comparison of the diastereoselectivities in (2-methylcyclopropyl)methanol (**75**) and (2-phenylcyclopropyl)methanol products (**115**).

Table 18: Comparison of diastereoselectivities in (2-methylcyclopropyl)methanol (**75**) and (2-phenylcyclopropyl)methanol (**115**).

Entry	Enzyme	X	*de trans*/*cis* [%]
1	Opr3 WT	Me	68
2	Opr3 WT	Ph	72
3	Opr3 Y190F	Me	57
4	Opr3 Y190F	Ph	71
5	Opr3 Y190W	Me	64
6	Opr3 Y190W	Ph	71
7	YqjM WT	Me	67
8	YqjM WT	Ph	-30
9	YqjM Y169F	Me	72
10	YqjM Y169F	Ph	94

As expected, diastereoselectivities of products were enhanced when a phenyl substituted substrate **31** was offered compared to a substrate which bears a methyl-function in β-position

27 (Table 18, Entries 1 to 10). Interestingly, YqjM WT displayed a reversed diastereoselectivity when (*E*)-4-chloro-3-phenylbut-2-enal (**31**) was offered as a substrate, since the *cis*-diastereomer of **115** was slightly favoured (Table 18, Entry 8). YqjM Y169F displayed a strong preference for one single diastereomer, *trans*-(2-phenylcyclopropyl)methanol (**115**) was obtained in a very good de of 94 %. Table 19 lists the enantiomeric excess of (2-phenylcyclopropyl)methanol (**115**) products.

Table 19: Determination of the absolute configruation and enantiomeric excess of (2 phenylcyclopropyl)methanol (**115**).

Entry	Enzyme	*ee* [%] 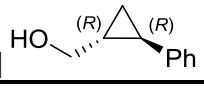	*ee* [%] 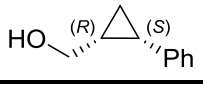
1	Opr3 WT	>99	54
2	Opr3 Y190F	>99	-43
3	Opr3 Y190W	>99	-51
4	YqjM WT	>99	-8
5	YqjM Y169F	>99	-29
6	YqjM Y169W	nd	nd

nd = not determined.

Substrate engineering strongly affected the enantiodiscrimination in the ene-reductase enabled carbocyclization. By offering (*E*)-4-chloro-3-phenylbut-2-enal (**31**) as a substrate for ene-reductase wild types and variants excellent stereoselectivities were obtained. All enzyme wild types as well as variants strongly favoured (*R,R*)-**115** of the *trans*-diastereomer. None of the enzymes seem to favour one single enantiomer of *cis*-(2-phenylcyclopropyl)methanol (**115**), only low to moderate ee's were obtained. The exchange of the Tyr residue against Phe in YqjM seems to be the key for achieving high diastereoselectivity and high enantioselectivity in this C-C bond forming reaction. In the conversion of (*E*)-4-chloro-3-phenylbut-2-enal with YqjM Y169F the (*R,R*)-(2 phenylcyclopropyl)methanol (**115**) was obtained in excellent 95 % conversion with a strong preference for one single diastereomer and one single enantiomer (de 94 % and ee >99 %).

4.4.5 Influence of EWG- and EDG-substituents on biocatalytic reductive carbocyclizations

In the previous chapter we discussed the influences of steric effects at the β-position on the reductive carbocyclization reactions enabled by ene-reductases. An even more interesting question is how electronic effects would influence the reductive cyclization reaction concerning the ring formation activity. Moreover, how would diastereoselectivites and enantioselectivities be affected by an electron-deficient or an electron-rich substituent.

Scheme 87 illustrates the attempted conversion of (*E*)-4-chloro-3-(4-methoxyphenyl)but-2-enal (**33**) and (*E*)-4-chloro-3-(4-(trifluoromethyl)phenyl)but-2-enal (**34**) by ene-rerductases.

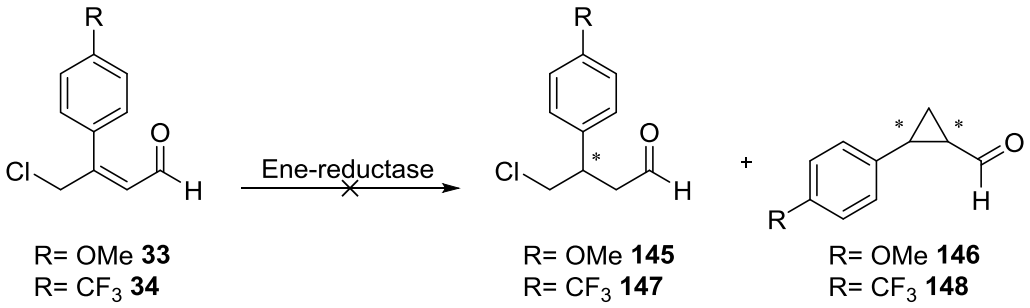

Scheme 87: Conversion of (*E*)-4-chloro-3-(4-methoxyphenyl)but-2-enal (**33**) and (*E*)-4-chloro-3-(4-(trifluoromethyl)phenyl)but-2-enal (**34**).

In the conversion of (*E*)-4-chloro-3-(4-methoxyphenyl)but-2-enal (**33**) and (*E*)-4-chloro-3-(4-(trifluoromethyl)phenyl)but-2-enal (**34**) by all ene-reductase wild types and variants it was not possible to interpret chromatograms obtained from GC-FID. Both substrates led to the formation of numerous by-products, which could not be identified by GC-MS. Unfortunately, it was not possible to generate any data which would provide trustworthy information.

5 Summary

The aim of this work was the investigation of a potential reductive C-C coupling reaction catalyzed by ene-reductases. Variants from Opr3 and YqjM were generated in which the Tyr-residue, which acts as a proton donor, is replaced against an amino acid which is not able to act as a proton donor (i.e. Phe, Trp). The reaction should follow the proposed mechanism shown in Scheme 88. The FMN-hydride should attack at C-β but the reprotonation step (usually a proton from a Tyr-residue is transferred to C-α) should be prevented. Instead of the reprotonation step (Scheme 88, red arrow) the enolate should alternatively attack the internal electrophile forming a cyclization product (Scheme 88, blue arrow).

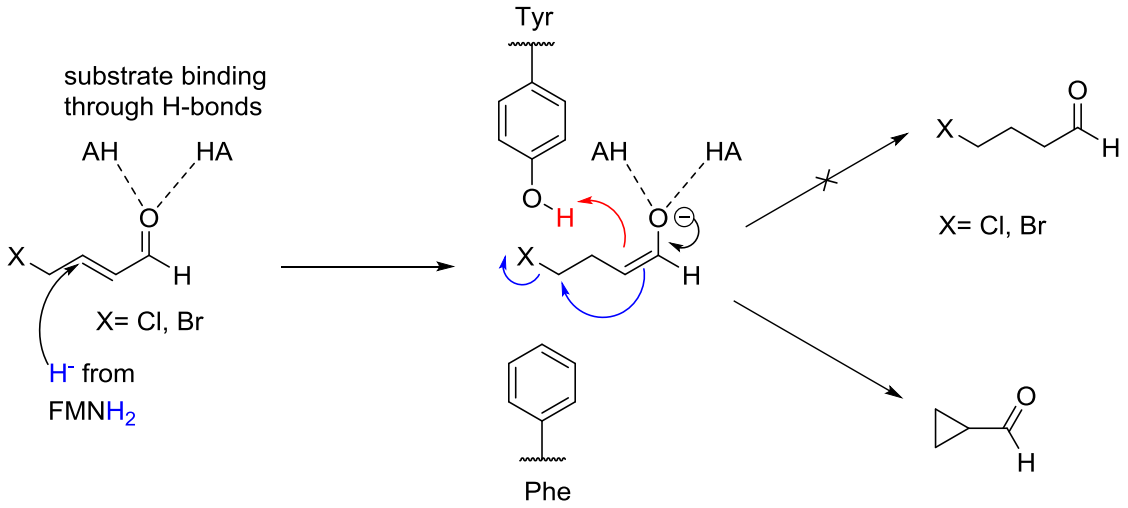

Scheme 88: Proposed mechanism for the reductive cyclization using engineered ene-reductases. Blue arrows indicate the reductive cyclization pathway, red arrows indicate the natural reduction pathway of ene-reductases.

Compounds which are suitable to serve as substrates for this reductive C-C bond forming reaction were synthesized and tested in biocatalytic experiments (Scheme 89).

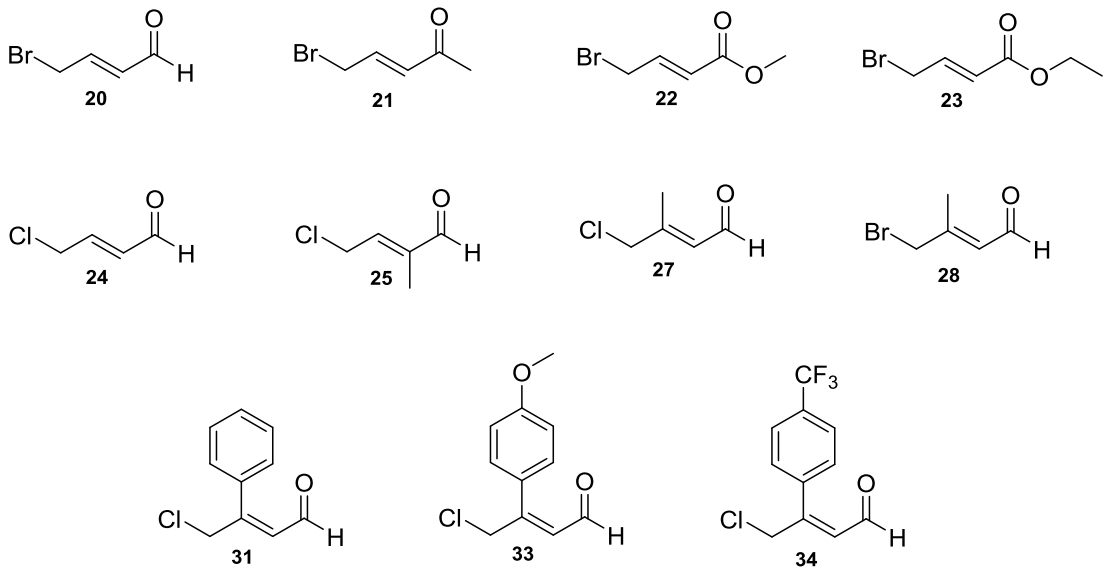

Scheme 89: Synthesized substrates for the reductive carbocycliaztion with engineered ene-reductases.

Aldehyde substrates (**20**, **24**, **25**, **27**, **28**, **31**, **33**, **34**) were prepared via WITTIG-olefination of the corresponding aldehyde or ketone. The hydroxyl-function of the allylic alcohol was converted to bromine or chlorine via an APPEL-reaction. In the last two steps of the synthetic sequence, the ester functionality was reduced with DIBAL-H to the corresponding allylic alcohol, which was then subsequently oxidized to the corresponding allylic aldehyde by MnO_2. A representative synthetic sequence is shown in Scheme 90.

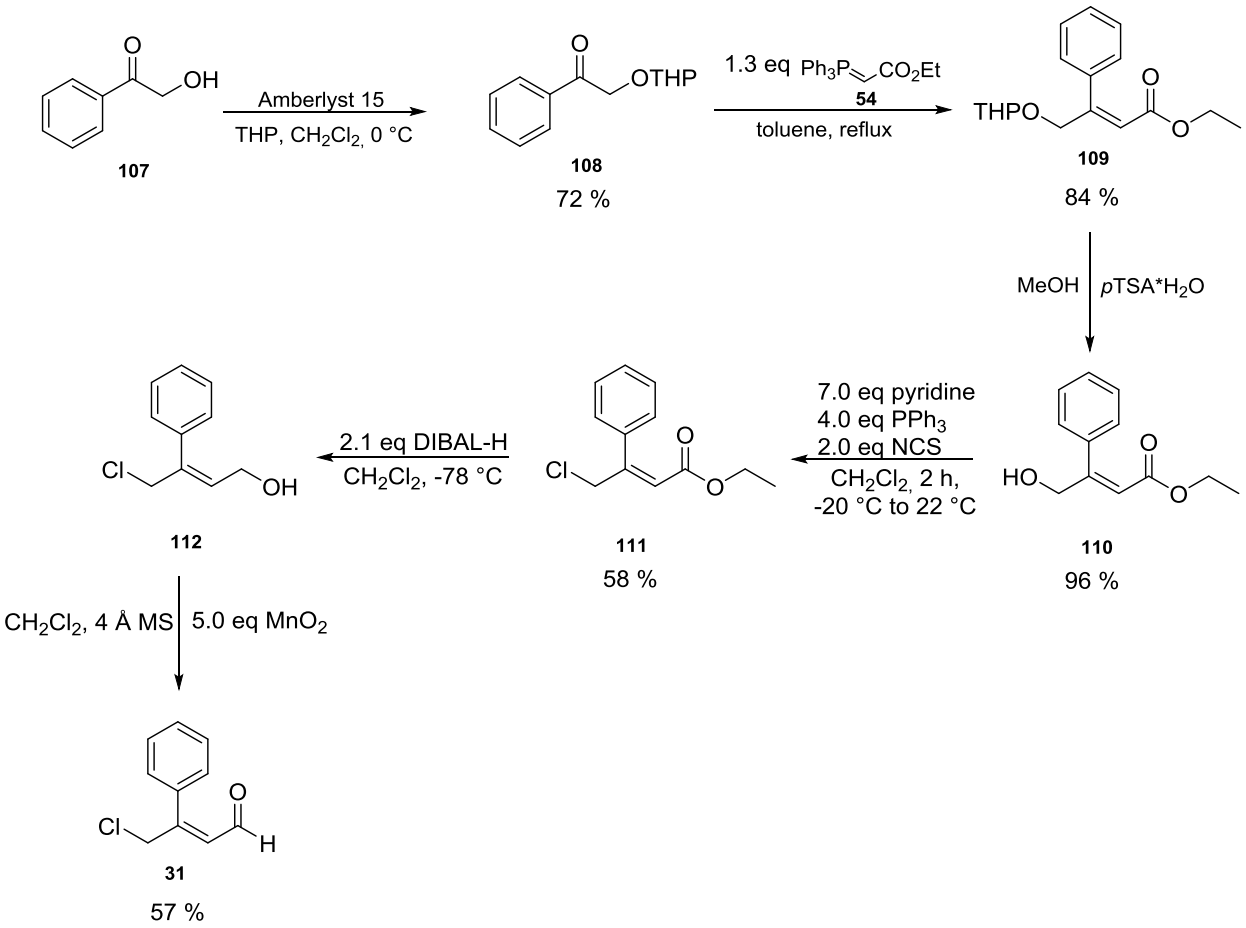

Scheme 90: Synthesis of (*E*)-4-chloro-3-phenylbut-2-enal (**31**).

The synthesis of the ketone substrate (*E*)-5-bromopent-3-en-2-one (**21**) was accomplished by WITTIG-olefination of 2-bromoacetaldehyde (**50**) (Scheme 91).

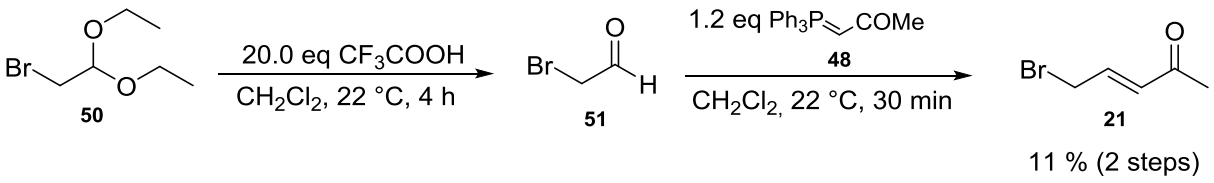

Scheme 91: Synthesis of (*E*)-5-bromopent-3-en-2-one (**21**).

Methyl-ester and ethyl-esters are unsuitable substrates for the ene-reductase enabled carbocyclization reaction, since substrates **22** and **23** were not converted by ene-reductase wild type enzymes and variants (Scheme 92). The aldehyde substrate **20** already indicated, upon the conversion with wild type enzymes, that a reductive cyclization reactions takes place, i.e. Opr3 WT delivered **37** in 30 % conversion. A two to three-fold improvement in the reductive cyclization activity was observed when variants of Opr3 and YqjM were used. Opr3 Y190F showed 88 % conversion to cyclopropanecarbaldehyde (**37**). The ketone substrate **21** showed comparable conversions to **38** when converted with ene-reductase variants, but when substrate **21** was converted with enzyme wild types, the conversion to **38** was rather low. The enzyme which displayed the best activity throughout this thesis was YqjM Y169F since it converted substrates **20** and **21** with full conversion and excellent selectivity for the reductive carbocyclization reaction (up to 98 %).

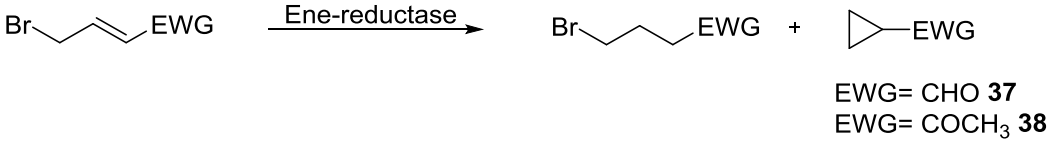

EWG= CO_2Me **22**	all enzymes	nc	nc
EWG= CO_2Et **23**	all enzymes	nc	nc
EWG= CHO **20**	Opr3 WT	70 %	30 %
EWG= CHO **20**	Opr3 Y190F	12 %	88 %
EWG= CHO **20**	YqjM Y169F	2 %	98 %
EWG= $COCH_3$ **21**	YqjM Y169F	2 %	98 %

Scheme 92: Substrates **20**, **21**, **22**, and **23** for the ring formation activity; nc = no conversion.

It was possible to scale-up the reaction with YqjM Y169F and substrate **20**. The cyclopropanecarbaldehyde was isolated as its (*E/Z*)-1-(cyclopropylmethylene)-2-(2,4-dinitrophenyl)hydrazine (**141**) in 60 % yield over 2 steps (Scheme 93).

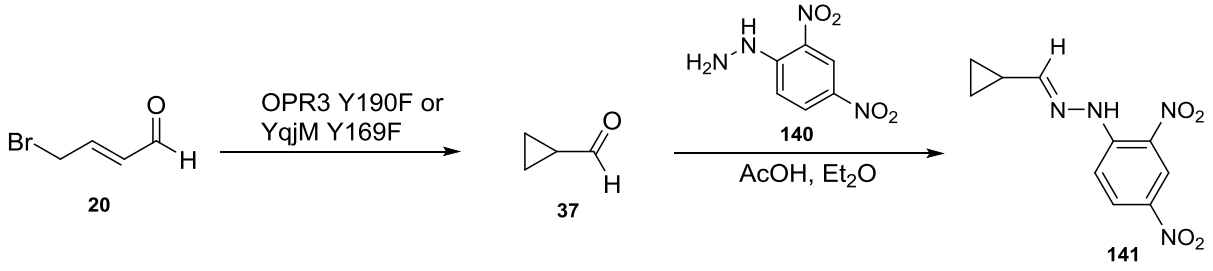

Scheme 93: Preparative reductive carbocyclization using YqjM Y169F.

The electrophilicity of the γ-carbon influences the formation of a cyclic product in the ene-reductase enabled carbocyclization reaction. One representative example is the conversion of bromine substrate **20**, which delivered upon conversion with YqjM Y169F, cyclopropanecarbaldehyde (**37**) in 98 %, while the conversion of chlorine substrate **24** delivered compound **37** in only 34 % (

Scheme **94**).

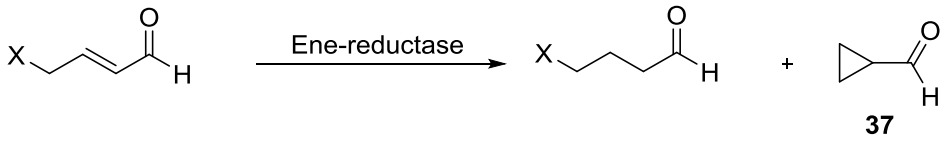

X= Br **20**	YqjM Y169F	2 %	98 %
X= Cl **24**	YqjM Y169F	66 %	34 %

Scheme 94: Conversion of (*E*)-4-chlorobut-2-enal (**24**) vs (*E*)-4-bromobut-2-enal (**20**).

A substituent in α-position of the double bond increases the formation of a cyclic product (Scheme 95). When (*E*)-4-chloro-2-methylbut-2-enal (**25**) was offered as a substrate for enzyme wild types and variants, a two to three-fold enhancement for the reductive cyclization activity was observed when compared to unsubstituted substrate **24**. For example, Opr3 Y190W transformed **24** in 18 % conversion to **37** and α-methyl substituted substrate **25** was converted in up to 65 % conversion to **41**.

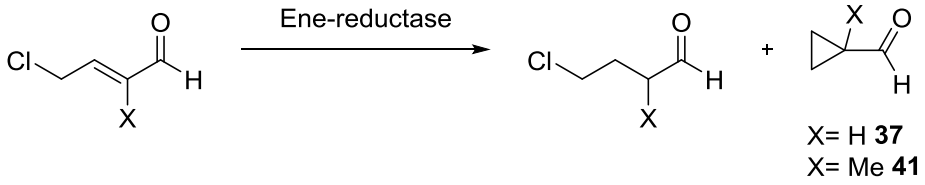

X= H **24**	Opr3 Y190W	82 %	18 %
X= Me **25**	Opr3 Y190W	35 %	65 %

Scheme 95: Conversion of (*E*)-4-chlorobut-2-enal (**24**) vs (*E*)-4-chloro-2-methylbut-2-enal (**25**).

Through the substitution at β-position of the substrate a two to three-fold improvement in the formation of a cyclic product was observed (Scheme 96). Again, the selectivity for the C-C bond forming reaction was increased when bromine substrate **28** was offered to all enzyme wild types and variants when compared to the chlorine substrate **27**. For example, when

substrate **28** was converted by YqjM Y169F the product of the C-C bond forming reaction **42** was obtained in 99 % conversion while the chlorine substrate delivered **42** in 88 % conversion. Overall, the diastereoselectivities and stereoselectivities of cyclopropane product **42** were moderate to low when substrates **27** and **28** were converted. The only exception was Opr3 WT, which accomplished ee's up to 90 %.

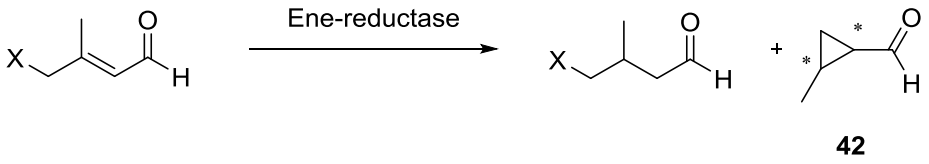

42

X= Cl **27**	YqjM Y169F	12 %	88 %
X= Br **28**	YqjM Y169F	2 %	98 %

Scheme 96: Conversion of (*E*)-4-chloro-3-methylbut-2-enal (**27**) vs (*E*)-4-bromo-3-methylbut-2-enal (**28**).

A substrate bearing a sterically demanding substituent at the β-position of the double bond led to an improved enantiodiscrimination (Scheme 97). All enzyme wild types as well as variants achieved excellent stereoselectivities by strongly favouring the (*R*,*R*)-enantiomer of **114**. It is worth mentioning, that with YqjM Y169F (*R*,*R*)-**114** was produced in an excellent conversion of 95 % with a strong preference for one single diastereomer and one single enantiomer (de 94 % and ee >99 %).

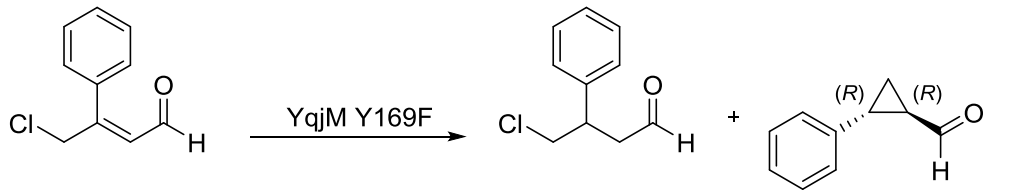

31 **113** **114**

conversion up to 95 %
de 94 %
ee > 99%

Scheme 97: Conversion of (*E*)-4-chloro-3-phenylbut-2-enal (**31**).

6 Future Work

Future work should aim for an extension of the substrate scope of this C-C bond forming reaction. Since the conversion of a substrate which bears a sterically demanding phenyl-group at position-β of the double bond drastically increased the enantiodiscrimination in the ene-reductase enabled carbocyclization reaction, it would be obvious to test the size limitation of the β-substituent. Scheme 98 displays possible substrates with sterically demanding substituent at C-β and their expected cyclization products.

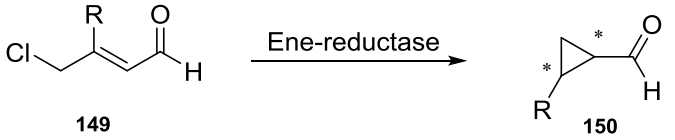

149 **150**

R= toluoyl, naphtyl, tert-butylbenzene

Scheme 98: Substrates bearing various sterically demanding substituents at the β-position of the double bond **149** and expected cyclization products **150**.

Since the focus of this work was mainly dedicated to aldehyde substrates, it would be highly desirable to expand this reductive carbocyclization reaction to ketone substrates. As it was already shown in previous chapters, the conversion of a ketone substrate did already display promising results regarding the reductive carbocyclization activity. The synthesis of various ketone substrates bearing different sizes of substituents at the double bond would be of great interest for the expansion of the substrate scope (Scheme 99).

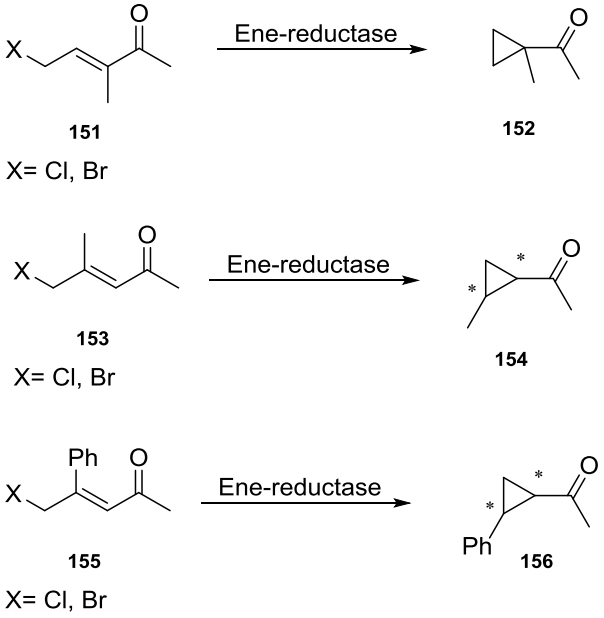

Scheme 99: Ketone substrates **151**, **153**, **155** and their expected cyclization products **152**, **154**, **156**.

Ene-reductases are known to perform the asymmetric reduction of the double bond in nitroolefins. It would be interesting to elucidate whether a nitroenolate undergoes a reductive cyclization reaction (Scheme 100).[23,39,97]

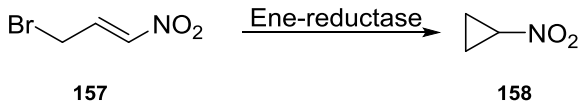

157 **158**

Scheme 100: Reductive cyclization of nitroolefin **157** to **158**.

Enzyme engineering could be used for further development of the ene-reductase enabled reductive cyclization reaction. In the conversion of various substrates we still observe the formation of the reduction byproduct, which is the result of the natural ene-reductase reaction. To further enhance the activity for the reductive cyclization reaction, it will be mandatory to exchange potentially proton donating active site residues to create a much more hydrophobic binding pocket. As already mentioned in the chapters before, through the conversion of the β-phenylsubstituted substrate **31** with YqjM Y169F, it was possible to obtain the cyclopropane product in excellent diastereoselectivities and stereoselectivities. To elucidate which active site residues are involved in the enantiodiscrimination, docking studies will be performed by Prof. Karl GRUBER. This docking study will be the starting point for the creation of new variants which possibly lead to cyclopropane products with enhanced and/or reversed diastereoselectivities and enantioselectivities. It would also be possible to further expand the enzyme repertoire by the creation of variants from different ene-reductases within the OYE family, i.e. OYE1.

7 Experimental Section

7.1 General aspects[98]

Commercially available reagents and solvents were purchased from Sigma Aldrich, Alfa Aesar, Roth, Lactan, ABCR, VWR, Fisher Scientific or Acros Organics and were used without further purification unless otherwise mentioned. All experiments were carried out using standard Schlenk techniques under an inert atmosphere of argon or nitrogen. When applying Schlenk techniques the glass apparatus was dried under oil pump vacuum by heating with a heat gun, cooled to RT, and flushed with inert gas. Dry solvents were prepared by the below-mentioned procedures and stored under an inert atmosphere. The stated temperatures generally refer to the oil bath or the cooling bath temperature. The water bath temperature of the rotary evaporator was usually set to 35 °C unless otherwise noted.

7.2 Dry Solvents[98]

Dry solvents were stored over 3 Å or 4 Å molecular sieves (Sigma Aldrich, beds, 8-12 mesh). The molecular sieves were activated by filling a 500 mL round bottom flask to one third of its volume and heating the flask in a heating mantle at level 1 under oil pump vacuum for 2 d until complete dryness was obtained.

Dry **dichloromethane** was prepared in two steps. First EtOH-stabilized dichloromethane was heated under reflux for 1 d over phosphorous pentoxide and distilled, then heated under reflux for 2 d over calcium hydride, and then distilled under argon atmosphere into a dry, brown 1 L Schlenk bottle with activated 4 Å molecular sieves.

Dry **dimethylsulfoxide** was purchased from Acros Organics and stored over activated 4 Å molecular sieves in a dry, brown 1 L Schlenk bottle under an argon atmosphere.

Dry **toluene** was purchased from Sigma Aldrich and was dried using an aluminum oxide column (Pure Solv® by Innovative Technology) and was stored over activated 4 Å molecular sieves in a dry, brown 1 L Schlenk bottle under an argon atmosphere.

Triethylamine was dried over calcium hydride and then distilled under argon atmosphere into a dry, brown 1 L Schlenk bottle with activated 4 Å molecular sieves.

Pyridine was purchased in anhydrous quality and stored over molecular sieves in a dark bottle under argon.

Non dry **diethylether** was purchased from Roth and the stabilizer was removed by distillation using a rotary evaporator. The solvent was stored in a brown glass bottle over KOH.

Dry **THF** was heated under reflux over sodium until benzophenone indicated the dryness of the solvent. It was stored in a brown 1 L Schlenk bottle with activated 4 Å molecular sieves. Non dry **THF** was distilled to remove the stabilizer using a rotary evaporator. It was stored over KOH in a brown glass-bottle.

Non dry solvents, i.e. cyclohexane, ethylacetate, methanol, dichloromethane, toluene, acetone, ethanol were purchased from VWR, Fisher Scientific, or Sigma Aldrich and used as obtained.

7.3 Analytical Methods[98]

7.3.1 Achiral GC-FID

Achiral GC-FID measurements were performed on an Agilent Technologies 6890N GC system with an Agilent Technologies J&W GC-column DB-17-01 ((14%-cyanopropylphenyl) methylpolysiloxane; 30 m x 250 µm x 0.25 µm). For injection, an Agilent Technologies 7683 Series auto sampler (split mode) was used. Nitrogen 5.0 served as carrier gas and hydrogen 5.0 and air were used for detection together with a flame ionization detector (FID).

Temperature program:

KH_80_30_280: 1 min at 80 °C, ramp 30 °C min^{-1} linear to 280 °C.

7.3.2 Chiral GC-FID

Chiral GC-FID measurements were performed on a Hewlett Packard 6890 GC System with an Agilent CP-Chirasil-Dex CB column (25 m×320 µm×0.25m). For injection, a Hewlett Packard 7683 Series autosampler (split mode) was used. Nitrogen 5.0 served as carrier gas and hydrogen 5.0 and air were used for detection together with a flame ionization detector (FID). Injector temperature was set to 200 °C and detector temperature was set to 250 °C, split ratio was set to 80:1.

Temperature program:

KH_40_60_155: Start at 40 °C, ramp 2 °C min^{-1} linear to 60 °C, 10 min at 60 °C, ramp 20 °C min^{-1} linear to 155 °C.

7.3.3 Achiral GC-MS

GC-MS measurements were performed on an Agilent Technologies 7890A (G3440A) GC system equipped with an Agilent Technologies J&W GC-column HP-5MS ((5%-phenyl) methylpolysiloxane; length: 30 m; inner-diameter: 0.250 mm; film: 0.25 μm) at a constant helium flow rate with He 5.0 as carrier gas. The sample was injected in split mode using an Agilent Technologies 7683 Series autosampler and an Agilent Technologies 7683B Series injector. The GC was coupled to a 5975C inert mass sensitive detector with triple-axis detector (MSD, EI, 70 eV; transfer line: 300°C; MS source: 240°C; MS quad: 180°C).

Temperature programm:

MT_50_S: 50°C 1 min, ramp: 40°C·min^{-1} linear to 300°C, 300°C 5 min, solvent delay: 4.0 min.

7.3.4 Reversed phase HPLC-MS

Analytical HPLC-MS measurements were performed on an Agilent 1200 Series MWD SL UV detector. Signals were detected at λ = 210 nm. The separation of the analytes was carried out using a "C-18 reversed-phase" column of the type „Poroshell® 120 EC-C18, 3.0 x 100 mm, 2.7 μm". The following methods were used for performing the separations:

method_1: 0.0 – 6.0 min 98% water/0.1% HCOOH and 2% CH_3CN linear decrease to 100% CH_3CN, 6.0 – 8.0 min 100% CH_3CN; 0.7 mL/min, 30 °C.

7.3.5 Chiral normal phase HPLC

Chiral HPLC measurements were performed on an Agilent 1100 Series HPLC system equipped with a temperature controlled column oven. Detection of the substances was accomplished with a Diode Array Detector at a wavelength of λ = 210 nm. The separations were carried out either on a Daicel Chiralcel OD-H column (0.46 cm×25 cm) or a Daicel Chiralcel OJ-H column (0.46 cm×25 cm). The following methods were used for the separation:

90_n-hexane_ODH: n-hexane: iPrOH 9:1, flow= 0.5 mL min^{-1}.

95_n-hexane_OJH: n-hexane: iPrOH 95:5, flow= 0.5 mL min^{-1}.

7.3.6 Nuclear Magnetic Resonance Spectroscopy

The described nuclear magnetic resonance spectra were recorded on a Bruker Avance III spectrometer (300.36 MHz for ^{1}H-NMR, 75.53 MHz for ^{13}C-NMR) with autosampler or a Varian Unity Inova NB high resolution spectrometer (499.90 MHz for ^{1}H-NMR, 125.71MHz for ^{13}C-NMR). The residual solvent peak was set as internal standard. Coupling constants (*J*) are reported as absolute values in Hertz (Hz) and chemical shifts are reported in parts per million (ppm). To confirm and identify a structure additional NMR experiments (NOESY, H,H-COSY, HSQC, APT, HMBC) were measured.

7.3.7 High resolution mass spectrometry

The measurement of high resolution mass spectrometry spectra was performed on a "Waters GCT Premier" system after ionisation with an EI ionisation source of a potential of 70 V. All measurements were performed by Prof. Robert Saf and Ing. Karin Bartl. The corresponding calculated and measured masses are noted for each compound.

7.3.8 Determination of melting points

Melting points were determinated using a Mel-Temp® melting point apparatus with integrated microscopical support from Electrothermal in open capillary tubes. Melting points were not corrected.

7.3.9 Specific Optical Rotation

The specific optical rotation was determined on a Perkin Elmer Polarimeter 341 with an integrated sodium vapor lamp. All samples were measured at the D-line of the sodium light (λ = 589 nm) under tempered conditions 20 °C. Concentrations between 5.0 g.L^{-1} (c = 0.50) and 20.0 g.L^{-1} (c = 2.00) depending on the solubility of the sample were chosen, CH_2Cl_2 and $CHCl_3$ were used as solvents.

7.3.10 Thin layer chromatography

Reactions were monitored by thin layer chromatography on commercial silica gel plates (TLC, aluminium foil, Merck, 60 F_{254}). The detection occurred by using an UV lamp (254 or 360 nm) or a stain reagent was applied and the plates were developed using a stream of hot air.

$KMnO_4$: 0.3 g $KMnO_4$ and 20 g K_2CO_3 were dissolved in 300 mL H_2O. Under stirring 5 mL 5 % aqueous NaOH were added.

CAM: 50 g Ammonium molybdate, 2.0 g $Ce(SO_4)_2$ and 50 mL concentrated sulfuric acid were dissolved in 400 mL distilled water.

Developing solvents and R_f-values are stated for each compound.

7.4 Flash column chromatography[98]

For preparative flash column chromatography silica gel from Acros Organics (silica gel, for chromatography 0.035 – 0.070 mm, 60 Å, nitrogen flushed) was used. The amount of silica depends on the specific separation problem and was in general the 20 to 100 fold amount of crude product. The column diameter was chosen to give a filling level between 15 and 25 cm. As fraction size, typically one third of the volume of the used silica gel volume was chosen. The eluent was selected to result in a R_f-value between 0.2 and 0.3 of the to-be-isolated substance. If the crude product was not soluble in the eluent, the sample was dissolved in a proper solvent (DCM or EtOAc) and the 1.5 fold amount of silica gel was added, followed by removing the solvent using a rotary evaporator and drying in vacuum.

7.5 Hydrogenation[98]

High pressure hydrogenation experiments were performed, utilizing an H-Cube™ continuous hydrogenation unit (HC-2.SS) from Thales Nanotechnology Inc. with a Knauer Smartline pump 100, equipped with a 10 mL ceramic pump head. As hydrogenation catalyst a 10 % palladium on carbon powder cartridge (Thales Nanotechnology Inc., THS 01111, 10 % Pd/C CatCart™), or a Raney-Nickel cartridge (Thales Nanotechnology Inc., THS 01112, Raney-Nickel CatCart™) was used.
The workup of batch hydrogenation experiments utilizing metal catalysts was performed by filtering off the catalyst using a pad of SiO_2 under inert conditions and elution with MeOH or EtOAc. The hydrogenation catalyst was washed with H_2O under inert gas and then stored in a glass bottle covered with water.

7.6 General considerations when synthesizing α,β-unsaturated aldehydes and performing reactions with α,β-unsaturated aldehydes

The reactions described in 7.7.7.1, 7.7.7.2, 7.8.1 and 7.8.3 had to be performed under the exclusion of light. The light in the laboratory and the fume hood was switched off. The glass

windows of the doors were covered with aluminum-foil and doors were closed during experiments. The windows were covered by blinds and the glass of the closed fume hood was covered by paper card boards. Working in the fume hood was achieved by opening just one window. Round bottom flask were covered with aluminum-foil or black garbage bags. When evaporation was needed a big paper card box was used to cover the water bath of the evaporator. Column chromatography was performed in the completely covered fume hood. α,β-unsaturated aldehydes were prepared freshly when biocatlytic experiments were performed. NMR experiments had to be done immediately when α,β- unsaturated aldehydes were isolated. It was not possible to store the α,β-unsaturated aldehydes.

7.7 Experimental Procedures

7.7.1 Synthesis of α,β-unsaturated esters and ketones

7.7.1.1 (2-Ethoxy-2-oxoethyl)triphenylphosphonium bromide (152)

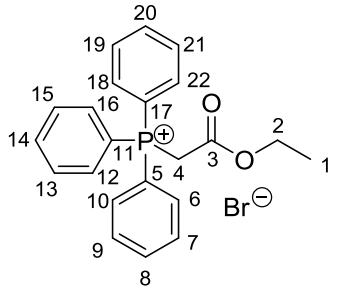

152

In a flame dried 250 mL two-neck round-bottom flask equipped with nitrogen inlet triphenylphosphine (42.15 g, 0.16 mol) was dissolved in 100 mL dry toluene. Ethylbromoacetate (16.2 mL, 0.14 mol) was added dropwise via a syringe in a N_2 counter-stream and a colourless precipitate was formed immediately. The suspension was stirred at 22 °C overnight. The colourless solid was washed with toluene (3×100 mL) and cyclohexane (3×100 mL) and was dried under oil pump vacuum.

yield: 62.25 g (99 %), white powder, $C_{22}H_{22}BrO_2P$, [429.29 g/mol].

m.p.= 153 °C.

^{1}H-NMR (300.36 MHz, DMSO-d_6): δ = 7.84 (ddd, $^3J_{HP}$= 19.1 Hz, $^4J_{HP}$= 12.0 Hz, $^5J_{HP}$= 5.5 Hz, 15H, H-6, H-7, H-8, H-9, H-10, H-12, H-13, H-14, H-15, H-16, H-18, H-19, H-20, H-21, H-22), 5.35 (d, $^2J_{HP}$= 14.5 Hz, 2H, H-4), 4.04 (q, $^3J_{HH}$= 7.1 Hz, 2 H, H-2), 0.97(t, $^3J_{HH}$= 7.1 Hz, 3H, H-1) ppm.

^{13}C-NMR (75.53 MHz, $CDCl_3$): δ = 164.6 (d,$^2J_{CP}$= 3.8 Hz, C-3), 135.1 (d, $^4J_{CP}$= 3.0 Hz, C-8, C-14, C-20), 133.7 (d, $^3J_{CP}$= 10.7 Hz, C-7, C-9, C-13, C-15, C-19, C-21), 130.1 (d, $^2J_{CP}$= 13.0 Hz, C-6, C-10, C-12, C-16, C-18, C-22), 118.2 (d, $^1J_{CP}$= 88.9 Hz, C-5, C-11, C-17), 62.3 (C-2), 29.6 (d,$^1J_{CP}$= 56.0 Hz, C-4), 13.5 (C-1) ppm.

The recorded spectra are in accordance with the reported in literature.[99]

7.7.1.2 Ethyl 2-(triphenyl-λ^5-phosphanylidene)acetate (54)

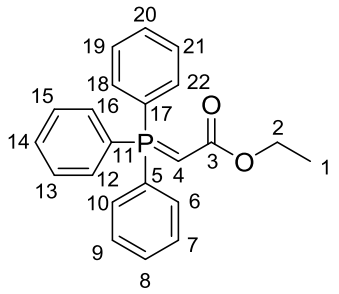

54

In a 1000 mL round bottom flask (2-ethoxy-2-oxoethyl)triphenylphosphonium bromide (**152**) (58.42 g, 136 mmol) was dissolved in 350 mL distilled H_2O and 400 mL toluene. Under stirring 10 % aqueous NaOH solution (50 mL) was added until a pH of 10 was achieved. The layers were separated and the aqueous phase was washed with dichloromethane (3×150 mL). The combined organic layers were dried over Na_2SO_4 and the solvent was removed under reduced pressure. After addition of 140 mL cyclohexane to the yellow oil, colourless crystals precipitated. The crystals were collected by filtration and washed with cold cyclohexane (3×150 mL). The white crystals were dried under oil pump vacuum.

yield: 27.95 g (59 %), colourless, crystalline solid, $C_{22}H_{21}O_2P$, [348.13 g/mol].

m.p.= 126-130 °C.

^{1}H-NMR (300.36 MHz, DMSO-d_6): δ = 7.64-7.57 (m, 15 H, H-6, H-7, H-8, H-9, H-10, H-12, H-13, H-14, H-15, H-16, H-18, H-19, H-20, H-21, H-22), 3.83 (q, $^3J_{HH}$= 6.9 Hz, 2H, H-2), 2.76 (d, $^2J_{HP}$= 22.7 Hz, 1H, H-4), 1.10 (t, $^3J_{HH}$= 7.0 Hz, 3H, H-1) ppm.

^{13}C-NMR (75.53 MHz, $CDCl_3$): δ = 170.4 (d,$^2J_{CP}$= 14.6 Hz, C-3), 132.5 (d, $^4J_{CP}$= 10.0 Hz, C-8, C-14, C-20), 132.1 (d, $^3J_{CP}$= 9.1 Hz, C-7, C-9, C-13, C-15, C-19, C-21), 128.9 (d, $^2J_{CP}$= 12.0 Hz, C-6, C-10, C-12, C-16, C-18, C-22), 127.4 (d, $^1J_{CP}$= 91.2 Hz, C-5, C-11, C-17), 56.6 (C-2), 28.8 (d,$^1J_{CP}$= 127.9 Hz, C-4), 14.7 (C-1) ppm.

The recorded spectra are in accordance with the reported in literature.[99]

7.7.1.3 Ethyl (*E*)-4-hydroxybut-2-enoate (55)

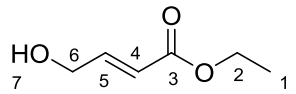

55

In a 250 mL round-bottom flask glycolaldehyde dimer (1.98 g,16.5 mmol) was dissolved in CH_2Cl_2. Ethyl 2-(triphenyl-λ^5-phosphanylidene)acetate (**54**) (11.48 g, 33.0 mmol) was added and the yellow reaction mixture was stirred under reflux at 45 °C for 4 h. After full conversion was indicated by TLC the solvent was removed under reduced pressure and the product was purified via flash chromatography (500 g silica gel, 20×7.5 cm, cyclohexane/ethylacetate 2/1, fraction size: 250 mL).

yield: 2.62 g (61 %), yellow oil, $C_6H_{10}O_3$, [130.14 g/mol]

R_f= 0.38 (cyclohexane/ethylacetate 1/1) ($KMnO_4$)

GC-FID (KH_80_30_280): t_R= 4.6 min

^{1}H-NMR (300.36 MHz, $CDCl_3$): δ = 7.00 (q, $^3J_{HH}$= 3.9 Hz, 1H, H-5), 6.07 (d, $^3J_{HH}$= 15.7 Hz, 1H, H-4), 4.31 (d, $^3J_{HH}$= 1.4 Hz, 2H, H-6), 4.17 (q, $^3J_{HH}$= 7.1 Hz, 2H, H-2), 1.27 (t, $^3J_{HH}$= 7.1 Hz, 3H, H-1) ppm.

^{13}C-NMR (75.53 MHz, $CDCl_3$): δ = 166.3 (C-3), 146.81 (C-4), 119.7 (C-5), 61.4 (C-6), 60.2 (C-2), 13.9 (C-1) ppm.

The recorded spectra are in accordance with the reported in literature.[99]

7.7.1.4 Ethyl (*E*)-4-chlorobut-2-enoate (56)

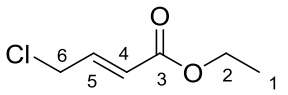

56

In a flame dried 250 mL two-neck round-bottom flask with nitrogen inlet and a bubble counter ethyl (*E*)-4-hydroxybut-2-enoate (**55**) (5.42 g, 41.6 mmol) was dissolved in 115 mL dry CH_2Cl_2 and cooled to -20 °C using an acetone/dry ice bath. Dry pyridine (23.5 mL, 23.0 g, 291 mmol) and PPh_3 (43.70 g, 166.6 mmol) were added and the clear, colorless solution was stirred for 20 min at -20 °C. NCS (11.12 g, 83.2 mmol) was added in small portions within 60 min and the reaction solution turned dark brown. After slowly warming the reaction mixture to 22 °C (2 h), TLC indicated complete consumption of starting material.

The reaction mixture was quenched by the addition of 1M HCl (100 mL). Addition of CH_2Cl_2 (50 mL) and centrifugation at 5000 rpm for 15 min produced two phases which were separated. The aqueous phase was extracted with CH_2Cl_2 (3x50 mL) and the combined organic layers were washed with 10 w% aq. $CuSO_4$ solution (3x100 mL) and brine (1x 100 mL). The organic phase was dried over Na_2SO_4 and the solvent was removed under reduced pressure. The product was purified via flash chromatography (250 g silica gel, 12×7.5 cm, cyclohexane/ethylacetate 20/1, fraction size: 125 mL).

yield: 3.15 g (51 %), slightly yellow liquid, $C_6H_9ClO_2$, [148.59 g/mol]

R_f= 0.58 (cyclohexane/ethylacetate 1/1) ($KMnO_4$)

^{1}H-NMR (300.36 MHz, $CDCl_3$): δ = 6.97 (q, $^3J_{HH}$= 6.1 Hz, 1H, H-5), 6.09 (d, $^3J_{HH}$= 15.4 Hz, 1H, H-4), 4.22 (d, $^3J_{HH}$= 7.1 Hz, 2H, H-6), 4.15 (q, $^3J_{HH}$= 4.1 Hz, 2H, H-2), 1.29 (t, $^3J_{HH}$= 7.1 Hz, 3H, H-1) ppm.

^{13}C-NMR (75.53 MHz, $CDCl_3$): δ = 165.6 (C-3), 141.6 (C-4), 124.1 (C-5), 60.7 (C-6), 42.5 (C-2), 14.2 (C-1) ppm.

The recorded spectra are in accordance with the reported in literature.[100]

7.7.1.5 1-(Triphenyl-λ^5-phosphanylidene)propan-2-one (48)

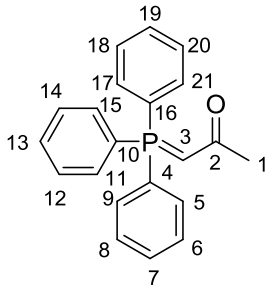

48

In a flame dried 250 mL three-neck round-bottom flask with nitrogen inlet triphenylphosphine (19.7 g, 75.2 mmol) and 1-chloropropan-2-one (5.0 mL, 5.8 g, 62.7 mmol) were dissolved in 50 mL dry chloroform. The mixture was heated to 65 °C under a nitrogen atmosphere for 10 h. A colourless precipitate was formed, which was washed with ice-cold Et_2O (3×50 mL). The solid was dissolved in a mixture of 250 mL distilled H_2O/CH_2Cl_2 (1/1) and under stirring 10 % aqueous NaOH solution was added (60 mL). The phases were separated and the aqueous phase was extracted with dichloromethane (1×50 mL). The combined organic phases

were washed with brine (2×100 mL), dried over Na_2SO_4, filtrated, and concentrated under reduced pressure. The colourless crystals were dried under oil pump vacuum for 5 h.

yield: 8.47 g (44 %), colourless, crystalline solid, $C_{21}H_{19}OP$, [318.26 g/mol].

m.p.= 202-205 °C

^{1}H-NMR (300.36 MHz, $CDCl_3$): δ = 7.90-7.29 (m, 15H, H-5, H-6, H-7, H-8, H-9. H-11, H-12, H-13, H-14, H-15, H-17, H-18, H-19, H-20, H-21), 3.63 (d, $^3J_{HH}$= 26.8 Hz, 1H, H-3), 2.02 (d, $^3J_{HH}$= 1.4 Hz, 3H, H-1) ppm.

^{13}C-NMR (75.53 MHz, $CDCl_3$): δ = 190.7 (d, $^2J_{CP}$= 1.7 Hz, C-2), 133.0 (d, $^3J_{CP}$= 2.7 Hz, C-6, C-8, C-12, C-14, C-18, C-20), 131.8 (d, $^4J_{CP}$= 2.7 Hz, C-7, C-13, C-19), 128.7 (d, $^2J_{CP}$= 12.1 Hz, C-5, C-9, C-11, C-15, C-17, C-21), 127.2 (d, $^1J_{CP}$= 90.7 Hz, C-4, C-10, C-16), 51.4 (d, $^1J_{CP}$= 107.5 Hz, C-3), 28.4 (d, $^3J_{CP}$= 15.6 Hz, C-1) ppm.

The recorded spectra are in accordance with the reported in literature.[101]

7.7.1.6 (*E*)-5-Bromopent-3-en-2-one (21)

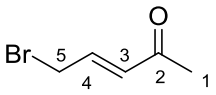

21

A 250 mL one-neck round-bottom flask was charged with 2-bromo-1,1-diethoxyethane (3.0 mL, 3.81 g, 19.3 mmol) and TFA (30.0 mL, 44.1 g, 387 mmol). The slightly yellow solution was stirred at 22 °C until GC-FID indicated complete consumption of starting material (4 h). The reaction mixture was diluted by the addition of distilled H_2O (40 mL), the phases were separated, and the aqueous phase was extracted with CH_2Cl_2 (3x40 mL). The combined organic layers were washed with brine (2x40 mL), dried over Na_2SO_4, and the solution was concentrated at a pressure of 600 mbar (with care to not exceed 35 °C bath temperature) until a final volume of 100 mL. Then 1-(triphenyl-λ^5-phosphanylidene)propan-2-one (**48**) (7.37 g, 23.2 mmol) was added and the reaction solution turned bright yellow. After stirring the reaction mixture for 2 h at 22 °C full conversion of the starting material was observed by GC-FID and the solvent was evaporated under reduced pressure. The crude product was purified via flash chromatography (500 g silica gel, 20×7.5 cm, cyclohexane/ethylacetate 6/1, fraction size: 250 mL).

yield: 406 mg (11 %), slightly yellow liquid, C_5H_7BrO, [163.01 g/mol]

R_f= 0.32 (cyclohexane/ethylacetate 4/1) ($KMnO_4$)

GC-FID (KH_80_30_280): t_R= 3.9 min

^{1}H-NMR (300.36 MHz, $CDCl_3$): δ = 6.82 (dt, $^3J_{HH}$= 15.7, 6.1 Hz, 1H, H-4), 6.23 (d, $^3J_{HH}$= 15.7 Hz, 1H, H-3), 4.03 (d, $^3J_{HH}$= 7.3 Hz, 2H, H-5), 2.29 (s, 3H, H-1) ppm.

^{13}C-NMR (75.53 MHz, $CDCl_3$): δ = 197.8 (C-2), 140.5 (C-4), 133.1 (C-3), 29.6 (C-5), 27.6 (C-1) ppm.

HRMS (EI): Calcd. (m/z) for C_5H_6O [M-HBr]: 82.0419; found: 82.0420.

7.7.2 Synthesis of α,β-unsaturated α-methyl substituted esters

7.7.2.1 (1-Ethoxy-1-oxopropan-2-yl)triphenylphosphonium bromide (153)

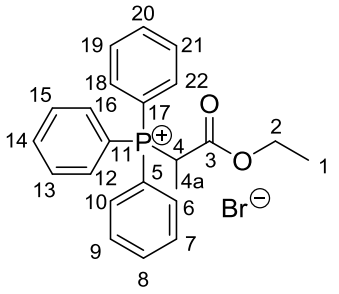

153

In a flame dried 250 mL three-neck round-bottom flask with nitrogen inlet triphenylphosphine (50.0 g, 190 mmol) was dissolved in ethyl 2-bromopropanoate (37 mL, 286 mmol). The mixture was heated to 51 °C under a nitrogen atmosphere for 10 h. Then cyclohexane (250 mL) was added to the solid and the solid cake was broken up with a spatula into smaller pieces. The colourless solid was washed with cyclohexane (3×150 mL) and dried under oil pump vacuum.

yield: 80.49 g (64 %), colourless powder, $C_{23}H_{24}BrO_2P$, [443.32 g/mol].

m.p.= 129-131 °C.

^{1}H-NMR (300.36 MHz, $CDCl_3$): δ = 7.93 (dd, $^3J_{HP}$= 12.6 Hz, $^3J_{HH}$= 7.4 Hz, 6H, H-6, H-10, H-12, H-16, H-18, H-22), 7.79-7.56 (m, 9H, H-7, H-8, H-9, H-13, H-14, H-15, H-19, H-20, H-21), 6.78 (dq, $^2J_{HP}$= 14.3 Hz, $^3J_{HH}$= 7.1 Hz, 1H, H-4), 3.95 (m, 2H, H-2),1.63 (dd, $^3J_{HP}$= 18.5 Hz, $^3J_{HH}$= 7.1 Hz, 3H, H-4a), 0.94 (t, $^3J_{HH}$= 7.1 Hz, 3H, H-1) ppm.

^{13}C-NMR(75.53 MHz, $CDCl_3$): δ = 168.0 (C-3), 134.9 (d, $^4J_{CP}$= 3.0 Hz, C-8, C-14, C-20), 134.3 (d, $^3J_{CP}$= 10.0 Hz, C-7, C-9, C-13, C-15, C-19, C-21), 130.2 (d, $^2J_{CP}$= 12.8 Hz, C-6, C-10, C-12, C-16, C-18, C-22), 117.9 (d, $^1J_{CP}$= 86.3 Hz, C-5, C-11, C-17), 62.9 (C-2), 36.7 (d, $^1J_{CP}$= 50.3 Hz, C-4), 29.6 (d,$^1J_{CP}$= 56.0 Hz, C-4), 13.6 (C-1), 13.0 (d, $^2J_{CP}$= 2.8 Hz, C-4a) ppm.

The recorded spectra are in accordance with the reported in literature.[102]

7.7.2.2 Ethyl 2-(triphenyl-λ^5-phosphanylidene)propanoate (60)

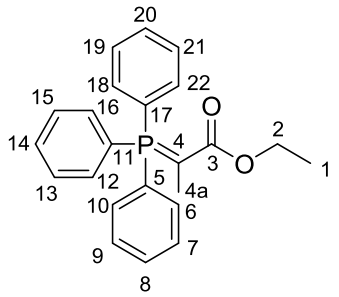

60

In a 500 ml round bottom flask NaOH (14.9 g, 373 mmol) was dissolved in 150 mL distilled H_2O. The solution was cooled to 0 °C using an ice/water bath and a solution of (1-ethoxy-1-oxopropan-2-yl)triphenylphosphonium bromide (**153**) (80.49 g, 182 mmol) in 75 mL dichloromethane was added slowly. The biphasic yellow solution was warmed to 22 °C over 2 h. The phases were separated and the aqueous phase was extracted with CH_2Cl_2 (1×50 mL). The combined organic layers were washed with brine (2×100 mL), dried over Na_2SO_4, and concentrated under reduced pressure. The yellow crystals were dried under oil pump vacuum for 5 h.

yield: 60.35 g (92 %), yellow, crystalline solid, $C_{23}H_{23}O_2P$, [362.41 g/mol].

m.p.= 155-157 °C

^{1}H-NMR (300.36 MHz, $CDCl_3$): δ = 7.65-7.36 (m, 15H, H-6, H-7, H-8, H-9, H-10. H-12, H-13, H-14, H-15, H-16, H-18, H-19, H-20, H-21, H-22), 4.03 (q, $^3J_{HH}$= 6.9 Hz, 2H, H-2$_{minor}$), 3.69 (q, $^3J_{HH}$= 7.0 Hz, 2H, H-2$_{major}$), 1.59 (dd, $^3J_{HP}$= 14.0 Hz, $^3J_{HH}$= 5.0 Hz, 3H, H-4a), 1.22 (t, $^3J_{HH}$= 6.9 Hz, 3H, H-1$_{minor}$), 0.43 (t, $^3J_{HH}$= 7.1 Hz, 3H, H-1$_{major}$) ppm.

^{13}C-NMR (75.53 MHz, $CDCl_3$): δ = 133.7 (d, $^4J_{CP}$= 9.5 Hz, C-8, C-14, C-20), 132.2 (d, $^3J_{CP}$= 9.9 Hz, C-7, C-9, C-13, C-15, C-19, C-21), 131.6 (C-6, C-10, C-12, C-16, C-18, C-22), 117.9 (d, $^1J_{CP}$= 12.0 Hz, C-5, C-11, C-17), 57.4 (C-2), 36.4(C-4), 14.2 (C-1), 13.0 (d, $^2J_{CP}$= 13.0 Hz, C-4a) ppm.

The recorded spectra are in accordance with the reported in literature.[102]

7.7.2.3 Ethyl (*E*)-4-hydroxy-2-methylbut-2-enoate (61)

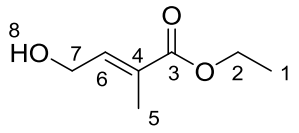

61

In a 250 mL one-neck round-bottom flask 1,4-dioxane-2,5-diol (1.98 mg, 33.0 mmol) was dissolved in 170 mL CH_2Cl_2. Ethyl 2-(triphenyl-λ^5-phosphanylidene)propanoate (**60**) (11.96 g, 33.0 mmol) was added in one portion and the reaction mixture was heated to 45 °C until TLC indicated full conversion of the starting material after 2 h. Then the solvent was removed under reduced pressure and the product was purified via flash chromatography (400 g silica gel, 18 × 7.5 cm, cyclohexane/ethylacetate 3/1, fraction size: 250 mL).

yield: 4.06 g (85 %), slightly yellow liquid, $C_7H_{12}O_3$, [144.17 g/mol]

R_f= 0.64 (cyclohexane/ethylacetate 1/1) ($KMnO_4$)

GC-FID (KH_80_30_280): t_R= 4.9 min

^{1}H-NMR (300.36 MHz, $CDCl_3$): δ = 6.82 (dd, $^3J_{HH}$= 6.0, 4.9 Hz, 1H, H-4), 4.34 (d, $^3J_{HH}$= 5.7 Hz, 2H, H-7), 4.19 (q, $^3J_{HH}$= 7.1 Hz, 2H, H-2), 1.90 (dd, $^3J_{HH}$= 12.9, 8.2 Hz, 1H, H-5), 1.83 (s, 3H, H-6), 1.29 (t, $^3J_{HH}$= 7.1 Hz, 3H, H-1) ppm.

^{13}C-NMR (75.53 MHz, $CDCl_3$): δ = 167.4 (C-3), 139.6 (C-4), 128.4 (C-5), 60.5 (C-2), 59.4 (C-7), 13.9 (C-1), 12.4 (C-6) ppm.

The recorded spectra are in accordance with the reported in literature.[103]

7.7.2.4 Ethyl (*E*)-4-chloro-2-methylbut-2-enoate (62)

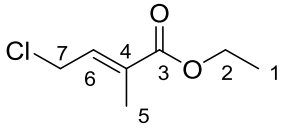

62

In a flame dried 250 mL two-neck round-bottom flask with nitrogen inlet and a bubble counter ethyl (*E*)-4-hydroxy-2-methylbut-2-enoate (**61**) (1.56 g, 10.8 mmol) was dissolved in 36 mL dry CH_2Cl_2 and cooled to -20 °C using an acetone/dry ice bath. Dry pyridine (6.10 mL, 5.98 g, 75.7 mmol) and PPh_3 (11.35 g, 43.3 mmol) were added and the clear, colorless

solution was stirred for 20 min at -20 °C. NCS (2.89 g, 21.6 mmol) was added in small portions within 30 min and the reaction solution turned dark brown. After slowly warming the reaction mixture to 22 °C (2 h), TLC indicated complete consumption of starting material. The reaction mixture was quenched by the addition of 1M HCl (50 mL). Addition of CH_2Cl_2 (50 mL) and centrifugation at 5000 rpm for 15 min produced two phases which were separated. The aqueous phase was extracted with CH_2Cl_2 (3x50 mL) and the combined organic layers were washed with 10 w% aq. $CuSO_4$ solution (3x60 mL) and brine (1x 100 mL). The organic phase was dried over Na_2SO_4 and the solvent was removed under reduced pressure. The product was purified via flash chromatography (250 g silica gel, 12×7.5 cm, cyclohexane/ethylacetate 20/1, fraction size: 125 mL).

yield: 1.04 g (59 %), slightly yellow liquid, $C_7H_{11}ClO_2$, [162.61 g/mol]

R_f= 0.28 (cyclohexane/ethylacetate 20/1) ($KMnO_4$)

^{1}H-NMR (300.36 MHz, $CDCl_3$): δ = 6.82 (t, $^3J_{HH}$= 7.2 Hz, 1H, H-6), 4.25-4.15 (m, 4H, H-2, H-7), 1.92 (s, 3H, H-5), 1.30 (t, $^3J_{HH}$= 7.1 Hz, 3H, H-1) ppm.

^{13}C-NMR (75.53 MHz, $CDCl_3$): δ = 166.8 (C-3), 134.4 (C-6), 131.5 (C-4), 60.6 (C-2), 38.8 (C-7), 13.8 (C-1), 12.0 (C-5) ppm.

Configuration of the double bond was confirmed via the observation of an NOE effect between the protons at C-5 and the protons at C-7.

HRMS (EI): Calcd. (m/z) for $C_7H_{10}O_2$ [M-HCl]: 126.0681; found: 126.0682.

7.7.2.5 Ethyl (*E*)-4-bromo-2-methylbut-2-enoate (69)

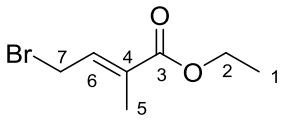

69

A 250 mL one-neck round-bottom flask was charged with ethyl (*E*)-4-hydroxy-2-methylbut-2-enoate (**61**) (4.80 g, 33.3 mmol) dissolved in 35 mL CH_2Cl_2 and was cooled using an ice/water bath. CBr_4 (16.6 g 50.0 mmol) was added and a solution of PPh_3 (5.76 g. 40.0 mmol) in 40 mL CH_2Cl_2 was added dropwise to the reaction mixture at 0 °C. After 30 min stirring at 22 °C TLC indicated full conversion of starting material and the reaction mixture was concentrated to dryness using a rotary evaporator. The product was purified via

flash chromatography (375 g silica gel, 15×8 cm, n-pentane/Et_2O 50/1, fraction size: 100 mL).

yield: 3.61 g (52 %), colourless liquid, $C_7H_{11}BrO_2$, [207.07 g/mol]

R_f= 0.35 (cyclohexane/ethylacetate 50/1) ($KMnO_4$)

^{1}H-NMR (300.36 MHz, $CDCl_3$): δ = 6.92 (td, $^3J_{HH}$= 8.5, 1.5 Hz, 1H, H-6), 4.20 (q, $^3J_{HH}$= 7.1 Hz, 2H, H-2), 4.03 (d, $^3J_{HH}$= 8.5 Hz, 2H, H-7), 1.92 (s, 3H, H-5), 1.30 (t, $^3J_{HH}$= 7.1 Hz, 3H, H-1) ppm.

^{13}C-NMR (75.53 MHz, $CDCl_3$): δ = 167.4 (C-3), 134.9 (C-6), 132.4 (C-4), 61.2 (C-2), 26.2 (C-7), 14.3 (C-1), 12.3 (C-5) ppm.

The recorded spectra are in accordance with the reported in literature.[104]

Configuration of the double bond was confirmed via the observation of an NOE effect between the protons at C-5 and the protons at C-7.

7.7.3 Synthesis of α,β-unsaturated β-methyl substituted esters

7.7.3.1 Ethyl (*E*)-4-hydroxy-3-methylbut-2-enoate (83)

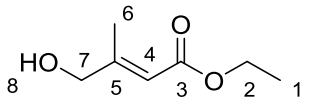

83

In a 250 mL one-neck round-bottom flask hydroxyacetone (3.0 mL, 3.18 g, 42.9 mmol) was dissolved in 100 mL MeCN. Ethyl 2-(triphenyl-λ^5-phosphanylidene)acetate (**54**) (18.3 g, 2.5 mmoL, 1.2 eq) was added in one portion and the reaction mixture was heated to 70 °C until TLC indicated full conversion of starting material after 3 h. Then the solvent was removed under reduced pressure and the product was purified via flash chromatography (225 g silica gel, 15×6.5 cm, cyclohexane/ethylacetate 8/1, fraction size: 100 mL).

yield: 3.45 g (55 %), slightly yellow liquid, $C_7H_{12}O_3$, [144.17 g/mol]

R_f= 0.23 (cyclohexane/ethylacetate 8/1) ($KMnO_4$)

^{1}H-NMR (300.36 MHz, DMSO-d_6): δ = 5.88 (s, 1H, H-8), 5.20 (t, $^3J_{HH}$= 5.6 Hz, 1H, H-4), 4.07 (q, $^3J_{HH}$= 7.1 Hz, 2H, H-2), 3.94 (d, $^3J_{HH}$= 5.0 Hz, 2H, H-7), 1.98 (s, 3H, H-6), 1.20 (t, $^3J_{HH}$= 7.1 Hz, 3H, H-1) ppm.

^{13}C-NMR (75.53 MHz, DMSO-d_6): δ = 166.0 (C-3), 159.6 (C-5), 112.0 (C-4), 65.2 (C-7), 59.0 (C-2), 15.3 (C-6), 14.2 (C-1) ppm.

The recorded spectra are in accordance with the reported in literature.[105]

7.7.3.2 Ethyl (*E*)-4-chloro-3-methylbut-2-enoate (72)

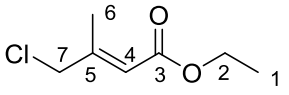

72

In a 100 mL one-neck round-bottom flask 1-chloropropan-2-one (0.8 mL, 925 mg, 9.94 mmol) was dissolved in 20 mL MeCN. Ethyl 2-(triphenyl-λ^5-phosphanylidene)acetate (**54**) (3.8 g, 10.9 mmoL) was added in one portion and the reaction mixture was heated to 70 °C until TLC indicated full conversion of starting material after 24 h. Then the solvent was

removed under reduced pressure and the product was purified via flash chromatography (125 g silica gel, 12.5×5.0 cm, cyclohexane/ethylacetate 50/1, fraction size: 25 mL).

yield: 350 mg (22 %), slightly yellow liquid, $C_7H_{11}ClO_2$, [162.61 g/mol]

R_f= 0.23 (cyclohexane/ethylacetate 50/1) ($KMnO_4$)

GC-FID (KH_80_30_280): t_R= 4.1 min

^{1}H-NMR (300.36 MHz, $CDCl_3$): δ = 5.95 (d, $^3J_{HH}$= 0.9 Hz, 1H, H-4), 4.17 (q, $^3J_{HH}$= 7.1 Hz, 2H, H-2), 4.03 (s, 2H, H-7), 2.23 (s, 3H, H-6), 1.28 (t, $^3J_{HH}$= 7.1 Hz, 3H, H-1) ppm.

^{13}C-NMR (75.53 MHz, $CDCl_3$): δ = 166.1 (C-3), 152.4 (C-5), 119.1 (C-4), 60.3 (C-2), 50.0 (C-7), 16.8 (C-6), 14.4 (C-1) ppm.

The recorded spectra are in accordance with the reported in literature.[106]

Configuration of the double bond was confirmed via the observation of an NOE effect between the proton at C-4 and the protons at C-7.

7.7.3.3 Ethyl (*E*)-4-bromo-3-methylbut-2-enoate (87)

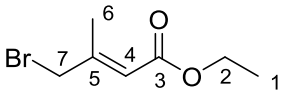

87

A 250 mL one-neck round-bottom flask was charged with ethyl (*E*)-4-hydroxy-3-methylbut-2-enoate (**83**) (6.31 g, 43.8 mmol) dissolved in 50 mL CH_2Cl_2 and was cooled using an ice/water bath. CBr_4 (19.9 g 60.0 mmol) was added and a solution of PPh_3 (15.7 g.60.0 mmol) in 150 mL CH_2Cl_2 was added dropwise to the reaction mixture at 0 °C. After 30 min stirring at 22 °C TLC indicated full conversion of starting material and the reaction mixture was concentrated to dryness using a rotary evaporator. The product was purified via flash chromatography (375 g silica gel, 15×8 cm, cyclohexane/ethylacetate 50/1, fraction size: 100 mL).

yield: 4.60 g (51 %), slightly yellow liquid, $C_7H_{11}BrO_2$, [207.07 g/mol]

R_f= 0.25 (cyclohexane/ethylacetate 50/1) ($KMnO_4$)

GC-FID (KH_80_30_280): t_R= 4.6 min

^{1}H-NMR (300.36 MHz, $CDCl_3$): δ = 5.95 (s, 1H, H-4), 4.17 (q, $^{3}J_{HH}$= 7.1 Hz, 2H, H-2), 3.94 (s, 2H, H-7), 2.27 (s, 3H, H-6), 1.28 (t, $^{3}J_{HH}$= 7.1 Hz, 3H, H-1) ppm.

^{13}C-NMR (75.53 MHz, $CDCl_3$): δ = 166.0 (C-3), 152.4 (C-5), 119.7 (C-4), 60.3 (C-2), 38.4 (C-7), 17.3 (C-6), 14.4 (C-1) ppm.

The recorded spectra are in accordance with the reported in literature.[105]

Configuration of the double bond was confirmed via the observation of an NOE effect between the proton at C-4 and the protons at C-7.

7.7.3.4 Ethyl 2-(diethoxyphosphoryl)-3-methylbutanoate (100)

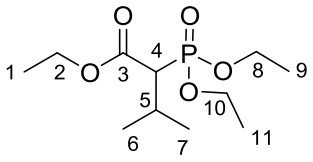

100

In a flame dried 250 mL two-neck round-bottom flask with nitrogen inlet and a bubble counter ethyl 2-(diethoxyphosphoryl)acetate (10 mL, 11.3 g, 50.4 mmol) was dissolved in 40 mL dry DMSO and cooled to 0 °C. KOtBu (6.77 g, 55.4 mmol) was added and the yellow, milky suspension was stirred for 30 min at 22 °C. 2-Iodopropane (5.5 mL, 9.35 g, 55.0 mmol) was added and the reaction solution was heated to 60 °C. After 2 h TLC indicated complete consumption of starting material and the reaction mixture was quenched by the addition of sat. aq. NH_4Cl-solution (50 mL). The aqueous phase was extracted with Et_2O (3x50 mL) and the combined organic layers were washed with brine (1x100 mL). The organic phase was dried over Na_2SO_4 and the solvent was removed under reduced pressure. The product was used in the next step without further purification.

yield: 12.8 g (48.1 mmol, 95 %), colorless liquid, $C_{11}H_{23}O_5P$ [266.27]

R_f= 0.48 (cyclohexane/ethylacetate 4/1) ($KMnO_4$)

^{1}H-NMR (300.36 MHz, $CDCl_3$): δ = 4.27-3.93 (m, 6H, H-2, H-8, H-10), 2.69 (dd, $^{3}J_{HH}$= 20.2, 9.3 Hz, 1H, H-4), 2.47-2.23 (m, 1H, H-5), 1.41-1.16 (m, 9H, H-1, H-9, H-11), 1.11 (d, $^{3}J_{HH}$= 6.7 Hz, 3H, H-6), 0.98 (d, $^{3}J_{HH}$= 6.6 Hz, 3H, H-7) ppm.

^{13}C-NMR (75.53 MHz, $CDCl_3$): δ = 169.4 (C-3), 62.5 (C-8, C-10), 61.2 (C-2), 53.5 (d, $^1J_{CP}$= 132.9 Hz, C-4), 31.3 (C-1), 28.4 (C-5), 21.6 (C-6, C-7), 16.5 (C-9), 14.2 (C-11) ppm.

The recorded spectra are in accordance with the reported in literature.[107]

7.7.3.5 2-((tert-Butyldimethylsilyl)oxy)acetaldehyde (105)

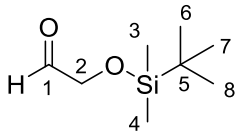

105

In a flame dried 250 mL two-neck round-bottom flask with nitrogen inlet and bubble counter 50 mL dry CH_2Cl_2 were cooled to -78 °C using an acetone/dry ice bath and oxalylchloride (1.84 mL, 2.67 g, 21.0 mmol) was added. DMSO (3.25 mL, 3.58 g, 45.8 mmol) was added dropwise via syringe to the reaction mixture in a N_2-counterstream and gas evolution was observed. After 30 min stirring at -78 °C 2-((tert-butyldimethylsilyl)oxy)ethan-1-ol (3.0 mL, 3.37 g, 19.1 mmol) dissolved in 10 mL dry CH_2Cl_2 and pyridine (3.1 mL, 3.02 g, 38.2 mmol) were added at -78 °C in a N_2-counterstream. After 30 min stirring at -78 °C dry Et_3N (13.4 mL, 9.66 g, 95.5 mmol) was added and the reaction mixture was warmed up to 22 °C, again evolution of gas was observed. After 30 min TLC indicated complete consumption of the starting material and the reaction mixture was quenched by addition of 1M HCl (45 mL), layers were separated, and the aqueous phase was extracted with CH_2Cl_2 (2x20 mL). The combined organic layers were washed with 10 w% $CuSO_4$ solution (3x50 mL), brine (3x50 mL), and dried over Na_2SO_4. The solvent was evaporated under reduced pressure and the crude product was purified via flash chromatography (125 g silica gel, 14×5 cm, cyclohexane/ethylacetate 15/1, fraction size: 75 mL).

yield: 1.29 g (39 %), slightly yellow liquid, $C_8H_{18}SiO_2$, [174.23 g/mol]

R_f= 0.23 (cyclohexane/ethylacetate 4/1) ($KMnO_4$)

^{1}H-NMR (300.36 MHz, $CDCl_3$): δ = 9.70 (s, 1H, H-1), 4.42 (s, 2H, H-2), 0.92 (s, 9H, H-6, H-7, H-8), 0.10 (s, 6H, H-3, H-4) ppm.

^{13}C-NMR (75.53 MHz, $CDCl_3$): δ = 202.4 (C-1), 69.8 (C-2), 25.9 (C-6, C-7, C-8), 18.5 (C-5), 5.30 (C-3, C-4) ppm.

The recorded spectra are in accordance with the reported in literature.[108]

7.7.3.6 4-((tert-Butyldiphenylsilyl)oxy)but-2-yn-1-ol (96)

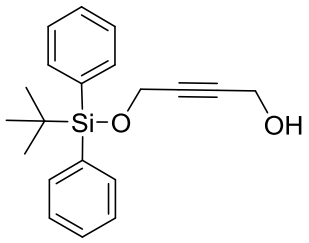

96

In a flame dried 100 mL two-neck round-bottom flask with nitrogen inlet but-2-yne-1,4-diol (1.72 g, 20.0 mmol) was dissolved in 20 mL dry CH_2Cl_2. Imidazole (817 mg, 12.0 mmol) was added and the clear, brown solution was stirred for 10 min at 22 °C. TBDPSCl (2.6 mL, 2.75 g, 10.0 mmol) was added and the reaction solution was stirred at 22 °C. After 3 h TLC indicated complete consumption of starting material and the reaction mixture was quenched by the addition of H_2O dist. (50 mL). The aqueous phase was extracted with CH_2Cl_2 (3x50 mL) and the combined organic layers were washed with brine (1x100 mL). The organic phase was dried over Na_2SO_4 and the solvent was removed under reduced pressure. The crude product was purified via flash chromatography (60 g silica gel, 13×3.5 cm, cyclohexane/ethylacetate 7/1, fraction size: 25 mL).

yield: 703 mg (2.16 mmol, 22 %), colorless liquid, $C_{20}H_{24}O_2Si$ [324.50]

R_f= 0.23 (cyclohexane/ethylacetate 7/1) ($KMnO_4$)

^{1}H-NMR (300.36 MHz, $CDCl_3$): δ = 7.72-7.70 (m, 4H), 7.44-7.37 (m, 6H), 4.36 (s, 2H), 4.20 (d, $^3J_{HH}$= 6.1 Hz, 2H), 1.31 (t, $^3J_{HH}$= 6.2 Hz, 1H), 1.06 (s, 9H) ppm.

The recorded spectra are in accordance with the reported in literature.[109]

7.7.3.7 Ethyl 2-isopropylbut-2-enoate (103)

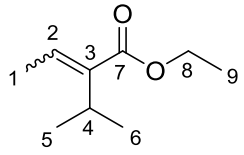

103

In a flame dried 250 mL two-neck round-bottom flask with nitrogen inlet and bubble counter ethyl 2-(diethoxyphosphoryl)-3-methylbutanoate (**100**) (6.0 g, 22.6 mmol) was dissolved in 70 mL dry THF and cooled to -78 °C using an acetone/dry ice bath. LHMDS (25.9 mL, 25.9 mmol, 1.0 M solution in THF) was added dropwise in a N_2-counterstream and the clear solution turned orange. After 30 min stirring at -78 °C acetaldehyde (4.4 mL, 5.60 g, 127 mmol) was added at -78 °C. The solution was warmed to 22 °C and stirred for 12 h. When TLC indicated complete consumption of the starting material, the reaction mixture was quenched by addition of sat. aq. NH_4Cl-solution (70 mL), layers were separated, and the aqueous phase was extracted with Et_2O (3x25 mL). The combined organic layers were washed with brine (3x50 mL) and dried over Na_2SO_4. The solvent was evaporated under reduced pressure and the crude product was purified via flash chromatography (150 g silica gel, 12×5.5 cm, cyclohexane/ethylacetate 100/1, fraction size: 100 mL).

yield: 1.52 g (43 %) mixture of *E/Z* 1/4, colorless liquid, $C_9H_{16}O_2$, [156.32 g/mol]

R_f= 0.52 (cyclohexane/ethylacetate 4/1) ($KMnO_4$)

^{1}H-NMR (300.36 MHz, $CDCl_3$): δ = 6.65 (q, $^3J_{HH}$= 7.2 Hz, 0.25H, H-2$^{Z\text{-isomer}}$), 5.81 (q, $^3J_{HH}$= 6.8 Hz, 1H, H-2), 4.20 (m, 2.4H, H-8$^{Z\text{-isomer}}$), 2.92 (dt, $^3J_{HH}$= 13.9, 7.0 Hz, 0.25H, H-4$^{Z\text{-isomer}}$), 2.68 (dt, $^3J_{HH}$= 13.6, 6.8 Hz, 1H, H-4), 1.87 (d, $^3J_{HH}$= 7.1 Hz, 3H, H-1), 1.79 (d, $^3J_{HH}$= 7.2 Hz, 0.75H, H-1$^{Z\text{-isomer}}$), 1.30 (m, 4H, H-9$^{E/Z\text{-isomer}}$), 1.17 (d, $^3J_{HH}$= 7.0 Hz, 1.5H, H-5$^{Z\text{-isomer}}$, H-6$^{Z\text{-isomer}}$), 1.04 (d, $^3J_{HH}$= 6.8 Hz, 6H, H-5, H-6) ppm.

^{13}C-NMR (75.53 MHz, $CDCl_3$): δ = 169.2 (C-7), 168.0 (C-7$^{Z\text{-isomer}}$), 140.1 (C-3), 139.1 (C-3$^{Z\text{-isomer}}$), 135.3 (C-2$^{Z\text{-isomer}}$), 129.8 (C-2), 60.2 (C-8), 31.6 (C-4), 27.1 (C-4$^{Z\text{-isomer}}$), 21.9 (C-5, C-6), 20.9 (C-5$^{Z\text{-isomer}}$, C-6$^{Z\text{-isomer}}$), 14.4 (C-9), 13.9 (C-9$^{Z\text{-isomer}}$) ppm.

The *E/Z* ratio was determined via ^{1}H-NMR experiments and the *E*-isomer showed an NOE-effect between the proton at C-2 and the protons at C-5 and C-6, which was not observed in the *Z*-isomer.

The recorded spectra are in accordance with the reported in literature.[107]

7.7.4 Synthesis of α,β-unsaturated β-aryl substituted esters

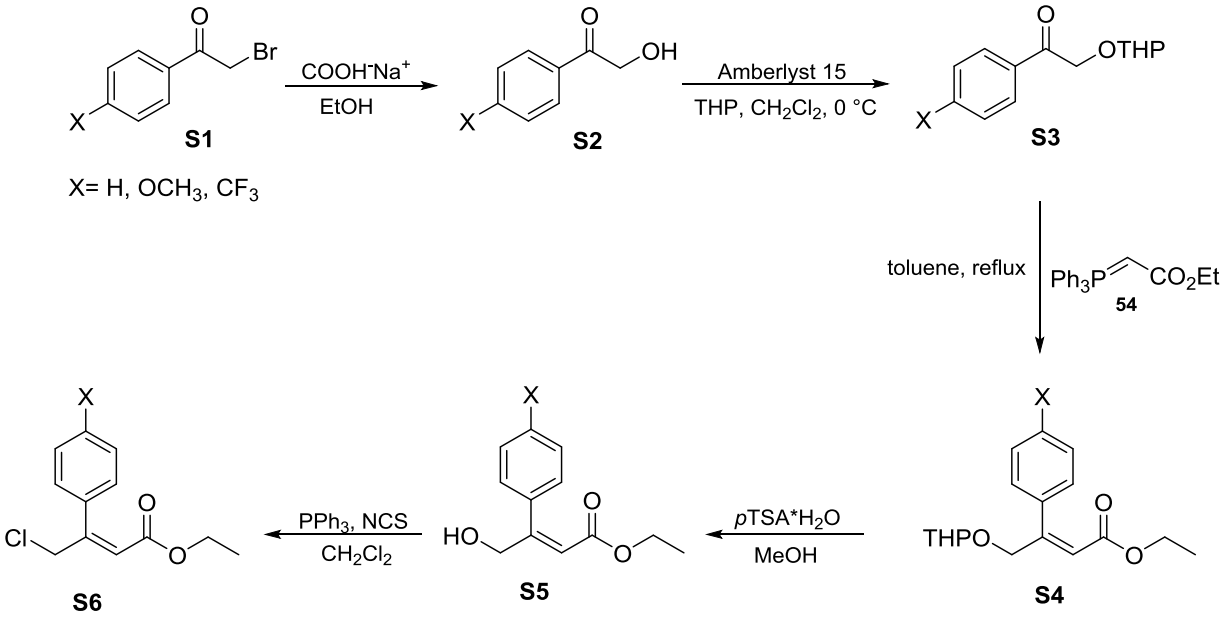

7.7.4.1 General procedure for the substiution of α-bromoketones S1

In a 250 mL round-bottom flask **S1** (22.0 mmol) was dissolved in 220 mL ethanol. Sodium formate (4.45 g, 65.5 mmol) was added and the solution was stirred under reflux until TLC indicated complete consumption of starting materials (12 h). Ethanol was evaporated under reduced pressure until dryness and H_2O (125 mL) was added. The aqueous phase was extracted with CH_2Cl_2 (3×50 mL), and the combined organic layers were dried over Na_2SO_4, and the solvent was removed under reduced pressure. The resulting product was used for the next step without further purification.

7.7.4.2 2-Hydroxy-1-(4-methoxyphenyl)ethan-1-one (127)

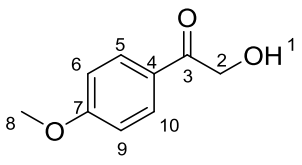

127

Starting from commercially available 2-bromo-1-(4-methoxyphenyl)ethan-1-one (5.0 g, 22.0 mmol) the reaction was executed as described in 7.7.4.1.

yield: 3.72 g (quant.), yellow solid, $C_9H_{10}O_3$, [166.17 g/mol]

R_f= 0.21 (cyclohexane/ethylacetate 4/1) ($KMnO_4$)

m.p.: 59 °C

^{1}H NMR (300.36 MHz; $CDCl_3$): δ = 7.90 (d, $^3J_{HH}$= 8.8 Hz, 2H, H-5, H-10), 6.97 (d, $^3J_{HH}$= 8.8 Hz, 2H, H-6, H-9), 4.82 (s, 2H, H-2), 3.88 (s, 3H, H-8) ppm.
^{13}C NMR (75.53 MHz; $CDCl_3$): δ = 196.8 (C-3), 164.6 (C-7), 130.3 (C-5, C-10), 126.5 (C-4), 114.3 (C-6, C-9), 65.1 (C-2), 55.7 (C-8) ppm.

The recorded spectra are in accordance with the reported in literature.[111]

7.7.4.3 2-Hydroxy-1-(4-(trifluoromethyl)phenyl)ethan-1-one (134)

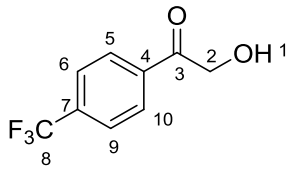

134

Starting from commercially available 2-bromo-1-[4-triflouromethyl)phenyl]ethan-1-one (10.0 g, 37.4 mmol) the reaction was executed as described in 7.7.4.1.

yield: 7.77 g (quant.), yellow solid, $C_9H_7F_3O_2$, [204.15 g/mol]

R_f= 0.26 (cyclohexane/ethylacetate 4/1) ($KMnO_4$)

m.p.: 110 °C

^{1}H NMR (300.36 MHz; $CDCl_3$): δ = 8.05 (d, $^3J_{HH}$= 8.4 Hz, 2H, H-5, H-10), 7.79 (d, $^3J_{HH}$= 8.4 Hz, 2H, H-6, H-9), 4.93 (s, 2H, H-2), 3.42 (s, 1H, H-1) ppm.
^{13}C NMR (75.53 MHz; $CDCl_3$): δ = 197.6 (C-3), 136.0 (C-7), 135.6 (C-5, C-10), 128.1 (C-8), 126.1 (C-6, C-9), 124.7 (C-4), 65.8 (C-2) ppm.

The recorded spectra are in accordance with the reported in literature.[110]

7.7.4.4 General procedure for the protection of α-hydroxyketones S3

In a flame dried 250 mL two-neck round-bottom flask with nitrogen inlet **S2** (18.4 mmol) was dissolved in 120 mL dry CH_2Cl_2. The colorless reaction solution was cooled in an ice/water bath and Amberlyst 15 (467 mg, 12 mol%) was added. 3,4-Dihydro-2*H*-pyran (8.30 mL, 7.72 g, 91.8 mmol) was added via dropping funnel within 20 min and the reaction mixture was stirred at 0 °C for 2 h until TLC indicated complete consumption of starting materials. The reaction mixture was quenched by the addition of sat. aq. $NaHCO_3$ solution (1×100 mL) and the aqueous phase was extracted with CH_2Cl_2 (3x30 mL). The combined organic layers were washed with brine (1x100 mL), dried over Na_2SO_4, and the solvent was removed under reduced pressure.

7.7.4.5 1-Phenyl-2-((tetrahydro-2*H*-pyran-2-yl)oxy)ethan-1-one (108)

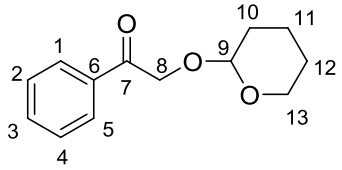

108

Starting from commercially available 2-hydroxyacetophenone (1.5 g, 11.0 mmol) the reaction was executed as described in 7.7.4.4 The crude product was purified via flash chromatography (500 g silica gel, 20×7.5 cm, cyclohexane/ethylacetate 20/1, fraction size: 250 mL).

yield: 2.92 g (72 %), slightly yellow liquid, $C_{13}H_{16}O_3$, [220.27 g/mol]

R_f= 0.47 (cyclohexane/ethylacetate 4/1) ($KMnO_4$)

^{1}H-NMR (300.36 MHz, $CDCl_3$): δ = 7.94 (d, $^3J_{HH}$= 7.3 Hz, 2H, H-1, H-5), 7.58 (t, $^3J_{HH}$= 7.4 Hz, 1H, H-3), 7.46 (t, $^3J_{HH}$= 7.5 Hz, 2H, H-2, H-4), 4.91 (q, $^3J_{HH}$= 17.0 Hz, 2H, H-8), 4.78 (d, $^3J_{HH}$= 3.3 Hz, 1H, H-9), 3.88 (m, 1H, H-13), 3.53 (m, 1H, H-13), 1.88 (m, 3H, H-10, H-12), 1.62 (m, 3H, H-10, H-11) ppm.

^{13}C-NMR (75.53 MHz, $CDCl_3$): δ = 196.2 (C-7), 135.2 (C-6), 133.6 (C-3), 128.8 (C-2, C-4), 128.0 (C-1, C-5), 98.8 (C-9), 69.5 (C-8), 62.4 (C-13), 30.4 (C-12), 25.5 (C-11), 19.2 (C-10) ppm.

The recorded spectra are in accordance with the reported in literature.[111]

7.7.4.6 1-(4-Methoxyphenyl)-2-((tetrahydro-2*H*-pyran-2-yl)oxy)ethan-1-one (128)

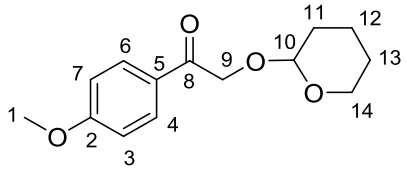

128

Starting from 2-hydroxy-1-(4-methoxyphenyl)ethan-1-one (**127**) (3.72 g, 22.3 mmol) the reaction was executed as described in 7.7.4.4. The crude product was purified via flash chromatography (500 g silica gel, 22×7.5 cm, cyclohexane/ethylacetate 20/1→ 5/1, fraction size: 250 mL).

yield: 4.62 g (83 %), slightly yellow liquid, $C_{14}H_{18}O_4$, [250.29 g/mol]

R_f= 0.52 (cyclohexane/ethylacetate 3/1) ($KMnO_4$)

^{1}H-NMR (300.36 MHz, $CDCl_3$): δ = 7.93 (d, $^3J_{HH}$= 7.8 Hz, 2H, H-4, H-6), 6.93 (d, $^3J_{HH}$= 8.8 Hz, 2H, H-3, H-7), 4.83 (dt, $^3J_{HH}$= 20.3, 10.1 Hz, 2H, H-9), 4.76 (d, $^3J_{HH}$= 3.5 Hz, 1H, H-10), 3.86 (m, 4H, H-1, H-14), 3.63-3.40 (m, 1H, H-14), 1.97-1.70 (m, 3H, H-11, H-13), 1.71-1.35 (m, 4H, H-11, H-12) ppm.

^{13}C-NMR (75.53 MHz, $CDCl_3$): δ = 194.7 (C-8), 163.8 (C-2), 130.3 (C-4, C-6), 128.3 (C-5), 114.0 (C-3, C-7), 98.8 (C-10), 69.3 (C-9), 62.4 (C-14), 55.6 (C-1), 30.4 (C-13), 25.5 (C-12), 19.2 (C-11) ppm.

The recorded spectra are in accordance with the reported in literature.[111]

7.7.4.7 2-((Tetrahydro-2*H*-pyran-2-yl)oxy)-1-(4-(trifluoromethyl)phenyl)ethan-1-one (135)

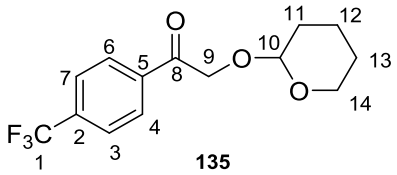

135

Starting from 2-hydroxy-1-(4-(trifluoromethyl)phenyl)ethan-1-one (**134**) (7.77 g, 37.4 mmol) the reaction was executed as described in 7.7.4.4. The crude product was purified via flash chromatography (500 g silica gel, 22×7.5 cm, cyclohexane/ethylacetate 15/1, fraction size: 250 mL).

yield: 6.10 g (57 %), slightly yellow liquid, $C_{14}H_{15}F_3O_3$, [288.27 g/mol]

R_f= 0.63 (cyclohexane/ethylacetate 3/1) ($KMnO_4$)

^{1}H-NMR (300.36 MHz, $CDCl_3$): δ = 8.06 (d, $^3J_{HH}$= 8.0 Hz, 2H, H-4, H-6), 7.73 (d, $^3J_{HH}$= 8.1 Hz, 2H, H-3, H-7), 4.86 (m, 3H, H-9, H-10), 3.88-3.82 (m, 1H, H-14), 3.55-3.53 (m, 1H, H-14), 2.06-1.71 (m, 3H, H-11, H-13), 1.74-1.33 (m, 4H, H-11, H-12) ppm.

^{13}C-NMR (75.53 MHz, $CDCl_3$): δ = 195.6 (C-8), 137.9 (C-5), 134.9 (q, $^2J_{CF}$= 19.1 Hz, C-2), 128.6 (C-4, C-6), 125.9 (q, $^3J_{CF}$= 2.3 Hz, C-3, C-7), 123.7 (q, $^1J_{CF}$= 163.1 Hz, C-1), 99.0 (C-10), 69.9 (C-9), 62.5 (C-14), 30.4 (C-13), 25.4 (C-12), 19.2 (C-11) ppm.

HRMS (EI): Calcd. (m/z) for $C_{14}H_{15}F_3O_3$ [M^+]: 288.0973; found: 288.0971.

7.7.4.8 General procedure for the WITTIG-reaction delivering α,β-unsaturated β-aryl substituted esters S4

In a 100 mL one-neck round-bottom flask **S3** (13.3 mmol) was dissolved in 35 mL toluene. Ethyl 2-(triphenyl-λ^5-phosphanylidene)acetate (**54**) (6.0 g, 17.2 mmoL) was added in one portion and the reaction mixture was heated to 135 °C until TLC indicated full conversion of starting material after 24 h. Then the solvent was removed under reduced pressure.

7.7.4.9 Ethyl (*E*)-3-phenyl-4-((tetrahydro-2*H*-pyran-2-yl)oxy)but-2-enoate (109)

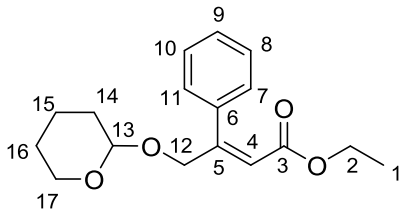

109

Starting from 1-phenyl-2-((tetrahydro-2*H*-pyran-2-yl)oxy)ethan-1-one (**108**) (2.92 g, 13.3 mmol) the reaction was executed as described in 7.7.4.8. The crude product was purified via flash chromatography (500 g silica gel, 20.0×7.5 cm, cyclohexane/ethylacetate 15/1, fraction size: 250 mL).

yield: 3.24 g (84 %), slightly yellow liquid, $C_{17}H_{22}O_4$, [290.36 g/mol]

R_f= 0.42 (cyclohexane/ethylacetate 9/1) ($KMnO_4$)

^{1}H-NMR (300.36 MHz, $CDCl_3$): δ = 7.49-7.07 (m, 5H, H-7, H-8, H-9, H-10, H-11), 6.21 (s, 1H, H-4), 4.72 (d, $^3J_{HH}$= 3.1 Hz, 1H, H-13), 4.47 (dd, $^3J_{HH}$= 16.4, 1.6 Hz, 1H, H-12), 4.19 (dd, $^3J_{HH}$= 16.4, 1.6 Hz, 1H, H-12), 4.01 (q $^3J_{HH}$= 7.1 Hz, 2H, H-2), 3.83 (m, 1H, H-17), 3.52 (m, 1H, H-17), 2.0-1.5 (m, 6H, H-14, H-15, H-16), 1.07 (t, $^3J_{HH}$= 7.1 Hz, 3H, H-1) ppm.

^{13}C-NMR (75.53 MHz, $CDCl_3$): δ = 166.2 (C-3), 155.1 (C-5), 137.6 (C-6), 128.2 (C-9), 128.1 (C-8, C-9), 127.6 (C-11, C-7), 116.3 (C-4), 98.2 (C-13), 70.1 (C-12), 62.2 (C-17), 60.0 (C-2), 30.5 (C-16), 25.5 (C-15), 19.3 (C-14), 14.1 (C-1) ppm.

NMR spectra are in accordance with previously reported ones.[111]

7.7.4.10 Ethyl (*E*)-3-(4-methoxyphenyl)-4-((tetrahydro-2*H*-pyran-2-yl)oxy)but-2-enoate (129)

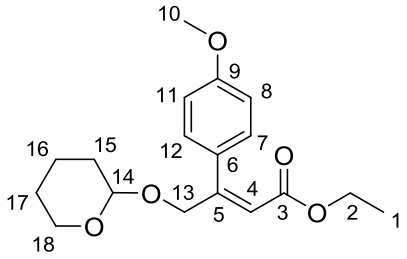

129

Starting from 1-(4-methoxyphenyl)-2-((tetrahydro-2*H*-pyran-2-yl)oxy)ethan-1-one (**128**) (4.39 g, 17.5 mmol) the reaction was executed as described in 7.7.4.8. The crude product was purified via flash chromatography (500 g silica gel, 20.0×7.5 cm, cyclohexane/ethylacetate 5/1, fraction size: 250 mL).

yield: 4.11 g (73 %), slightly yellow liquid, $C_{18}H_{24}O_5$, [320.39 g/mol]

R_f= 0.65 (cyclohexane/ethylacetate 3/1) ($KMnO_4$)

^{1}H-NMR (300.36 MHz, $CDCl_3$): δ = 7.17 (d, $^3J_{HH}$= 8.6 Hz, 2H, H-7, H-12), 6.88 (d, $^3J_{HH}$= 8.6 Hz, 2H, H-8, H-11), 6.17 (s, 1H, H-4), 4.71 (s, 1H, H-14), 4.46 (dd, $^3J_{HH}$= 16.3 Hz, 1H, H-13), 4.24-4.12 (m, 1H, H-13), 4.04 (q, $^3J_{HH}$= 7.1 Hz, 2H, H-2), 3.82 (m, 4H, H-10, H-18), 3.52 (d, $^3J_{HH}$= 11.1 Hz, 1H, H-18), 1.90-1.46 (m, 6H, H-15, H-16, H-17), 1.13 (t, $^3J_{HH}$= 7.1 Hz, 3H, H-1) ppm.

^{13}C-NMR (75.53 MHz, $CDCl_3$): δ = 166.4 (C-3), 162.5 (C-9), 159.7 (C-6), 154.6 (C-5), 129.1 (C-7, C-12), 115.9 (C-4), 133.5 (C-8, C-11), 98.2 (C-14), 70.1 (C-13), 62.2 (C 18), 60.0 (C-2), 55.3 (C-10), 30.5 (C-17), 25.5 (C-16), 19.3 (C-15), 14.2 (C-1) ppm.

NMR spectra are in accordance with previously reported ones.[111]

7.7.4.11 Ethyl (*E*)-4-((tetrahydro-2*H*-pyran-2-yl)oxy)-3-(4-(trifluoromethyl)phenyl)but-2-enoate (136)

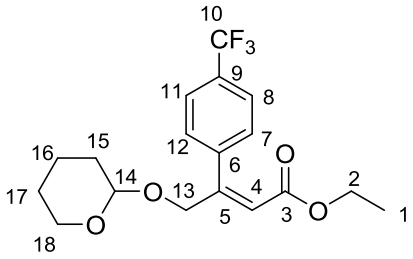

136

Starting from 2-((tetrahydro-2*H*-pyran-2-yl)oxy)-1-(4-(trifluoromethyl)phenyl)ethan-1-one (**135**) (5.48 g, 19.0 mmol) the reaction was executed as described in 7.7.4.8. The crude product was purified via flash chromatography (500 g silica gel, 20.0×7.5 cm, cyclohexane/ethylacetate 15/1, fraction size: 250 mL).

yield: 3.50 g (51 %), slightly yellow liquid, $C_{18}H_{21}O_4F_3$, [358.36 g/mol]

R_f= 0.62 (cyclohexane/ethylacetate 3/1) ($KMnO_4$)

^{1}H-NMR (300.36 MHz, $CDCl_3$): δ = 7.61 (d, $^3J_{HH}$= 8.9 Hz, 2H, H-8, H-11), 7.33 (d, $^3J_{HH}$= 7.9 Hz, 2H, H-7, H-12), 6.25 (s, 1H, H-4), 4.71 (s, 1H, H-14), 4.46 (dd, $^3J_{HH}$= 16.2, 1.7 Hz, 1H, H-13), 4.35–4.04 (m, 1H, H-13), 4.05 (dd, $^3J_{HH}$= 24.7, 7.2 Hz, 2H, H-2), 3.79 (dd, $^3J_{HH}$= 14.1, 5.7 Hz, 1H, H-18), 3.54 (t, $^3J_{HH}$= 12.8 Hz, 1H, H-18), 1.99 – 1.38 (m, 6H, H-15, H-16, H-17), 1.08 (t, $^3J_{HH}$= 7.1 Hz, 3H, H-1) ppm.

^{13}C-NMR (75.53 MHz, $CDCl_3$): δ = 165.7 (C-3), 153.8 (C-4), 141.5 (C-6), 130.2 (q, $^2J_{CF}$= 32.5 Hz, C-9), 128.1 (C-7, C-12), 125.1 (q, $^3J_{CF}$= 3.7 Hz, C-8, C-11), 124.2 (q, $^1J_{CF}$= 271.9 Hz, C-10), 117.6 (C-4), 98.3 (C-14), 70.0 (C-13), 62.3 (C-18), 60.3 (C-2), 30.5 (C-17), 25.5 (C-16), 19.2 (C-15), 14.0 (C-1) ppm.

HRMS (EI): Calcd. (m/z) for $C_{18}H_{21}F_3O_4$ [M^+]: 358.1392; found: 358.1389.

7.7.4.12 General procedure for the deprotection of S4

In a 100 mL one-neck round-bottom flask **S4** (11.2 mmol) was dissolved in 65 mL MeOH. *p*-Toluenesulfonic acid monohydrate (106 mg, 558 µmoL) was added in one portion and the reaction mixture was stirred at 22 °C until TLC indicated full conversion of starting material after 12 h. Then the solvent was removed under reduced pressure and the product was dissolved in 60 mL ethylacetate. The organic phase was washed with sat. aq. $NaHCO_3$ solution (2×50 mL) and the aqueous phase was extracted with EtOAc (3x30 mL). The combined organic layers were washed with brine (1x100 mL), dried over Na_2SO_4, and the solvent was removed under reduced pressure. The product was used in the next step without further purification.

7.7.4.13 Ethyl (*E*)-4-hydroxy-3-phenylbut-2-enoate (110)

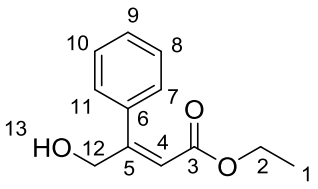

110

Starting from ethyl (*E*)-3-phenyl-4-((tetrahydro-2*H*-pyran-2-yl)oxy)but-2-enoate (**109**) (3.24 g, 11.2 mmol) the reaction was executed as described in 7.7.4.12.

yield: 2.20 g (96 %), slightly yellow liquid, $C_{12}H_{14}O_3$, [206.24 g/mol]

R_f= 0.32 (cyclohexane/ethylacetate 9/1) ($KMnO_4$)

^{1}H-NMR (300.36 MHz, DMSO-d_6): δ = 7.33 (d, $^3J_{HH}$= 3.5 Hz, 3H, H-10, H-9, H-8), 7.28-7.05 (m, 2H, H-11, H-7), 6.09 (s, 1H, H-4), 5.48 (t, $^3J_{HH}$= 5.5 Hz, 1H, H-13), 4.18 (d, $^3J_{HH}$= 4.0 Hz, 2H, H-12), 3.92 (q, $^3J_{HH}$= 7.0 Hz, 1H, H-2), 1.00 (t, $^3J_{HH}$= 7.1 Hz, 3H, H-1) ppm.

^{13}C-NMR (75.53 MHz, DMSO-d_6): δ = 165.4 (C-3), 158.8 (C-6), 137.5 (C-5), 127.8 (C-10, C-9, C-8), 127.7 (C-11, C-7), 114.4 (C-4), 64.9 (C-12), 59.2 (C-2), 13.8 (C-1) ppm.

The recorded spectra are in accordance with the reported in literature.[111]

7.7.4.14 Ethyl (*E*)-4-hydroxy-3-(4-methoxyphenyl)but-2-enoate (130)

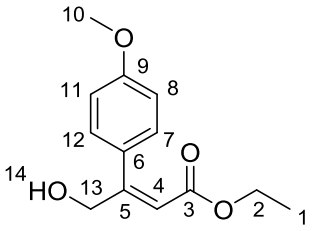

130

Starting from ethyl (*E*)-3-(4-methoxyphenyl)-4-((tetrahydro-2*H*-pyran-2-yl)oxy)but-2-enoate (**129**) (4.11 g, 14.2 mmol) the reaction was executed as described in 7.7.4.12.

yield: 3.03 g (90 %), slightly yellow liquid, $C_{13}H_{16}O_4$, [236.27 g/mol]

R_f= 0.33 (cyclohexane/ethylacetate 3/1) ($KMnO_4$)

^{1}H-NMR (300.36 MHz, $CDCl_3$): δ = 7.15 (d, $^3J_{HH}$= 8.5 Hz, 2H, H-8, H-11), 6.89 (d, $^3J_{HH}$= 8.4 Hz, 2H, H-7, H-12), 6.15 (s, 1H, H-4), 4.36 (s, 2H, H-13), 4.04 (q, $^3J_{HH}$= 7.1 Hz, 2H, H-2), 3.81 (s, 3H, H-10), 2.41 (s, 1H, H-14), 1.13 (t, $^3J_{HH}$= 7.1 Hz, 3H, H-1) ppm.

^{13}C-NMR (75.53 MHz, $CDCl_3$): δ = 166.4 (C-3), 163.8 (C-6), 159.8 (C-9), 157.0 (C-5), 129.0 (C-8, C-11), 115.5 (C-4), 113.7 (C-7, C-12), 66.8 (C-13), 60.1 (C-2), 55.4 (C-10), 14.2 (C-1) ppm.

The recorded spectra are in accordance with the reported in literature.[111]

7.7.4.15 Ethyl (*E*)-4-hydroxy-3-(4-(trifluoromethyl)phenyl)but-2-enoate (137)

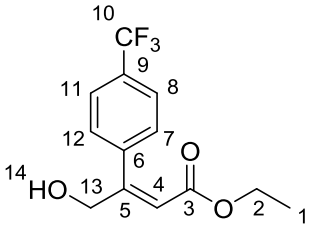

137

Starting from ethyl (*E*)-4-((tetrahydro-2*H*-pyran-2-yl)oxy)-3-(4-(trifluoromethyl)phenyl)but-2-enoate (**136**) (3.50 g, 9.77 mmol) the reaction was executed as described in 7.7.4.12. The crude product was purified via flash chromatography (300 g silica gel, 12×7.5 cm, cyclohexane/ethylacetate 4/1, fraction size: 180 mL).

yield: 1.65 g (60 %), slightly yellow liquid, $C_{13}H_{13}O_3F_3$, [274.24 g/mol]

R_f= 0.28 (cyclohexane/ethylacetate 3/1) ($KMnO_4$)

^{1}H-NMR (300.36 MHz, DMSO-d_6): δ = 7.71 (d, $^3J_{HH}$= 8.0 Hz, 2H, H-8, H-11), 7.41 (d, $^3J_{HH}$= 7.9 Hz, 2H, H-7, H-12), 6.14 (s, 1H, H-4), 5.55 (t, $^3J_{HH}$= 5.6 Hz, 1H, H-14), 4.33-4.05 (m, 2H, H-13), 3.92 (q, $^3J_{HH}$= 7.1 Hz, 2H, H-2), 1.00 (t, $^3J_{HH}$= 7.1 Hz, 3H, H-1) ppm.

^{13}C-NMR (75.53 MHz, DMSO-d_6): δ = 165.0 (C-3), 158.0 (C-5), 142.0 (C-6), 128.29 (C-7, C-12), 128.2 (q, $^2J_{CF}$= 31.7 Hz, C-9), 124.6 (q, $^3J_{CF}$= 3.7 Hz, C-8, C-11), 124.3 (q, $^1J_{CF}$= 271.9 Hz, C-10), 115.4 (C-4), 64.8 (C-13), 59.4 (C-2), 13.7 (C-1) ppm.

HRMS (EI): Calcd. (m/z) for $C_{13}H_{13}F_3O_3$ [M^+]: 274.0817; found: 274.0816.

7.7.4.16 General procedure for APPEL-reaction of S5

In a flame dried 250 mL two-neck round-bottom flask with nitrogen inlet and a bubble counter **S5** (10.7 mmol) was dissolved in 30 mL dry CH_2Cl_2 and cooled to -20 °C using an acetone/dry ice bath. Dry pyridine (6.0 mL, 5.90 g, 74.7 mmol) and PPh_3 (11.20 g, 42.7 mmol) were added and the clear, colorless solution was stirred for 20 min at -20 °C. NCS (2.85 g, 21.3 mmol) was added in small portions within 60 min and the reaction solution turned dark brown. After slowly warming the reaction mixture to 22 °C (2 h), TLC indicated complete consumption of starting material. The reaction mixture was quenched by the addition of 1M HCl (100 mL). Addition of CH_2Cl_2 (100 mL) and centrifugation at 5000 rpm for 15 min produced two phases which were separated. The aqueous phase was extracted with CH_2Cl_2 (3x50 mL) and the combined organic layers were washed with 10 w% aq. $CuSO_4$ solution (3x60 mL) and brine (1x100 mL). The organic phase was dried over Na_2SO_4 and the solvent was removed under reduced pressure.

7.7.4.17 Ethyl (*E*)-4-chloro-3-phenylbut-2-enoate (111)

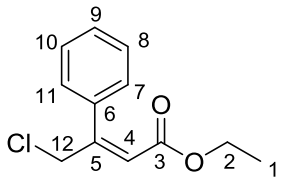

111

Starting from ethyl (*E*)-4-hydroxy-3-phenylbut-2-enoate (**110**) (2.20 g, 10.7 mmol) the reaction was executed as described in 7.7.4.16. The crude product was purified via flash chromatography (300 g silica gel, 12×7.5 cm, cyclohexane/ethylacetate 25/1, fraction size: 180 mL).

yield: 1.40 g (58 %), slightly yellow liquid, $C_{12}H_{13}ClO_2$, [224.86 g/mol]

R_f= 0.54 (cyclohexane/ethylacetate 9/1) ($KMnO_4$)

^{1}H-NMR (300.36 MHz, DMSO-d_6): δ = 7.56-7.50 (m, 5H, H-11, H-10, H-9, H-8, H-7), 6.32 (s, 1H, H-4), 4.63 (s, 2H, H-12), 3.94 (q, $^3J_{HH}$= 7.1 Hz, 2H, H-2), 1.01 (t, $^3J_{HH}$= 7.1 Hz, 3H, H-1) ppm.

^{13}C-NMR (75.53 MHz, DMSO-d_6): δ = 164.9 (C-3), 151.3 (C-6), 136.4 (C-5), 128.3 (C-9), 127.8 (C-11, C-10, C-8, C-7), 120.4 (C-4), 59.8 (C-2), 48.5 (C-12), 13.7 (C-1) ppm.

Configuration of the double bond was confirmed via the observation of an NOE effect between the proton at C-4 and the protons at C-12.

HRMS (EI): Calcd. (m/z) for $C_{12}H_{13}ClO_2$ [M^+]: 224.0604; found: 224.0600.

7.7.4.18 Ethyl (*E*)-4-chloro-3-(4-methoxyphenyl)but-2-enoate (131)

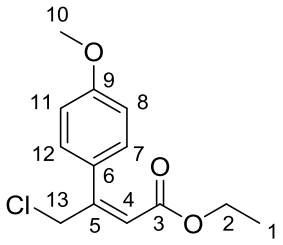

131

Starting from ethyl (*E*)-4-hydroxy-3-(4-methoxyphenyl)but-2-enoate (**130**) (1.0 g, 4.23 mmol) the reaction was executed as described in 7.7.4.16. The crude product was purified via flash chromatography (250 g silica gel, 12×6 cm, cyclohexane/ethylacetate 25/1→15/1, fraction size: 100 mL).

yield: 595 mg (55 %), slightly yellow liquid, $C_{13}H_{15}ClO_3$, [254.71 g/mol]

R_f= 0.83 (cyclohexane/ethylacetate 3/1) ($KMnO_4$)

GC-MS (EI, 70 eV, MT_50_S): t_R= 6.5 min; *m/z* (%): 254.1 (23) [M^+], 208.0 (100) [M^+-C_2H_5O]

^{1}H-NMR (300.36 MHz, $CDCl_3$): δ = 7.19 (d, $^3J_{HH}$= 8.5 Hz, 2H, H-7, H-12), 6.91 (d, $^3J_{HH}$= 8.5 Hz, 2H, H-8, H-11), 6.21 (s, 1H, H-4), 4.30 (s, 2H, H-13), 4.05 (q, $^3J_{HH}$= 7.1 Hz, 2H, H-2), 3.82 (s, 3H, H-10), 1.14 (t, $^3J_{HH}$= 7.1 Hz, 3H, H-1) ppm.

^{13}C-NMR (75.53 MHz, $CDCl_3$): δ = 165.7 (C-3), 160.0 (C-9), 151.8 (C-5), 129.3 (C-7, C-12), 128.9 (C-6), 120.0 (C-4), 113.7 (C-8, C-11), 60.4 (C-2), 55.4 (C-10), 48.6 (C-13), 14.1 (C-1) ppm.

Configuration of the double bond was confirmed via the observation of an NOE effect between the proton at C-4 and the protons at C-13.

HRMS (EI): Calcd. (m/z) for $C_{13}H_{15}ClO_3$ [M^+]: 254.0710; found: 254.0710.

7.7.4.19 Ethyl (*E*)-4-chloro-3-(4-(trifluoromethyl)phenyl)but-2-enoate (138)

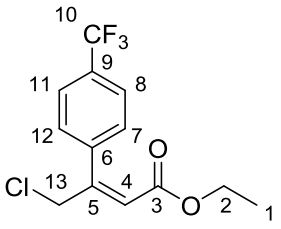

138

Starting from ethyl (*E*)-4-hydroxy-3-(4-(trifluoromethyl)phenyl)but-2-enoate (**137**) (1.47 g, 5.36 mmol) the reaction was executed as described in 7.7.4.16. The crude product was purified via flash chromatography (500 g silica gel, 12×6 cm, cyclohexane/ethylacetate 20/1, fraction size: 250 mL).

yield: 1.03 g (66 %), slightly yellow liquid, $C_{13}H_{12}ClO_2F_3$, [292.68 g/mol]

R_f= 0.72 (cyclohexane/ethylacetate 4/1) ($KMnO_4$)

GC-MS (EI, 70 eV, MT_50_S): t_R= 5.7 min; *m/z* (%): 292.0 (68) [M^+], 246.0 (100) [M^+-C_2H_5O]

^{1}H-NMR (300.36 MHz, DMSO-d_6): δ = 7.75 (d, $^3J_{HH}$= 8.0 Hz, 2H, H-8, H-11), 7.51 (d, $^3J_{HH}$= 8.5 Hz, 2H, H-7, H-12), 6.41 (s, 1H, H-4), 4.67 (s, 2H, H-13), 3.95 (q, $^3J_{HH}$= 7.1 Hz, 2H, H-2), 1.00 (t, $^3J_{HH}$= 7.1 Hz, 3H, H-1) ppm.

^{13}C-NMR (75.53 MHz, DMSO-d_6): δ = 164.4 (C-3), 150.6 (C-5), 141.0 (C-6), 128.8 (C-8, C-11), 128.7 (q, $^2J_{CF}$= 32.5 Hz, C-9), 124.8 (q, $^3J_{CF}$= 3.7 Hz, C-8, C-11), 124.2 (q, $^1J_{CF}$= 271.9 Hz, C-10), 121.5 (C-4), 60.0 (C-2), 48.2 (C-13), 13.6 (C-1) ppm.

Configuration of the double bond was confirmed via the observation of an NOE effect between the proton at C-4 and the protons at C-13.

HRMS (EI): Calcd. (m/z) for $C_{13}H_{12}ClO_2F_3$ [M^+]: 292.0478; found: 292.0478.

7.7.5 Synthesis of saturated aldehydes and ketones

7.7.5.1 4-Bromobutanal (45)

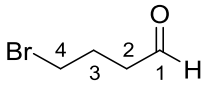

45

In a flame dried 250 mL two-neck round-bottom flask with nitrogen inlet commercially available ethyl 4-bromobutanoate (0.74 mL, 1.00 g, 5.16 mmol) was dissolved in 75 mL dry CH_2Cl_2 and was cooled to -78 °C using an acetone/dry ice bath. DIBAL-H solution (6.2 mL, 6.2 mmol, 1.0 M in CH_2Cl_2) was added dropwise to the reaction mixture in a N_2-counterstream. After full conversion of starting material was indicated by TLC and GC-FID (30 min) the reaction mixture was quenched at -78 °C by addition of 1M HCl (50 mL) and then warmed to 24 °C. The colorless layers were separated and the aqueous phase was extracted with CH_2Cl_2 (3x15 mL). The combined organic layers were washed with brine (1x50 mL) and dried over Na_2SO_4. The solvent was evaporated at 650 mbar taking care that the bath temperature did not exceed 35 °C.

yield: 473 mg (60 %), slightly red liquid, C_4H_7BrO, [151.00 g/mol]

R_f= 0.68 (cyclohexane/ethylacetate 4/1) ($KMnO_4$)

GC-FID (KH_80_30_280): t_R= 3.1 min

^{1}H-NMR (300.36 MHz, $CDCl_3$): δ = 9.81 (s, 1H, H-1), 3.46 (t, $^3J_{HH}$ = 6.4 Hz, 2H, H-4), 2.67 (t, $^3J_{HH}$ = 6.9 Hz, 2H, H-2), 2.36–2.07 (m, 2H, H-3) ppm.

^{13}C-NMR (75.53 MHz, $CDCl_3$): δ = 200.83 (C-1), 42.25 (C-2), 32.85 (C-4), 25.08 (C-3) ppm.

NMR spectra are in accordance with previously reported ones.[112]

7.7.5.2 4-Chlorobutanal (58)

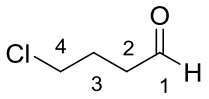

58

In a flame dried 25 mL Schlenk-flask 4-chlorobutan-1-ol (92 µL, 100 mg, 921 µmol) was dissolved in 5 mL dry CH_2Cl_2. PCC (298 mg, 1.38 mmol) and 4 Å molecular sieves (0.5 g) were added in a N_2-counterstream and the brownish solution was stirred at 22 °C. After full conversion of starting material was indicated by TLC and GC-FID, the reaction mixture was filtrated through a pad of silica and the pad rinsed with CH_2Cl_2 (3×50 mL). The solvent was evaporated at 650 mbar taking care that the bath temperature did not exceed 35 °C.

yield: 65 mg (66 %), slightly yellow liquid, C_4H_7ClO, [106.55 g/mol]

R_f= 0.68 (cyclohexane/ethylacetate 4/1) ($KMnO_4$)

GC-FID (KH_80_30_280): t_R= 2.6 min

^{1}H-NMR (300.36 MHz, $CDCl_3$): δ = 9.78 (s, 1H, H-1), 3.57 (t, $^3J_{HH}$ = 6.4 Hz, 2H, H-4), 2.64 (t, $^3J_{HH}$ = 6.8 Hz, 2H, H-2), 2.24–2.07 (m, 2H, H-3) ppm.

^{13}C-NMR (75.53 MHz, $CDCl_3$): δ = 201.1 (C-1), 44.3 (C-2), 41.1 (C-4), 25.0 (C-3) ppm.

NMR spectra are in accordance with previously reported ones.[113]

7.7.5.3 5-Bromopentan-2-one (52)

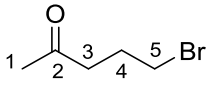

52

In a 25 mL one-neck round-bottom flask 3-acetyldihydrofuran-2(3*H*)-one (1.0 mL, 1.19 g, 9.3 mmol) was dissolved in 4 mL toluene. HBr (48 w% in water, 1.6 mL, 2.73 g, 14.0 mmol) was added in one portion and the reaction mixture was heated to 80 °C until TLC indicated full conversion of the staring material (8 h). The reaction solution was diluted by the addition of distilled H_2O (10 mL), the phases were separated, and the aqueous phase was extracted with Et_2O (6x10 mL). The combined organic layers were washed with brine (1x60 mL), dried over Na_2SO_4, and the solvent was removed under reduced pressure. The brown oil was

purified via flash chromatography (125 g silica gel, 12×4.0 cm, cyclohexane/ethylacetate 4/1, fraction size: 50 mL).

yield: 791 mg (52 %), orange liquid, C_5H_9BrO, [165.03 g/mol]

R_f= 0.62 (cyclohexane/ethylacetate 4/1) ($KMnO_4$)

GC-FID (KH_80_30_280): t_R= 3.6 min

^{1}H-NMR (300.36 MHz, $CDCl_3$): δ = 3.44 (t, $^3J_{HH}$= 6.3 Hz, 2H, H-5), 2.64 (t, $^3J_{HH}$= 6.9 Hz, 2H, H-3), 2.12 (m, 5H, H-1, H-4) ppm.

^{13}C-NMR (75.53 MHz, $CDCl_3$): δ = 207.5 (C-2), 41.6 (C-3), 33.4 (C-5), 30.2 (C-1), 26.5 (C-4) ppm.

HRMS (EI): Calcd. (m/z) for C_3H_6Br [M-CH_3CO]: 120.9653; found: 120.9653.

NMR spectra are in accordance with previously reported ones.[114]

7.7.5.4 Ethyl 4-hydroxy-3-methylbutanoate (90)

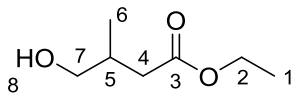

90

In a 250 mL two-neck round-bottom flask with nitrogen inlet ethyl (*E*)-4-hydroxy-3-methylbut-2-enoate (**83**) (682 mg, 4.73 mmol) was dissolved in 160 mL EtOAc. Et_3N (394 µL, 288 mg, 2.85 mmol) and 10 % Pd/C (160 mg, 150 µmol) were added. The grey suspension was cooled to 0 °C and after providing hydrogen atmosphere by evacuating and back-flushing with hydrogen gas (3 x), the reaction mixture was stirred for 3 h at 0 °C with an attached balloon filled with H_2. Complete consumption of starting material was detected by GC-FID indicating the formation of an unknown byproduct (50 %). The reaction solution was filtrated through a pad of celite, which was rinsed with ethylacetate (3×30 mL), and the solvent was evaporated under reduced pressure. The crude product was used immediately in the next step without further purification.

7.7.5.5 Ethyl 4-chloro-3-methylbutanoate (85)

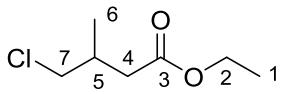

85

In a flame dried 100 mL two-neck round-bottom flask with nitrogen inlet and a bubble counter ethyl 4-hydroxy-3-methylbutanoate (**84**) (998 mg, 6.83 mmol) was dissolved in 30 mL dry CH_2Cl_2 and cooled to -20 °C using an acetone/dry ice bath. Dry pyridine (4.0 mL, 3.84 g, 49.0 mmol) and PPh_3 (7.28 g, 27.7 mmol) were added and the clear, colorless solution was stirred for 20 min at -20 °C. NCS (1.85 g, 13.8 mmol) was added in small portions within 30 min and the reaction solution turned dark brown. After slowly warming the reaction mixture to 22 °C (2 h), TLC indicated complete consumption of starting material. The reaction mixture was quenched by the addition of 1M HCl (40 mL). The aqueous phase was extracted with CH_2Cl_2 (3x50 mL) and the combined organic layers were washed with 10 w% aq. $CuSO_4$ solution (3x60 mL) and brine (1x100 mL). The organic phase was dried over Na_2SO_4 and the solvent was removed under reduced pressure. The product was purified via flash chromatography (500 g silica gel, 20×8 cm, cyclohexane/ethylacetate 70/1, fraction size: 250 mL).

yield: 653 mg (3.91 mmol, 58 %), colorless liquid, $C_7H_{13}O_2Cl$ [164.63]

R_f= 0.61 (cyclohexane/ethylacetate 10/1, UV and $KMnO_4$)

^{1}H NMR (300.36 MHz, $CDCl_3$): δ = 4.14 (q, $^3J_{HH}$= 7.1 Hz, 2H, H-2), 3.75-3.27 (m, 2H, H-7), 2.53 (dd, $^3J_{HH}$= 15.2, 6.0 Hz, 1H, H-4), 2.44-2.27 (m, 1H, H-5), 2.24 (dd, $^3J_{HH}$= 15.2, 7.2 Hz, 1H, H-4), 1.26 (t, $^3J_{HH}$= 7.1 Hz, 3H, H-1), 1.07 (d, $^3J_{HH}$= 6.6 Hz, 3H, H-6).

^{13}C NMR (75.53 MHz, $CDCl_3$): δ = 172.4 (C-3), 60.6 (C-2), 50.3 (C-7), 38.6 (C-4), 32.7 (C-5), 17.9 (C-6), 14.4 (C-1).

HRMS (EI): Calcd. (m/z) for $C_7H_{12}O_2$ [M-HCl]: 128.0837, found: 128.0837.

7.7.5.6 Ethyl 4-hydroxy-2-methylbutanoate (65)

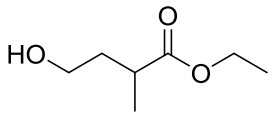

65

The preparation was executed as described in 7.7.5.4 starting from ethyl (*E*)-4-hydroxy-2-methylbut-2-enoate (**61**) (1.0 g, 7.0 mmol). The crude product was used immediately in the next step without further purification.

7.7.5.7 Ethyl 4-chloro-2-methylbutanoate (66)

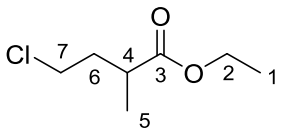

66

The preparation was executed as described in 7.7.5.5 starting from ethyl 4-hydroxy-2-methylbutanoate (**65**) (1.25 g, 8.55 mmol). The product was purified via flash chromatography (500 g silica gel, 22×7.5 cm, cyclohexane/ethylacetate 70/1, fraction size: 250 mL).

yield: 865 mg (5.25 mmol, 61 %), colorless liquid, $C_7H_{13}O_2Cl$ [164.63]

R_f= 0.67 (cyclohexane/ethylacetate 10/1, UV and $KMnO_4$)

^{1}H NMR (300.36 MHz, $CDCl_3$): δ = 4.14 (q, $^3J_{HH}$= 7.1 Hz, 2H, H-2), 3.56 (t, $^3J_{HH}$= 6.7 Hz, 2H, H-7), 2.83-2.45 (m, 1H, H-4), 2.18 (td, $^3J_{HH}$= 14.3, 6.6 Hz, 1H, H-6), 1.83 (dt, $^3J_{HH}$= 13.4, 6.7 Hz, 1H, H-6), 1.41-0.99 (m, 6H, H-1, H-5).

^{13}C NMR (75.53 MHz, $CDCl_3$): δ = 175.9 (C-3), 60.7 (C-2), 42.7 (C-7), 36.9 (C-4), 36.2 (C-6), 17.0 (C-5), 14.3 (C-1).

NMR spectra are in accordance with previously reported ones.[115]

7.7.5.8 Ethyl 4-bromo-3-methylbutanoate (91)

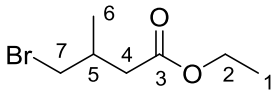

91

A 250 mL one-neck round-bottom flask was charged with ethyl 4-hydroxy-3-methylbutanoate (**90**) (557 mg, 3.81 mmol) dissolved in 5 mL CH_2Cl_2 and cooled in an ice/water bath. CBr_4 (1.98 g 6.0 mmol) was added and a solution of PPh_3 (1.20 g, 4.57 mmol) in 5 mL CH_2Cl_2 was added dropwise to the reaction mixture at 0 °C. After 30 min stirring at 22 °C TLC indicated full conversion of starting material and the reaction mixture was concentrated to dryness without further workup. The product was purified via flash chromatography (200 g silica gel, 6×14 cm, cyclohexane/ethylacetate 70/1, fraction size: 120 mL).

yield: 536 mg (67 %), colourless liquid, $C_7H_{13}BrO_2$, [209.08 g/mol]

R_f= 0.45 (cyclohexane/ethylacetate 10/1) ($KMnO_4$)

GC-FID (KH_80_30_280): t_R= 4.0 min

^{1}H NMR (300.36 MHz, $CDCl_3$): δ = 4.38-391 (m, 2H, H-2), 3.63-3.25 (m, 2H, H-7), 2.52 (dd, $^3J_{HH}$= 14.9, 5.7 Hz, 1H, H-4), 2.43-2.15 (m, 2H, H-4, H-5), 1.26 (t, $^3J_{HH}$= 7.1 Hz, 3H, H-1), 1.08 (d, $^3J_{HH}$= 6.4 Hz, 3H, H-6).

^{13}C NMR (75.53 MHz, $CDCl_3$): δ = 172.3 (C-3), 60.6 (C-2), 40.3 (C-7), 39.5 (C-4), 32.3 (C-5), 18.9 (C-6), 14.4 (C-1).

NMR spectra are in accordance with previously reported ones.[116]

7.7.5.9 Ethyl 4-hydroxy-3-phenylbutanoate (112)

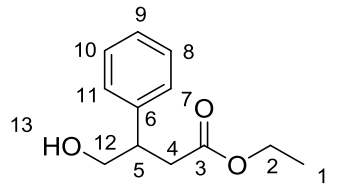

120

A 0.05 M solution of ethyl (*E*)-4-hydroxy-3-phenylbut-2-enoate (**110**) (1.14 g, 5.53 mmol) in 110 mL methanol was prepared in a 200 mL Erlenmeyer flask. The reduction was carried out using a continuous-flow hydrogenation reactor (H-cube™) with a 10 % Pd/C catalyst

cartridge with the following conditions: 1 mL/min, 60 °C, 60 bar H_2. The product solution was collected in a 250 mL Erlenmeyer flask and the solvent was removed under reduced pressure. The product was purified via flash chromatography (50 g silica gel, 11×3.5 cm, cyclohexane/ethylacetate 4/1, fraction size: 25 mL).

yield: 536 mg (67 %), colorless liquid, $C_{12}H_{16}O_3$, [208.26 g/mol]

R_f= 0.45 (cyclohexane/ethylacetate 10/1) ($KMnO_4$)

^{1}H-NMR (300.36 MHz, MeOD): δ = 7.38-7.08 (m, 5H, H-7, H-8, H-9, H-10, H-11), 4.00 (q, $^3J_{HH}$= 7.1 Hz, 2H, H-2), 3.77-3.57 (m, 2H, H-12), 3.27 (dd, $^3J_{HH}$= 10.8, 4.9 Hz, 1H, H-5), 2.87 (dd, $^3J_{HH}$= 15.4, 5.8 Hz, 1H, H-4), 2.59 (dd, $^3J_{HH}$= 15.3, 9.4 Hz, 1H, H-4), 1.11 (t, $^3J_{HH}$= 7.1 Hz, 3H, H-1) ppm.

^{13}C-NMR (75.53 MHz, MeOD): δ = 164.8 (C-3), 133.3 (C-6), 120.0 (C-7, C-11), 119.5 (C-8, C-10), 118.3 (C-9), 57.7 (C-12), 51.9 (C-2), 36.9 (C-5), 28.9 (C-4), 4.9 (C-1) ppm.

HRMS (EI): Calcd. (m/z) for $C_{12}H_{16}O_3$ [M^+]: 208.1099; found: 208.1091.

7.7.5.10 Ethyl 4-chloro-3-phenylbutanoate (121)

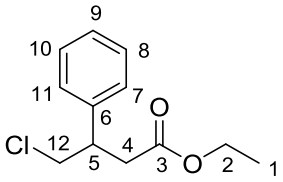

121

In a flame dried 250 mL two-neck round-bottom flask with nitrogen inlet and a bubble counter ethyl 4-hydroxy-3-phenylbutanoate (**120**) (747 mg, 3.59 mmol) was dissolved in 14 mL dry CH_2Cl_2 and cooled to -20 °C using an acetone/dry ice bath. Dry pyridine (2.0 mL, 1.99 g, 24.8 mmol) and PPh_3 (3.76 g, 14.3 mmol) were added and the clear, colorless solution was stirred for 20 min at -20 °C. NCS (957 mg, 7.17 mmol) was added in small portions within 30 min and the reaction solution turned dark brown. After slowly warming the reaction mixture to 22 °C (2 h), TLC indicated complete consumption of starting material. The reaction mixture was quenched by the addition of 1M HCl (20 mL). Addition of CH_2Cl_2 (20 mL) and centrifugation at 5000 rpm for 15 min produced two phases which were separated. The aqueous phase was extracted with CH_2Cl_2 (3x20 mL) and the combined organic layers were washed with 10 w% aq. $CuSO_4$ solution (3x20 mL) and brine (1x50 mL).

The organic phase was dried over Na_2SO_4 and the solvent was removed under reduced pressure. The product was purified via flash chromatography (250 g silica gel, 17.5×5.5 cm, cyclohexane/ethylacetate 25/1, fraction size: 150 mL).

yield: 1.40 g (58 %), slightly yellow liquid, $C_{12}H_{15}ClO_2$, [226.70 g/mol]

R_f= 0.56 (cyclohexane/ethylacetate 9/1) ($KMnO_4$)

GC-FID (KH_80_30_280): t_R= 6.3 min

^{1}H-NMR (300.36 MHz, DMSO-d_6): δ = 7.30-7.26 (m, 5H, H-7, H-8, H-9, H-10, H-11), 3.99-3.79 (m, 4H, H-2, H-12), 3.40 (dd, $^3J_{HH}$= 14.1, 7.5 Hz 2H, H-5), 2.89 (dd, $^3J_{HH}$= 15.8, 5.9 Hz, 1H, H-4), 2.69 (dd, $^3J_{HH}$= 15.8, 9.0 Hz, 1H, H-4), 1.05 (t, $^3J_{HH}$= 7.1 Hz, 3H, H-1) ppm.

^{13}C-NMR (75.53 MHz, DMSO-d_6): δ = 171.0 (C-3), 140.6 (C-6), 128.3 (C-8, C-10), 127.8 (C-7, C-11), 127.0 (C-9), 59.9 (C-2), 48.7 (C-12), 43.8 (C-5), 37.5 (C-4), 13.9 (C-1) ppm.

HRMS (EI): Calcd. (m/z) for $C_{12}H_{14}O_2$ [M-HCl]: 190.0994; found: 190.0996.

7.7.5.11 General Procedure for the reduction of saturated esters (66, 85, 91, 121) to the corresponding aldehydes (64, 74, 89, 113)

In a flame dried 50 mL two-neck round-bottom flask with nitrogen inlet, saturated ester **66**, **85**, **91**, **121** (1.48 mmol) was dissolved in 5 mL dry CH_2Cl_2. The reaction solution was cooled to -78 °C using an acetone/dry ice bath. A solution of DIBAL-H (1.0 M in CH_2Cl_2, 1.6 mL, 1.6 mmol) was added dropwise via syringe to the reaction mixture in a N_2-counterstream. After 15 min TLC indicated complete consumption of the starting material and overreduction to the alcohol. The reaction mixture was quenched by addition of 1M HCl at -78 °C and then warmed to 22 °C. The colorless layers were separated and the aqueous phase was extracted with CH_2Cl_2 (2 x 50 mL). The combined organic layers were washed with brine (1x100 mL) and dried over Na_2SO_4. The reaction solution was added to a flame dried 50 mL two-neck round-bottom flask with nitrogen inlet. PCC (487 mg, 2.22 mmol) and 4 Å molecular sieves (0.5 g) were added in a N_2-counterstream and the brownish solution was stirred at 22 °C. After full conversion was indicated by TLC and GC-FID, the reaction mixture was filtrated through a pad of silica, which was then rinsed with CH_2Cl_2 (3×50 mL). The solvent was evaporated under reduced pressure.

7.7.5.12 4-Bromo-3-methylbutanal (89)

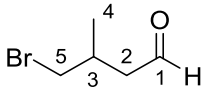

89

Starting from ethyl 4-bromo-3-methylbutanoate (**91**) (294 mg, 1.41 mmol) reduction to the aldehyde was executed as described in 7.7.5.11. The product did not require further purification.

yield: 172 mg (74 %), slightly green liquid, C_5H_9BrO, [165.03 g/mol]

GC-FID (KH_80_30_280): t_R= 3.4 min

R_f= 0.27 (cyclohexane/ethylacetate 10/1) ($KMnO_4$)

^{1}H-NMR (300.36 MHz, $CDCl_3$): δ = 9.78 (s, 1H, H-1), 3.42 (ddd, $^3J_{HH}$= 27.7, 10.0 5.1 Hz, 2H, H-5), 2.81-2.60 (m, 1H, H-2), 2.55-2.24 (m, 2H, H-2, H-3), 1.08 (d, $^3J_{HH}$= 6.5 Hz, 3H, H-4) ppm.

^{13}C-NMR (75.53 MHz, $CDCl_3$): δ = 201.0 (C-1), 48.9 (C-2), 40.2, (C-5), 30.0 (C-3), 19.1 (C-4) ppm.

HRMS (EI): Calcd. (m/z) for C_5H_8O [M-HBr]: 84.0575; found: 84.0574.

7.7.5.13 4-Chloro-3-methylbutanal (74)

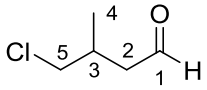

74

Starting from ethyl 4-chloro-3-methylbutanoate (**85**) (400 mg, 2.43 mmol) reduction to the aldehyde was executed as described in 7.7.5.11. The product was purified via flash chromatography (40 g silica gel, 9.0×4.5 cm, n-pentane/diethylether 20/1, fraction size: 25 mL).

yield: 59 mg (20 %), colourless liquid, C_5H_9ClO, [120.58 g/mol]

R_f= 0.26 (cyclohexane/ethylacetate 10/1) ($KMnO_4$)

GC-FID (KH_80_30_280): t_R= 2.9 min

^{1}H-NMR (300.36 MHz, $CDCl_3$): δ = 9.78 (s, 1H, H-1), 3.52 (ddd, $^3J_{HH}$= 29.6, 10.8 5.3 Hz, 2H, H-5), 2.71 (dd, $^3J_{HH}$= 16.7, 5.0 Hz, 1H, H-2), 2.63-2.20 (m, 2H, H-2, H-3), 1.07 (d, $^3J_{HH}$= 6.6 Hz, 3H, H-4) ppm.

^{13}C-NMR (75.53 MHz, $CDCl_3$): δ = 201.1 (C-1), 50.3 (C-5), 48.0, (C-2), 30.4 (C-3), 18.1 (C-4) ppm.

HRMS (EI): Calcd. (m/z) for C_5H_8O [M-HCl]: 84.0575; found: 84.0575.

7.7.5.14 4-Chloro-2-methylbutanal (64)

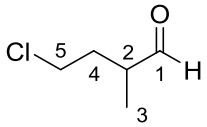

64

Starting from ethyl 4-chloro-2-methylbutanoate (**66**) (400 mg, 2.43 mmol) reduction to the aldehyde was executed as described in 7.7.5.11. The product was purified via flash

chromatography (25 g silica gel, 7.0×2.5 cm, n-pentane/diethylether 20/1, fraction size: 25 mL).

yield: 20 mg (7 %), colourless liquid, C_5H_9ClO, [120.58 g/mol]

R_f= 0.64 (cyclohexane/ethylacetate 2/1) ($KMnO_4$)

GC-FID (KH_80_30_280): t_R= 2.9 min

^{1}H-NMR (300.36 MHz, $CDCl_3$): δ = 9.68 (s, 1H, H-1), 3.78-3.45 (m, 2H, H-5), 2.67 (dq, $^3J_{HH}$= 13.8, 6.9 Hz, 1H, H-2), 2.24 (td, $^3J_{HH}$= 13.7, 6.7 Hz, 1H, H-4), 1.88-1.65 (m, 1H, H-4), 1.16 (d, $^3J_{HH}$= 7.2 Hz, 3H, H-3) ppm.

^{13}C-NMR (75.53 MHz, $CDCl_3$): δ = 203.7 (C-1), 43.7 (C-2), 42.2, (C-5), 33.0 (C-4), 13.1 (C-3) ppm.

NMR spectra are in accordance with previously reported ones.[115]

7.7.5.15 4-Chloro-3-phenylbutanal (113)

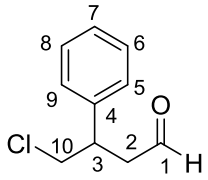

113

Starting from ethyl 4-chloro-3-phenylbutanoate (**121**) (336 mg, 1.48 mmol) reduction to the aldehyde was executed as described in 7.7.5.11. The product was purified via flash chromatography (15 g silica gel, 4.5×2.0 cm, cyclohexane/ethylacetate 12/1, fraction size: 10 mL).

yield: 114 mg (42 %), slightly yellow liquid, $C_{10}H_{11}ClO$, [182.65 g/mol]

R_f= 0.41 (cyclohexane/ethylacetate 4/1) ($KMnO_4$)

GC-FID (KH_80_30_280): t_R= 5.9 min

^{1}H-NMR (300.36 MHz, DMSO-d_6): δ = 9.60 (s, 1H, H-1), 7.33-7.24 (m, 5H, H-5, H-6, H-7, H-8, H-9), 4.02-3.71 (m, 2H, H-10), 3.72-3.39 (m, 1H, H-3), 3.16-2.66 (m, 2H, H-2) ppm.

^{13}C-NMR (75.53 MHz, DMSO-d_6): δ = 201.7 (C-1), 140.9 (C-4), 128.4 (C-6, C-8), 127.8 (C-5, C-9), 127.0 (C-7), 49.0 (C-10), 46.4 (C-2), 41.3 (C-3) ppm.

HRMS (EI): Calcd. (m/z) for $C_{10}H_{10}O$ [M-HCl]: 146.0732; found: 146.0736.

7.7.6 Synthesis of racemic and chiral cyclopropanes

7.7.6.1 1-Methylcyclopropane-1-carbaldehyde (41)

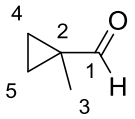

41

In a flame dried 50 mL two-neck round-bottom flask with nitrogen inlet (1-methylcyclopropyl)methanol (250 mg, 2.9 mmol) was dissolved in 18 mL abs. CH_2Cl_2. PCC (1.25 g, 5.80 mmol) and 4 Å molecular sieves (0.5 g) were added in a N_2-counterstream and the brownish solution was stirred at 22 °C. After full conversion of starting material was indicated by GC-FID (8 h), the reaction mixture was filtrated through a pad of silica, which was then rinsed with CH_2Cl_2 (3×50 mL). The clear and colorless filtrate was concentrated at a pressure of 200 mbar (with care to not exceed 35 °C water bath temperature).

yield: 61 mg (25 %), colorless liquid, C_5H_8O, [84.12 g/mol]

GC-FID (KH_80_30_280): t_R= 1.8 min

^{1}H-NMR (300.36 MHz, $CDCl_3$): δ = 8.63 (s, 1H, H-5), 5.29 (s, 3H, H-3), 1.19-1.08 (m, 2H, H-5), 0.92 (q, $^3J_{HH}$= 4.1 Hz, 2H, H-4) ppm.

^{13}C-NMR (75.53 MHz, $CDCl_3$): δ = 202.1 (C-1), 27.7 (C-2), 15.7 (C-3), 14.0 (C-4, C-5) ppm.

The recorded spectra are in accordance with the reported in literature.[117]

7.7.6.2 *trans*-(2-Phenylcyclopropyl)methanol (*rac*) (*trans*-115)

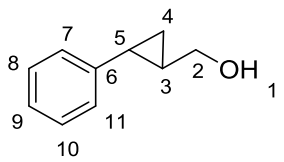

trans-**115**

In a flame dried 50 mL three-neck round-bottom flask equipped with nitrogen inlet and a bubble counter, freshly distilled CH_2I_2 (360 µL, 1.20 g, 4.47 mmol) was dissolved in 26 mL dry CH_2Cl_2 (0.17 M). The reaction mixture was cooled to 0 °C using an ice/water bath and

Et_2Zn (1.0 M solution in hexanes, 2.8 mL, 2.8 mmol) was added dropwise via syringe forming a colorless precipitate. In the meanwhile, in a second flame dried 25 mL Schlenk flask (*E*)-3-phenylprop-2-en-1-ol (300 mg, 2.24 mmol) was dissolved in 6.3 mL dry CH_2Cl_2 (0.33 M). The reaction mixture was cooled to 0 °C using an ice/water bath and Et_2Zn (1.0 M solution in hexanes, 2.8 mL, 2.8 mmol) was added dropwise. After 30 min stirring at 0 °C the content of the second flask was added to the first flask via cannula. The reaction solution was stirred at 22 °C until GC-FID indicated complete consumption of starting material (8 h). The reaction was quenched by the addition of sat. aq. NH_4Cl-solution (26 mL, 11.5 mL/mmol allylic alcohol). The aqueous phase was extracted with CH_2Cl_2 (3x15 mL) and the combined organic layers were washed with brine (1x50 mL), dried over Na_2SO_4, and the solvent was evaporated under reduced pressure. The product was purified via flash chromatography (30 g silica gel, 7×3.5 cm, cyclohexane/ethylacetate 5/1, fraction size: 15 mL).

yield: 160 mg (48 %), colourless liquid, $C_{10}H_{12}O$, [148.21 g/mol]

R_f= 0.24 (cyclohexane/ethylacetate 5/1) ($KMnO_4$)

^{1}H-NMR (300.36 MHz, $CDCl_3$): δ = 7.24-7.05 (m, 5H, H-7, H-8, H-9, H-10, H-11), 3.60 (m, 2H, H-2), 1.80 (m, 1H, H-5), 1.58 (s, 1H, H-1), 1.43 (m, 1H, H-3), 0.93 (m, 2H, H-4) ppm.

^{13}C-NMR (75.53 MHz, $CDCl_3$): δ = 142.6 (C-6), 128.5 (C-7, C-11), 126.0 (C-8, C-10), 125.8 (C-9), 66.7 (C-2), 25.4 (C-3), 21.4 (C-5), 13.9 (C-4) ppm.

The recorded spectra are in accordance with the reported in literature.[118]

7.7.6.3 *trans*-2-Phenylcyclopropane-1-carbaldehyde (*rac*) (*trans*-114)

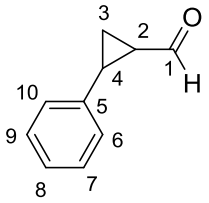

trans-**114**

The preparation was executed as described in 7.7.6.1 starting from racemic *trans*-(2-phenylcyclopropyl)methanol (*trans*-**115**) (100 mg, 675 µmol).

yield: 53 mg (53 %), yellowish liquid, $C_{10}H_{12}O$, [148.21 g/mol]

GC-FID (KH_80_30_280): t_R= 5.2 min

^{1}H-NMR (300.36 MHz, $CDCl_3$): δ = 9.33 (d, $^{3}J_{HH}$= 4.6 Hz, 1H, H-1), 7.33-7.11 (m, 5H, H-6, H-7, H-8, H-9, H-10), 2.66-2.61 (m, 1H, H-4), 2.21-2.15 (m, 1H, H-2), 1.76-1.71 (m, 1H, H-3), 1.56-1.51 (m, 1H, H-3) ppm.

^{13}C-NMR (75.53 MHz, $CDCl_3$): δ = 199.6 (C-1), 138.9 (C-5), 128.5 (C-6, C-10), 126.7 (C-7, C-9), 126.2 (C-8), 33.7 (C-2), 26.5 (C-4), 16.4 (C-3) ppm.

The recorded spectra are in accordance with the reported in literature.[119]

7.7.6.4 (*Z*)-2-Phenylethen-1-ol (119)

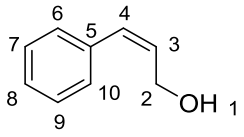

119

In a 20 mL two-neck round-bottom flask equipped with nitrogen inlet 3-phenylprop-2-yn-1-ol (1.0 mL, 1.08 g, 8.16 mmol), quinoline (102 µL, 111 mg, 860 µmol), and Lindlar catalyst (208 mg, 1.96 mmol) were suspended in 12 mL ethylacetate. After ensuring hydrogen atmosphere by evacuating and back-flushing with hydrogen gas (3 x), the reaction mixture was stirred at 22 °C with an attached balloon filled with H_2 until GC-FID indicated complete consumption of starting material (1 h). The reaction solution was filtrated through a pad of celite, which was rinsed with ethylacetate (2×8 mL), and the solvent was evaporated under reduced pressure. The product was purified via flash chromatography (100 g silica gel, 12×1.5 cm, cyclohexane/ethylacetate 5/1, fraction size: 50 mL).

yield: 760 mg (69 %), colorless liquid, $C_9H_{10}O$, [134.18 g/mol]

R_f= 0.23 (cyclohexane/ethylacetate 5/1) ($KMnO_4$)

^{1}H-NMR (300.36 MHz, $CDCl_3$): δ = 7.31-7.13 (m, 5H, H-6, H-7, H-8, H-9, H-10), 6.51 (d, $^{3}J_{HH}$= 11.7 Hz, 1H, H-4), 5.81 (dt, $^{3}J_{HH}$= 11.7, 6.3 Hz, 1H, H-3), 4.37 (dd, $^{3}J_{HH}$= 6.3, 1.1 Hz, 2H, H-2), 1.62 (s, 1H, H-1) ppm.

^{13}C-NMR (75.53 MHz, $CDCl_3$): δ = 136.7 (C-5), 131.3 (C-3), 131.2 (C-4), 128.9 (C-6, C-10), 128.4 (C-7, C-9), 127.4 (C-8), 59.8 (C-2) ppm.

The recorded spectra are in accordance with the reported in literature.[120]

7.7.6.5 *cis*-(2-Phenylcyclopropyl)methanol (*rac*) (*cis*-115)

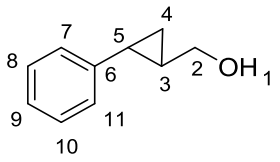

(*cis*-**115**)

Starting from (*Z*)-2-phenylethen-1-ol (**119**) (760 mg, 5.66 mmol) cyclopropanation was executed as described in 7.7.6.2. The product was purified via flash chromatography (100 g silica gel, 12×1.5 cm, cyclohexane/ethylacetate 5/1, fraction size: 50 mL).

yield: 584 mg (70 %), colorless liquid, $C_{10}H_{12}O$, [148.21 g/mol]

R_f= 0.24 (cyclohexane/ethylacetate 5/1) ($KMnO_4$)

^{1}H-NMR (300.36 MHz, $CDCl_3$): δ = 7.28-7.15 (m, 5H, H-7, H-8, H-9, H-10, H-11), 3.43 (dd, $^3J_{HH}$= 11.6, 6.4 Hz, 1H, H-2), 3.24 (dd, $^3J_{HH}$= 11.6, 8.5 Hz, 1H, H-2), 2.27 (dd, $^3J_{HH}$= 14.7, 8.3 Hz, 1H, H-3), 1.48-1.37 (m, 2H, H-1, H-5), 1.02 (td, $^3J_{HH}$= 8.3, 5.4 Hz, 1H, H-4), 0.85 (dd, $^3J_{HH}$= 11.2, 5.6 Hz, 1H, H-4) ppm.

^{13}C-NMR (75.53 MHz, $CDCl_3$): δ = 138.4 (C-6), 129.0 (C-7, C-11), 128.4 (C-8, C-10), 126.3 (C-9), 63.0 (C-2), 21.0 (C-3), 20.8 (C-5), 7.8 (C-4) ppm.

The recorded spectra are in accordance with the reported in literature.[121]

7.7.6.6 *cis*-2-Phenylcyclopropane-1-carbaldehyde (*rac*) (*cis*-114)

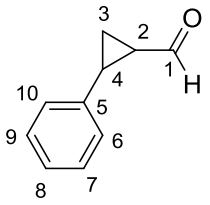

cis-**114**

The preparation was executed as described in 7.7.6.1 starting from racemic *cis*-(2-phenylcyclopropyl)methanol (*cis*-**115**) (108 mg, 729 µmol).

yield: 65 mg (60 %), yellowish liquid, $C_{10}H_{12}O$, [148.21 g/mol]

GC-FID (KH_80_30_280): t_R= 5.3 min

^{1}H-NMR (300.36 MHz, $CDCl_3$): δ = 8.66 (d, $^{3}J_{HH}$= 6.6 Hz, 1H, H-1), 7.32-7.21 (m, 5H, H-6, H-7, H-8, H-9, H-10), 2.83 (q, $^{3}J_{HH}$= 8.2 Hz, H-2), 2.14-2.00 (m, 1H, H-4), 1.88-1.79 (dt, $^{3}J_{HH}$= 7.2, 5.3 Hz, 1H, H-3), 1.64-1.55 (dt, $^{3}J_{HH}$= 8.2, 5.6 Hz 1H, H-3) ppm.

^{13}C-NMR (75.53 MHz, $CDCl_3$): δ = 201.3 (C-1), 135.7(C-5), 129.1 (C-6, C-10), 128.5 (C-7, C-9), 127.1 (C-8), 29.6 (C-4), 26.3 (C-2), 11.5 (C-3).

The recorded spectra are in accordance with the reported in literature.[122]

7.7.6.7 (*Z*)-But-2-en-1-ol (*cis*-77)

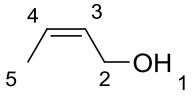

cis-**77**

In a 250 mL two-neck round-bottom flask equipped with nitrogen inlet 2-butyn-1-ol (5.0 mL, 4.69 g, 66.8 mmol) and Lindlar catalyst (133 mg, 1.25 mmol) were suspended in 100 mL MeOH. After ensuring hydrogen atmosphere by evacuating and back-flushing with hydrogen gas (3 x), the reaction mixture was stirred at 22 °C with an attached balloon filled with H_2 until GC-FID indicated complete consumption of starting material (3 d). The reaction solution was filtrated through a pad of celite, which was then rinsed with MeOH (3×50 mL). The filtrate was concentrated at a pressure of 200 mbar (with care to not exceed 35 °C water bath temperature). The yellow liquid was purified by distillation at atmospheric pressure (b.p. = 112 °C).

yield: 2.07 g (43 %), colourless liquid, C_4H_8O, [72.06 g/mol]

GC-FID (KH_80_30_280): t_R= 1.8 min

^{1}H NMR (300.36 MHz, $CDCl_3$): δ = 5.72–5.47 (m, 2H, H-3, H-4), 4.20 (d, $^{3}J_{HH}$= 4.3 Hz, 2H, H-2), 1.69–1.63 (m, 3H, H-5), 1.57 (s, 1H, H-1) ppm.

^{13}C-NMR (75.53 MHz, $CDCl_3$): δ = 129.4 (C-4), 127.3 (C-3), 58.4 (C-2), 13.1 (C-5) ppm.

The recorded spectra are in accordance with the reported in literature.[123]

7.7.6.8 (*E*)-But-2-en-1-ol (*trans*-77)

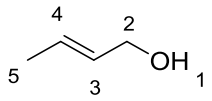

trans-**77**

In a flame dried 250 mL two-neck round-bottom flask equipped with nitrogen inlet and bubble counter, $LiAlH_4$ (5.32 g, 140 mmol) was suspended in 25 mL dry Et_2O at 0 °C. A solution of 2-butyn-1-ol (5.0 mL, 4.69 g, 66.8 mmol) in 25 mL dry Et_2O was added dropwise to the reaction mixture and the grey suspension was stirred at 22 °C until GC-FID indicated complete consumption of starting material (8 h). The reaction mixture was cooled using an ice/water bath and dist. H_2O (5.3 mL), 15 w% NaOH (5.3 mL), and dist. H_2O (15.9 mL) were added carefully in the stated sequence. After the reaction mixture was stirred at 22 °C for 30 min the colorless precipitate was removed by filtration through a fritted funnel, which was washed with Et_2O (3×30 mL). The filtrate was concentrated at a pressure of 200 mbar (with care to not exceed 35 °C water bath temperature). The yellow solution was purified by distillation at atmospheric pressure (b.p. = 114 °C).

yield: 2.97 g (62 %), colourless liquid, C_4H_8O, [72.06 g/mol]

GC-FID (KH_80_30_280): t_R= 1.7 min

^{1}H NMR (300.36 MHz, $CDCl_3$): δ = 5.98–5.35 (m, 2H, H-3, H-4), 4.05 (d, $^3J_{HH}$= 3.8 Hz, 2H, H-2), 1.70 (d, $^3J_{HH}$= 4.9 Hz, 3H, H-5), 1.60 (s, 1H, H-1) ppm.

^{13}C-NMR (75.53 MHz, $CDCl_3$): δ = 130.3 (C-4), 128.2 (C-3), 63.8 (C-2), 17.8 (C-5) ppm.

The recorded spectra are in accordance with the reported in literature.[123]

7.7.6.9 *cis*-(2-Methylcyclopropyl)methanol (*rac*) (*cis*-75)

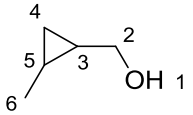

cis-**75**

Starting from (*Z*)-but-2-en-1-ol (*cis*-**77**) (500 mg, 6.94 mmol) cyclopropanation was executed as described in 7.7.6.2. The product was purified via flash chromatography (100 g silica gel, 12×5 cm, n-pentane/diethylether 4/1, fraction size: 25 mL).

yield: 155 mg (26 %), colourless liquid, $C_5H_{10}O$, [86.13 g/mol]

R_f= 0.33 (cyclohexane/ethylacetate 4/1) (CAM)

GC-FID (KH_80_30_280): t_R= 2.1 min

^{1}H-NMR (300.36 MHz, $CDCl_3$): δ = 3.89–3.63 (m, 1H, H-2), 3.63–3.35 (m, 1H, H-2), 1.36 (s, 1H, H-1), 1.07 (dd, $^3J_{HH}$= 14.2, 6.4 Hz, 4H, H-6, H-5), 1.00–0.85 (m, 1H, H-3), 0.81–0.46 (m, 1H, H-4), -0.07 (dd, , $^3J_{HH}$= 10.0, 5.0 Hz, 1H, H-4) ppm.

^{13}C-NMR (75.53 MHz, $CDCl_3$): δ = 63.3 (C-2), 18.2 (C-5), 13.2 (C-6), 10.7 (C-4), 9.8 (C-3) ppm.

The recorded spectra are in accordance with the reported in literature.[124]

7.7.6.10 *trans*-(2-Methylcyclopropyl)methanol (*rac*) (*trans*-75)

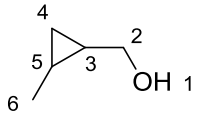

trans-**75**

Starting from (*E*)-but-2-en-1-ol (*trans*-**77**) (500 mg, 6.94 mmol) cyclopropanation was executed as described in 7.7.6.2. The product was purified via flash chromatography (75 g silica gel, 12×4.5 cm, n-pentane/diethylether 4/1, fraction size: 25 mL).

yield: 175 mg (28 %), colourless liquid, $C_5H_{10}O$, [86.13 g/mol]

R_f= 0.33 (cyclohexane/ethylacetate 4/1) (CAM)

GC-FID (KH_80_30_280): t_R= 2.0 min

^{1}H-NMR (300.36 MHz, $CDCl_3$): δ = 3.48–3.37 (p, $^3J_{HH}$= 11.1 Hz, 1H, H-2), 1.53 (s, 1H, H-1), 1.04 (d, $^3J_{HH}$= 5.9 Hz, 3H, H-6), 0.90–0.71 (m, 1H, H-3), 0.71–0.53 (m, 1H, H-5), 0.45-0.05 (m, 2H, H-4) ppm.

^{13}C-NMR (75.53 MHz, $CDCl_3$): δ = 67.3 (C-2), 22.4 (C-3), 18.6 (C-6), 11.3 (C-5), 11.2 (C-4) ppm.

The recorded spectra are in accordance with the reported in literature.[125]

7.7.6.11 ((1*S*,2*R*)-2-Methylcyclopropyl)methanol ((*S*,*R*)-75)

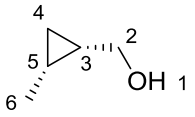

(*S*,*R*)-**75**

In a flame dried 80 mL Schlenk-flask, 1,2-DME (2.0 mL, 19.0 mmol) was dissolved in 18 mL dry CH_2Cl_2. In the meanwhile, in a second flame dried 250 mL three-neck round-bottom flask equipped with nitrogen inlet and a bubble counter, (*Z*)-but-2-en-1-ol (*cis*-**77**) (540 mg, 7.50 mmol) and (4*S*,5*S*)-2-butyl-N^4,N^4,N^5,N^5-tetramethyl-1,3,2-dioxaborolane-4,5-dicarboxamide ((4*S*,5*S*)-**81**) (2.2 g, 8.14 mmol) were dissolved in 37 mL dry CH_2Cl_2. Both reaction mixtures were cooled to -10 °C using a NaCl/ice-water bath. To the solution of 1,2-DME and CH_2Cl_2, Et_2Zn (1.0 M solution in hexanes, 19.0 mL, 19.0 mmol) was added dropwise via syringe forming a cloudy suspension. Then CH_2I_2 (3.0 mL, 37.0 mmol) was added dropwise and after the reaction mixture was stirred for 15 min at -10 °C, the $Zn(CH_2I)_2$*DME solution was added to the 250 mL three-neck round-bottom flask containing the allylic alcohol via cannula. The reaction solution was stirred at 0 °C for 2 h and the reaction was quenched by the addition of sat. aq. NH_4Cl-solution (50 mL). The aqueous phase was extracted with CH_2Cl_2 (3x30 mL), dried over Na_2SO_4, and the solvent was evaporated under reduced pressure. The product was purified via flash chromatography (200 g silica gel, 17×5.5 cm, n-pentane/diethylether 4/1, fraction size: 75 mL).

yield: 57 mg (9 %), colourless liquid, $C_5H_{10}O$, [86.13 g/mol]

R_f= 0.33 (cyclohexane/ethylacetate 4/1) (CAM)

GC-FID (KH_80_30_280): t_R= 2.1 min

^{1}H-NMR (300.36 MHz, $CDCl_3$): δ = 3.89–3.63 (m, 1H, H-2), 3.63–3.35 (m, 1H, H-2), 1.36 (s, 1H, H-1), 1.07 (dd, $^3J_{HH}$= 14.2, 6.4 Hz, 4H, H-6, H-5), 1.00–0.85 (m, 1H, H-3), 0.81–0.46 (m, 1H, H-4), -0.07 (dd, , $^3J_{HH}$= 10.0, 5.0 Hz, 1H, H-4) ppm.

^{13}C-NMR (75.53 MHz, $CDCl_3$): δ = 63.3 (C-2), 18.2 (C-5), 13.2 (C-6), 10.7 (C-4), 9.8 (C-3) ppm.

$[\alpha]^{20}_D$ = +37.4 (c 0.9, CH_2Cl_2); lit.: $[\alpha]^{23}_D$ = +43.4 (c 0.9, CH_2Cl_2).[Ref. 124]

The recorded spectra are in accordance with the reported in literature.[124]

Racemic sample: GC-FID (CP-Chirasil-Dex CB, KH_40_60_155)

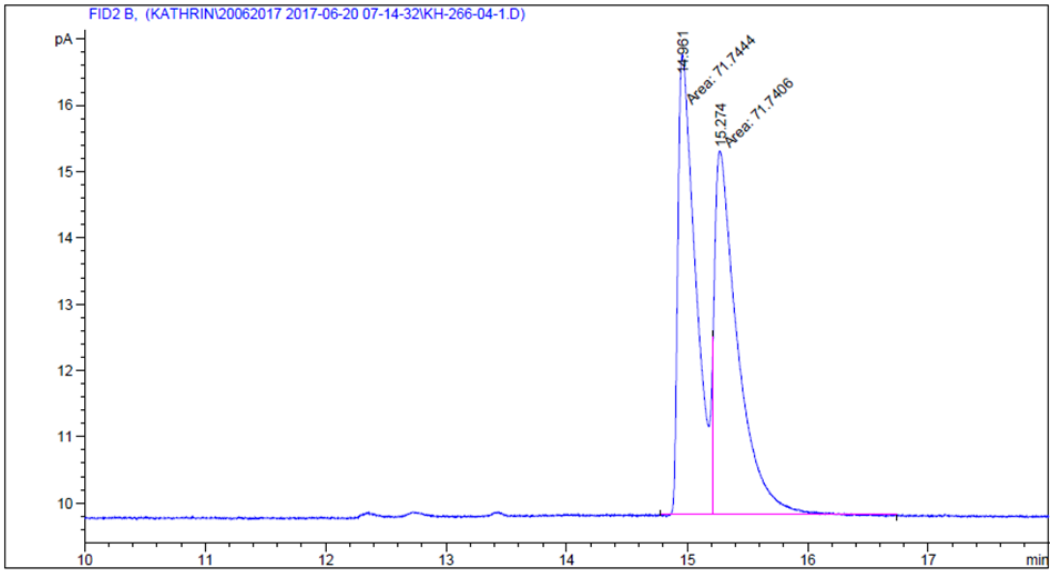

Peak #	RetTime [min]	Type	Width [min]	Area [pA*s]	Height [pA]	Area %
1	14.961	MF	0.1722	71.74436	6.94476	50.00133
2	15.274	FM	0.2181	71.74055	5.48316	49.99867

Enantioenriched sample: GC-FID (CP-Chirasil-Dex CB, KH_40_60_155), 73 % ee

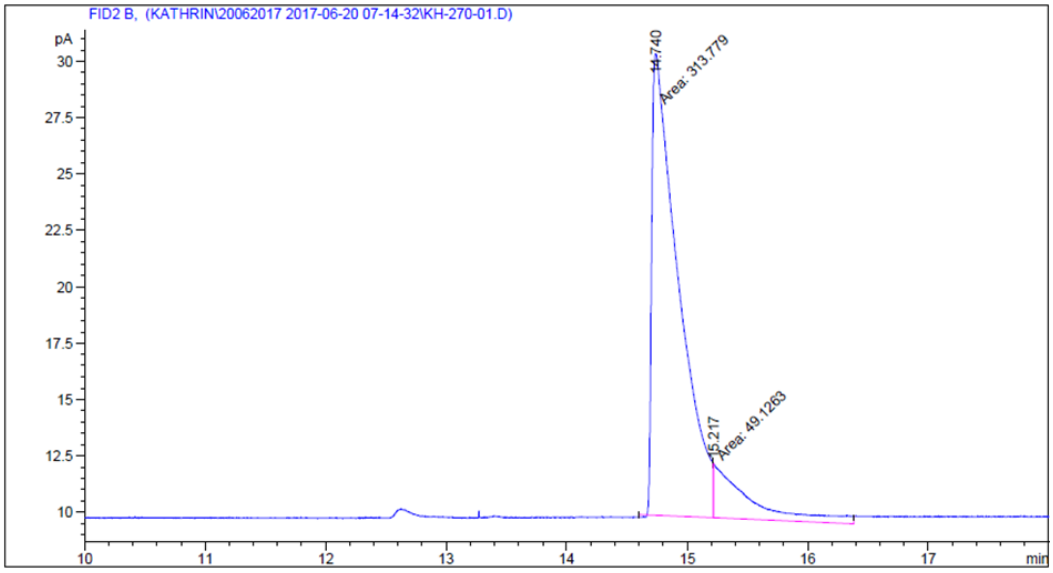

Peak #	RetTime [min]	Type	Width [min]	Area [pA*s]	Height [pA]	Area %
1	14.740	MF	0.2555	313.77863	20.46783	86.46304
2	15.217	FM	0.3373	49.12629	2.42716	13.53696

7.7.6.12 ((1*S*,2*S*)-2-Methylcyclopropyl)methanol ((*S*,*S*)-75)

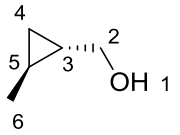

(*S*,*S*)-**75**

In a flame dried 80 mL Schlenk-flask, 1,2-DME (2.0 mL, 19.0 mmol) was dissolved in 18 mL dry CH_2Cl_2. In the meanwhile, in a second flame dried 250 mL three-neck round-bottom flask equipped with nitrogen inlet and a bubble counter, (*E*)-but-2-en-1-ol (*trans*-**77**) (540 mg, 7.50 mmol) and (4*R*,5*R*)-2-butyl-N^4,N^4,N^5,N^5-tetramethyl-1,3,2-dioxaborolane-4,5-dicarboxamide ((4*R*,5*R*)-**81**) (2.2 g, 8.14 mmol) were dissolved in 37 mL dry CH_2Cl_2. Both reaction mixtures were cooled to -10 °C using a NaCl/ice-water bath. To the solution of 1,2-DME and CH_2Cl_2, Et_2Zn (1.0 M solution in hexanes, 19.0 mL, 19.0 mmol) was added dropwise via syringe forming a cloudy suspension. Then CH_2I_2 (3.0 mL, 37.0 mmol) was added dropwise and after the reaction mixture was stirred for 15 min at -10 °C, the $Zn(CH_2I)_2$*DME solution was added to the 250 mL three-neck round-bottom flask containing the allylic alcohol via cannula. The reaction solution was stirred at 0 °C for 2 h and the reaction was quenched by the addition of saturated aqueous NH_4Cl-solution (50 mL). The aqueous phase was extracted with CH_2Cl_2 (3x30 mL), dried over Na_2SO_4, and the solvent was evaporated under reduced pressure. The product was purified via flash chromatography (150 g silica gel, 15×4.5 cm, n-pentane/diethylether 4/1, fraction size: 50 mL).

yield: 247 mg (38 %), colourless liquid, $C_5H_{10}O$, [86.13 g/mol]

R_f= 0.33 (cyclohexane/ethylacetate 4/1) (CAM)

GC-FID (KH_80_30_280): t_R= 2.0 min

^{1}H-NMR (300.36 MHz, $CDCl_3$): δ = 3.48–3.37 (p, $^3J_{HH}$= 11.1 Hz, 1H, H-2), 1.53 (s, 1H, H-1), 1.04 (d, $^3J_{HH}$= 5.9 Hz, 3H, H-6), 0.90–0.71 (m, 1H, H-3), 0.71–0.53 (m, 1H, H-5), 0.45-0.05 (m, 2H, H-4) ppm.

^{13}C-NMR (75.53 MHz, $CDCl_3$): δ = 67.3 (C-2), 22.4 (C-3), 18.6 (C-6), 11.3 (C-5), 11.2 (C-4) ppm.

$[\alpha]^{20}_D$ = +46.5 (c 0.13, CH_2Cl_2); lit.: value not available.[Ref.126]

The recorded spectra are in accordance with the reported in literature.[126]

Racemic sample: GC-FID (CP-Chirasil-Dex CB, KH_40_60_155)

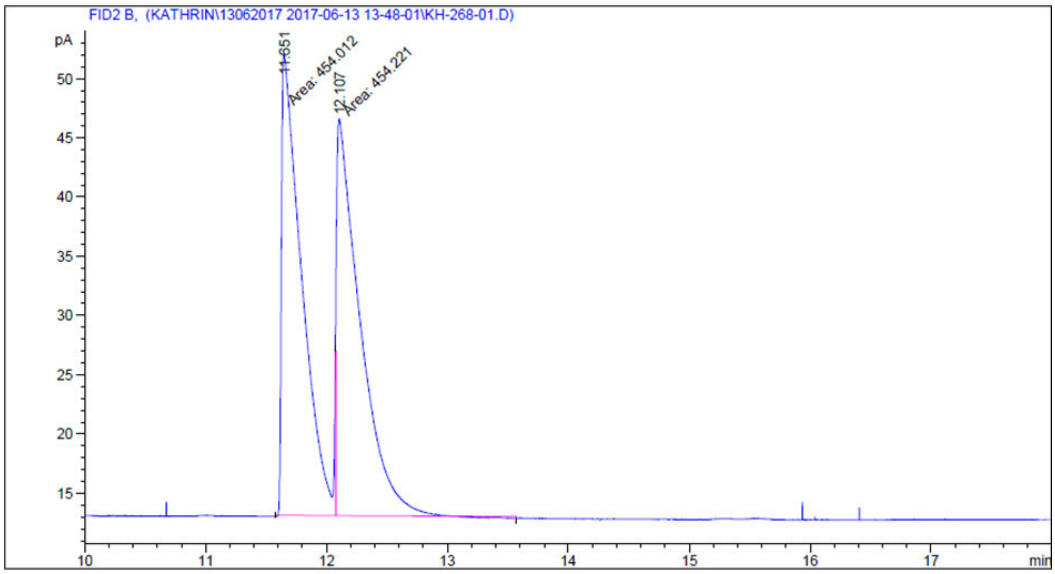

Peak #	RetTime [min]	Type	Width [min]	Area [pA*s]	Height [pA]	Area %
1	11.651	MF	0.1946	454.01233	38.88210	49.98851
2	12.107	FM	0.2262	454.22104	33.47151	50.01149

Enantioenriched sample: GC-FID (CP-Chirasil-Dex CB, KH_40_60_155),86 % ee

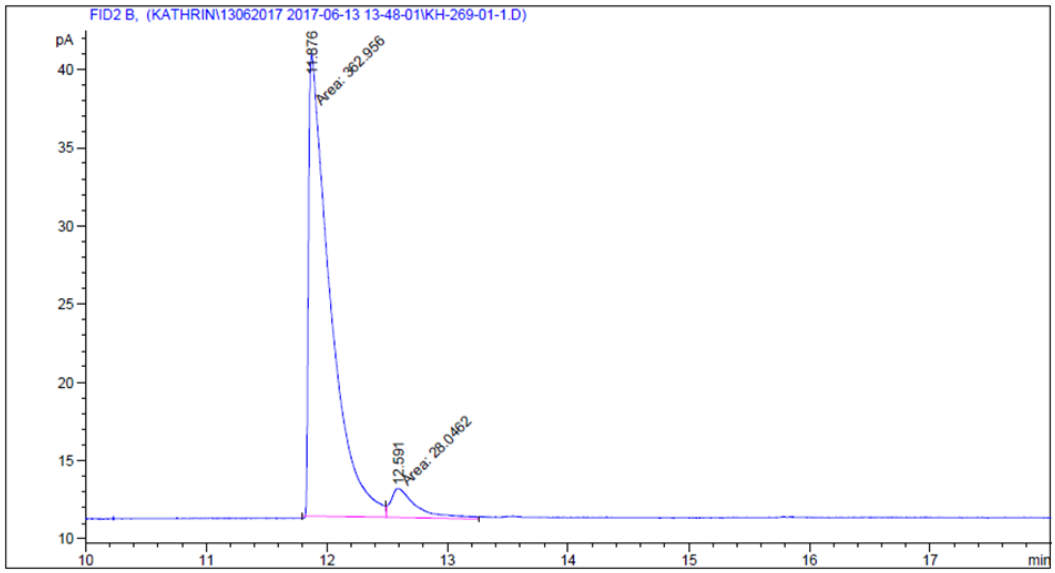

Peak #	RetTime [min]	Type	Width [min]	Area [pA*s]	Height [pA]	Area %
1	11.876	MF	0.2051	362.95566	29.49018	92.82710
2	12.591	FM	0.2505	28.04618	1.86611	7.17290

7.7.6.13 (4*S*,5*S*)-2-Butyl-N^4,N^4,N^5,N^5-tetramethyl-1,3,2-dioxaborolane-4,5-dicarboxamide ((4*S*,5*S*)-81)

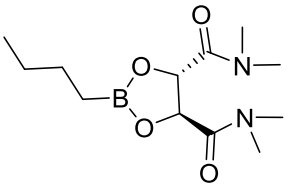

In a 50 mL round–bottom flask equipped with a Dean-Stark apparatus (2*S*,3*S*)-2,3-dihydroxy-N^1,N^1,N^4,N^4-tetramethylsuccinamide (1.30 g, 6.4 mmol) and n-butylboronic acid (615 mg, 6.0 mmol) were heated under reflux in toluene (60 mL) until no more water distilled (8 h). The mixture was cooled to 22 °C and the solids were collected by filtration and washed with toluene (3×10 mL). The combined filtrates were concentrated under reduced pressure and the colourless oil was dried under oil pump vacuum for 6 h.

yield: 1.66 g (97 %), colourless liquid, $C_{12}H_{23}BN_2O_4$, [270.13 g/mol]

^{1}H-NMR (300.36 MHz, $CDCl_3$): δ = 5.40 (s, 2H, CHO), 3.03 (s, 6H, $N(CH_3)_2$), 2.86 (s, 6H, $N(CH_3)_2$), 1.29 (m, 4H, CH_2-CH_2), 0.81 (m, 5H, CH_2, CH_3) ppm.

^{13}C-NMR (75.53 MHz, $CDCl_3$): δ = 167.9 (C_q, C=O), 75.1 (CHO), 36.4 (CH_3), 35.3 (CH_3), 25.6 (CH_2), 24.5 (CH_2), 13.7 (CH_3), 9.6 (CH_2) ppm.

$[\alpha]^{20}_D$ = +90.4 (c 0.18, $CHCl_3$); lit.: value not available.[Ref.124]

The recorded spectra are in accordance with the reported in literature.[124]

7.7.6.14 (4*R*,5*R*)-2-Butyl-N^4,N^4,N^5,N^5-tetramethyl-1,3,2-dioxaborolane-4,5-dicarboxamide ((4*R*,5*R*)-81)

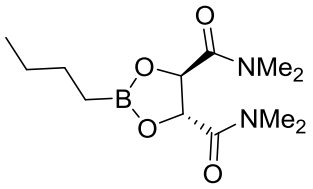

In a 50 mL round–bottom flask equipped with a Dean-Stark apparatus (2*R*,3*R*)-2,3-dihydroxy-N^1,N^1,N^4,N^4-tetramethylsuccinamide (2.14 g, 10.5 mmol) and n-butylboronic acid (1.02 g, 10.0 mmol) were heated under reflux in toluene (60 mL) until no more water distilled (8 h). The mixture was cooled to 22 °C and the solids were collected by filtration and washed with

toluene (3×10 mL). The combined filtrates were concentrated under reduced pressure and the colourless oil was dried under oil pump vacuum for 6 h.

yield: 2.53 g (94 %), colourless liquid, $C_{12}H_{23}BN_2O_4$, [270.13 g/mol]

^{1}H-NMR (300.36 MHz, $CDCl_3$): δ = 5.40 (s, 2H, CHO), 3.04 (s, 6H, $N(CH_3)_2$), 2.86 (s, 6H, $N(CH_3)_2$), 1.29 (m, 4H, CH_2-CH_2), 0.82 (m, 5H, CH_2, CH_3) ppm.

^{13}C-NMR (75.53 MHz, $CDCl_3$): δ = 167.9 (C_q, C=O), 75.1 (CHO), 36.4 (CH_3), 35.3 (CH_3), 25.6 (CH_2), 24.5 (CH_2), 13.7 (CH_3), 9.6 (CH_2) ppm.

$[\alpha]^{20}_D$ = -82.1 (c 0.17, $CHCl_3$); lit.: $[\alpha]_D$ = -114.3 (c 1.71, $CHCl_3$).[Ref.127]

The recorded spectra are in accordance with the reported in literature.[127]

7.7.6.15 (*E*)-3-(4-Methoxyphenyl)prop-2-en-1-ol (*trans*-154)

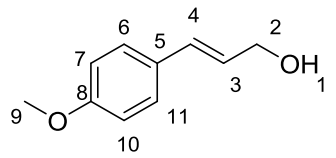

trans-**154**

In a flame dried 100 mL two-neck round-bottom flask equipped with nitrogen inlet and bubble counter, ethyl (*E*)-3-(4-methoxyphenyl)acrylate (1.00 g, 4.85 mmol) was suspended in 12 mL dry CH_2Cl_2 and was cooled to -78 °C using an acetone/dry ice bath. DIBAL-H solution (12.0 mL, 12.0 mmol, 1.0 M in CH_2Cl_2) was added dropwise to the reaction mixture in a N_2-counterstream. After full conversion of starting material was indicated by TLC (5 min) the reaction mixture was quenched by addition of 1M HCl (50 mL) at 0 °C and then warmed to 22 °C. The colorless layers were separated and the aqueous phase was extracted with CH_2Cl_2 (3x20 mL). The combined organic layers were washed with brine (1x60 mL) and dried over Na_2SO_4. The solvent was evaporated under reduced pressure. The product was used in the next step without further purification.

yield: 713 mg (89 %), colourless crystals, $C_{10}H_{12}O_2$, [164.20 g/mol]

R_f= 0.18 (cyclohexane/ethylacetate 4/1) ($KMnO_4$)

m.p.: 76 °C

GC-FID (KH_80_30_280): t_R= 5.2 min

^{1}H-NMR (300.36 MHz, $CDCl_3$): δ = 7.23 (d, $^3J_{HH}$= 8.6 Hz, 2H, H-7, H-10), 6.86 (d, $^3J_{HH}$= 8.6 Hz, 2H, H-6, H-11), 6.55 (d, $^3J_{HH}$= 15.9 Hz, 1H, H-4), 6.23 (dt, $^3J_{HH}$= 15.8, 5.9 Hz, 1H, H-3), 4.29 (d, $^3J_{HH}$= 5.8 Hz, 2H, H-2), 3.81 (s, 3H, H-9), 1.63 (s, 1H, H-1) ppm.

^{13}C-NMR (75.53 MHz, $CDCl_3$): δ = 159.4 (C-8), 131.1 (C-4), 129.6 (C-5), 127.8 (C-7, C-10), 126.4 (C-3), 144.1 (C-6, C-11), 64.0 (C-2), 55.4 (C-9) ppm.

The recorded spectra are in accordance with the reported in literature.[128]

7.7.6.16 *trans*-(2-(4-Methoxyphenyl)cyclopropyl)methanol (*trans*-155)

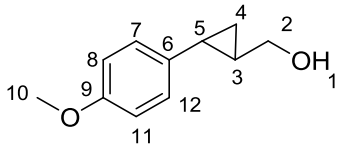

trans-**155**

The preparation was executed as described in 7.7.6.2 starting from (*E*)-3-(4-methoxyphenyl)prop-2-en-1-ol (*trans*-**154**) (695 mg, 4.23 mmol).

yield: 534 mg (71 %), colorless liquid, $C_{11}H_{14}O_2$, [178.23 g/mol]

R_f= 0.41 (toluene/ethylacetate 3/1) (CAM)

^{1}H-NMR (300.36 MHz, $CDCl_3$): δ = 7.01 (d, $^3J_{HH}$= 8.6 Hz, 2H, H-8, H-11), 6.81 (d, $^3J_{HH}$= 8.6 Hz, 2H, H-7, H-12), 3.78 (s, 3H, H-10), 3.71-3.48 (m, 2H, H-2), 1.87-1.71 (m, 1H, H-5), 1.59 (s, 1H, H-1), 1.48-1.32 (m, 1H, H-3), 0.99-0.74 (m, 2H, H-4) ppm.

^{13}C-NMR (75.53 MHz, $CDCl_3$): δ = 157.9 (C-9), 134.5 (C-6), 127.1 (C-8, C-11), 114.0 (C-7, C-12), 66.8 (C-2), 55.5 (C-10), 24.9 (C-3), 20.7 (C-5), 13.4 (C-4) ppm.

The recorded spectra are in accordance with the reported in literature.[129]

7.7.7 Synthesis of aldehydes for reductive cyclization reactions

7.7.7.1 General procedure for reduction with DIBAL-H for unsaturated esters 43, 56, 62, 72, 87, 111, 131, 138

These experiments were executed under the complete exclusion of light. In a flame dried 250 mL two-neck round-bottom flask with nitrogen inlet a 0.30 M (1.0 eq) solution of the corresponding ester in dry CH_2Cl_2 was cooled to -78 °C using an acetone/dry ice bath. 2.1 eq DIBAL-H (1.0 M solution in CH_2Cl_2) were added dropwise to the reaction mixture in a N_2-counterstream. After 15 min full conversion was indicated by TLC. The reaction mixture was quenched by the addition of excess 1 M HCl at -78 °C and warmed to 24 °C. After stirring for 30 min the colorless layers were separated and the aqueous phase was extracted with CH_2Cl_2 (2x50 mL). The combined organic layers were washed with brine (1x100 mL) and dried over Na_2SO_4. The solution of the allylic alcohol was immediately used in the next reaction without further purification.

7.7.7.2 General oxidation procedure with MnO_2 to substrates 20, 24, 25, 27, 28, 31, 33, 34

These experiments were executed under the complete exclusion of light. 1.0 g anhydrous 4 Å MS was transferred into a flame dried 250 mL two-neck round-bottom flask with nitrogen inlet. A 0.10 M (1.0 eq) solution of the corresponding allylic alcohol in CH_2Cl_2 and activated MnO_2 (5.0 eq) were added in a N_2-counterstream. The black reaction mixture was stirred for 8 h. After full conversion of the starting material was indicated by TLC and GC-FID, MnO_2 was removed via filtration through a pad of silica which was rinsed with CH_2Cl_2. The filtrate was collected and the solvent was evaporated under reduced pressure taking care that the bath temperature did not exceed 35 °C. Purification procedure and analytical data are stated for each substrate.

7.7.7.3 (*E*)-4-Bromobut-2-enal (20)

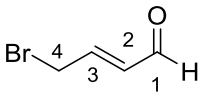

20

Starting from ethyl-4-bromocrotonate (**43**) (2.0 mL, 2.8 g, 14.5 mmol) reduction with DIBAL-H and oxidation with activated MnO_2 was executed as described in 7.7.7.1 and 7.7.7.2.

yield: 700 mg (33 %), brown liquid, C_4H_5BrO, [148.99 g/mol]

R_f= 0.68 (cyclohexane/ethylacetate 1/1) ($KMnO_4$)

GC-FID (KH_80_30_280): t_R= 3.6 min

^{1}H-NMR (300.36 MHz, $CDCl_3$): δ = 9.63 (dd, $^3J_{HH}$= 15.7, 7.5 Hz, 1H, H-1), 6.88 (dt, $^3J_{HH}$= 14.6, 7.3 Hz, 1H, H-3), 6.24 (dt, $^3J_{HH}$= 18.0, 9.0 Hz, 1H, H-2), 4.11 (dd, $^3J_{HH}$= 7.3, 1.0 Hz, 2H, H-4) ppm.

^{13}C-NMR (75.53 MHz, $CDCl_3$): δ = 192.8 (C-1), 149.5 (C-3), 134.3 (C-2), 28.7 (C-4) ppm.
NMR spectra are in accordance with previously reported ones.[130]

7.7.7.4 (*E*)-4-Chlorobut-2-enal (24)

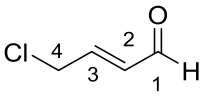

24

Starting from ethyl-4-chlorocrotonate (**56**) (750 mg, 5.05 mmol) reduction with DIBAL-H and oxidation with activated MnO_2 was executed as described described in 7.7.7.1 and 7.7.7.2

yield: 70 mg (13 %), orange-brownish liquid, C_4H_5ClO, [104.53 g/mol]

R_f= 0.64 (cyclohexane/ethylacetate 1/1) ($KMnO_4$)

GC-FID (KH_80_30_280): t_R= 2.9 min

^{1}H-NMR (300.36 MHz, $CDCl_3$): δ = 9.62 (d, $^3J_{HH}$= 7.6 Hz, 1H, H-1), 6.85 (dt, $^3J_{HH}$= 15.4, 5.9 Hz, 1H, H-3), 6.35 (dd, $^3J_{HH}$= 15.4, 7.6 Hz, 1H, H-2), 4.27-4.20 (m, 2H, H-4) ppm.

^{13}C-NMR (75.53 MHz, $CDCl_3$): δ = 192.7 (C-1), 149.6 (C-3), 134.0 (C-2), 42.4 (C-4) ppm.

NMR spectra are in accordance with previously reported ones.[131]

7.7.7.5 (*E*)-4-Chloro-3-methylbut-2-enal (27)

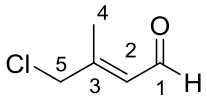

27

Starting from ethyl (*E*)-4-chloro-3-methylbut-2-enoate (**72**) (700 mg, 4.30 mmol) reduction with DIBAL-H and oxidation with activated MnO_2 was executed as described in 7.7.7.1 and 7.7.7.2.

yield: 130 mg (26 %), yellowish liquid, C_5H_7ClO, [118.02 g/mol]

R_f= 0.23 (cyclohexane/ethylacetate 5/1) ($KMnO_4$)

GC-FID (KH_80_30_280): t_R= 3.6 min

^{1}H-NMR (300.36 MHz, $CDCl_3$): δ = 10.0 (d, $^3J_{HH}$= 7.6 Hz, 1H, H-1), 6.10 (d, $^3J_{HH}$= 6.9 Hz, 1H, H-2), 4.10 (s, 2H, H-5), 2.26 (s, 3H, H-4) ppm.

^{13}C-NMR (75.53 MHz, $CDCl_3$): δ = 191.6 (C-1), 155.3 (C-3), 128.7 (C-2), 49.4 (C-5), 15.7 (C-4) ppm.
HRMS (EI): Calcd. (m/z) for C_5H_7ClO [M^+]: 118.0185; found: 118.0185.

7.7.7.6 (*E*)-4-Bromo-3-methylbut-2-enal (28)

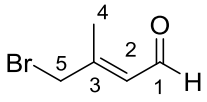

28

Starting from ethyl (*E*)-4-bromo-3-methylbut-2-enoate (**87**) (1.0 g, 4.83 mmol) reduction with DIBAL-H and oxidation with activated MnO_2 was executed as described in 7.7.7.1 and 7.7.7.2.

yield: 270 mg (34 %), yellow and brownish liquid, C_5H_7BrO, [163.01 g/mol]

R_f= 0.45 (cyclohexane/ethylacetate 5/1) ($KMnO_4$)

GC-FID (KH_80_30_280): t_R= 3.6 min

^{1}H-NMR (300.36 MHz, $CDCl_3$): δ = 10.0 (d, $^{3}J_{HH}$= 7.6 Hz, 1H, H-1), 6.10 (d, $^{3}J_{HH}$= 7.4 Hz, 1H, H-2), 4.00 (s, 2H, H-5), 2.30 (s, 3H, H-4) ppm.

^{13}C-NMR (75.53 MHz, $CDCl_3$): δ = 191.1 (C-1), 155.5 (C-3), 129.1 (C-2), 37.3 (C-5), 16.0 (C-4) ppm.

NMR spectra are in accordance with previously reported ones.[132]

7.7.7.7 (*E*)-4-Chloro-3-phenylbut-2-enal (31)

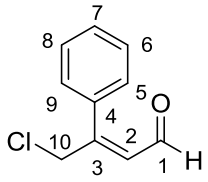

31

Starting from ethyl (*E*)-4-chloro-3-phenylbut-2-enoate (**111**) (395 mg, 1.76 mmol) reduction with DIBAL-H and oxidation with activated MnO_2 was executed as described in 7.7.7.1 and 7.7.7.2. The product was purified via flash chromatography (50 g silica gel, 10×1.5 cm, cyclohexane/ethylacetate 12/1, fraction size: 25 mL).

yield: 181 mg (57 %), yellowish liquid, $C_{10}H_9ClO$, [180.23 g/mol]

R_f= 0.53 (cyclohexane/ethylacetate 4/1) ($KMnO_4$)

GC-FID (KH_80_30_280): t_R= 6.1 min

^{1}H-NMR (300.36 MHz, DMSO-d_6): δ = 9.42 (d, $^{3}J_{HH}$= 7.9 Hz, 1H, H-1), 7.50 (s, 5H, H-5, H-6, H-7, H-8, H-9), 6.40 (d, $^{3}J_{HH}$= 7.9 Hz, 1H, H-2), 4.82 (s, 2H, H-10) ppm.

^{13}C-NMR (75.53 MHz, DMSO-d_6): δ = 192.5 (C-1), 158.7 (C-2), 134.3 (C-3), 129.7 (C-4), 129.2 (C-5, C-9), 128.9 (C-7), 128.5 (C-6, C-8), 47.7 (C-10) ppm.

HRMS (EI): Calcd. (m/z) for $C_{10}H_8O$ [M-HCl]: 180.0342; found: 180.0347.

7.7.7.8 (*E*)-4-Chloro-2-methylbut-2-enal (25)

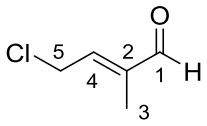

25

Starting from ethyl (*E*)-4-chloro-2-methylbut-2-enoate (**62**) (1.0 g, 6.20 mmol) reduction with DIBAL-H and oxidation with activated MnO_2 was executed as described in 7.7.7.1 and 7.7.7.2.

yield: 328 mg (45 %), yellowish liquid, C_5H_7ClO, [118.02 g/mol]

R_f= 0.72 (cyclohexane/ethylacetate 3/1) ($KMnO_4$)

GC-FID (KH_80_30_280): t_R= 3.2 min

^{1}H-NMR (300.36 MHz, $CDCl_3$): δ = 9.48 (s, 1H, H-1), 6.55 (dd, $^3J_{HH}$= 7.4, 6.3 Hz, 1H, H-2), 4.30 (d, $^3J_{HH}$= 7.4 Hz, 2H, H-5), 1.82 (s, 3H, H-3) ppm.

^{13}C-NMR (75.53 MHz, $CDCl_3$): δ = 194.4 (C-1), 145.8 (C-4), 141.3 (C-2), 38.8 (C-5), 9.3 (C-3) ppm.
The recorded spectra are in accordance with the reported in literature.[133]

7.7.7.9 (*E*)-4-Chloro-3-(4-methoxyphenyl)but-2-enal (33)

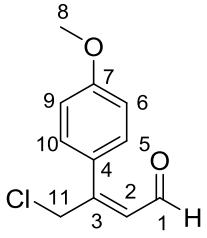

33

Starting from ethyl (*E*)-4-chloro-3-(4-methoxyphenyl)but-2-enoate (**131**) (571 mg, 2.24 mmol) reduction with DIBAL-H and oxidation with activated MnO_2 was executed as described in 7.7.7.1 and 7.7.7.2. The product was purified via flash chromatography (25 g silica gel, 7×2.5 cm, cyclohexane/ethylacetate 10/1, fraction size: 15 mL).

yield: 206 mg (44 %), yellow-brownish liquid, $C_{11}H_{11}ClO$, [210.66 g/mol]

R_f= 0.56 (cyclohexane/ethylacetate 1/1) ($KMnO_4$)

GC-FID (KH_80_30_280): t_R= 7.3 min

^{1}H-NMR (300.36 MHz, $CDCl_3$): δ = 9.54 (d, $^{3}J_{HH}$= 7.8 Hz, 1H, H-1), 7.27 (d, $^{3}J_{HH}$= 8.7 Hz, 2H, H-6, H-11), 6.96 (d, $^{3}J_{HH}$= 8.6 Hz, 2H, H-7, H-10), 6.35 (d, $^{3}J_{HH}$= 7.8 Hz, 1H, H-3), 4.42 (s, 2H, H-12), 3.84 (s, 3H, H-9) ppm.

^{13}C-NMR (75.53 MHz, $CDCl_3$): δ = 193.2 (C-2), 161.2 (C-8), 158.1 (C-5), 130.7 (C-6, C-11), 129.4 (C-3), 126.9 (C-4), 114.3 (C-7, C-10), 55.4 (C-9), 47.6 (C-12) ppm.

HRMS (EI): Calcd. (m/z) for $C_{11}H_{11}ClO_2$ [M^+]: 210.0448; found: 210.0448.

7.7.7.10 (*E*)-4-Chloro-3-(4-(trifluoromethyl)phenyl)but-2-enal (34)

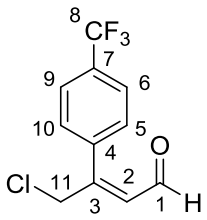

34

Starting from ethyl (*E*)-4-chloro-3-(4-(trifluoromethyl)phenyl)but-2-enoate (**138**) (500 mg, 1.71 mmol) reduction with DIBAL-H and oxidation with activated MnO_2 was executed as described in 7.7.7.1 and 7.7.7.2. The product was purified via flash chromatography (50 g silica gel, 7.0×2.5 cm, cyclohexane/ethylacetate 9/1, fraction size: 25 mL).

yield: 215 mg (51 %), colorless oil, $C_{11}H_8ClOF_3$, [248.63 g/mol]

R_f= 0.65 (cyclohexane/ethylacetate 4/1) ($KMnO_4$)

^{1}H-NMR (300.36 MHz, DMSO-d_6): δ = 9.41 (d, $^{3}J_{HH}$= 7.9 Hz, 1H, H-1), 7.81 (dd, $^{3}J_{HH}$= 32.1, 8.0 Hz, 1H, H-5, H-6, H-9, H-10), 6.47 (d, $^{3}J_{HH}$= 7.9 Hz, 1H, H-2), 4.85 (s, 2H, H-11) ppm.

^{13}C-NMR (75.53 MHz, DMSO-d_6): δ = 192.3 (C-1), 156.8 (C-3), 138.5 (C-4), 130.1 (C-5, C-10), 129.8 (q, $^{2}J_{CF}$= 32.5 Hz, C-7), 125.4 (q, $^{3}J_{CF}$= 3.7 Hz, C-6, C-9), 124.0 (q, $^{1}J_{CF}$= 272.7 Hz, C-8), 47.5 (C-11) ppm.

HRMS (EI): Calcd. (m/z) for $C_{11}H_7OF_3$ [M-HCl]: 212.0449; found: 212.0448.

7.8 Biocatalysis Section

7.8.1 Analytical scale procedure for enzymatic reductive cyclization reactions

These experiments were executed under complete exclusion of light. An aliquot of enzyme (5 µM final concentration) was rehydrated in NaPi buffer (50 mM, 150 mM NaCl, pH 7.5) to a volume of 300 µL. The reaction was started by the addition of a stock solution (300 µL) containing the substrate (10 mM), NADH (15 mM), DMF (1 % final concentration), and 1,2 DME as an internal standard ($V_{Substrate}$=$V_{InternalStandard}$). The samples were incubated for 180 min at 25 °C and 300 rpm in an Eppendorf Thermomixer comfort. For work-up MTBE (300 µL) was added to each sample, which was then intensely vortexed and centrifuged for 10 min at 13.000 rpm. The organic layer was then separated and dried over $MgSO_4$. After centrifugation (10 min, 13.000 rpm), the organic layer was transferred into GC glass-vials and the samples were measured directly using GC-FID or HPLC. Conversions are stated as an average of three independent experiments.

Blank reactions were prepared for every screening run. One set of blanks was run without enzyme and the other set of blanks was run without NADH.

7.8.2 Determination of diastereomeric excess, enantiomeric excess and assignment of absolute configuration

A solution of $NaBH_4$ (10 wt% in dist. water, 50 µL per sample) was added to the finished biocatalytic reaction mixtures in an Eppendorf vial and the samples were incubated for 30 min at 22 °C. The reaction mixtures were quenched by the addition of 1 M HCl (100 µL) and TBME (300 µL) was added. The samples were intensely vortexed and after centrifugation (10 min, 13.000 rpm) the organic layer was separated and dried over $MgSO_4$. Once more, the samples were centrifuged (10 min, 13.000 rpm) and the organic layer was transferred into GC glass-vials and analysed as stated for each compound.

7.8.2.1 Diastereomeric excess and enantiomeric excess of (2-methylcyclopropyl)methanol

All samples were reduced as it is described in 7.8.2. The diastereomeric and the enantiomeric excess of (2-methylcyclopropylmethanol) (**75**) was determined as follows (Scheme 101):

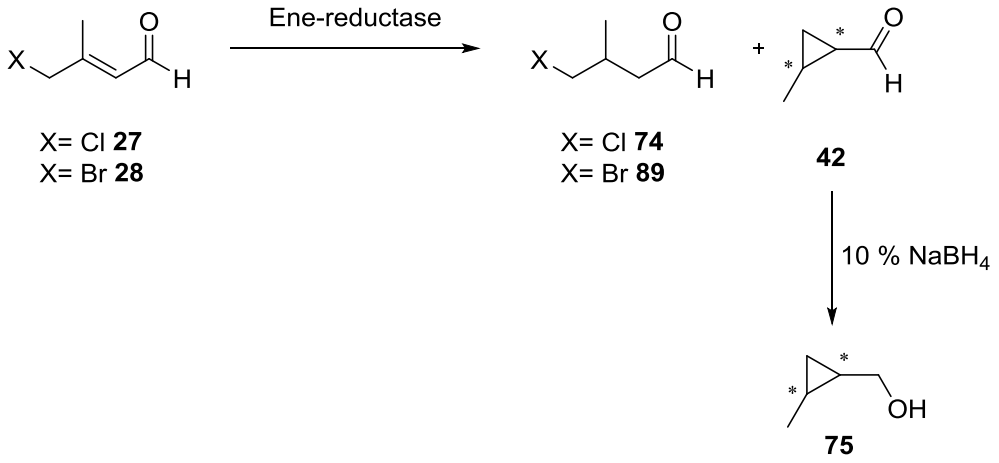

Scheme 101: Determination of diastereomeric excess and enantiomeric excess of (2-methylcyclopropyl)methanol (**75**).

Separation of diastereomers was achieved on achiral GC-FID using an Agilent Technologies J&W GC-column DB-17-01 and method KH_80_30_280. As shown in Figure 14 and Figure 15 the *cis*-diastereomer (*cis*-**75**) and the *trans*-diastereomer (*trans*-**75**) were identified by the injection of synthesized reference materials on achiral GC-FID. Figure 16 shows GC-FID chromatogram of the conversion of (*E*)-4-chloro-3-methylbut-2-enal (**27**) by YqjM Y169F after the sample had been reduced with $NaBH_4$.

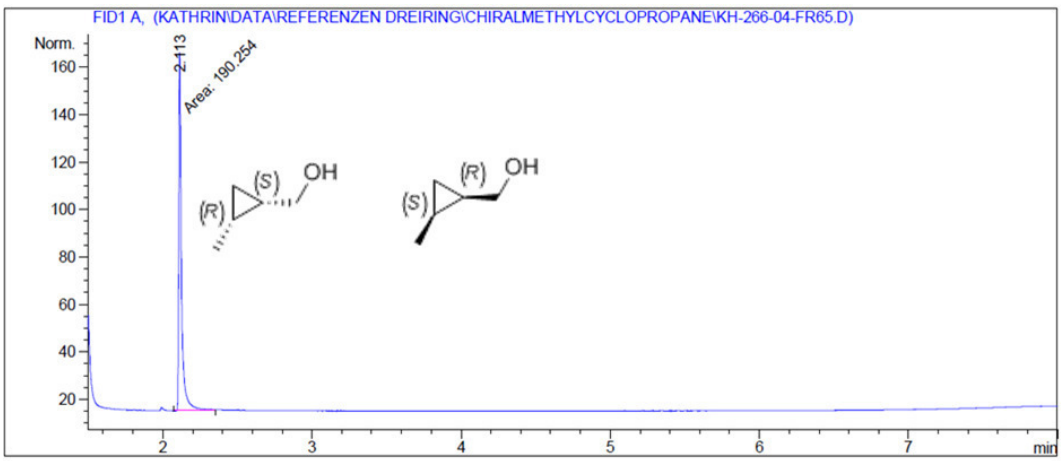

Figure 14: GC-FID chromatogram of (2-methylcyclopropyl)methanol *cis*-**75**.

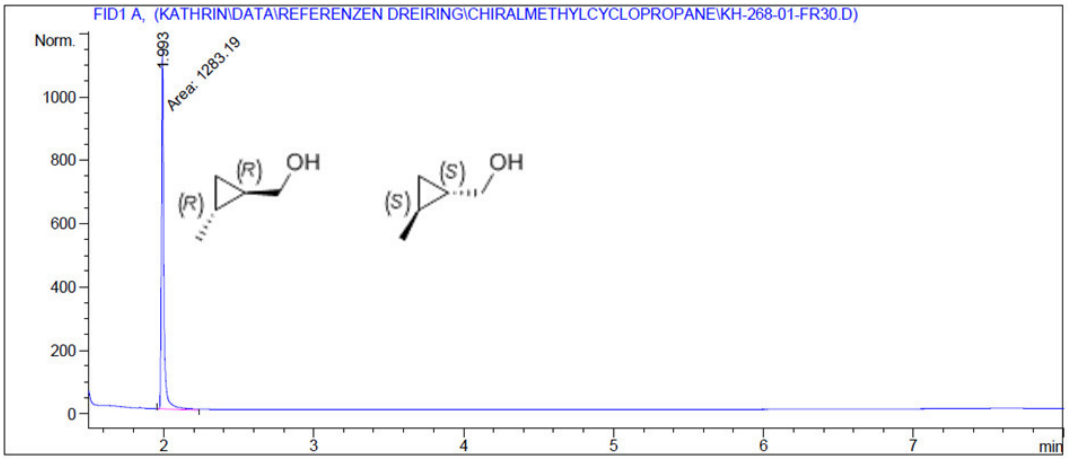

Figure 15: GC-FID chromatogram of (2-methylcyclopropyl)methanol *trans*-**75**.

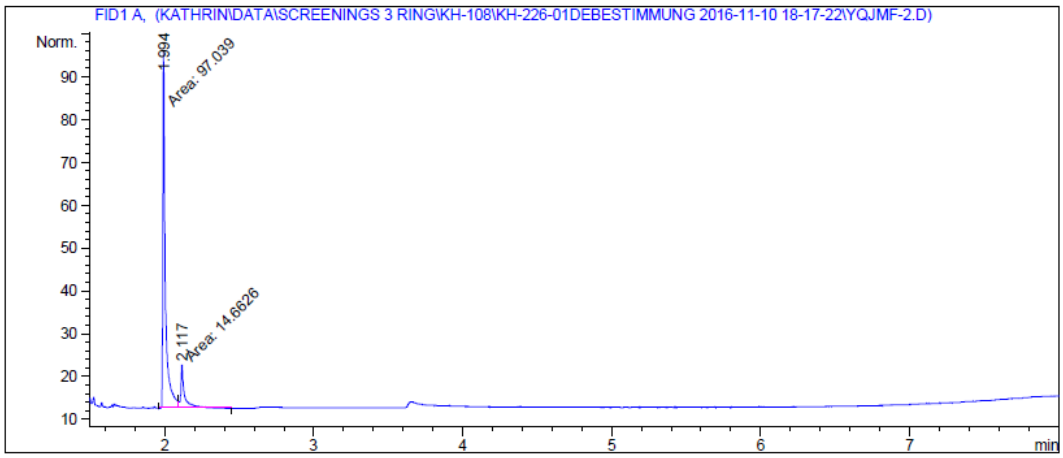

Figure 16: GC-FID chromatogram of the conversion of (*E*)-4-chloro-3-methylbut-2-enal (**27**) by YqjM Y169F after the sample had been reduced with $NaBH_4$.

For the determination of the absolute configuration and the enantiomeric excess samples were injected in chiral GC-FID. Separation of enantiomers was achieved on chiral GC-FID using an Agilent CP-Chirasil-Dex CB column and method KH_40_60_155. Synthesized reference material was injected to perform the determination of the absolute configuration (chromatograms were already shown in 7.7.6.11 and 7.7.6.12). Figure 17 shows the conversion of (*E*)-4-chloro-3-methylbut-2-enal (**27**) by Opr3 WT after reduction with $NaBH_4$.

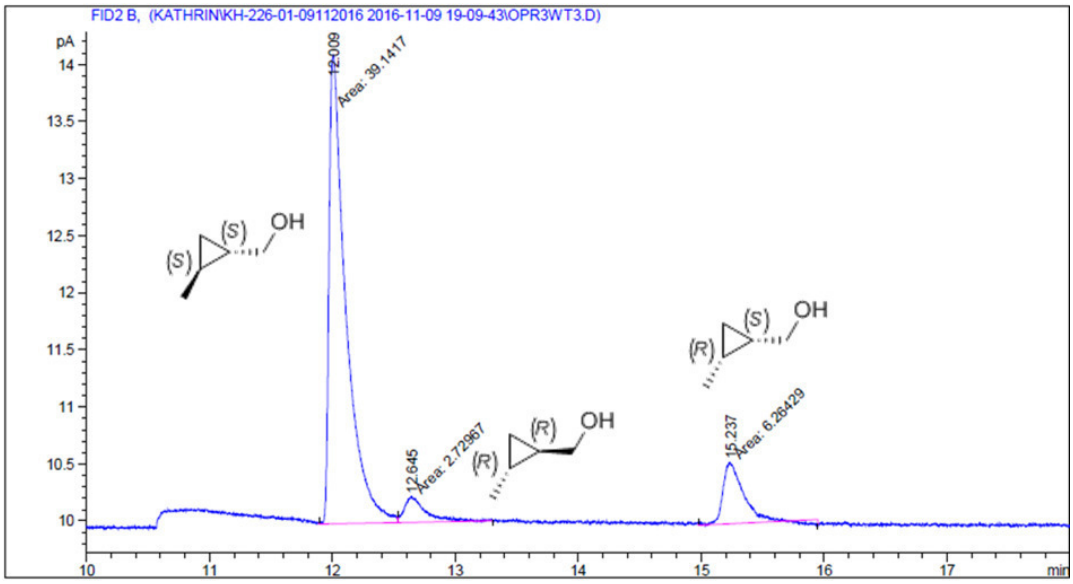

Figure 17: GC-FID chromatogram of the conversion of (*E*)-4-chloro-3-methylbut-2-enal (**27**) by Opr3 WT after reduction with $NaBH_4$.

7.8.2.2 Diastereomeric excess and enantiomeric excess of (2-phenylcyclopropyl)methanol

The diastereomeric excess of 2-phenylcyclopropane-1-carbaldehyde (**114**) and the enantiomeric excess of (2-phenylcyclopropylmethanol) (**115**) was determined as follows (Scheme 102):

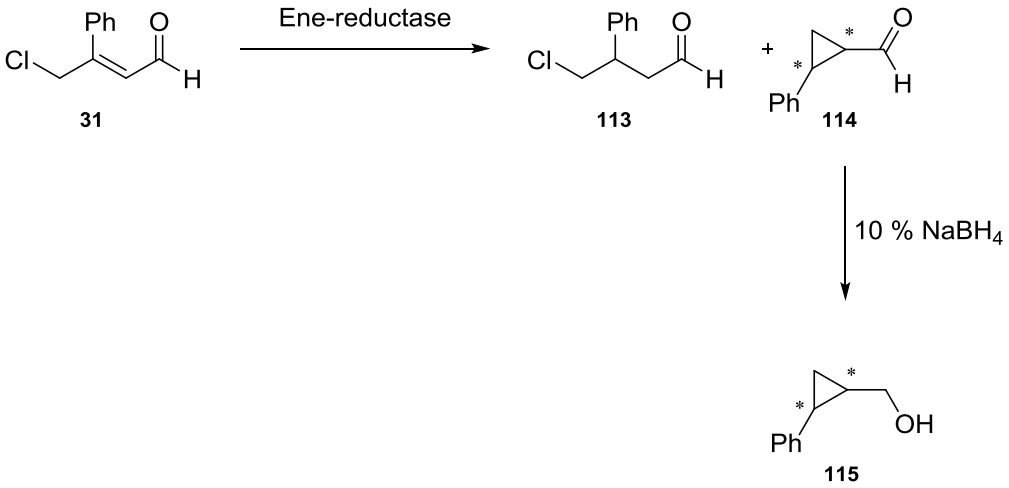

Scheme 102: Determination of diastereomeric excess of 2-phenylcyclopropane-1-carbaldehyde (**114**) and enantiomeric excess of (2-phenylcyclopropyl)methanol (**115**).

Separation of diastereomers was achieved on achiral GC-FID using an Agilent Technologies J&W GC-column DB-17-01 and method KH_80_30_280. As shown in Figure 18 and Figure 19 the *cis*-diastereomer (*cis*-**114**) and the *trans*-diastereomer (*trans*-**114**) were identified by the injection of synthesized reference materials on achiral GC-FID. Figure 20 shows GC-FID chromatogram of the conversion of (*E*)-4-chloro-3-phenylbut-2-enal by Opr3 Y190F.

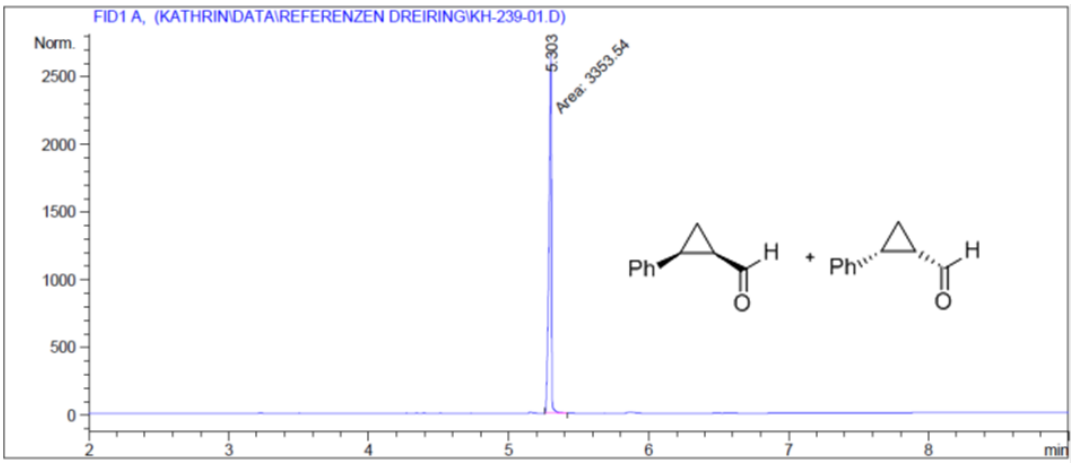

Figure 18: GC-FID chromatogram of 2-phenylcyclopropane-1-carbaldehyde (*cis*-**114**).

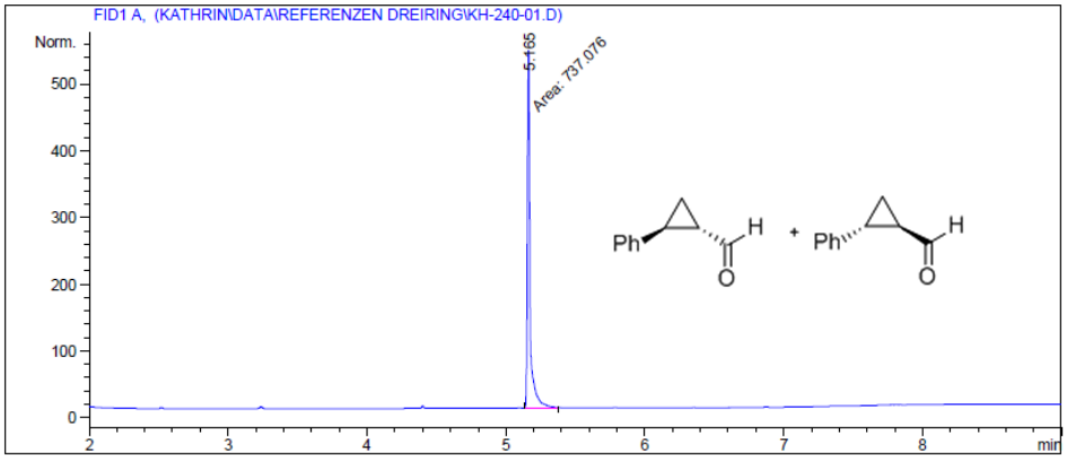

Figure 19: GC-FID chromatogram of 2-phenylcyclopropane-1-carbaldehyde (*trans*-**114**).

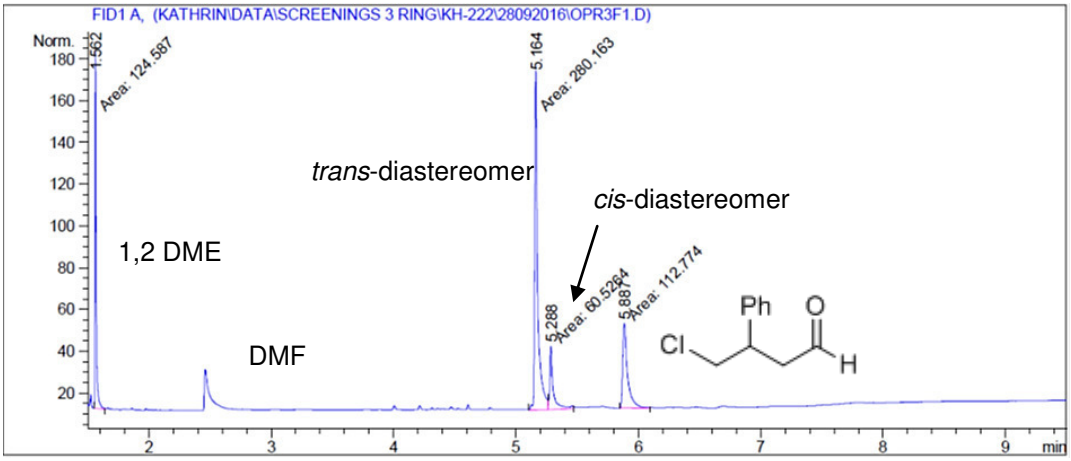

Figure 20: GC-FID chromatogram of the conversion of (*E*)-4-chloro-3-phenylbut-2-enal (**31**) by Opr3 Y190F.

For the determination of the absolute configuration and the enantiomeric excess, samples were reduced as it is described in 7.8.2. Separation of enantiomers of *trans*-(2-phenylcyclopropyl)methanol (*trans*-**115**) was achieved as follows (Figure 21): Daicel Chiralcel OD-H, n-hexane: iPrOH 9:1, flow= 0.5 mL min^{-1}. Elution order of enantiomers was previously described in literature.[134]

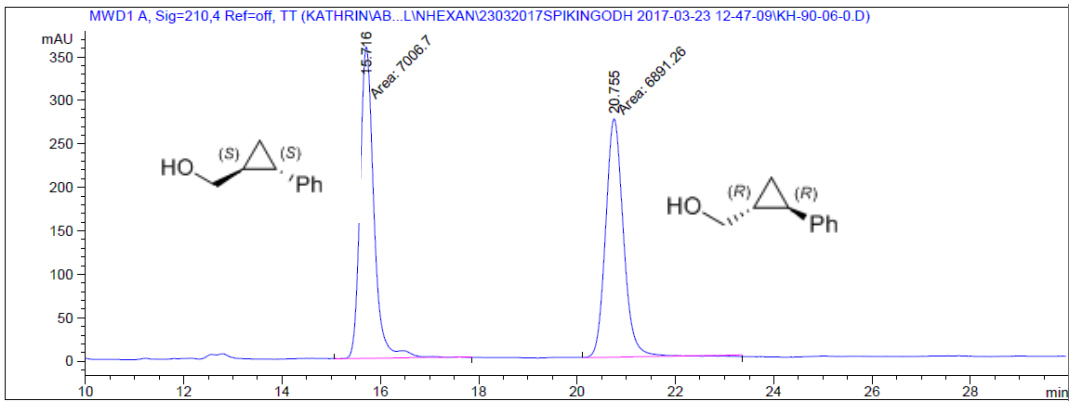

Peak #	RetTime [min]	Type	Width [min]	Area [mAU*s]	Height [mAU]	Area %
1	15.716	MM	0.3232	7006.69678	361.29327	50.4153
2	20.755	MM	0.4169	6891.25684	275.51080	49.5847

Figure 21: HPLC chromatogram of racemic sample of *trans*-(2-phenylcyclopropyl)methanol (*trans*-**115**).

Figure 22 illustrates a HPLC chromatogram of the conversion of (*E*)-4-chloro-3-phenylbut-2-enal (**31**) by Opr3 Y190F using the above mentioned column and method. For the determination of the enantiomeric excess the sample was spiked with 0.2 µL of racemic *trans*-(2-phenylcyclopropyl)methanol (*trans*-**115**) (see Figure 23).

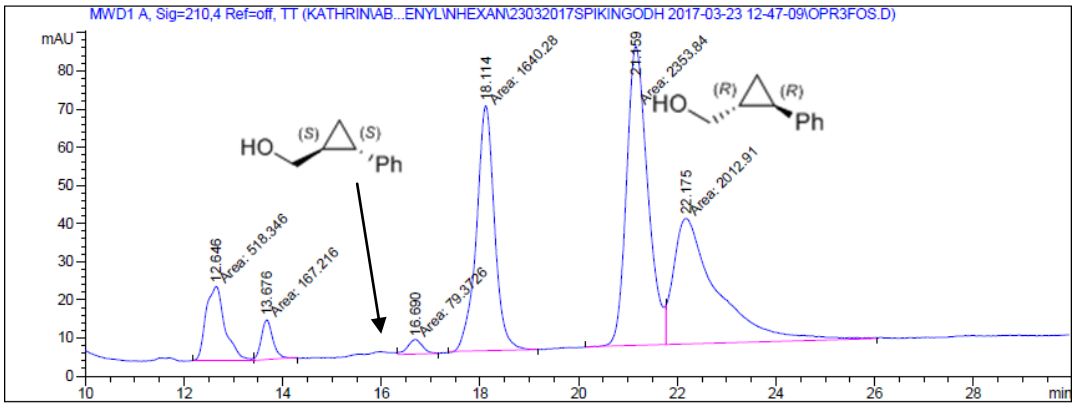

Figure 22: HPLC chromatogram of sample of Opr3 Y190F.

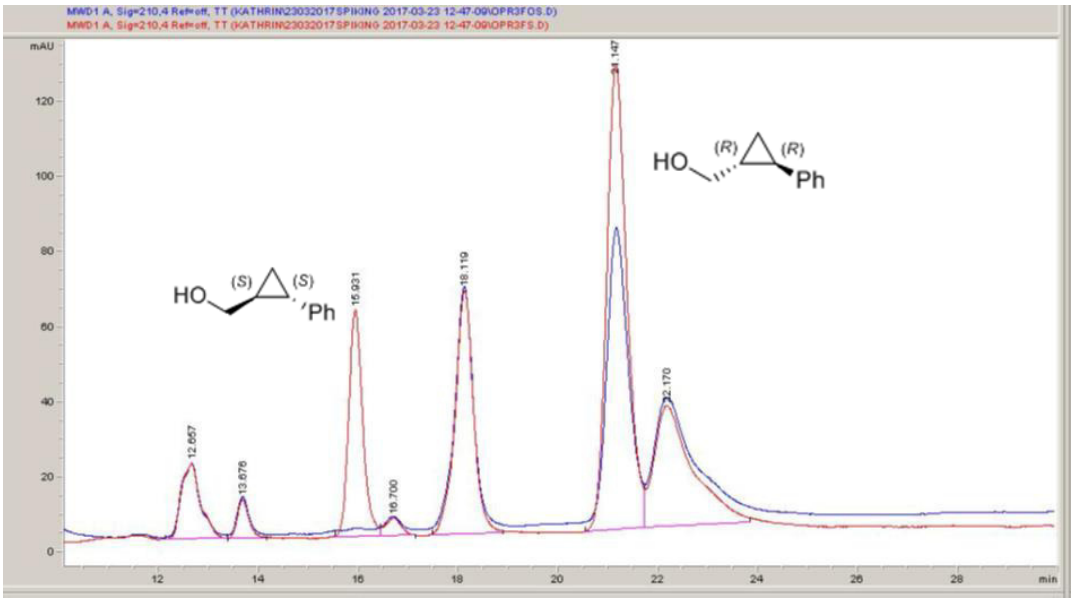

Figure 23: HPLC chromatogram of sample of Opr3 Y190F spiked with 0.2 µL of racemic *trans*-(2-phenylcyclopropyl)methanol (*trans*-**115**).

Separation of enantiomers of *cis*-(2-phenylcyclopropyl)methanol was achieved as follows: Daicel Chiralcel OJ-H, n-hexane: iPrOH 95:5, flow= 0.5 mL min^{-1}. Elution order of enantiomers was previously described in literature.[134]

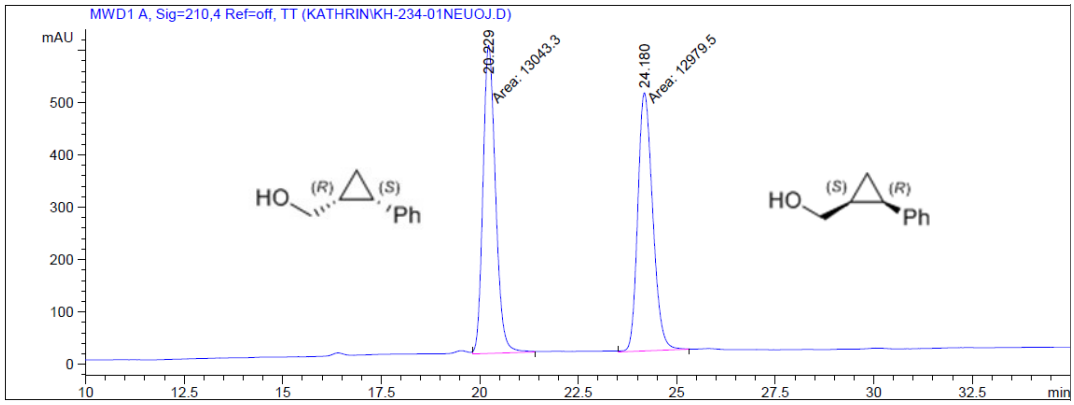

Peak #	RetTime [min]	Type	Width [min]	Area [mAU*s]	Height [mAU]	Area %
1	20.229	MM	0.3682	1.30433e4	590.42200	50.1226
2	24.180	MM	0.4366	1.29795e4	495.41827	49.8774

Figure 24: HPLC chromatogram of racemic sample of *cis*-(2-phenylcyclopropyl)methanol (*cis*-**115**).

Figure 25 illustrates a HPLC chromatogram of the conversion of (*E*)-4-chloro-3-phenylbut-2-enal (**31**) by Opr3 Y190F using the above mentioned column and method. For the determination of the enantiomeric excess the sample was spiked with 0.2 µL of racemic *cis*-(2-phenylcyclopropyl)methanol (*trans*-**115**) (see Figure 26).

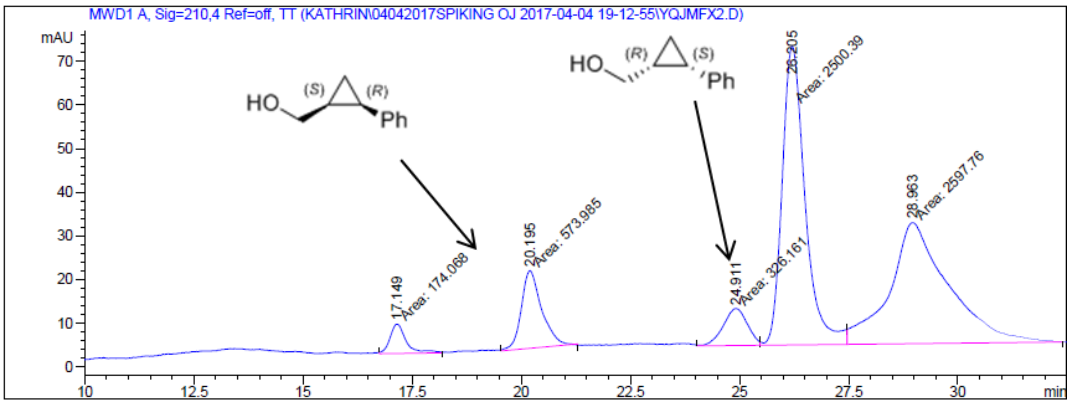

Figure 25: HPLC chromatogram of sample of YqjM Y169F.

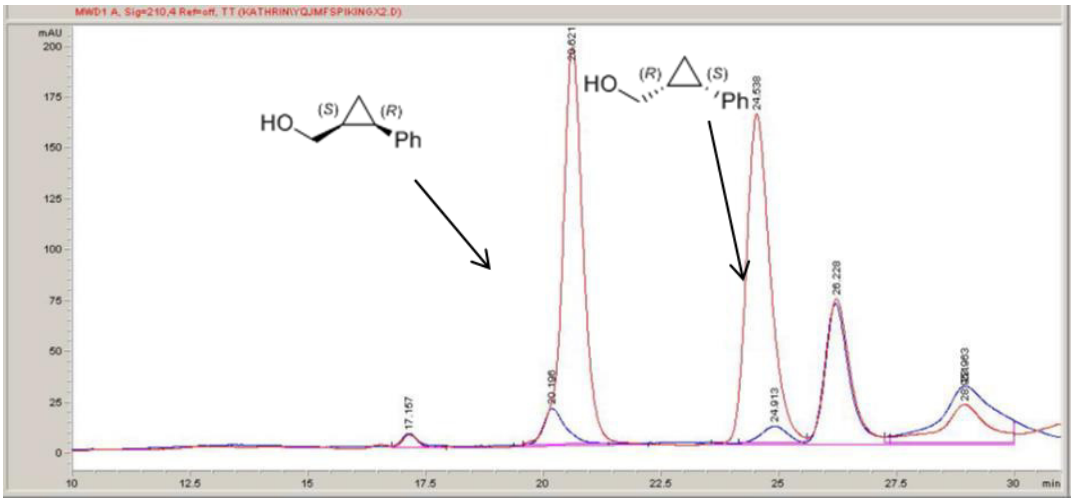

Figure 26: HPLC chromatogram of sample of YqjM Y169F spiked with 0.2 µL of racemic *cis*-(2-phenylcyclopropyl)methanol (*cis*-**115**).

7.8.3 Preparative scale procedure for enzymatic reductive cyclization reactions

These experiments were executed under complete exclusion of light in a 50 mL Greiner vial with screw cap. An aliquot of enzyme (5 µM final concentration) was rehydrated in NaPi buffer (50 mM, 150 mM NaCl, pH 7.5) to a volume of 23.25 mL. The reaction was started by the addition of a stock solution (23.25 mL) containing the substrate (10 mM), NADH (15 mM), DMF (1 % final concentration), and 1,2 DME as an internal standard ($V_{Substrate}$=$V_{InternalStandard}$). The flask was incubated for 180 min at 25 °C and 300 rpm in an Eppendorf Thermomixer comfort. For work-up Et_2O (50 mL) was added, intensely mixed, and centrifuged for 10 min at 4000 rpm. The organic layer was then separated, 20 mL AcOH and 0.9 eq* 2,4-dinitrophenylhydrazine were added and the orange solution was stirred for 48 h at 22 °C. The solvent was evaporated under reduced pressure and the 2,4 dinitrophenylhydrazone adduct was purified as stated for each compound.

* If an excess of 2,4-dinitrophenylhydrazine was used, purification of the corresponding 2,4-dinitrophenylhydrazone was not possible.

7.8.3.1 1-(Cyclopropylmethylene)-2-(2,4-dinitrophenyl)hydrazine (141)

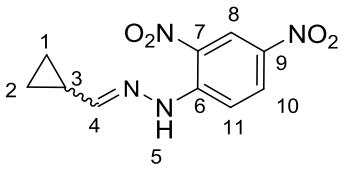

141

Starting from (*E*)-4-bromobut-2-enal (78 mg, 480 µmol) reductive cyclization with YqjM Y169F and conversion of the aldehyde with 2,4-dinitrophenylhydrazine was executed as described in 7.8.3. The product was purified via flash chromatography (30 g silica gel, 9×3.5 cm, cyclohexane/ethylacetate 5/1, fraction size: 15 mL).

yield: 71 mg (60 %), orange powder, $C_{10}H_9N_4O_4$, [250.07 g/mol]

R_f= 0.56 (cyclohexane/ethylacetate 5/1) (UV and $KMnO_4$)

HPLC-MS (**method_1, ESI$^+$**): t_R= 6.9 min; *m/z:* 251 [M+H$^+$]; λ_{max} = 210 nm.

^{1}H-NMR (300.36 MHz, DMSO-d_6): δ = 11.32 (s, 1H, H-5), 8.84 (d, $^{3}J_{HH}$= 2.5 Hz, 1H, H-4), 8.32 (dd, $^{3}J_{HH}$= 9.7, 2.2 Hz, 1H, H-8), 7.86 (d, $^{3}J_{HH}$= 9.6 Hz, 1H, H-10), 7.56 (d, $^{3}J_{HH}$= 7.9 Hz, 1H, H-11), 1.85–1.63 (m, 1H, H-3), 0.99 (d, $^{3}J_{HH}$= 5.5 Hz, 2H, H-1), 0.79 (d, $^{3}J_{HH}$= 2.1 Hz, 2H, H-2).

^{13}C-NMR (75.53 MHz, DMSO-d_6): δ = 158.5 (C-4), 144.4 (C-6), 136.2 (C-9), 129.8 (C-10), 128.3 (C-7), 123.1 (C-8), 116.2 (C-11), 14.0 (C-3), 6.7 (C-1, C-2) ppm.
m.p.: 185-187 °C

The recorded spectra are in accordance with the reported in literature.[135]

7.9 Biological Section

7.9.1 Generation of enzyme variants of Opr3 and YqjM

For generation of enzyme variants of Opr3 and YqjM, suitable mutagenesis primer were designed and ordered (see Table 20). Plasmids pET21a(*opr3*) and pET21a(*yqjM*) were used as templates. Site-directed mutagenesis was performed according to the manual of *QuikChange* Site-directed mutagenesis kit. Plasmids were isolated (from three colonies respectively) after mutagenesis PCR and transformation into *E.coli* Top10 cells. Sequencing was done in order to control the mutations. The respective plasmids were transformed into $CaCl_2$-competent *E.coli* BL21-CodonPlus™-(DE3)-RIL cells (Stratagene). Opr3 WT and the Opr3 variants were expressed with a hexahistidine tag at the C-terminus.

Table 20: Mutagenesis primers of Opr3 and YqjM.

Entry	Enzyme variant	Mutagenesis primer 5'-3'
1	Opr3 Y190F	ccatgg agctcacggt ttcttgattg atcaattctt gaaagatgg
2	Opr3 Y190W	ccatgg agctcacggt tggttgattg atcaattctt gaaagatgg
3	YqjM Y169F	c atgcggcgca cggatttta attcatgaat ttttgtctcc gc
4	YqjM Y169W	cgca cggatggtta attcatgaat ttttg

7.9.2 DNA sequences and translated amino acid sequenes of ene-reductase variants

The gene of Opr3 wild type with the 6x His-tag underlined.

ATGGCTAGCCACCACCACCACCACCACATGGCGTCTTCAGCTCAAGATGGAAACA
ATCCCCTTTTCTCTCCTTACAAGATGGGCAAGTTCAATCTATCCCACAGGGTAGTA
TTGGCTCCGATGACAAGGTGCAGAGCACTGAATAATATTCCACAGGCGGCGCTAG
GGGAGTATTACGAGCAGAGAGCGACGGCCGGTGGATTTCTGATCACTGAAGGCA
CTATGATTTCTCCGACTTCAGCTGGGTTTCCTCATGTGCCAGGGATTTTCACAAAG
GAACAAGTAAGGGAATGGAAGAAAATAGTTGATGTAGTGCATGCAAAGGGTGCT
GTCATATTTTGTCAGCTGTGGCATGTTGGTCGTGCATCTCATGAAGTGTATCAACC
TGCTGGAGCTGCACCAATATCATCCACTGAGAAGCCTATATCAAATAGGTGGAGA
ATTCTAATGCCTGATGGAACTCATGGGATTTATCCAAAACCAAGAGCAATTGGAA
CCTATGAGATCTCACAAGTTGTTGAAGATTATCGCAGGTCGGCCTTGAATGCTAT
TGAAGCAGGTTTCGATGGTATTGAAATCCATGGAGCTCACGGTTACTTGATTGAT
CAATTCTTGAAAGATGGGATCAATGACCGGACAGATGAGTATGGTGGATCACTA
GCCAACCGGTGCAAATTCATCACACAGGTGGTTCAAGCAGTAGTCTCAGCAATAG
GAGCTGATCGCGTAGGCGTTAGAGTTTCACCAGCAATAGATCATCTTGATGCCAT
GGACTCTAATCCACTCAGCCTTGGCTTAGCAGTTGTTGAAAGACTAAACAAAATC
CAACTCCATTCTGGTTCCAAGCTTGCCTATCTTCATGTAACACAGCCACGATACGT
AGCATATGGGCAAACTGAAGCAGGCAGACTTGGCAGTGAAGAGGAAGAGGCTCG
TTTAATGAGGACTTTGAGGAACGCGTATCAGGGGACATTCATTTGCAGTGGTGGA
TACACTAGGGAACTAGGAATTGAGGCTGTGGCACAAGGTGATGCTGATCTCGTGT
CATATGGTCGTCTTTTCATCTCTAATCCTGATTTGGTTATGAGAATCAAGCTAAAT
GCACCTCTAAATAAGTATAACAGGAAGACATTCTATACTCAAGATCCAGTTGTGG
GATACACAGATTACCCTTTCCTTCAAGGAAATGGAAGCAATGGACCGTTATCGCG
TCTGTGA

MASHHHHHHMASSAQDGNNPLFSPYKMGKFNLSHRVVLAPMTRCRALNNIPQAAL
GEYYEQRATAGGFLITEGTMISPTSAGFPHVPGIFTKEQVREWKKIVDVVHAKGAVIF
CQLWHVGRASHEVYQPAGAAPISSTEKPISNRWRILMPDGTHGIYPKPRAIGTYEISQ
VVEDYRRSALNAIEAGFDGIEIHGAHGYLIDQFLKDGINDRTDEYGGSLANRCKFITQ
VVQAVVSAIGADRVGVRVSPAIDHLDAMDSNPLSLGLAVVERLNKIQLHSGSKLAYL
HVTQPRYVAYGQTEAGRLGSEEEEARLMRTLRNAYQGTFICSGGYTRELGIEAVAQG
DADLVSYGRLFISNPDLVMRIKLNAPLNKYNRKTFYTQDPVVGYTDYPFLQGNGSNG
PLSRL

The gene of Opr3 Y190F variant with the 6x His-tag underlined and mutagenesis primer in bold.

ATGGCTAGCCACCACCACCACCACCACATGGCGTCTTCAGCTCAAGATGGAAACA
ATCCCCTTTTCTCTCCTTACAAGATGGGCAAGTTCAATCTATCCCACAGGGTAGTA
TTGGCTCCGATGACAAGGTGCAGAGCACTGAATAATATTCCACAGGCGGCGCTAG
GGGAGTATTACGAGCAGAGAGCGACGGCCGGTGGATTTCTGATCACTGAAGGCA
CTATGATTTCTCCGACTTCAGCTGGGTTTCCTCATGTGCCAGGGATTTTCACAAAG
GAACAAGTAAGGGAATGGAAGAAAATAGTTGATGTAGTGCATGCAAAGGGTGCT
GTCATATTTTGTCAGCTGTGGCATGTTGGTCGTGCATCTCATGAAGTGTATCAACC
TGCTGGAGCTGCACCAATATCATCCACTGAGAAGCCTATATCAAATAGGTGGAGA
ATTCTAATGCCTGATGGAACTCATGGGATTTATCCAAAACCAAGAGCAATTGGAA
CCTATGAGATCTCACAAGTTGTTGAAGATTATCGCAGGTCGGCCTTGAATGCTAT
TGAAGCAGGTTTCGATGGTATTGAAAT**CCATGGAGCTCACGGTTTCTTGATTGA**
TCAATTCTTGAAAGATGGGATCAATGACCGGACAGATGAGTATGGTGGATCACT
AGCCAACCGGTGCAAATTCATCACACAGGTGGTTCAAGCAGTAGTCTCAGCAATA
GGAGCTGATCGCGTAGGCGTTAGAGTTTCACCAGCAATAGATCATCTTGATGCCA
TGGACTCTAATCCACTCAGCCTTGGCTTAGCAGTTGTTGAAAGACTAAACAAAAT
CCAACTCCATTCTGGTTCCAAGCTTGCCTATCTTCATGTAACACAGCCACGATACG
TAGCATATGGGCAAACTGAAGCAGGCAGACTTGGCAGTGAAGAGGAAGAGGCTC
GTTTAATGAGGACTTTGAGGAACGCGTATCAGGGGACATTCATTTGCAGTGGTGG
ATACACTAGGGAACTAGGAATTGAGGCTGTGGCACAAGGTGATGCTGATCTCGTG
TCATATGGTCGTCTTTTCATCTCTAATCCTGATTTGGTTATGAGAATCAAGCTAAA
TGCACCTCTAAATAAGTATAACAGGAAGACATTCTATACTCAAGATCCAGTTGTG
GGATACACAGATTACCCTTTCCTTCAAGGAAATGGAAGCAATGGACCGTTATCGC
GTCTGTGA

MASHHHHHHMASSAQDGNNPLFSPYKMGKFNLSHRVVLAPMTRCRALNNIPQAAL
GEYYEQRATAGGFLITEGTMISPTSAGFPHVPGIFTKEQVREWKKIVDVVHAKGAVIF
CQLWHVGRASHEVYQPAGAAPISSTEKPISNRWRILMPDGTHGIYPKPRAIGTYEISQ
VVEDYRRSALNAIEAGFDGIEIHGAHG**F**LIDQFLKDGINDRTDEYGGSLANRCKFITQ
VVQAVVSAIGADRVGVRVSPAIDHLDAMDSNPLSLGLAVVERLNKIQLHSGSKLAYL
HVTQPRYVAYGQTEAGRLGSEEEEARLMRTLRNAYQGTFICSGGYTRELGIEAVAQG
DADLVSYGRLFISNPDLVMRIKLNAPLNKYNRKTFYTQDPVVGYTDYPFLQGNGSNG
PLSRL

The gene of Opr3 Y190W variant with the 6x His-tag underlined and mutagenesis primer in bold.

ATGGCTAGCCACCACCACCACCACCACATGGCGTCTTCAGCTCAAGATGGAAACA
ATCCCCTTTTCTCTCCTTACAAGATGGGCAAGTTCAATCTATCCCACAGGGTAGTA
TTGGCTCCGATGACAAGGTGCAGAGCACTGAATAATATTCCACAGGCGGCGCTAG
GGGAGTATTACGAGCAGAGAGCGACGGCCGGTGGATTTCTGATCACTGAAGGCA
CTATGATTTCTCCGACTTCAGCTGGGTTTCCTCATGTGCCAGGGATTTTCACAAAG
GAACAAGTAAGGGAATGGAAGAAAATAGTTGATGTAGTGCATGCAAAGGGTGCT
GTCATATTTTGTCAGCTGTGGCATGTTGGTCGTGCATCTCATGAAGTGTATCAACC
TGCTGGAGCTGCACCAATATCATCCACTGAGAAGCCTATATCAAATAGGTGGAGA
ATTCTAATGCCTGATGGAACTCATGGGATTTATCCAAAACCAAGAGCAATTGGAA
CCTATGAGATCTCACAAGTTGTTGAAGATTATCGCAGGTCGGCCTTGAATGCTAT
TGAAGCAGGTTTCGATGGTATTGAAAT**CCATGGAGCTCACGGTTGGTTGATTG**
ATCAATTCTTGAAAGATGGGATCAATGACCGGACAGATGAGTATGGTGGATCAC
TAGCCAACCGGTGCAAATTCATCACACAGGTGGTTCAAGCAGTAGTCTCAGCAAT
AGGAGCTGATCGCGTAGGCGTTAGAGTTTCACCAGCAATAGATCATCTTGATGCC
ATGGACTCTAATCCACTCAGCCTTGGCTTAGCAGTTGTTGAAAGACTAAACAAAA
TCCAACTCCATTCTGGTTCCAAGCTTGCCTATCTTCATGTAACACAGCCACGATAC
GTAGCATATGGGCAAACTGAAGCAGGCAGACTTGGCAGTGAAGAGGAAGAGGCT
CGTTTAATGAGGACTTTGAGGAACGCGTATCAGGGGACATTCATTTGCAGTGGTG
GATACACTAGGGAACTAGGAATTGAGGCTGTGGCACAAGGTGATGCTGATCTCGT
GTCATATGGTCGTCTTTTCATCTCTAATCCTGATTTGGTTATGAGAATCAAGCTAA
ATGCACCTCTAAATAAGTATAACAGGAAGACATTCTATACTCAAGATCCAGTTGT
GGGATACACAGATTACCCTTTCCTTCAAGGAAATGGAAGCAATGGACCGTTATCG
CGTCTGTGA

MASHHHHHHMASSAQDGNNPLFSPYKMGKFNLSHRVVLAPMTRCRALNNIPQAAL
GEYYEQRATAGGFLITEGTMISPTSAGFPHVPGIFTKEQVREWKKIVDVVHAKGAVIF
CQLWHVGRASHEVYQPAGAAPISSTEKPISNRWRILMPDGTHGIYPKPRAIGTYEISQ
VVEDYRRSALNAIEAGFDGIEIHGAHG**W**LIDQFLKDGINDRTDEYGGSLANRCKFITQ
VVQAVVSAIGADRVGVRVSPAIDHLDAMDSNPLSLGLAVVERLNKIQLHSGSKLAYL
HVTQPRYVAYGQTEAGRLGSEEEEARLMRTLRNAYQGTFICSGGYTRELGIEAVAQG
DADLVSYGRLFISNPDLVMRIKLNAPLNKYNRKTFYTQDPVVGYTDYPFLQGNGSNG
PLSRL

The gene of YqjM wild type (*Bacillus subtilis*)

ATGGCCAGAAAATTATTTACACCTATTACAATTAAAGATATGACGTTAAAAAACC
GCATTGTCATGTCGCCAATGTGCATGTATTCTTCTCATGAAAAGGACGGAAAATT
AACACCGTTCCACATGGCACATTACATATCGCGCGCAATCGGCCAGGTCGGACTG
ATTATTGTAGAGGCGTCAGCGGTTAACCCTCAAGGACGAATCACTGACCAAGACT
TAGGCATTTGGAGCGACGAGCATATTGAAGGCTTTGCAAAACTGACTGAGCAGGT
CAAAGAACAAGGTTCAAAAATCGGCATTCAGCTTGCCCATGCCGGACGTAAAGC
TGAGCTTGAAGGAGATATCTTCGCTCCATCGGCGATTGCGTTTGACGAACAATCA
GCAACACCTGTAGAAATGTCAGCAGAAAAAGTAAAAGAAACGGTCCAGGAGTTC
AAGCAAGCGGCTGCCCGCGCAAAAGAAGCCGGCTTTGATGTGATTGAAATTCAT
GCGGCGCACGGATATTTAATTCATGAATTTTTGTCTCCGCTTTCCAACCATCGAAC
AGATGAATATGGCGGCTCACCTGAAAACCGCTATCGTTTCTTGAGAGAGATCATT
GATGAAGTCAAACAAGTATGGGACGGTCCTTTATTTGTCCGTGTATCTGCTTCTGA
CTACACTGATAAAGGCTTAGACATTGCCGATCACATCGGTTTTGCAAAATGGATG
AAGGAGCAGGGTGTTGACTTAATTGACTGCAGCTCAGGCGCCCTTGTTCACGCAG
ACATTAACGTATTCCCTGGCTATCAGGTCAGCTTCGCTGAGAAAATCCGTGAACA
GGCGGACATGGCTACTGGTGCCGTCGGCATGATTACAGACGGTTCAATGGCTGAA
GAAATTCTGCAAAACGGACGTGCCGACCTCATCTTTATCGGCAGAGAGCTTTTGC
GGGATCCATTTTTTGCAAGAACTGCTGCGAAACAGCTCAATACAGAGATTCCGGC
CCCTGTTCAATACGAAAGAGGCTGGTAA

MARKLFTPITIKDMTLKNRIVMSPMCMYSSHEKDGKLTPFHMAHYISRAIGQVGLIIV
EASAVNPQGRITDQDLGIWSDEHIEGFAKLTEQVKEQGSKIGIQLAHAGRKAELEGDI
FAPSAIAFDEQSATPVEMSAEKVKETVQEFKQAAARAKEAGFDVIEIHAAHGYLIHEF
LSPLSNHRTDEYGGSPENRYRFLREIIDEVKQVWDGPLFVRVSASDYTDKGLDIADHI
GFAKWMKEQGVDLIDCSSGALVHADINVFPGYQVSFAEKIREQADMATGAVGMITD
GSMAEEILQNGRADLIFIGRELLRDPFFARTAAKQLNTEIPAPVQYERGW

The gene of YqjM Y169F variant with the mutagenesis primer in bold.

ATGGCCAGAAAATTATTTACACCTATTACAATTAAAGATATGACGTTAAAAAACC
GCATTGTCATGTCGCCAATGTGCATGTATTCTTCTCATGAAAAGGACGGAAAATT
AACACCGTTCCACATGGCACATTACATATCGCGCGCAATCGGCCAGGTCGGACTG
ATTATTGTAGAGGCGTCAGCGGTTAACCCTCAAGGACGAATCACTGACCAAGACT
TAGGCATTTGGAGCGACGAGCATATTGAAGGCTTTGCAAAACTGACTGAGCAGGT
CAAAGAACAAGGTTCAAAAATCGGCATTCAGCTTGCCCATGCCGGACGTAAAGC
TGAGCTTGAAGGAGATATCTTCGCTCCATCGGCGATTGCGTTTGACGAACAATCA
GCAACACCTGTAGAAATGTCAGCAGAAAAAGTAAAAGAAACGGTCCAGGAGTTC
AAGCAAGCGGCTGCCCGCGCAAAAGAAGCCGGCTTTGATGTGATTGAAATT**CAT**
GCGGCGCACGGATTTTTAATTCATGAATTTTTGTCTCCGCTTTCCAACCATCG
AACAGATGAATATGGCGGCTCACCTGAAAACCGCTATCGTTTCTTGAGAGAGATC
ATTGATGAAGTCAAACAAGTATGGGACGGTCCTTTATTTGTCCGTGTATCTGCTTC
TGACTACACTGATAAAGGCTTAGACATTGCCGATCACATCGGTTTTGCAAAATGG
ATGAAGGAGCAGGGTGTTGACTTAATTGACTGCAGCTCAGGCGCCCTTGTTCACG
CAGACATTAACGTATTCCCTGGCTATCAGGTCAGCTTCGCTGAGAAAATCCGTGA
ACAGGCGGACATGGCTACTGGTGCCGTCGGCATGATTACAGACGGTTCAATGGCT
GAAGAAATTCTGCAAAACGGACGTGCCGACCTCATCTTTATCGGCAGAGAGCTTT
TGCGGGATCCATTTTTTGCAAGAACTGCTGCGAAACAGCTCAATACAGAGATTCC
GGCCCCTGTTCAATACGAAAGAGGCTGGTAA

MARKLFTPITIKDMTLKNRIVMSPMCMYSSHEKDGKLTPFHMAHYISRAIGQVGLIIV
EASAVNPQGRITDQDLGIWSDEHIEGFAKLTEQVKEQGSKIGIQLAHAGRKAELEGDI
FAPSAIAFDEQSATPVEMSAEKVKETVQEFKQAAARAKEAGFDVIEIHAAHGFLIHEF
LSPLSNHRTDEYGGSPENRYRFLREIIDEVKQVWDGPLFVRVSASDYTDKGLDIADHI
GFAKWMKEQGVDLIDCSSGALVHADINVFPGYQVSFAEKIREQADMATGAVGMITD
GSMAEEILQNGRADLIFIGRELLRDPFFARTAAKQLNTEIPAPVQYERGW

The gene of YqjM Y169W variant with the mutagenesis primer in bold.

ATGGCCAGAAAATTATTTACACCTATTACAATTAAAGATATGACGTTAAAAAACC
GCATTGTCATGTCGCCAATGTGCATGTATTCTTCTCATGAAAAGGACGGAAAATT
AACACCGTTCCACATGGCACATTACATATCGCGCGCAATCGGCCAGGTCGGACTG
ATTATTGTAGAGGCGTCAGCGGTTAACCCTCAAGGACGAATCACTGACCAAGACT
TAGGCATTTGGAGCGACGAGCATATTGAAGGCTTTGCAAAACTGACTGAGCAGGT
CAAAGAACAAGGTTCAAAAATCGGCATTCAGCTTGCCCATGCCGGACGTAAAGC
TGAGCTTGAAGGAGATATCTTCGCTCCATCGGCGATTGCGTTTGACGAACAATCA
GCAACACCTGTAGAAATGTCAGCAGAAAAAGTAAAAGAAACGGTCCAGGAGTTC
AAGCAAGCGGCTGCCCGCGCAAAAGAAGCCGGCTTTGATGTGATTGAAATTCAT
GCGG**CGCACGGATGGTTAATTCATGAATTTTTG**TCTCCGCTTTCCAACCATCGA
ACAGATGAATATGGCGGCTCACCTGAAAACCGCTATCGTTTCTTGAGAGAGATCA
TTGATGAAGTCAAACAAGTATGGGACGGTCCTTTATTTGTCCGTGTATCTGCTTCT
GACTACACTGATAAAGGCTTAGACATTGCCGATCACATCGGTTTTGCAAAATGGA
TGAAGGAGCAGGGTGTTGACTTAATTGACTGCAGCTCAGGCGCCCTTGTTCACGC
AGACATTAACGTATTCCCTGGCTATCAGGTCAGCTTCGCTGAGAAAATCCGTGAA
CAGGCGGACATGGCTACTGGTGCCGTCGGCATGATTACAGACGGTTCAATGGCTG
AAGAAATTCTGCAAAACGGACGTGCCGACCTCATCTTTATCGGCAGAGAGCTTTT
GCGGGATCCATTTTTTGCAAGAACTGCTGCGAAACAGCTCAATACAGAGATTCCG
GCCCCTGTTCAATACGAAAGAGGCTGGTAA

MARKLFTPITIKDMTLKNRIVMSPMCMYSSHEKDGKLTPFHMAHYISRAIGQVGLIIV
EASAVNPQGRITDQDLGIWSDEHIEGFAKLTEQVKEQGSKIGIQLAHAGRKAELEGDI
FAPSAIAFDEQSATPVEMSAEKVKETVQEFKQAAARAKEAGFDVIEIHAAHGWLIHEF
LSPLSNHRTDEYGGSPENRYRFLREIIDEVKQVWDGPLFVRVSASDYTDKGLDIADHI
GFAKWMKEQGVDLIDCSSGALVHADINVFPGYQVSFAEKIREQADMATGAVGMITD
GSMAEEILQNGRADLIFIGRELLRDPFFARTAAKQLNTEIPAPVQYERGW

7.9.3 Preparation of buffers

NaH_2PO_4/Na_2HPO_4 buffer (50 mM, pH 7.5, 150 mM NaCl)

$Na_2HPO_4*2H_2O$ (8.29 g, 46.6 mmol), $NaH_2PO_4*H_2O$ (0.47 g, 3.4 mmol) and NaCl (8.77 g, 150 mmol) were dissolved in 1 L H_2O bidest. Under vigorous stirring H_3PO_4 conc. or NaOH-solution (conc., in H_2O) were added until a calibrated pH-meter indicated pH 7.5. Buffer solution was filtered sterile.

When different concentrations of imidazole were needed, amount of imidazole is added prior to the adjustment of the pH.

Buffer A: Tris-HCl buffer (50 mM, pH 7.5)

Tris-HCl (7.88 g, 50 mmol) was dissolved in 1 L H_2O bidest. Under vigorous stirring HCl conc. or NaOH-solution (conc., in H_2O) were added until a calibrated pH-meter indicated pH 7.5. Buffer solution was filtered sterile.

Buffer B: Tris-HCl buffer (50 mM, pH 7.5, 400 mM KCl)

Tris-HCl (7.88 g, 50 mmol) and KCl (29.8 g, 400 mmol) were dissolved in 1 L H_2O bidest. Under vigorous stirring HCl conc. or NaOH-solution (conc., in H_2O) were added until a calibrated pH-meter indicated pH 7.5. Buffer solution was filtered sterile.

Buffer C: Tris-HCl buffer (50 mM, pH 7.5, 1.5 M ammonium sulfate)

Tris-HCl (7.88 g, 50 mmol) and $(NH_4)_2SO_4$ (198.2 g, 1.5 mol) were dissolved in 1 L H_2O bidest. Under vigorous stirring HCl conc. or NaOH-solution (conc., in H_2O) were added until a calibrated pH-meter indicated pH 7.5. Buffer solution was filtered sterile.

7.9.4 Expression of Opr3 and YqjM wild types and variants

10 mL of an overnight cell culture was used to inoculate one flask with 800 mL LB medium supplemented with ampicillin (100 µg/mL) and chloramphenicol (10 µg/mL). The cell culture was incubated at 37 °C at 250 rpm until an OD_{600} of 0.6-0.8 was reached. The protein expression was induced by the addition of IPTG (0.125 mM) and incubated at 20 °C for 16 h. The cells were harvested by centrifugation at 4 °C and the pellets were stored at -32 °C.

7.9.5 Purification of Opr3 wild type and variants

The cell pellet was resuspended in lysis buffer (50 mM sodium phosphate buffer, pH 7.5, 20 mM imidazole, 150 mM NaCl, 3 mL/g cell pellet) and phenylmethylsulfonyl fluoride (final concentration 1.3 mM) and lysozyme (final concentration 1 mg/mL) were added. After 20 min at 4 °C the cells were further lysed in an ice bath by ultra-sonication for 10 min (0.5 s pulse, power 60 %). The sonicated suspension was centrifuged at 20.000 rpm for 45 min at 4 °C. The supernatant was subjected to Ni-NTA affinity chromatography on a HisTrap FF 5 mL column. After washing with increasing amount of imidazole (up to 50 mM), the bound protein was eluted with elution buffer (50 mM sodium phosphate buffer, pH 7.5, 300 mM imidazole, 150 mM NaCl). The yellow fractions containing Opr3 were pooled, concentrated, and dialyzed overnight in sodium phosphate buffer (50 mM, pH 7.5, 150 mM NaCl) at 4 °C. The progress of protein purification was monitored by SDS-PAGE. Aliquots of Opr3 WT and variants were stored at 4 °C.

7.9.6 Purification of YqjM WT and variants[136]

The cell pellet was resuspended in buffer A (50 mM Tris-HCl, pH 7.5, 4 mL/g cell pellet) and phenylmethylsulfonyl fluoride (final concentration 1.3 mM) and lysozyme (final concentration 1 mg/mL) were added. After 20 min at 4 °C the cells were further lysed in an ice bath by ultra-sonication for 10 min (0.5 s pulse, power 60 %). The sonicated suspension was centrifuged at 20.000 rpm for 45 min at 4 °C. The supernatant was subjected to ion exchange chromatography on a DEAE-Sephacel FF column (20 mL) freshly equilibrated in buffer A. After extensive washing with buffer A, the bound protein was eluted with a linear gradient of 250 mL of a 1:1 mixture of buffer A/buffer B (buffer B: 50 mM Tris-HCl, pH 7.5, 400 mM KCl). The yellow fractions containing YqjM were pooled, concentrated, and dialyzed overnight in buffer A at 4 °C. The dialysate was brought to 30 % ammonium sulfate saturation and applied to a phenyl-Sepharose column (25 mL) freshly equilibrated with buffer C (50 mM Tris-HCl, pH 7.5, 1.5 M ammonium sulfate). After washing with buffer A, the bound protein was eluted with a linear gradient of 250 mL buffer C and 250 mL buffer A. The yellow fractions containing YqjM were pooled, concentrated, and dialyzed overnight in buffer A at 4 °C. The progress of protein purification was monitored by SDS-PAGE. Aliquots of YqjM WT and variants were stored at -32 °C.

7.9.7 Estimation of enzyme concentrations and FMN absorbance spectra

Enzyme concentration was photometrically estimated (ε = 9500 $L \cdot mol^{-1} \cdot cm^{-1}$) at the FMN absorbance maximum (summarized in Table 21).

Table 21: Absorbance maxima of Opr3 and YqjM wild type enzymes and variants.

Entry	Enzyme variant	Absorbance maximum [nm]
1	Opr3 WT	466
2	Opr3 Y190F	467
3	Opr3 Y190W	466
4	YqjM WT	455
5	YqjM Y169F	454
6	YqjM Y169W	454

All spectra were recorded using a spectrophotometer Specord 200 plus from Analytik Jena. The measurements were carried out in disposable cuvettes (semimicro, dimension 12.5×12.5×45 mm) from Brand. Spectra are shown in Figure 27, Figure 28, Figure 29, Figure 30, Figure 31 and Figure 32.

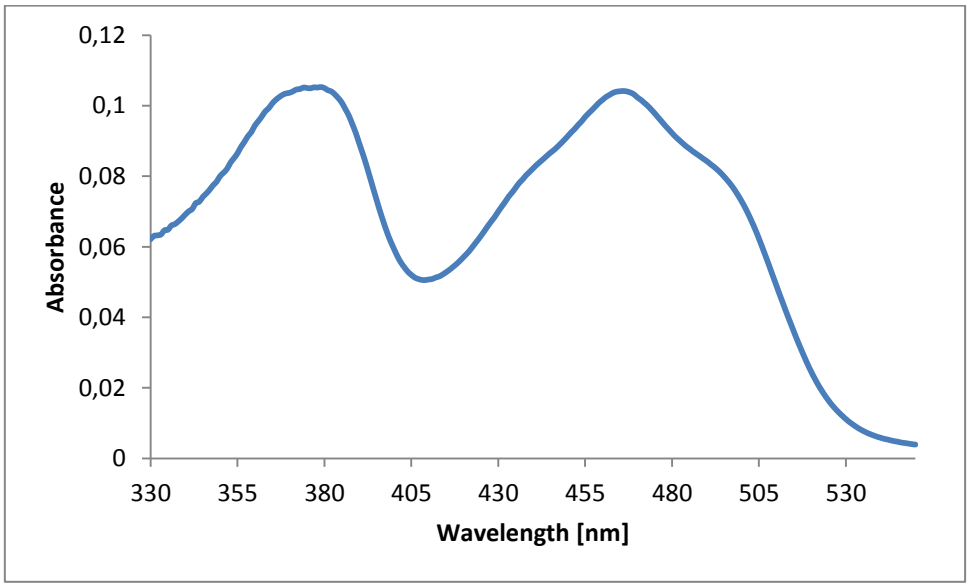

Figure 27: FMN absorbance spectrum of Opr3 WT.

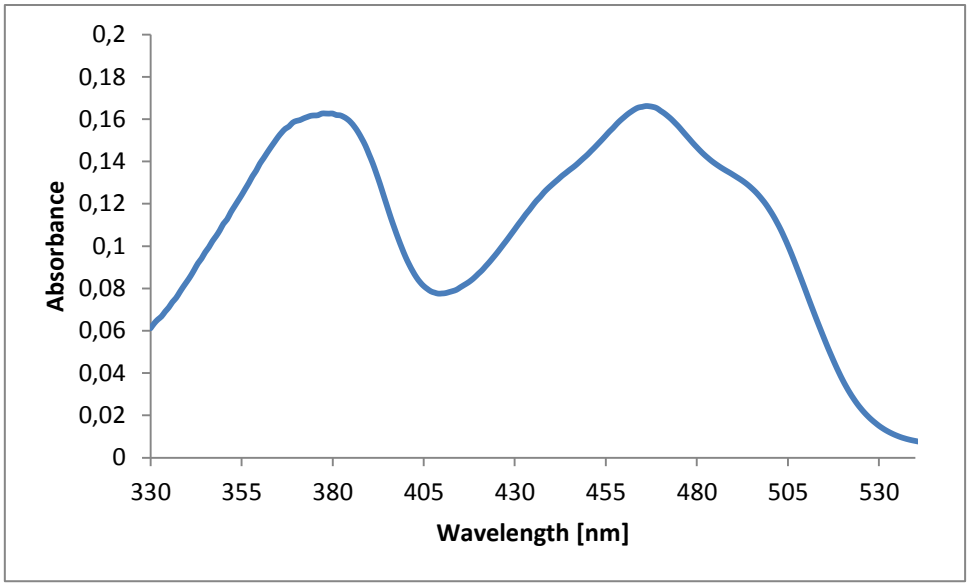

Figure 28: FMN absorbance spectrum of Opr3 Y190F.

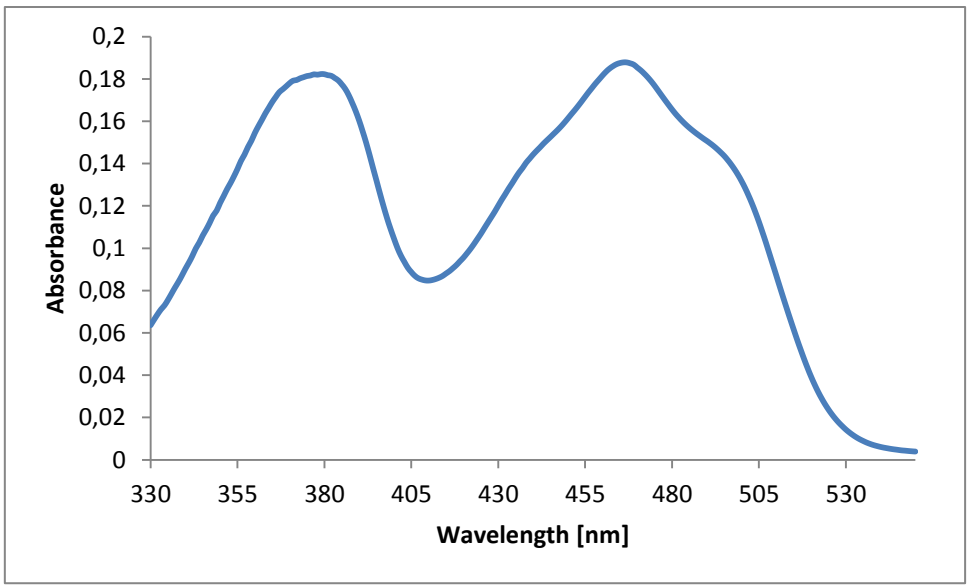

Figure 29: FMN absorbance spectrum of Opr3 Y190W.

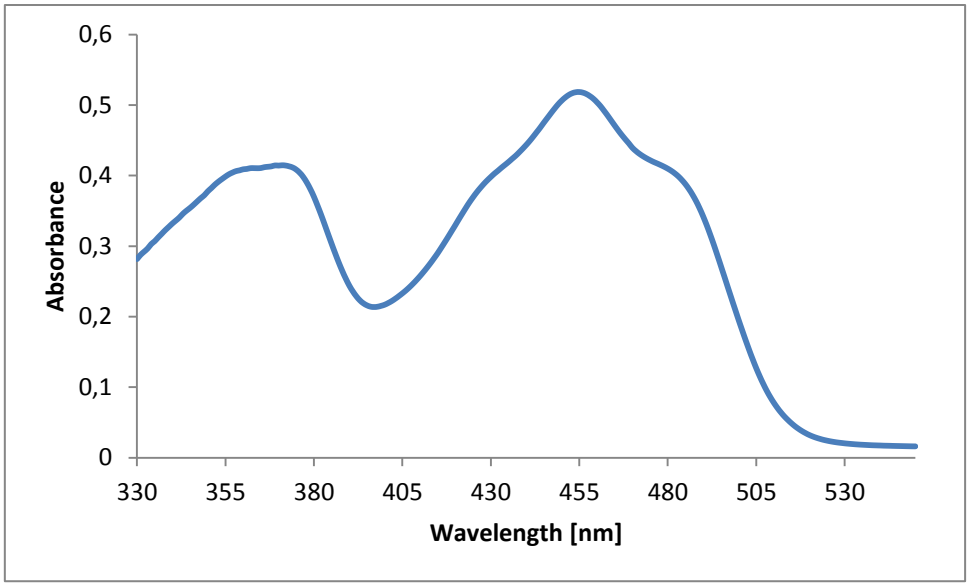

Figure 30: FMN absorbance spectrum of YqjM WT.

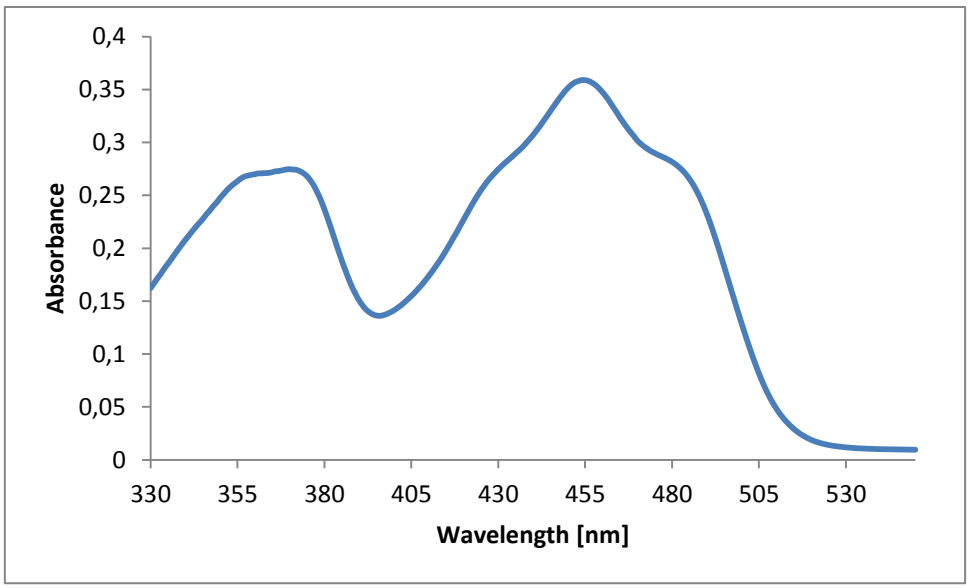

Figure 31: FMN absorbance spectrum of YqjM Y169F.

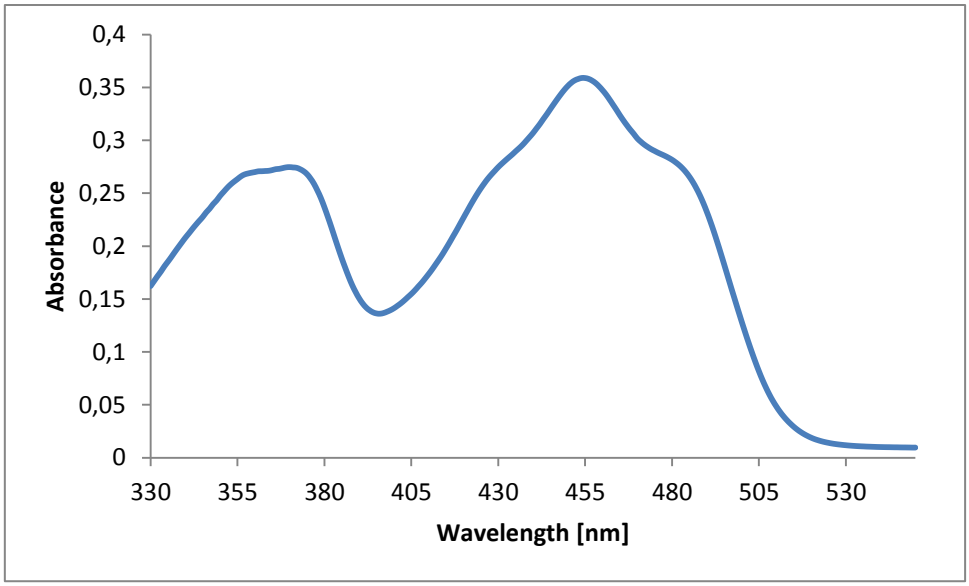

Figure 32: FMN absorbance spectrum of YqjM Y169W.

8 References

[1] K. W**.** Quasdorf, L. E. Overman, *Nature* **2014**, *516*, 181-191.
[2] C. K Prier, F. H. Arnold, *J. Am. Chem. Soc.* **2015**, *137*, 13992-14006.
[3] N. G. Schmidt, E. Eger, W. Kroutil, *ACS Catal.* **2016**, *6*, 4286-4311.
[4] K. Fesko, M. Gruber-Khadjawi, *ChemCatChem* **2013**, *5*, 1248–1272.
[5] V. E. Gouverneur, K. N. Houk, B. de Pascual-Teresa, B. Beno, K. D. Janda, A. R. Lerner,. *Science* **1993**, *262*, 204-208.
[6] P. G. Schultz, R. A. Lerner, *Science* **1995**, *269*, 1835-1842.
[7] D. Hilvert, *Annu. Rev. Biochem*. **2000**, *69*, 751-793.
[8] D. Rothilsberger, O. Khersonsky, A. M. Wollacott, L. Jiang, J. DeChancie, J. Betker, J. L. Gallaher, E. A. Althoff, A. Zanghellini, O. Dym, S. Albeck, K. N. Houk, D. S. Tawfik, D. Baker, *Nature* **2008**, *453*, 190-195.
[9] J. B. Siegel, A. Zanghellini, H. M. Lovick, G. Kiss, A. R. Lambert, J. L. St. Clair, J. L. Gallaher, D. Hilvert, B. L. Stoddart, K. N. Houk, F. E. Michael, D. Baker, *Science* **2010**, *329*, 309-313.
[10] S. D. Kare, Y. Kipnis, P. J. Greisen, R. Takeuchi, Y. Ashani, M. Goldsmith, Y. Song, J. L. Gallagher, I. Silman, H. Leader, J. L. Sussmann, B. L. Stoddart, D. S. Tawfik, D. Baker, *Nat. Chem. Biol.* **2012**, *8*, 294-300.
[11] D. Hilvert, *Annu. Rev. Biochem* **2013**, *82*, 447-470.
[12] G. Kiss, N. Celeb-Ölcüm, R. Moretti, D. Baker, K. N. Houk, *Angew. Chem. Int. Ed.* **2013**, *52*, 5700-5725.
[13] U. T. Bornscheuer, R. J. Kazlauskas, *Angew. Chem. Int. Ed.* **2004**, *43*, 6032-6040.
[14] U. T. Bornscheuer, *Angew. Chem. Int. Ed.* **2016**, *55*, 4372-4373.
[15] O. Warburg, W. Christian, *Sci. Nat.* **1932**, *20*, 688-688.
[16] O. Warburg, W. Christian, *FEBS J*. **1933**, *266*, 377-411.
[17] H. Theorell, *FEBS J*. **1934**, *275*, 344-346.
[18] H. Theorell, *Arch. Biochem. Biophys.* **1956**, *65*, 439-448.
[19] K. Stott, K. Saito, D. J. Thiele, V. Massey, *J. Biol. Chem.* **1993**, *268*, 6097-6106.
[20] B. J. Brown, Z, Deng, O. A. Karplus, V. Massey, *J. Biol. Chem.* **1998**, *273*, 32753-32762.
[21] M. Kataoka, A. Kotaka, A. Hasegawa, M. Wada, M. Yoshizumi, S. Nakamori, S. Shimizu, *Biosci. Biotechnol. Biochem.* **2002**, *66*, 2651-2657.
[22] C. Breithaupt, J. Strassner, U. Breitinger, R. Huber, P. Macheroux, A. Schaller, T. Clausen, *Structure* **2001**, *9*, 419-429.
[23] M. Hall, C. Stueckler, H. Ehammer, E. Pointer, G. Oberdorfer, K. Gruber, B. Hauer, R. Stuermer, W. Kroutil, P. Macheroux, K. Faber. *Adv. Synth. Catal.* **2008**, *350*, 411-418.
[24] A. S. Abramovitz, V. Massey, *J. Biol. Chem.* **1976**, *251*, 5327-5336.
[25] J. K. Eweg, F. Miller W. J. H. VanBerkel, *Eur. J. Biochem* **1982**, *129*, 303-316
[26] K. M. Fox, P. A. Karplus, *Structure* **1994**, *2*, 1089-1105.
[27] R. M. Kohli, V. Massey, *J. Biol. Chem.* **1998**, *273*, 32763-32770.
[28] V. Massey, L. M. Schopfer, *J. Biol. Chem.* **1986**, *261*, 1215-1222.
[29] J. Basran, R. J. Harris, M. J. Sutcliffe, N. S. Scrutton, *J. Biol. Chem.* **2003**, *278*, 43973-43982.
[30] A. D. N. Vaz, S. Chakraborty, V. Massey, *Biochemistry* **1995**, *34*, 4246-4256.
[31] R. Lonsdale, M. T. Reetz, *J. Am. Chem. Soc.* **2015**, *137*, 14733-14742.
[32] D. Xu, R. M. Kohli, V. Massey, *Proc. Natl. Acad. Sci. USA* **1999**, *96*, 3556-3561.

[33] F. Schaller, C. Biesgen, C. Müssig, T. Altmann, E. W. Weiler, *Planta* **2000**, *210*, 979-984.
[34] C. Breithaupt, R. Kurzbauer, H. Lilie, A. Schaller, J. Strassner, R. Huber, P. Macheroux, T. Clausen. *Proc. Natl. Acad. Sci. USA* **2006**, *103*, 14337-14342.
[35] T. M. Barna, H. Khan, N. C. Bruce, I. Barsukov, N. S. Scrutton, P. C. E. Moody, *J. Mol. Biol.* **2001**, *310*, 433-447.
[36] T. M. Barna, I. I. L. Messiha, C. Petosa, N. C. Bruce, N. S. Scrutton, P. C. E. Moody, *J. Biol. Chem* **2002**, *277*, 30976-30983.
[37] T. B. Fitzpatrick, N. Amrhein, P. Macheroux, *J. Biol. Chem.* **2003**, *278*, 19891-19897.
[38] K. Kitzing, T. B. Fitzpatrick, C. Wilken, J. Sawa, G. P. Bourenkov, P. Macheroux, T. Clausen, *J. Biol. Chem.* **2005**, *280*, 27904-27913.
[39] M. Hall, C. Stueckler, W. Kroutil, P. Macheroux, K. Faber, *Angew. Chem. Int. Ed.* **2007**, *46*, 3934-3937.
[40] E. D. Amato, J. D. Stewart, *Biotechnol. Adv.* **2015**, *33*, 624-631.
[41] D. J. Bougioukou, S. Kille, A. Taglieber, M. T. Reetz, *Adv. Synth. Catal.* **2009**, *351*, 3287-3305.
[42] M. T. Reetz, M. Bocola, J. D. Caballeira, D. Zha, A. Vogel, *Angew. Chem. Int. Ed.* **2005**, *117*, 4246-4268.
[43] M. T. Reetz, M. Bocola, J. D. Caballeira, D. Zha, A. Vogel, *Angew. Chem. Int. Ed.* **2008**, *44*, 4192-4196.
[44] C. M. Coulthier, M. M. Kayser, M. T. Reetz, *J. Org. Chem.* **2006**, *71*, 8431-8437.
[45] J. D. Caballeira, P. Krumlinde, M. Bocola, A. Vogel, M. T. Reetz, J. -E. Bäckvall, *Chem. Commun.* **2007**, 1913-1915.
[46] G. Steinkellner, C. C. Gruber, T. Pavkov-Kellner, A. Binter, K. Steiner, C. Winkler, A. Lyskowki, O. Schwamberger, M. Oberer, H. Schwab, K. Faber, P. Macheroux, K. Gruber, *Nat. Commun.* **2014**, *5*, 4150-4159.
[47] N. J. Turner, E. O'Reilly, *Nat. Chem. Biol.* **2013**, *9*, 285-288.
[48] M. Hönig, P. Sondermann, N. J. Turner, E. M. Carreira, *Angew. Chem. Int. Ed.* **2017**, *56*, 8942-8973.
[49] D. A. Evans, K. A. Woerpel, M. M. Hinman, M. M. Faul, *J. Am. Chem. Soc.* **1991**, *131*, 726-728.
[50] H. Suematsu, S. Kanchiku, T. Uchida, J. Katsuki, *J. Am. Chem. Soc.* **2008**, *130*, 10327-10337.
[51] V. N. G. Lindsay, W. Lin, A. B. Charette, *J. Am. Chem. Soc.* **2009**, *131*, 16383-16385.
[52] Y. Chen, J. V. Ruppel, X. P. Zhang, *J. Am. Chem. Soc.* **2007**, *129*, 12074-12074.
[53] J. I. Ito, S. Ujiie, H. Nishiyama, *Chem. Eur. J.* **2010**, *16*, 4986-4990.
[54] P. S. Coelho, E. M. Brustad, A. Kannan, F. H. Arnold, *Science* **2013**, *339,* 307–310.
[55] P. S. Coelho, Z. J. Wang, M. E. Ener, S. A. Baril, A. Kannan, F. H. Arnold, E. M. Brustad, *Nat. Chem. Biol.* **2013**, *9,* 485–487.
[56] Z. J. Wang, H. Renata, N. E. Peck, C. C. Farwell, P. S. Coelho, F. H. Arnold, *Angew. Chem. Int. Ed.* **2014**, *53,* 6810–6813.
[57] J. G. Gober, A. E. Rydeen, E. J. Gibson-O'Grady, J. B. Leuthaeuser, J. S. Fetrow, E. M. Brustad, *ChemBioChem* **2016**, *17,* 394–397.
[58] M. Bordeaux, V. Tyagi, R. Fasan, *Angew. Chem. Int. Ed.* **2015**, *54,* 1744–1748.
[59] V. Tyagi, R. Fasan, *Angew. Chem. Int. Ed.* **2016**, *55,* 2512–2516.
[60] D. Enders, U. Kallfass, *Angew. Chem. Int. Ed.*, **2002**, *41*, 1743-1745.
[61] P. Dünkelmann, D. Kolter-Jung, A. Nitsche, A. S. Demir, P. Siegert, B. Lingen, M. Baumann, M. Pohl, M. Müller, *J. Am. Chem. Soc.* **2002**, *124*, 12084-12085.
[62] H. Stetter, *Angew. Chem. Int. Ed.* **1976**, *15*, 639-712.

[63] C. Dresden, M. Richter, M. Pohl, S. Lüdeke, M. Müller, *Angew. Chem. Int. Ed.* **2010**, *49*, 6600-6603.
[64] M. Yamaguchi, N. Yokota, T. Minami, *J. Chem. Soc. Chem. Commun.* **1991**, 1088–1089.
[65] M. Yamaguchi, T. Shiraishi, M. Hirama, *Angew. Chem. Int. Ed.* **1993**, *105,* 1243–1245.
[66] M. Yamaguchi, T. Shiraishi, M. Hirama, *Angew. Chem. Int. Ed.* **1993**, *32,* 1176–1178.
[67] E. Zandvoort, E. M. Geertsema, B. J. Baas, W, J, Quax, G. J. Poelarends, *Angew. Chem. Int. Ed.* **2012**, *51*, 1240-1243.
[68] X. Garrabou, R. Verez, D. Hilvert, *J. Am. Chem. Soc.* **2017**, *139*, 103-106.
[69] H. Y. Jang, R. Huddleston, M. Krische, *J. Am. Chem. Soc.* **2002**, *124,* 15156-15157.
[70] H. Y. Jang, M. Krische, *Eur. J. Org. Chem.* **2004**, 3953-3958.
[71] R. Schrock, J. Osborn, *J. Am. Chem. Soc.* **1976**, *98*, 2134-2143.
[72] R. Schrock, J. Osborn, *J. Am. Chem. Soc.* **1976**, *98*, 2143-2147.
[73] R. Schrock, J. Osborn, *J. Am. Chem. Soc.* **1976**, *98*, 4450-4455.
[74] H. Y. Jang, M. Krische, *Acc. Chem. Res.* **2004**, *37*, 653-661.
[75] R. R. Huddleston, M. Krische, *Org. Lett.* **2003**, *5*, 1143-1146.
[76] D. Cauble, J. Gipson, M. Krische, *J. Am. Chem. Soc.* **2003**, *125*, 1110-1111.
[77] P. Koech, M. Krische, *Org. Lett.* **2004**, *6*, 691-694.
[78] T. G. Baik, A. L. Luis, L. C. Wang, M. J. Krische, *J. Am. Chem. Soc.* **2001**, *123*, 5112-5113.
[79] L. C. Wang, H. Y. Jang, Y. Roh, V. Lynch, A. J. Schultz, X. Wang, M. J. Krische, *J. Am. Chem. Soc.* **2002**, *124*, 9448-9453.
[80] A. Schweiger, *MSc Thesis*, Graz University of Technology, Graz, **2016**.
[81] M. A. Casadei, C. Galli, L. Mandolini, *J. Am. Chem. Soc.* **1984**, *106*, 1051-1059.
[82] C. Fuganti, P. Grasselli, *J. Chem. Soc. Chem. Commun*. **1982**, 205-206.
[83] C. Fuganti, P. Grasselli, S. Servi, *J. Chem. Soc. Perkin Trans 1.* **1983**, 241-244.
[84] A. Kergomard, M. F. Renard, H. Veschambre, *J. Org. Chem.* **1982**, *47*, 792-798.
[85] C. J. Sih, J. B. Heather, R. Sood, P. Prize, G. Peruzzotti, H. F. H. Lee, S. S. Lee, *J. Am. Chem. Soc* **1975**, *97*, 865-867.
[86] P. Ferraboschi, P. Grisenti, R. Casati, A. Fiecchi, E. Santaniello, *J. Chem. Soc. Perkin Trans 1*. **1987**, 1743-1748.
[87] T. Kitazume, N. Ishikawa, *Chem. Lett.* **1984**, 587-590.
[88] W. Li, J. Li, Y. Wu, N. Fuller, M. A. Markus, *J. Org. Chem.* **2010**, *75*, 1077-1086.
[89] E. Brenna, F. G. Gatti, D. Monti, F. Parmeggiani, A. Sacchetti, J. Valoti, *J. Mol. Catal., B Enzym.* **2015**, *114*, 77-85.
[90] S. J. Fox, S. Guardain, A. Coulthurst, C. Fox, I. Kuprov, J. W. Essex, C. K. Skylaris, B. Linclau, *Chem. Eur. J.* **2015**, *21*, 1682-1691.
[91] P. Fistrup, T. Jensen, J. Hoppe, P. Norrby, *Chem. Eur. J.* **2006**, *12*, 5352-5360.
[92] A. B. Charette, H. Juteau, *J. Am. Chem. Soc.* **1994**, *116*, 2651-2652.
[93] Y. Ishino, K. Wakamoto, T. Hirashima, *Chem. Lett.* **1984**, *13*, 765-768.
[94] I. S. Kim, G. R. Dong, Y. H. Jung, *J. Org. Chem.* **2007**, *72*, 5424-5426.
[95] K. Heckenbichler, *MSc Thesis*, University of Graz, Graz, **2013**.
[96] H. Kries, L. Caputi, C. E. M. Stevenson, M. O. Kamileen, N. H. Sherden, F. Geu-Flores, D. M. Lawson, S. E. O'Connor, *Nat. Chem. Biol.* **2015**, *12*, 6-8.
[97] M. Hall, C. Stueckler, H. Ehammer, E. Pointner, W. Kroutil, P. Macheroux, K. Faber, *Org. Lett.* **2007**, *9*, 5409-5411.
[98] M. Trobe, *Dissertation*, Graz Universitiy of Technology, Graz, **2015**.
[99] S. Sadhukhan, G. F. Zhang, G. P. Tochtrop, *ACS Chem. Biol.* **2014**, *9*, 1706-1711.
[100] M. P. Doyle, M. Yan, W. Hu, L. S. Gronenberg, *J. Am. Chem. Soc* **2003**, *125*, 4692-4693.

[101] M. Dischmann, T. Frassetto, M. A. Breuning, U. Koert, *Chem. Eur. J.* **2014**, *20*, 11300-11302.
[102] Denmark S., T. Kobayashi, R. Christopher, *Tetrahedron* **2010**, *66*, 4745-4759.
[103] Y. Nakagawa, S. Chanthamath, K. Shibatomi, S. Iwasa, *Org. Lett.* **2015**, *17*, 2792-2795.
[104] I. Shiina, Y. Umezaki, Y. Ohashi, Y. Yamazaki, S. Dan, T. Yamori, *J. Med. Chem.* **2013**, *56*, 150-159.
[105] G. E. Magoulas, S. E. Bariamis, C. M. Athanassopoulos, A. Haskopoulos, P. G. Dedes, M. G. Krokidis, N. K. Karamanos, D. Kletsas, D. Papaioannou, G. Maroulis, *Eur. J. Med. Chem.* **2011**, *46*, 721-737.
[106] G. L. Olson, H. C. Cheung, K. D. Morgan, C. Neukom, G. Saucy, *J. Org. Chem.* **1976**, *41*, 3287-3293.
[107] T. J. Senter, O. O. Fadeeyi, C. W. Lindsley, *Org. Lett.* **2012**, *14*, 1869-1871.
[108] P. Gersbach, A. Jantsch, F. Flyen, N. Scherr, J. Dengy, G. Pluschke, K. Altmann, *Chem. Eur. J.* **2011**, *17*, 13017-13031.
[109] B. M. Trost, R. C. Livingston*, J. Am. Chem. Soc.* **2008**, *130*, 11970-11978.
[110] X. Wu, Q. M. Lian, S. Liu, A. Wu, *RSC Adv.* **2014**, *4*, 51180-51183.
[111] H. Lu, J. Y. Liu, C. G. Li, J. B. Lin, Y. M. Liang, P. F. Xu, *Chem. Commun.* **2015**, *51*, 4473-4476.
[112] P. D. Brown, A. C. Willis, M. S. Sherburn, A. L. Lawrence, *Angew. Chem. Int. Ed.* **2013**, *52*, 13273-13275.
[113] X. Han, P. E. Floreancig, *Angew. Chem. Int. Ed.* **2014**, *53*, 11075-11078.
[114] D. J. Miller, F. Yu, D. W. Knight, K. Allemann, *Org. Biomol. Chem.* **2009**, *7*, 962-975.
[115] D. J. Collins, A. M. James, *Aust. J. Chem.* **1989**, *45*, 223-228.
[116] M. Schmid, R. Barner, *Helv. Chim. Acta* **1979**, *62*, 464-473.
[117] H. O. House, P. D. Weeks, *J. Am. Chem. Soc.* **1975**, *97*, 2778-2785.
[118] J. Pietruszka, A. C. M. Rieche, T. Wilhelm, A. Witt, *Adv. Synth. Catal.* **2003**, *345*, 1273-1286.
[119] M. Schmittel, A. A. Mahajan, G. Bucher, J. W. Bats, *J. Org. Chem.* **2007**, *72*, 2166-2173.
[120] S. Fan, F. Chen, X. Zhang, *Angew. Chem. Int. Ed.* **2011**, *50*, 5918-5923.
[121] S. E. Denmark, S. P. O`Connor, *J. Org. Chem.* **1997**, *62*, 584-594.
[122] P. Mauleon, J. L. Krinsky, F. D. Toste, *J. Am. Chem. Soc*. **2009**, *131*, 4513–4520.
[123] J. Rehbein, S. Leick, M. Hiersemann, *J. Org. Chem.* **2009**, *74*, 1531-1540.
[124] J. D. White, T. S Kim, M. Nambu, *J. Am. Chem. Soc.* **1995**, *117*, 5612-5613.
[125] E. C. Friedrich, S. E. Lunetta, E. J. Lewis, *J. Org. Chem.* **1989**, *54*, 2388-2390.
[126] V. M. T. Carneiro, C. M. Avila, M. J. Balunas, W. H. Gerwick, R. A. Pilli, *J. Org. Chem.* **2014**, *79*, 630-642.
[127] R. Anthes, O. Bello, S. Benoit, C.-K. Chen, E. Corbett, R. M. Corbett, A. J. DelMonte, S. Gingras, R. Livingston, J. Sausker, M. Soumeillant, *Org. Process Res. Dev.* **2008**, *12*, 168-177.
[128] M. H. Yang, D. L. Orsi, R. A. Altmann, *Angew. Chem. Int. Ed.* **2015**, *54*, 2361-2365.
[129] A. M. del Hoyo, A: G. Herraiz, M. G. Suero, *Angew. Chem. Int. Ed.* **2017**, *56*, 1610-1613.
[130] M.S.C. Pedras, A. Abdoli, *Bioorg. Med. Chem.* **2013**, *21*, 4541-4549.
[131] M. J. Berenguer, J. Castells, J. Fernandez, R. M. Galard, *Tetrahedron Lett.* **1971**, *6*, 493-494.
[132] L. Duhamel, J. Guillemont, J. M. Poirier, *Tetrahedron Lett.* **1992**, *33*, 5051-5054.
[133] G. Eletti-Bianchi, F. Centini, L. Re, *J. Org. Chem.* **1976**, *41*, 1648-1650.
[134] H. Shitama, T. Katsuki, *Angew. Chem. Int. Ed.* **2008**, *47*, 2450-2453.
[135] M. Lageron, M. B. Fleury, *Angew. Chem. Int. Ed.* **2012**, *57*, 5409-5412.
[136] T. B. Fitzpatrick, N. Amrhein, P. Macheroux, *J. Biol. Chem.* **2003**, *278*, 19891-19897.

9 Abbreviations

Analytical methods:

^{13}C-NMR	carbon NMR
^{1}H-NMR	proton NMR
APT	attached proton test
Ar	aryl
Cq	quaternary carbon
bs	broad singlet
d	doublet
dd	doublet of doublets
ddd	doublet of doublet of doublets
DI	direct inlet
EI	electron impact ionization
eV	electron volt
GC	gas chromatography
GC-MS	gas chromatography mass spectrometry
GC-FID	gas chromatography flame ionization detector
H,H-COSY	H,H correlated spectroscopy
HMBC	heteronuclear multiple bond correlation
HRMS	high resolution mass spectrometry
HSQC	hetero single quantum coherence
Hz	Hertz
J	coupling constant
m	multiplet
m.p.	melting point
m/z	mass to charge ratio
MHz	mega Hertz
NOESY	Nuclear Overhauser effect spectroscopy

ppm	chemical shift
Rf	ratio of fronts
RT	room temperature
s	singlet
t	triplet
TLC	thin layer chromatography
t_R	retention time
UV	ultra violet
δ	chemical shift

Chemical abbreviations:

Ac	acetyl
Bu	butyl
CH	cyclohexane
DCM	dichloromethane
DIBAL-H	diisobutylaluminium hydride
DIPA	diisopropyl amine
DMAP	4-dimethylaminopyridine
DME	dimethoxyethane
DMF	*N*,*N*-dimethylformamide
DMSO	dimethyl sulfoxide
Et	ethyl
EA	ethyl acetate
EtOH	ethanol
Hal	halide
LDA	lithium diisopropylamide
Me	methyl
OEt	ethoxy
OMe	methoxy
OTf	triflate

PCC	pyridinium chlorochromate
pHBA	para-hydroxybenzaldehyde
THF	tetrahydrofuran
TMS-Cl	trimethyl silyl chloride
TNT	2,4,6-trinitrotoluene

Biological abbreviations:

ADH	alcohol dehydrogenase
CAST	combinatorial active-site saturation test
ER	enoate reductase
FMN	flavin mononucleotide
GDH	glucose dehydrogenase
ISM	iterative saturation mutagenesis
JA	jasmonic acid
NAD(P)H	nicotinamide adenine dinucleotide (phosphate)
OPC-8:0	3-oxo- 2(2'[*Z*]-pentenyl)-cyclopentane-1-octanoate
OPDA	9*S*,13*S*-12-oxo-phytodienoate
Opr1	12-oxophytodienoate reductase 3
Opr3	12-oxophytodienoate reductase 3
OYE	old yellow enzyme

Amino acids:

A / Ala	alanine
R / Arg	arginine
N / Asn	aspargine
D / Asp	aspartic acid
C / Cys	cysteine
Q / Gln	glutamine
E / Glu	glutamic acid
G / Gly	glycine
H / His	histidine

I / Ile	isoleucine
L / Leu	leucine
K / Lys	lysine
M / Met	methionine
F / Phe	phenylalanine
P / Pro	proline
S / Ser	serine
T / Thr	threonine
W / Trp	tryptophane
Y / Tyr	tyrosine
V / Val	valine

Others:

Å	angstrom
%	percentage
°C	degree Celsius
µg	microgram
µL	microliter
µmol	micromol
abs.	absolute
cm	centimeter
conc.	concentrated
conv.	conversion
d	days
de	diastereomeric excess
ee	enantiomeric excess
eq	equivalent
et al	et alii
g	gram
h	hours
M	molar

mbar	millibar
mg	milligram
min	minute
mL	milliliter
mmol	millimol
nm	nanometer
w%	percentage by weight

10 Acknowledgements

Als erstes möchte ich Prof. Dr. Rolf Breinbauer danken. Vielen Dank, dass ich vier Jahre lang ein Teil der Arbeitsgruppe sein durfte und dass du mir die Möglichkeit geboten hast, viele neue Dinge zu lernen und Erfahrungen zu sammeln. Vor allem möchte ich mich für deine Unterstützung bei der Planung meines Projektes und deinem Engagement bei der Planung meiner beruflichen Zukunft bedanken. Herzlichen Dank für dein in mich gesetztes Vertrauen und deine stetige Bereitschaft konstruktive Ideen und Anregungen mit mir zu teilen.

Prof. Dr. Karl Gruber und Prof. Dr. Wolfgang Kroutil möchte ich recht herzlich für die Begutachtung meiner Dissertation danken.

Prof. Dr. Peter Macheroux und seiner Arbeitsgruppe möchte ich für die erfolgreiche Zusammenarbeit in den letzten Jahren danken. Ich danke Dr. Alexandra Binter, Marina Toplak, Eva Frießer, Dr. Karin Koch, Eveline Brodl und Dr. Peter Augustin für die geduldige Beantwortung aller meiner Fragen und für euer Engagement für mein Projekt.

Ich bedanke mich bei meinen Studenten Lea Brandner, Christoph Gradwohl, Anna Schweiger, Andrea Walzl, Jakob Dohr und Leo Krammer. Ihr habt einen großen Beitrag zu dieser Arbeit geleistet und mich mit viel Enthusiasmus und Synthesekraft unterstützt. Danke für die vielen gemeinsamen Tage im Labor, eure Ergebnisse haben wesentlich zu dieser Arbeit beigetragen.

Ganz besonderer Dank gilt Anna Schweiger, die mich für ein Jahr an meinem Projekt unterstützt hat. Ich bedanke mich für die langen Labortage an denen wir gemeinsam Probleme lösen durften, wodurch wir nicht nur ein Team sondern auch Freundinnen geworden sind.

Prof. Dr. Robert Saf und Ing. Karin Bartl danke ich für die Messung der exakten Massen.

Ich möchte dem gesamten Institut für Organische Chemie für die freundliche Aufnahme, für die Hilfsbereitschaft und Unterstützung danken. Ich möchte vor allem Elisabeth Seitler für ihre Freundschaft danken. Es macht mich sehr traurig, dass unsere gemeinsame Arbeitszeit nun endet und wir uns nicht mehr jeden Tag sehen könnnen. Besonders bedanken möchte ich mich bei Prof. Dr. Hansjörg Weber und Carina Illaszewicz-Trattner. Danke, dass ihr immer für mich und meine NMR-Anliegen Zeit gefunden habt. Ich bedanke mich bei Peter Plachota, Peter Urdl, Alexander Fragner und Gerhard Thomann für die zahlreichen Unterstützungen.

Spezieller Dank geht an Astrid Nauta für ihre Geduld und ihre positive Einstellung, die mich jeden Tag angesteckt hat.

An dieser Stelle möchte ich mich bei Dr. Gernot Strohmeier bedanken. Ohne deine Hilfe wäre vieles nicht möglich gewesen, du hast sehr viel zu der erfolgreichen Umsetzung meines Projektes beigetragen.

Großer Dank geht an die ganze Arbeitsgruppe, vor allem an meine Mädels, Julia Blesl und Anna Migglautsch. Ich freue mich auf jeden Tag an dem ich mit euch gemeinsam im Labor oder auch im Schreibraum sein darf. Ohne euch, hätte ich vieles nicht geschafft, vielen Dank! Ich danke Thomas Schlatzer, für seine enorme Unterstützung beim Laborbetreuen und die vielen lustigen Stunden in diversen Praktika. Ich danke Patrick Dobrounig, Marko Kljajic, Carina Doler, Bernhard Berg, Martin Vareka, Christian Lembacher-Fadum, Dr. Nikolaus Guttenberger und Dr. Rita Fürst. Danke für die hilfreichen Diskussionen und den Spaß, den wir hatten.

Auch meiner Familie gilt großer Dank. Besonders meine Eltern haben mich immer unterstützt und an mich geglaubt. Ohne euch hätte ich weder studieren noch diese Arbeit verfassen können. Danke an meine Mama, du warst immer für mich da und ich komme für dich bis heute stets an erster Stelle. Ich weiß, dass das absolut nicht selbstverständlich ist und ich danke dir, für all die Dinge die du mir beigebracht hast.

Danke Daniel, dass auch du immer für mich da bist. Du bist für mich der beste Bruder, den man sich nur wünschen kann, und ich freue mich schon auf all die Dinge, die wir noch gemeinsam unternehmen werden.

Ganz zum Schluss möchte ich mich noch bei einem der wichtigsten Menschen in meinem Leben bedanken, meinem Freund Stefan. Ich bedanke mich, dass wir jeden Tag Seite an Seite verbringen dürfen und dass du deine Freunde und Brüder in Graz zurück lässt, um mich nach Linz zu begleiten.

11 Appendix

NMR-Spectra

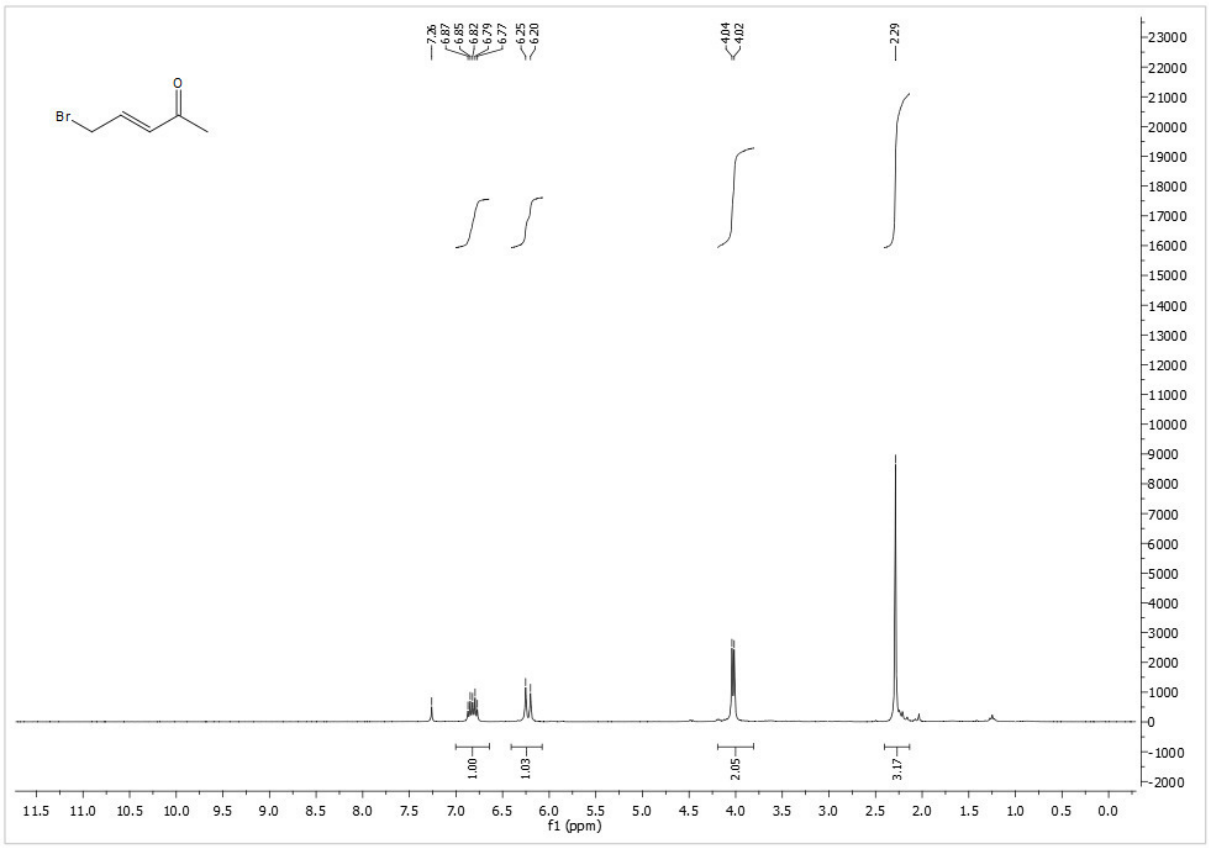

Figure 33: ^{1}H-NMR (300.36 MHz, $CDCl_3$) of compound **21**.

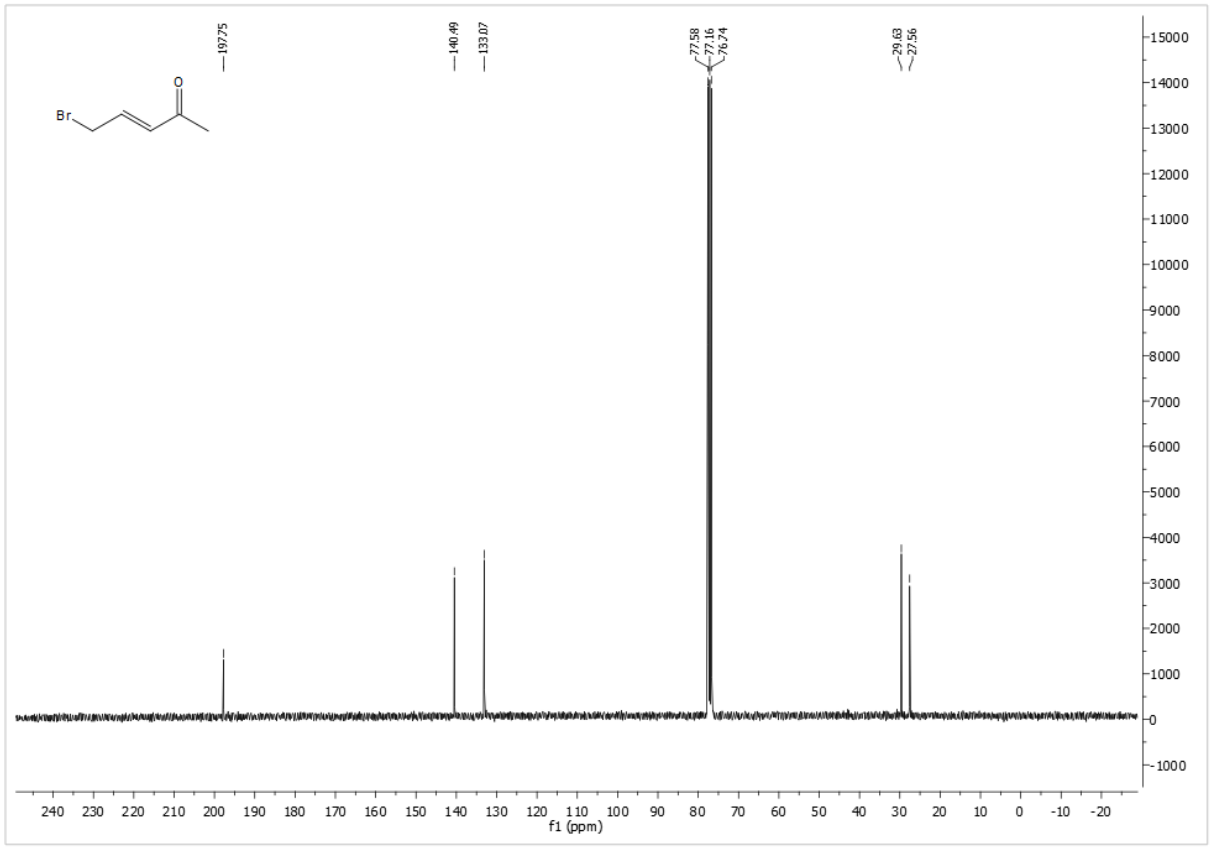

Figure 34: ^{13}C-NMR (75.53 MHz, $CDCl_3$) of compound **21**.

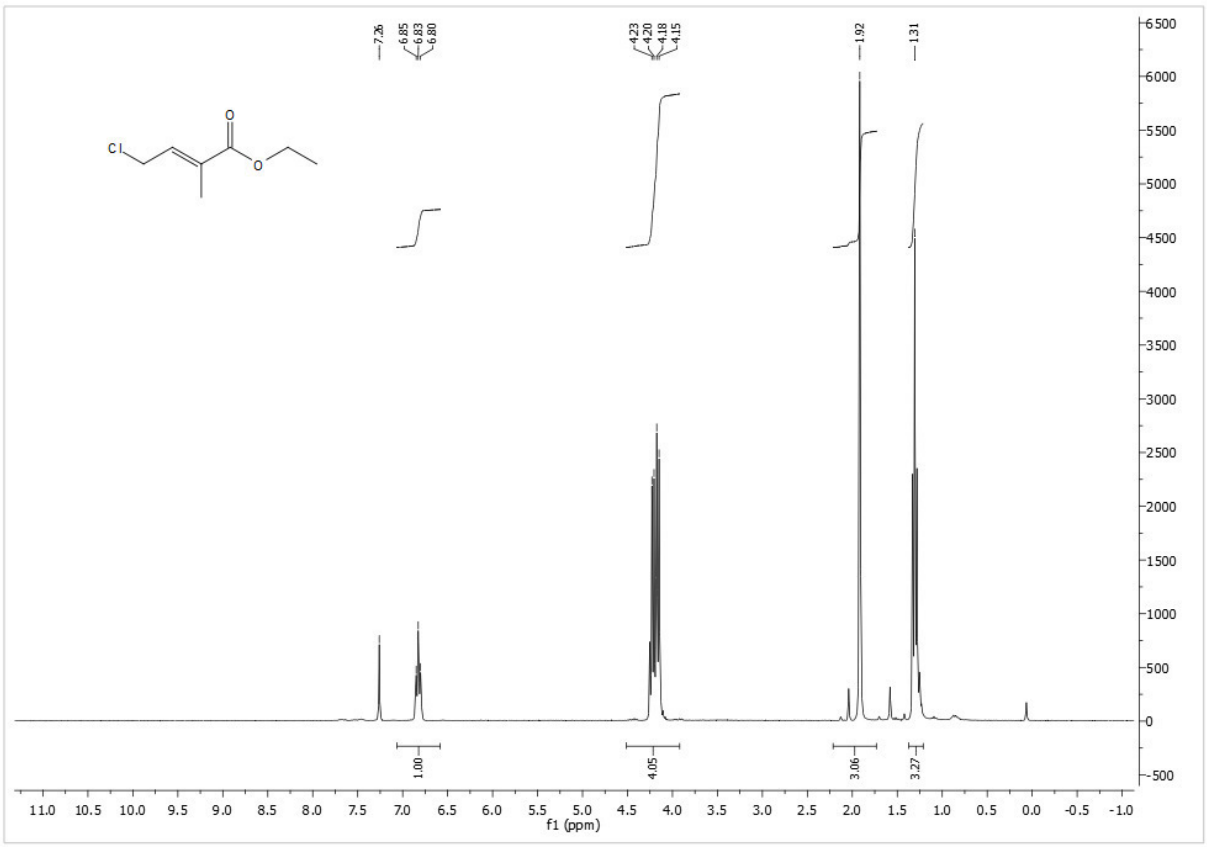

Figure 35: ^{1}H-NMR (300.36 MHz, $CDCl_3$) of compound **62**.

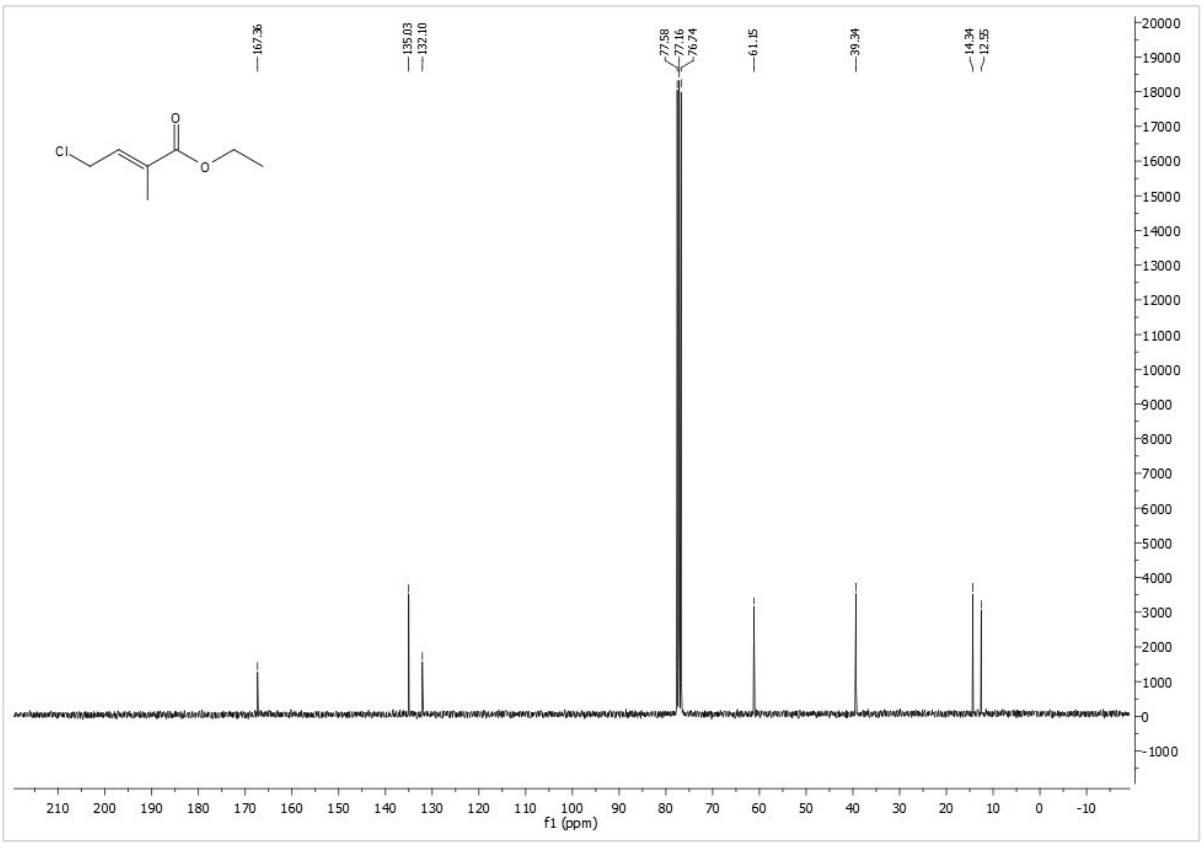

Figure 36: ^{13}C-NMR (75.53 MHz, $CDCl_3$) of compound **62**.

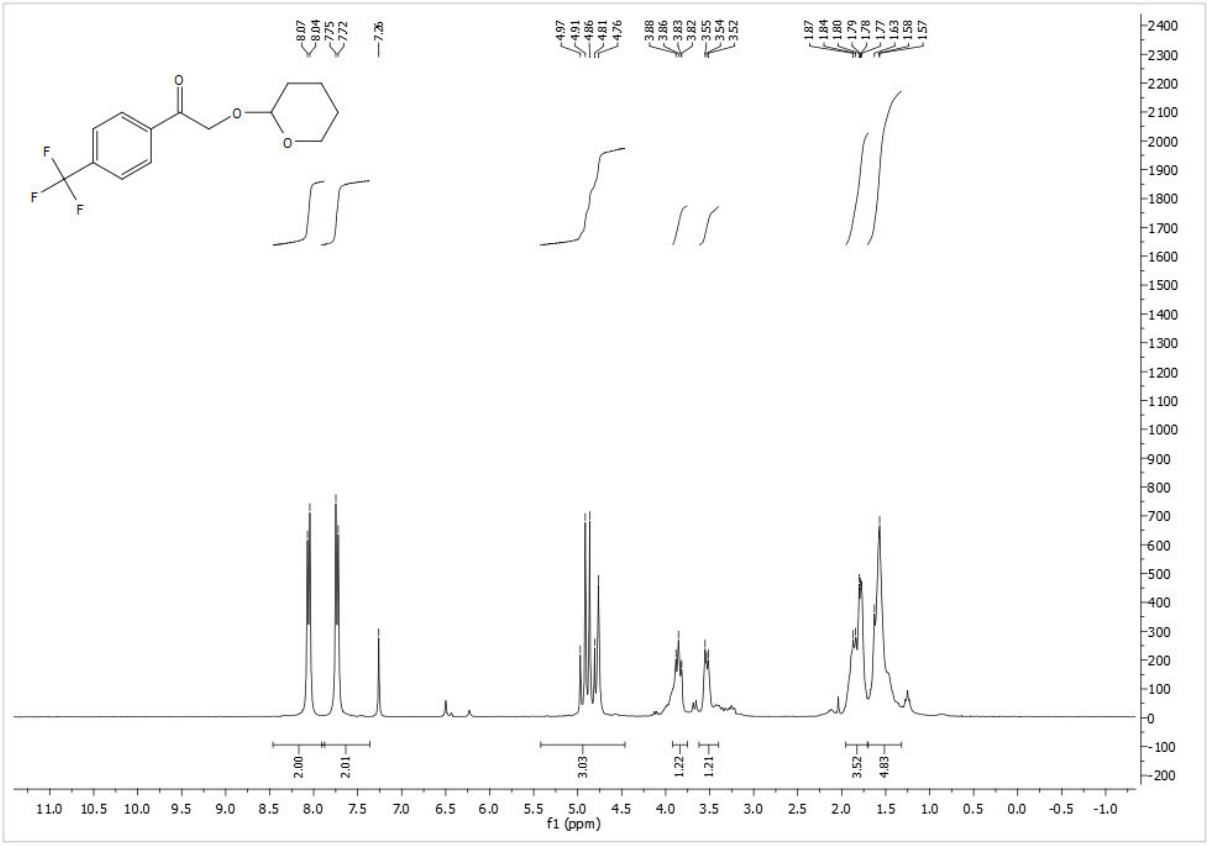

Figure 37: ^{1}H-NMR (300.36 MHz, $CDCl_3$) of compound **135**.

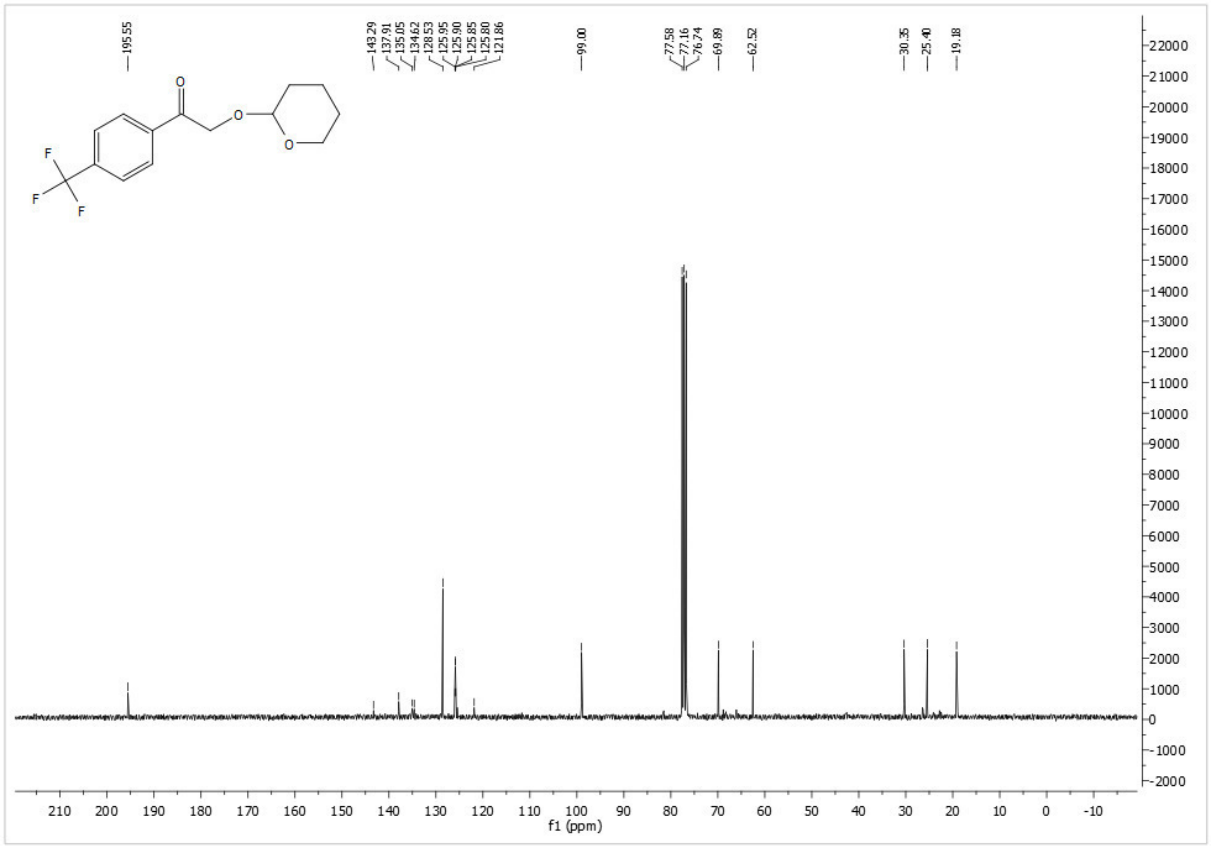

Figure 38: ^{13}C-NMR (75.53 MHz, $CDCl_3$) of compound **135**.

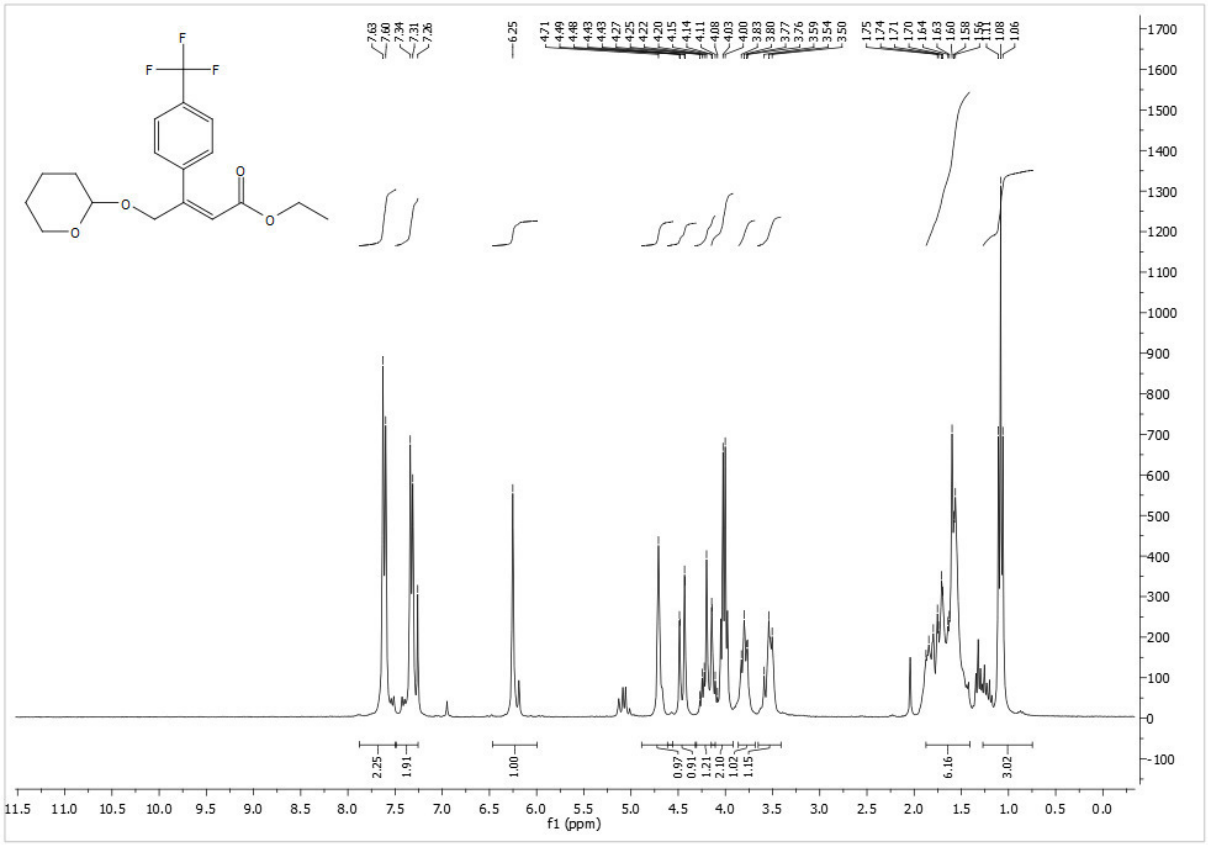

Figure 39: ^{1}H-NMR (300.36 MHz, $CDCl_3$) of compound **136**.

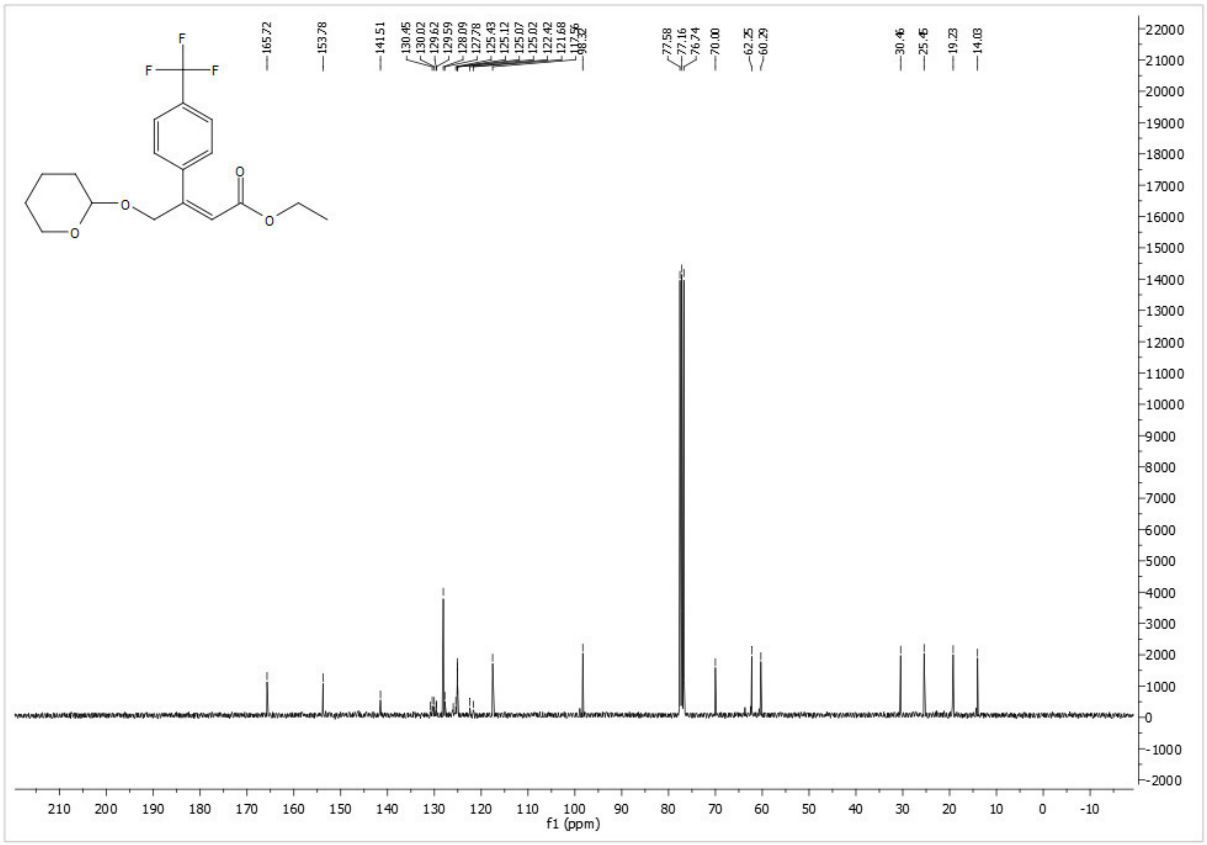

Figure 40: ^{13}C-NMR (75.53 MHz, $CDCl_3$) of compound **136**.

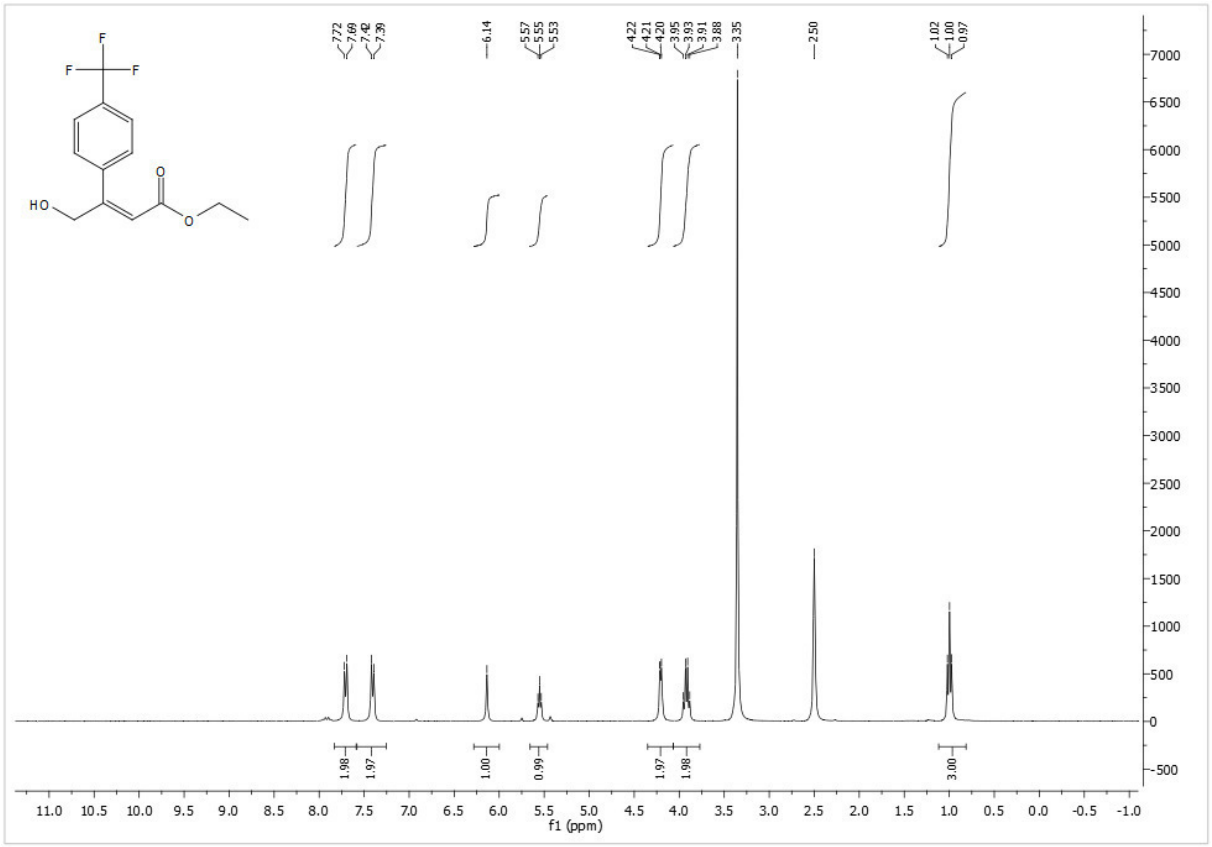

Figure 41: ^{1}H-NMR (300.36 MHz, $CDCl_3$) of compound **137**.

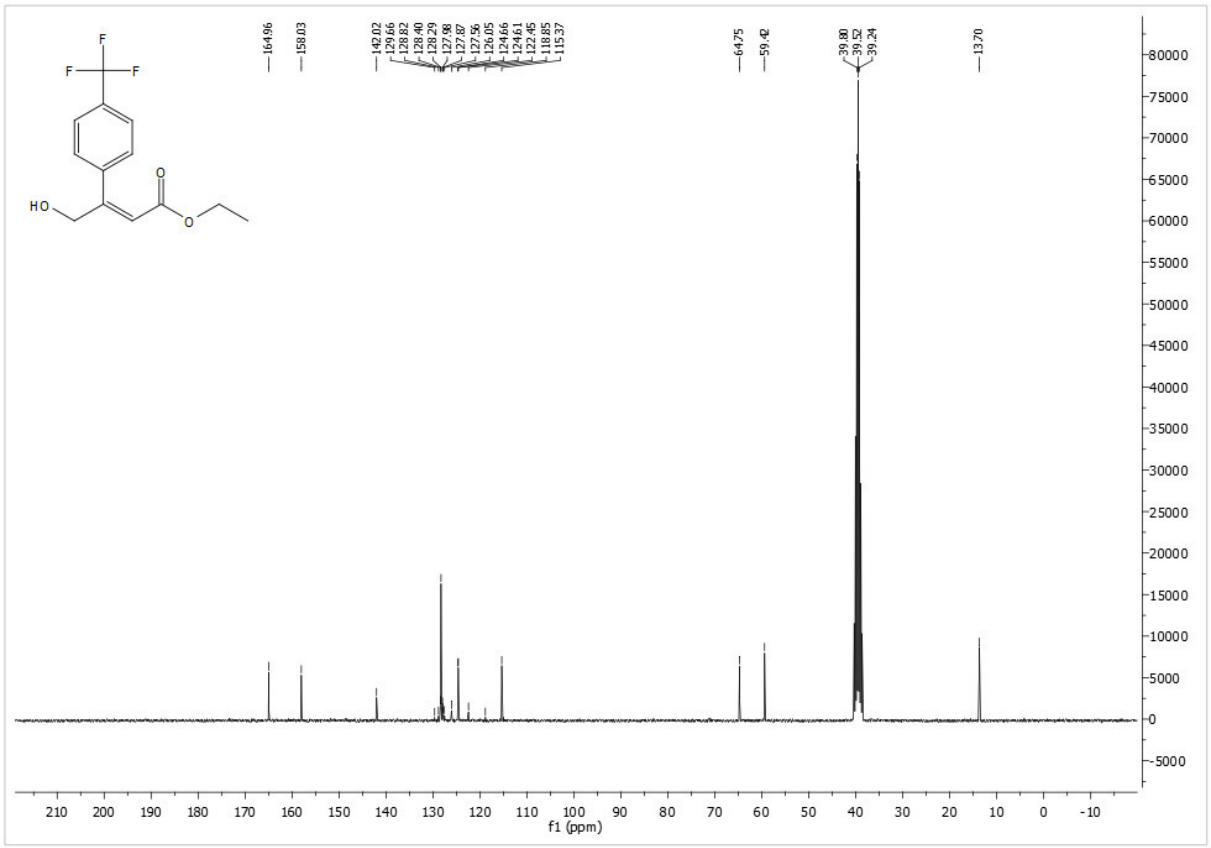

Figure 42: ^{13}C-NMR (75.53 MHz, $CDCl_3$) of compound **137**.

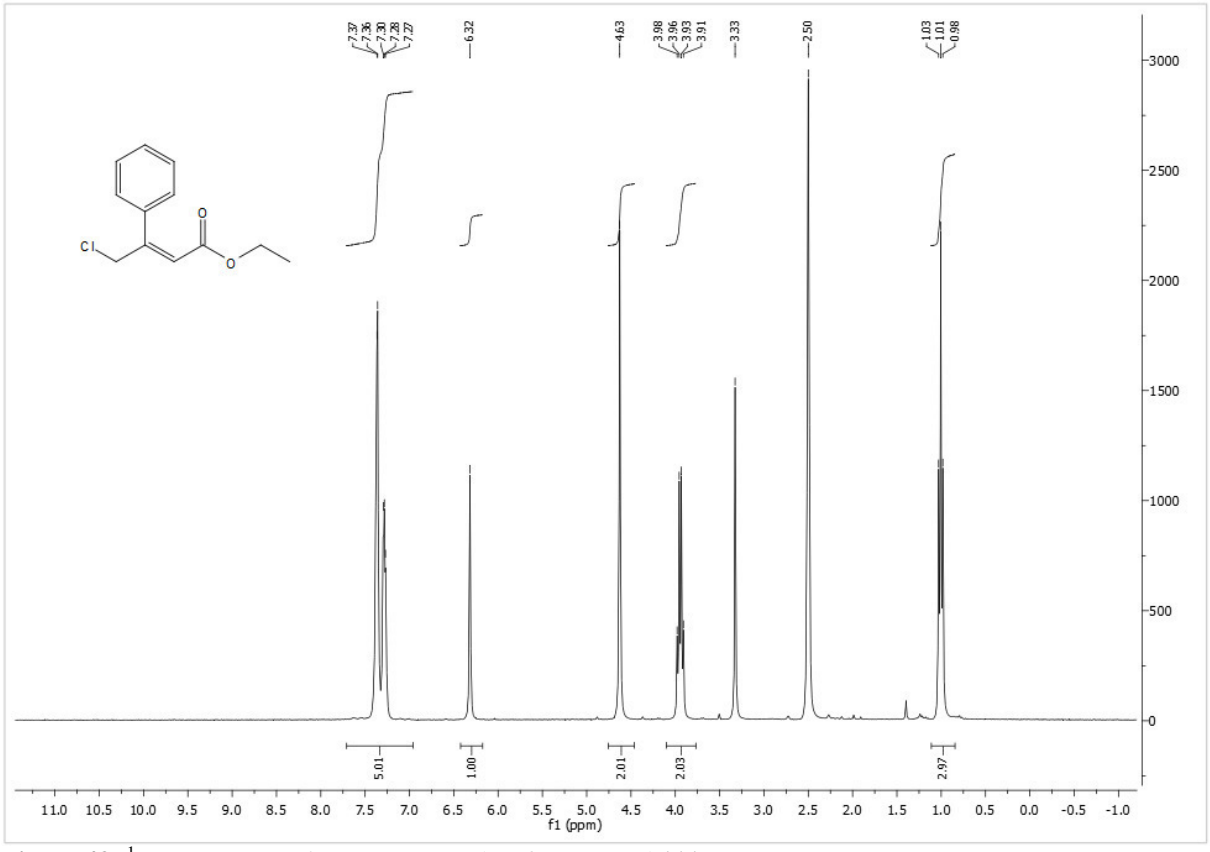

Figure 43: ^{1}H-NMR (300.36 MHz, DMSO-d_6) of compound **111**.

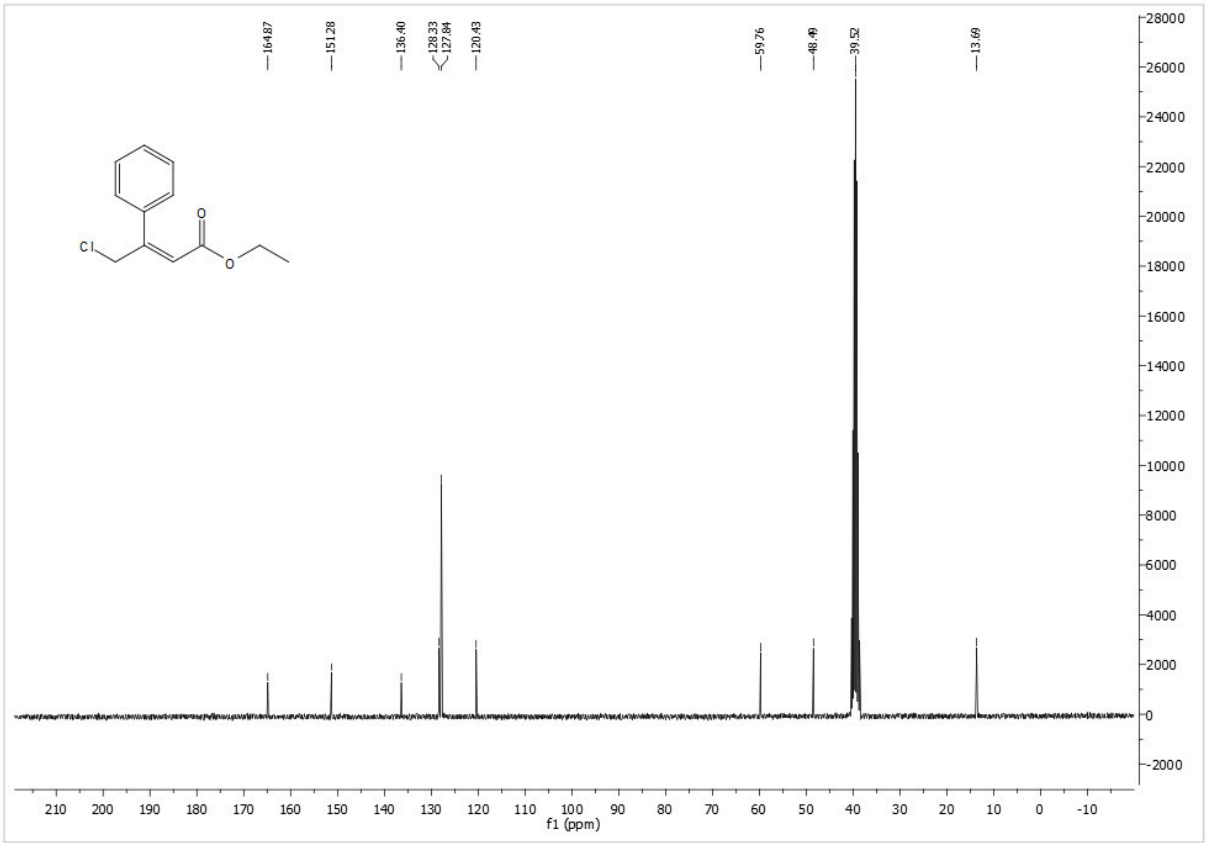

Figure 44: ^{13}C-NMR (75.53 MHz, DMSO-d_6) of compound **111**.

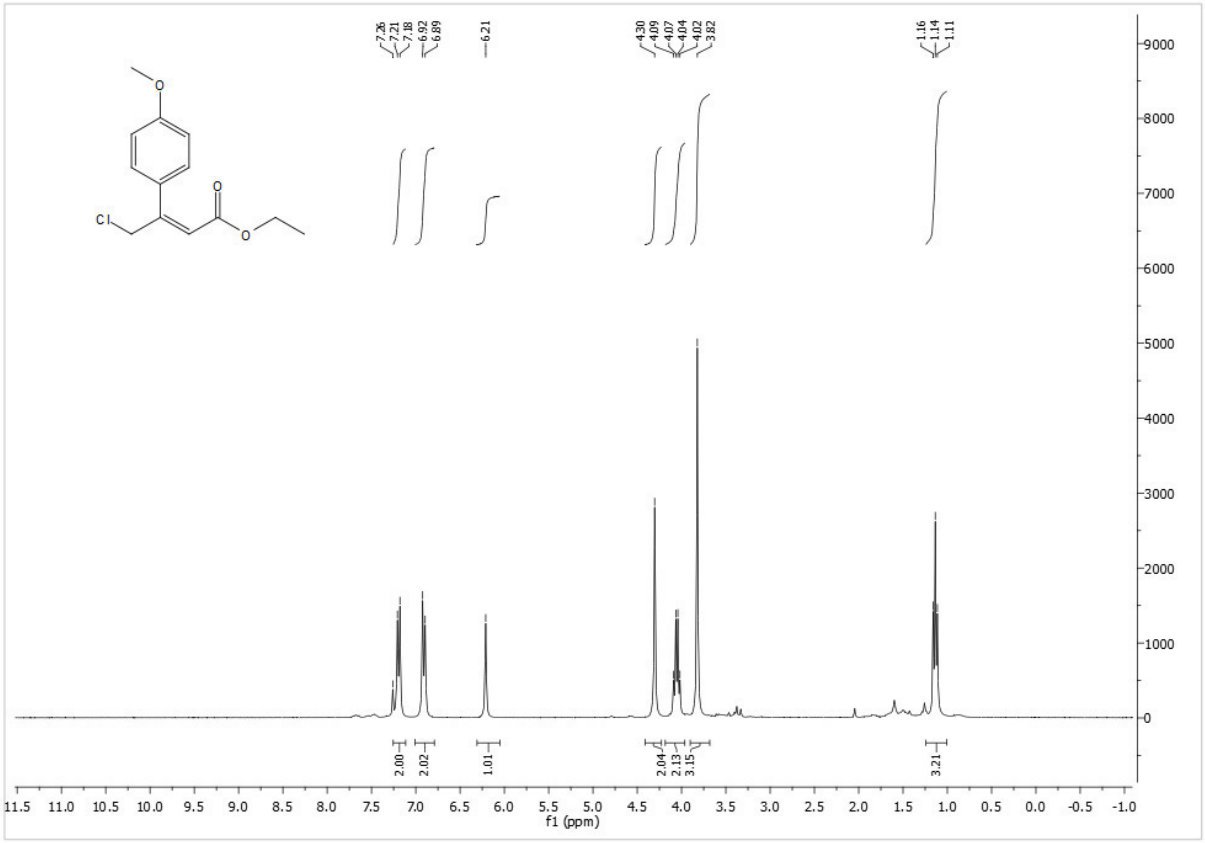

Figure 45: ^{1}H-NMR (300.36 MHz, $CDCl_3$) of compound **131**.

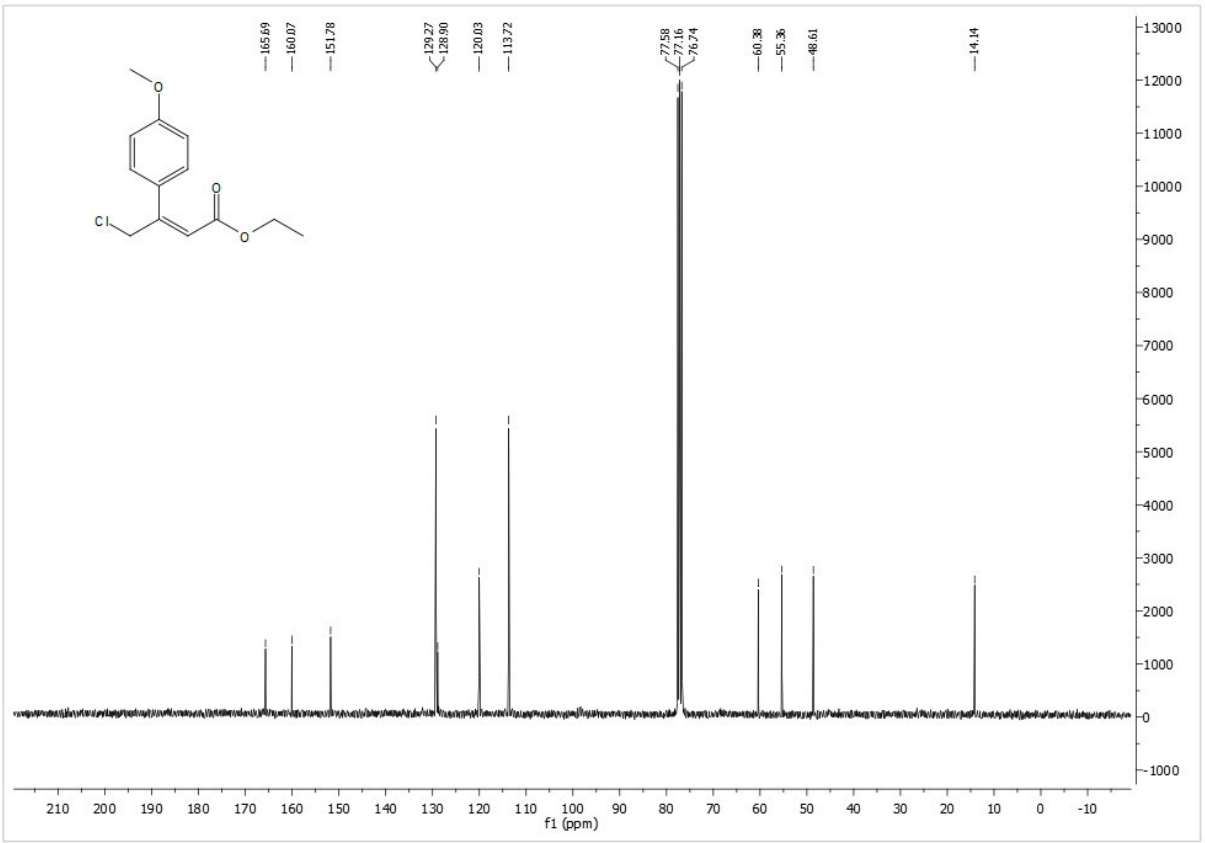

Figure 46: ^{13}C-NMR (75.53 MHz, $CDCl_3$) of compound **131**.

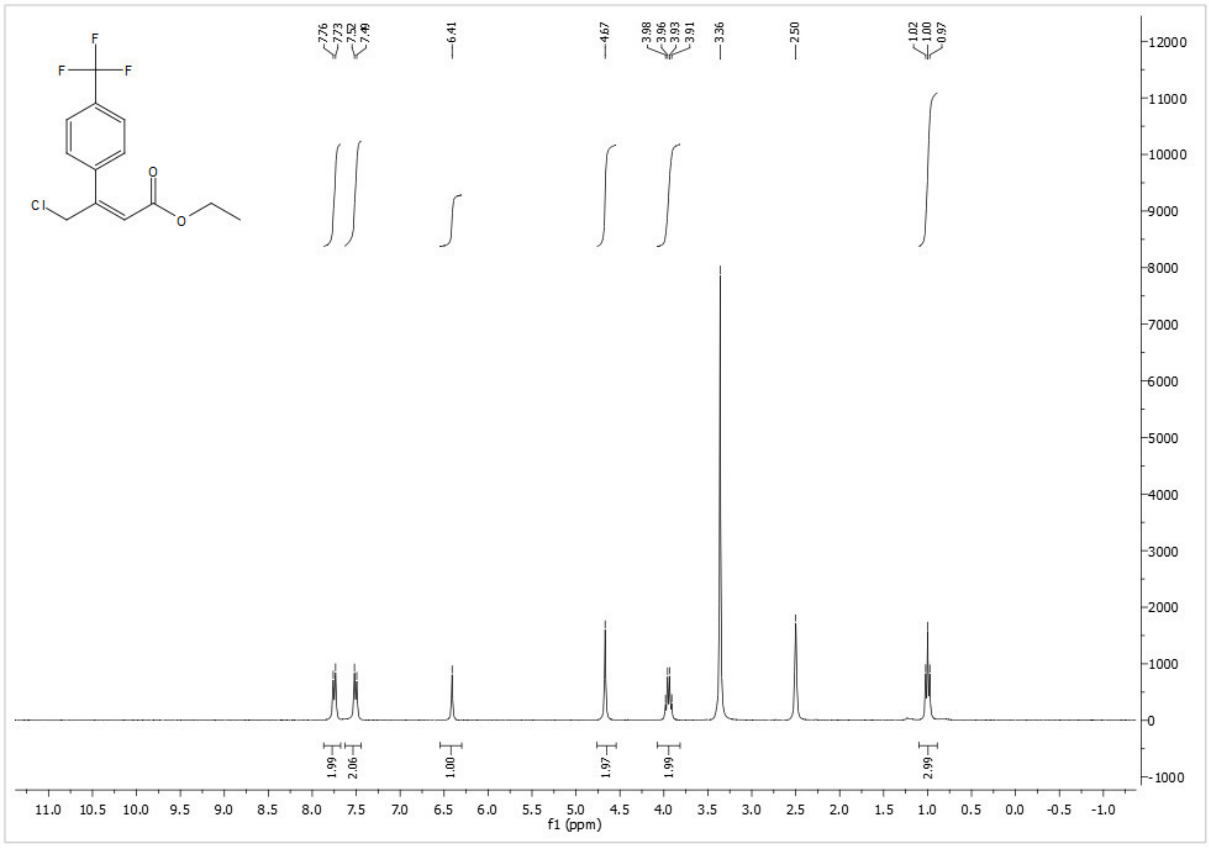

Figure 47: ^{1}H-NMR (300.36 MHz, DMSO-d_6) of compound **138**.

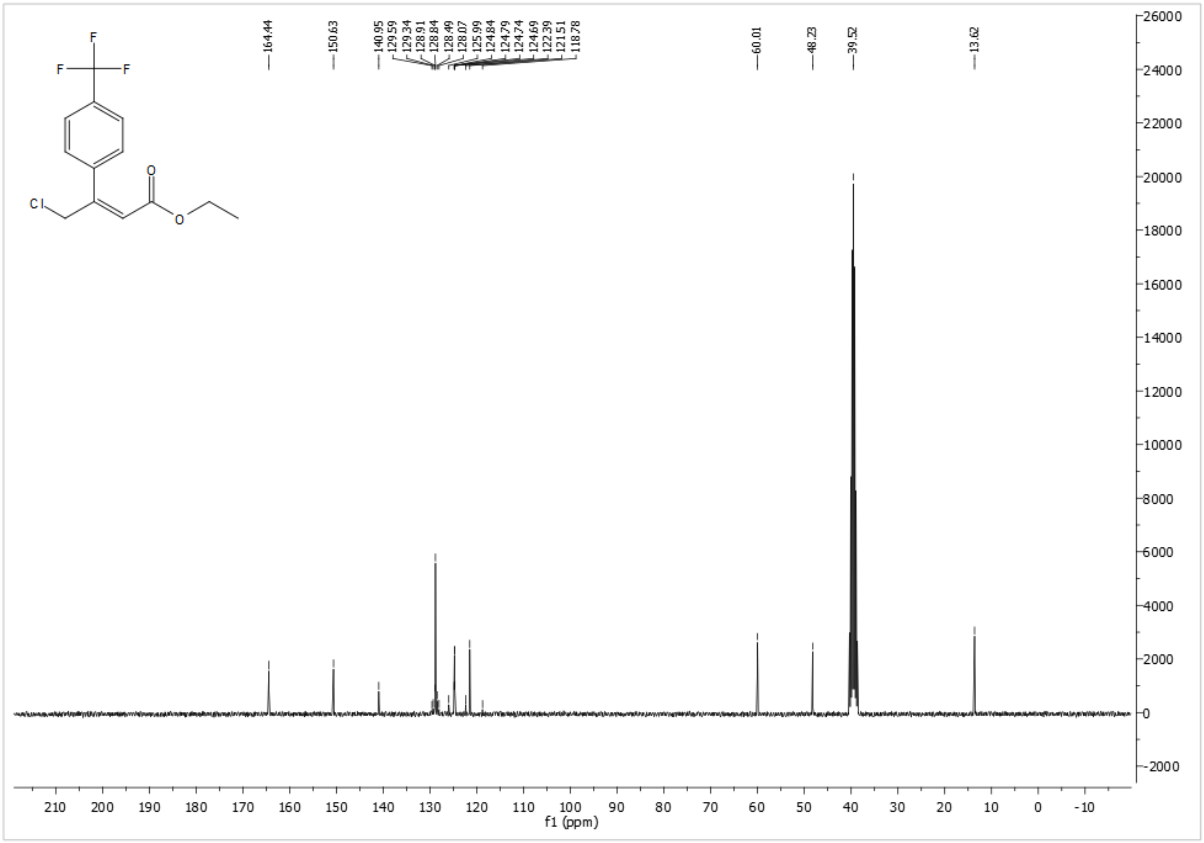

Figure 48: ^{13}C-NMR (75.53 MHz, DMSO-d_6) of compound **138**.

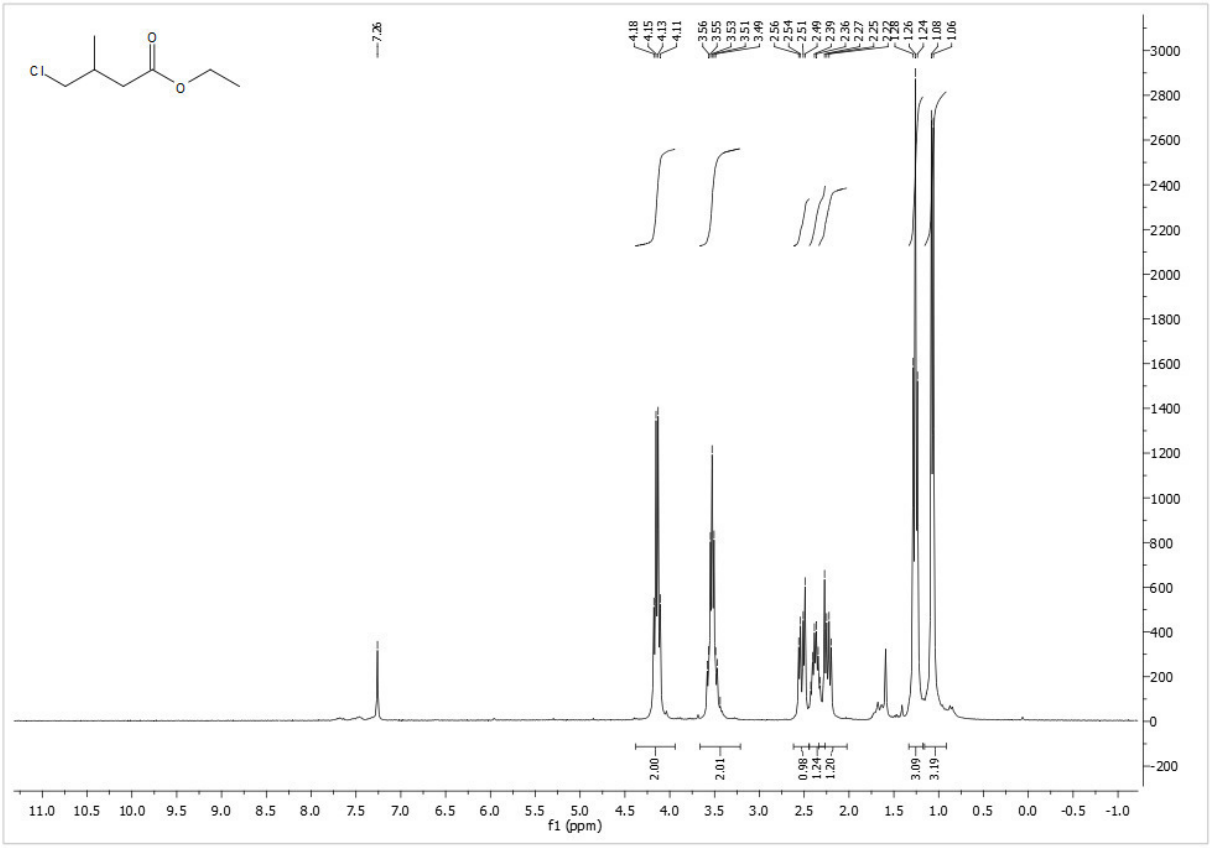

Figure 49: ^{1}H-NMR (300.36 MHz, $CDCl_3$) of compound **85**.

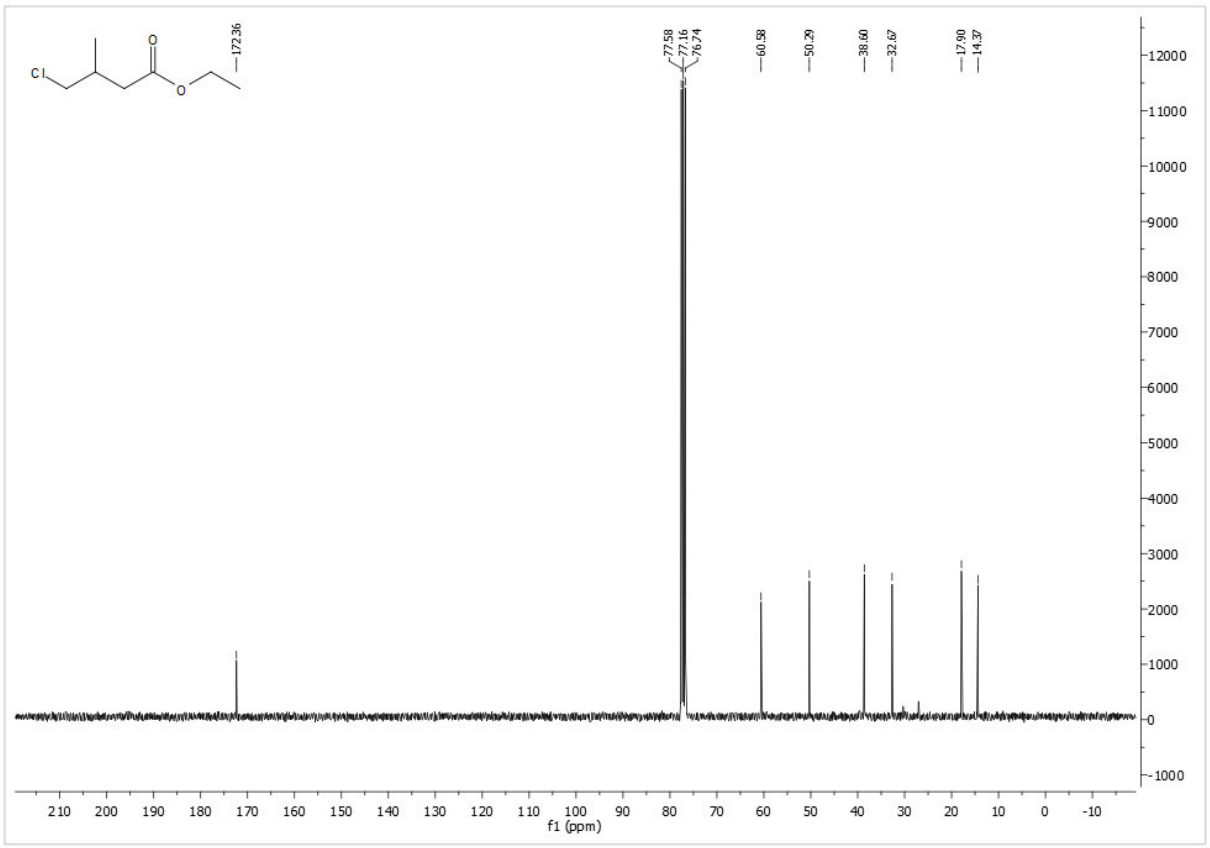

Figure 50: ^{13}C-NMR (75.53 MHz, $CDCl_3$) of compound **85**.

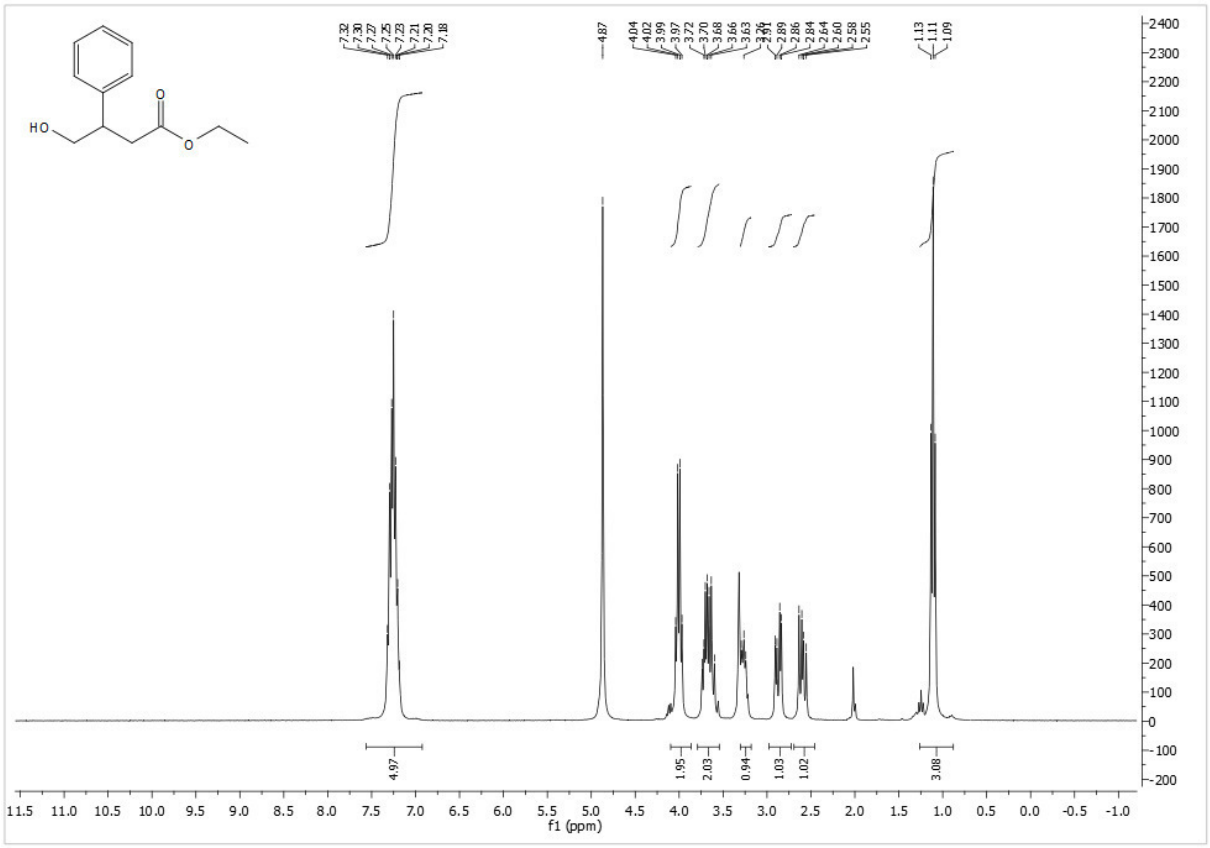

Figure 51: [1]H-NMR (300.36 MHz, MeOD) of compound **120**.

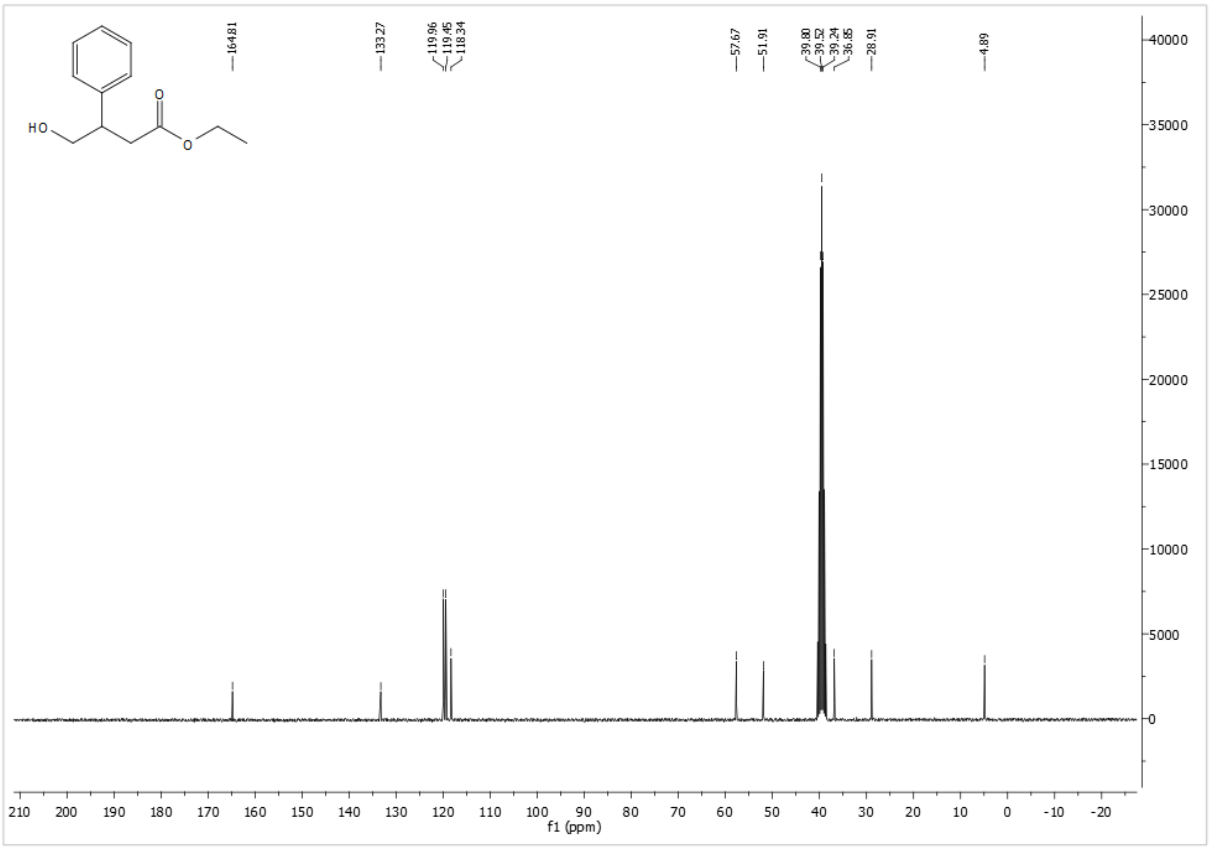

Figure 52: [13]C-NMR (75.53 MHz, MeOD) of compound **120**.

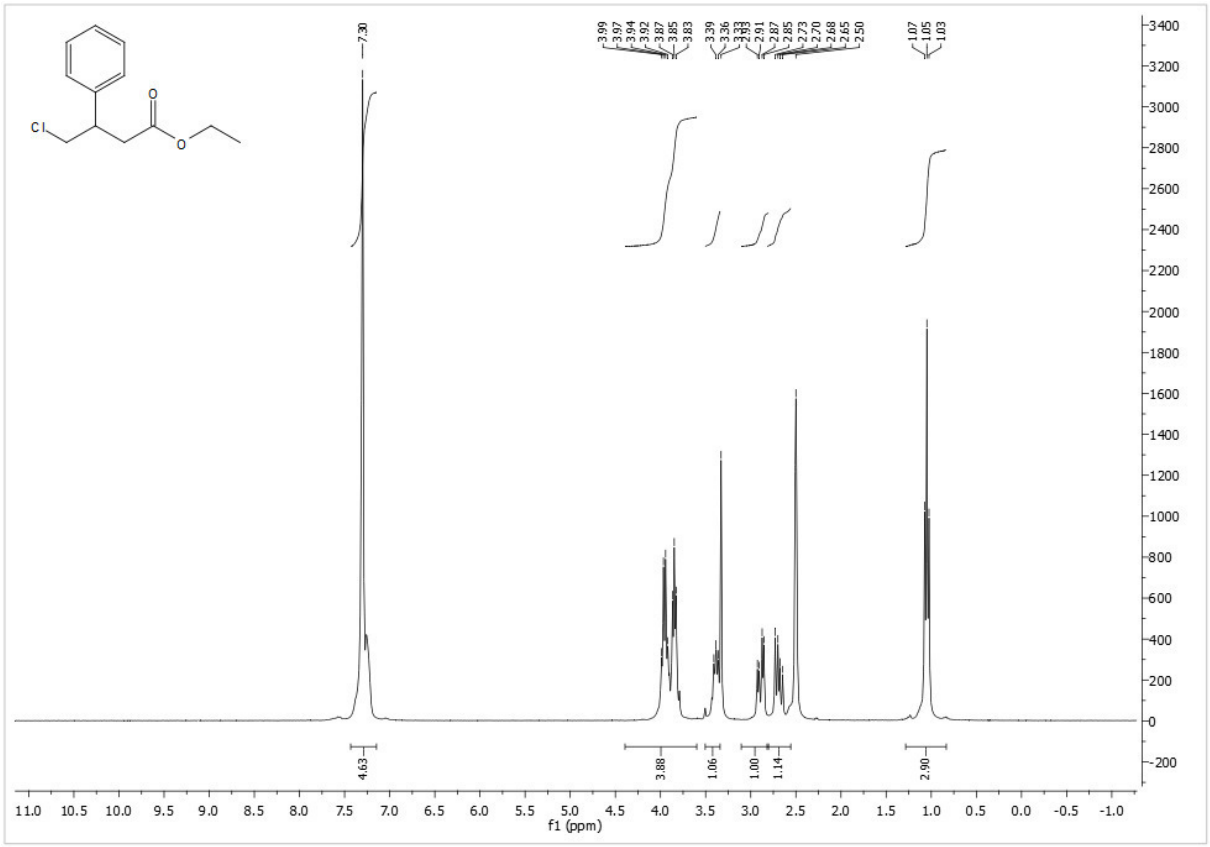

Figure 53: ^{1}H-NMR (300.36 MHz, DMSO-d_6) of compound **121**.

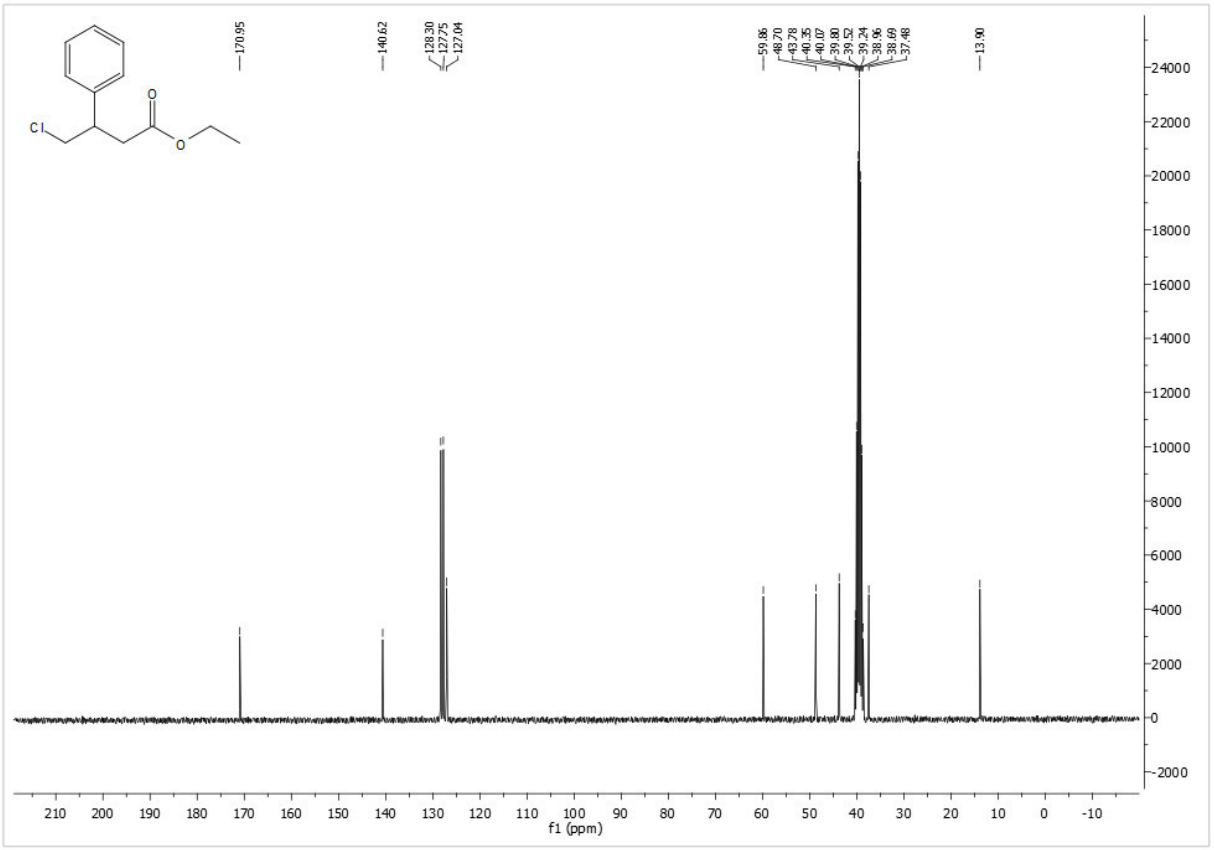

Figure 54: ^{13}C-NMR (75.53 MHz, DMSO-d_6) of compound **121**.

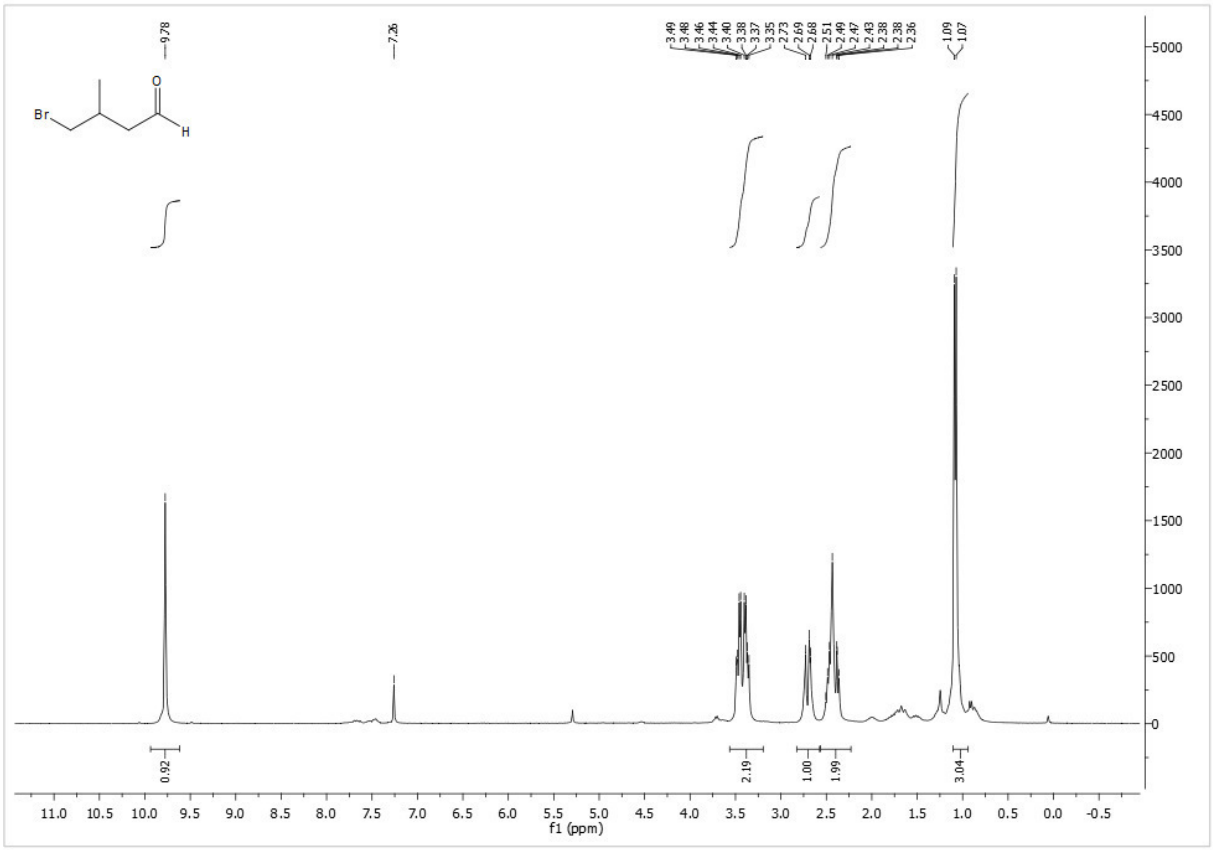

Figure 55: ^{1}H-NMR (300.36 MHz, $CDCl_3$) of compound **89**.

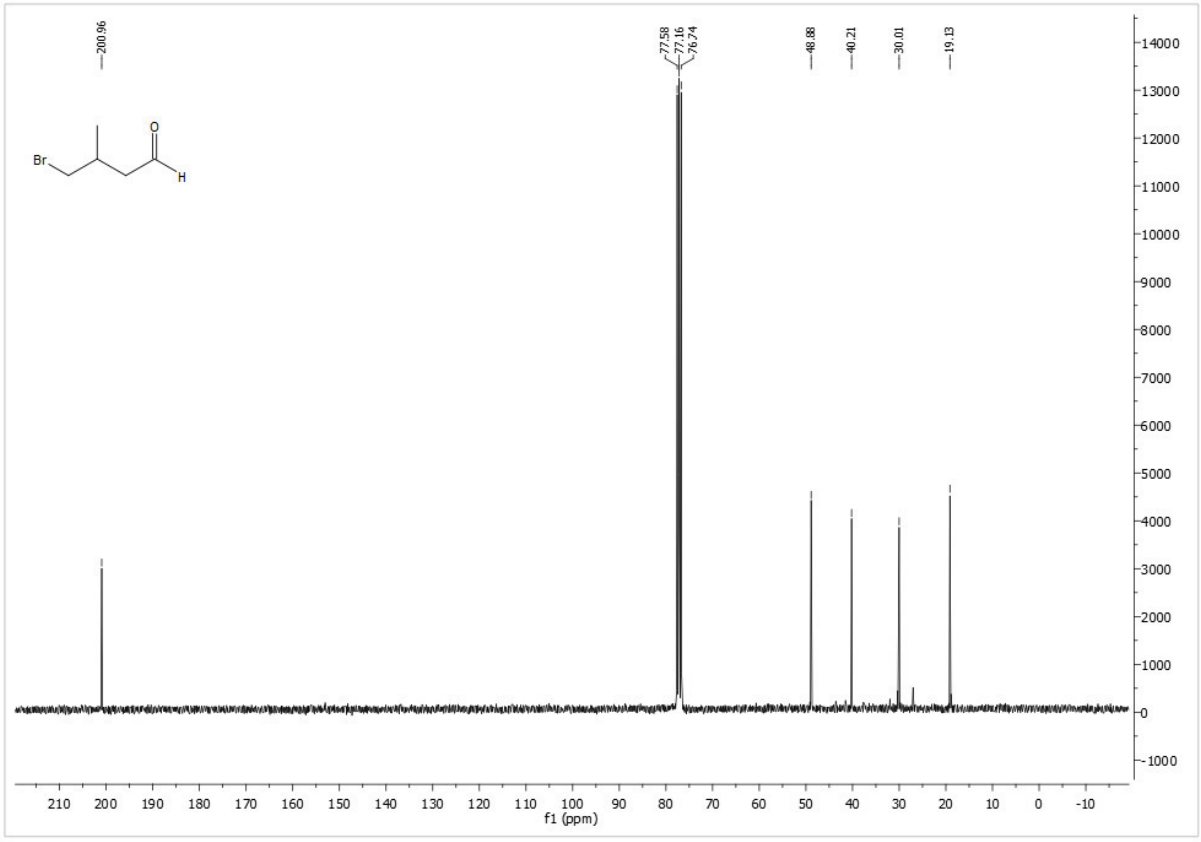

Figure 56: ^{13}C-NMR (75.53 MHz, $CDCl_3$) of compound **89**.

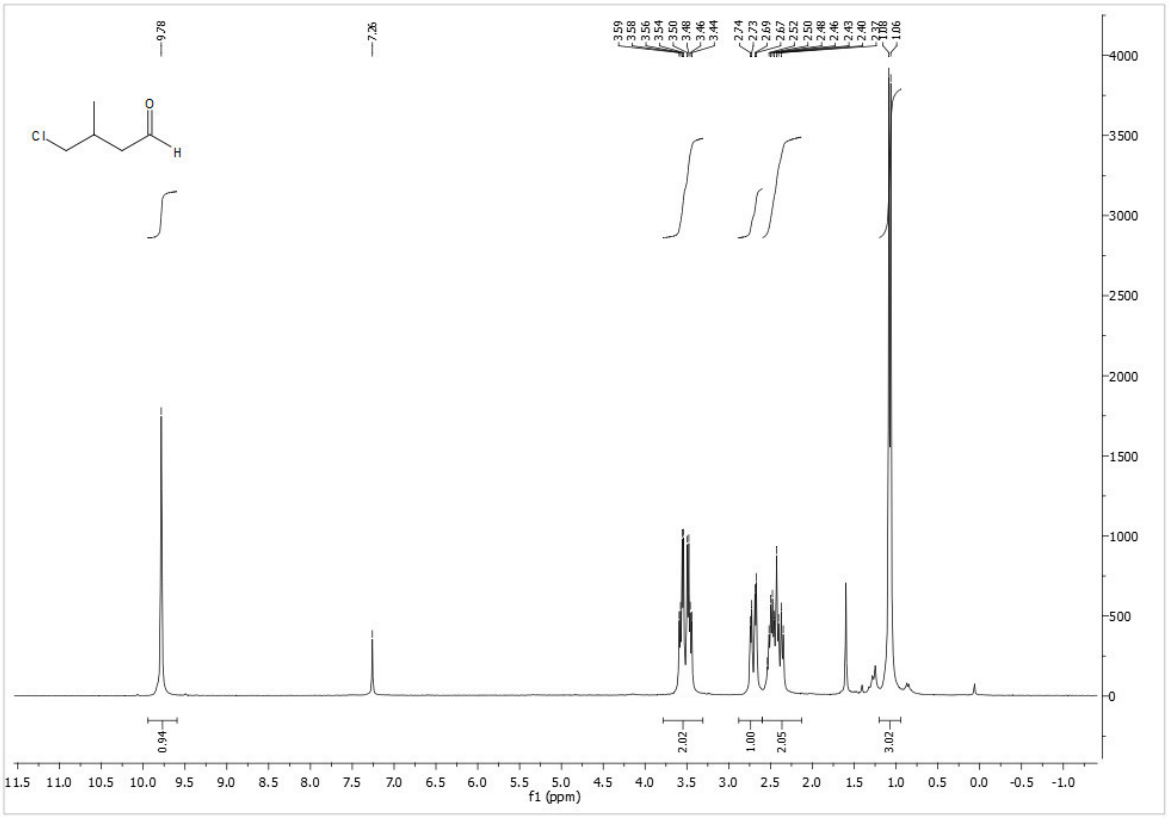

Figure 57: ^{1}H-NMR (300.36 MHz, $CDCl_3$) of compound **74**.

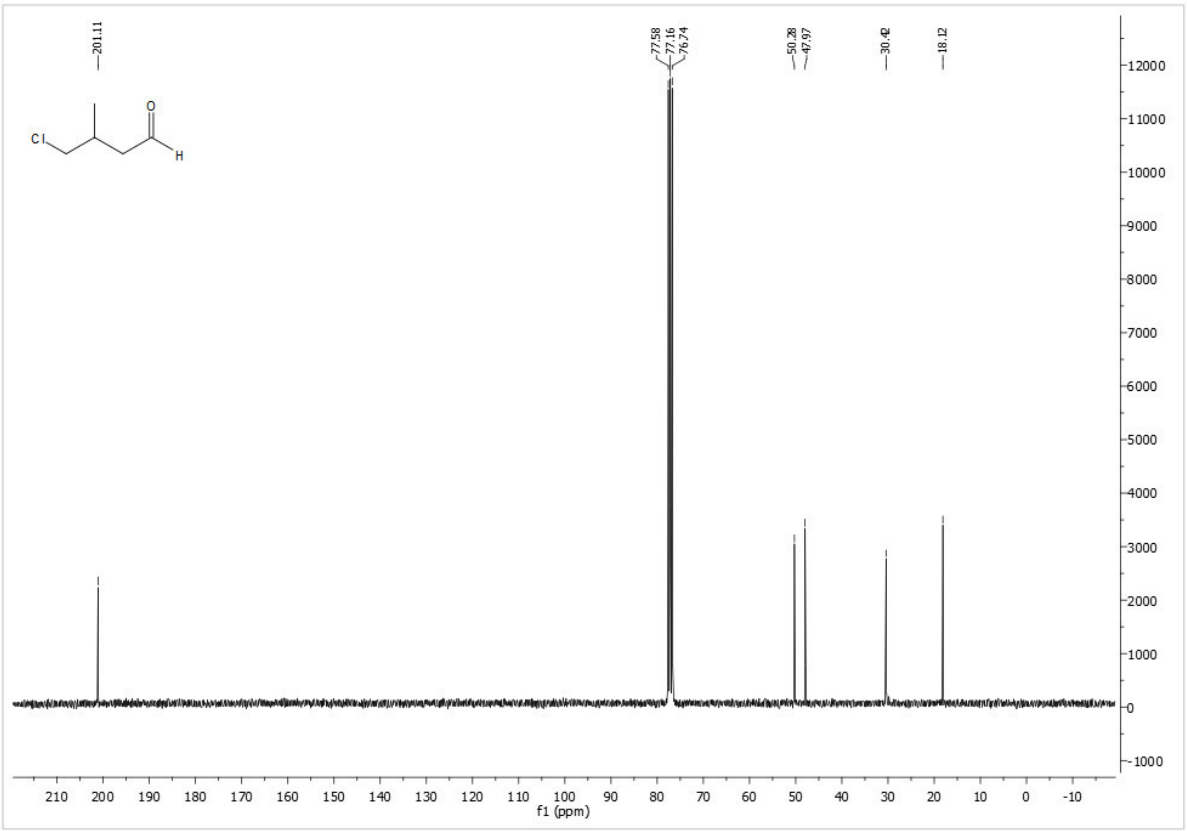

Figure 58: ^{13}C-NMR (75.53 MHz, $CDCl_3$) of compound **74**.

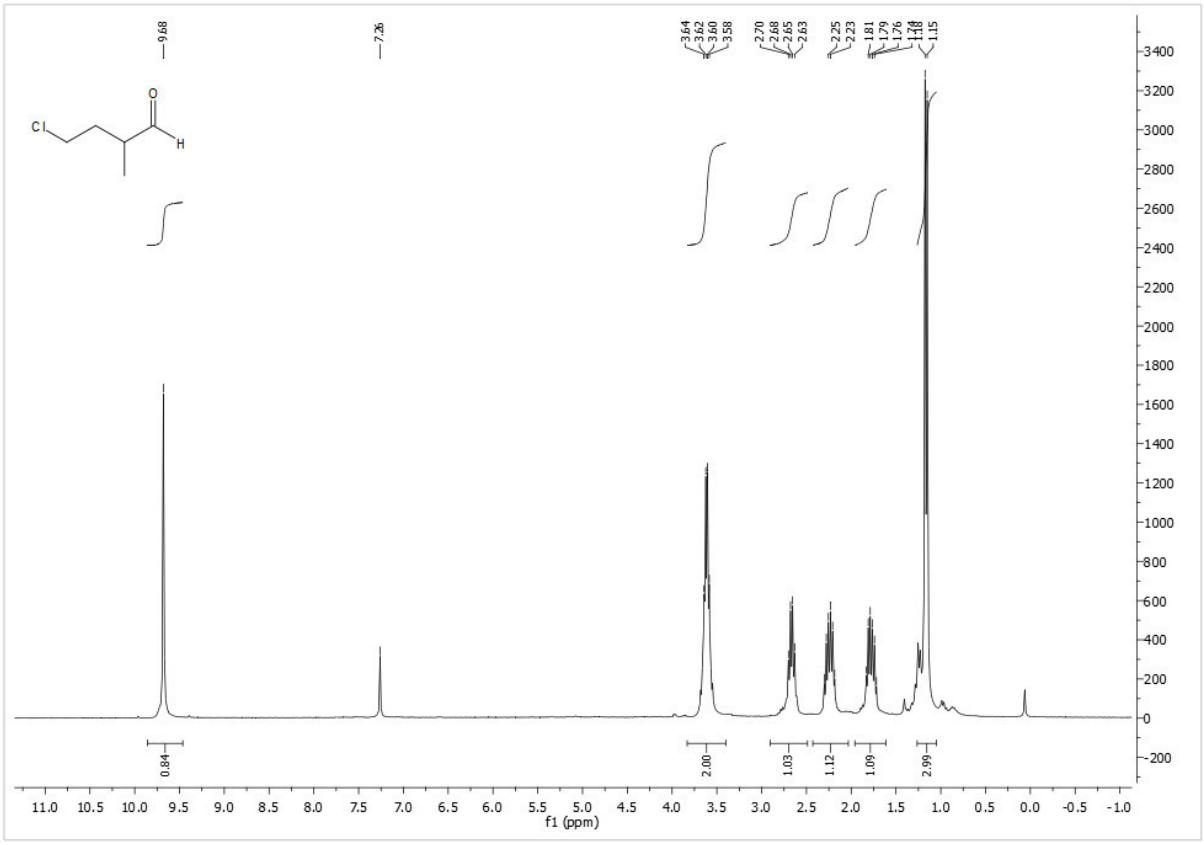

Figure 59: ^{1}H-NMR (300.36 MHz, $CDCl_3$) of compound **64**.

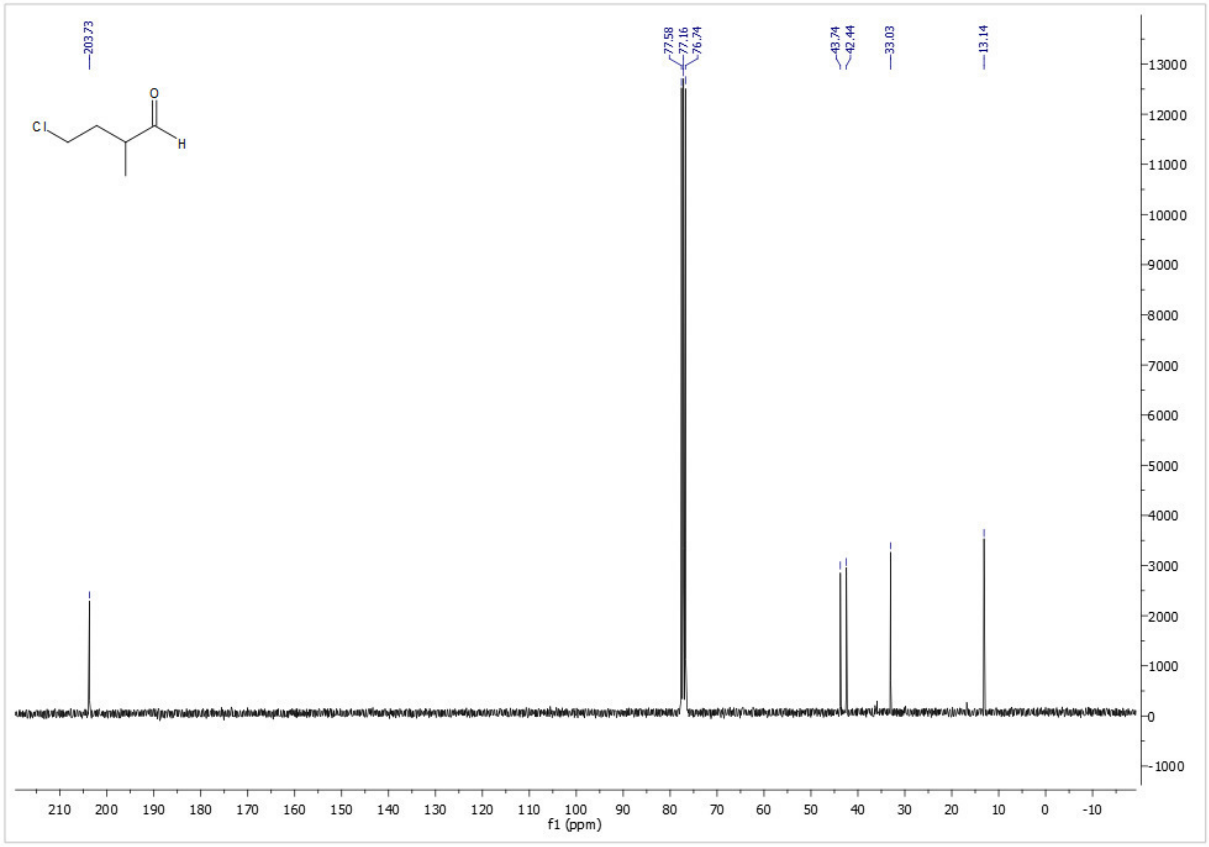

Figure 60: ^{13}C-NMR (75.53 MHz, $CDCl_3$) of compound **64**.

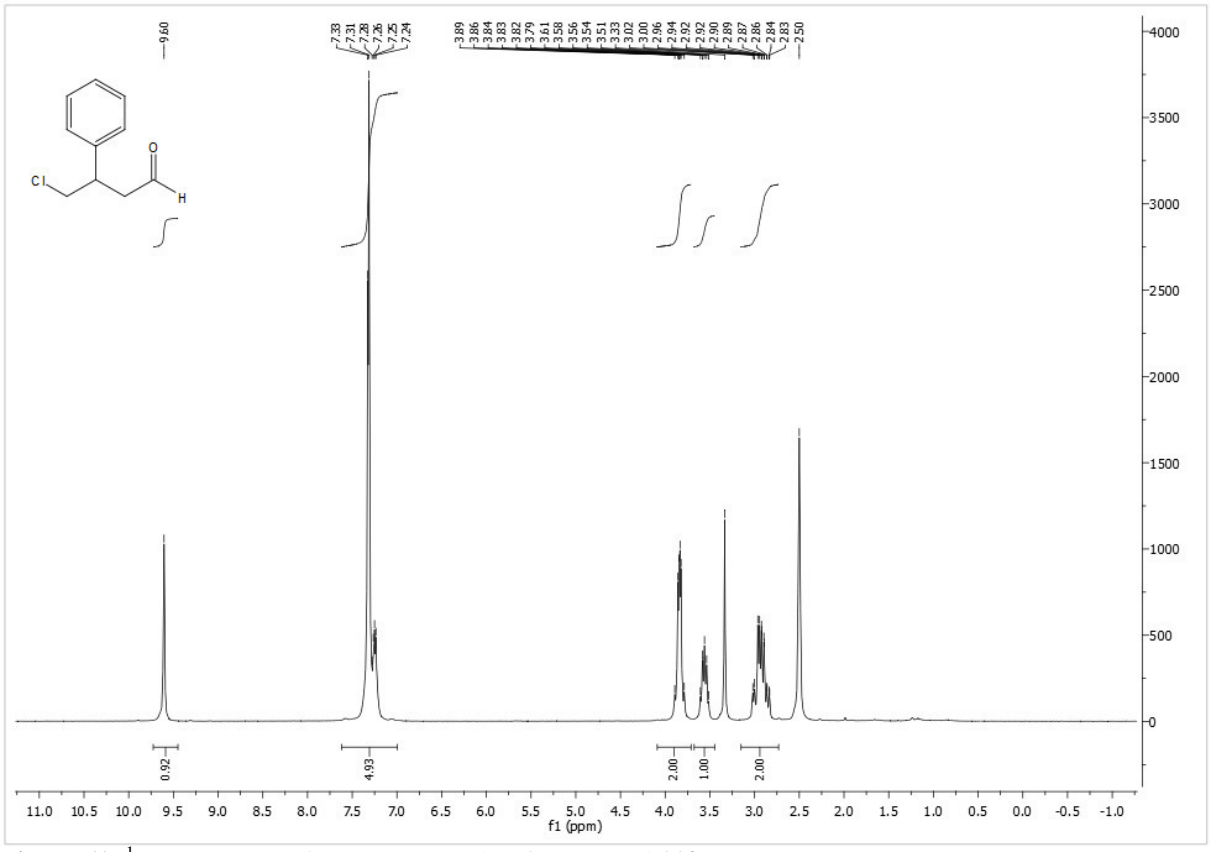

Figure 61: ^{1}H-NMR (300.36 MHz, DMSO-d_6) of compound **113**.

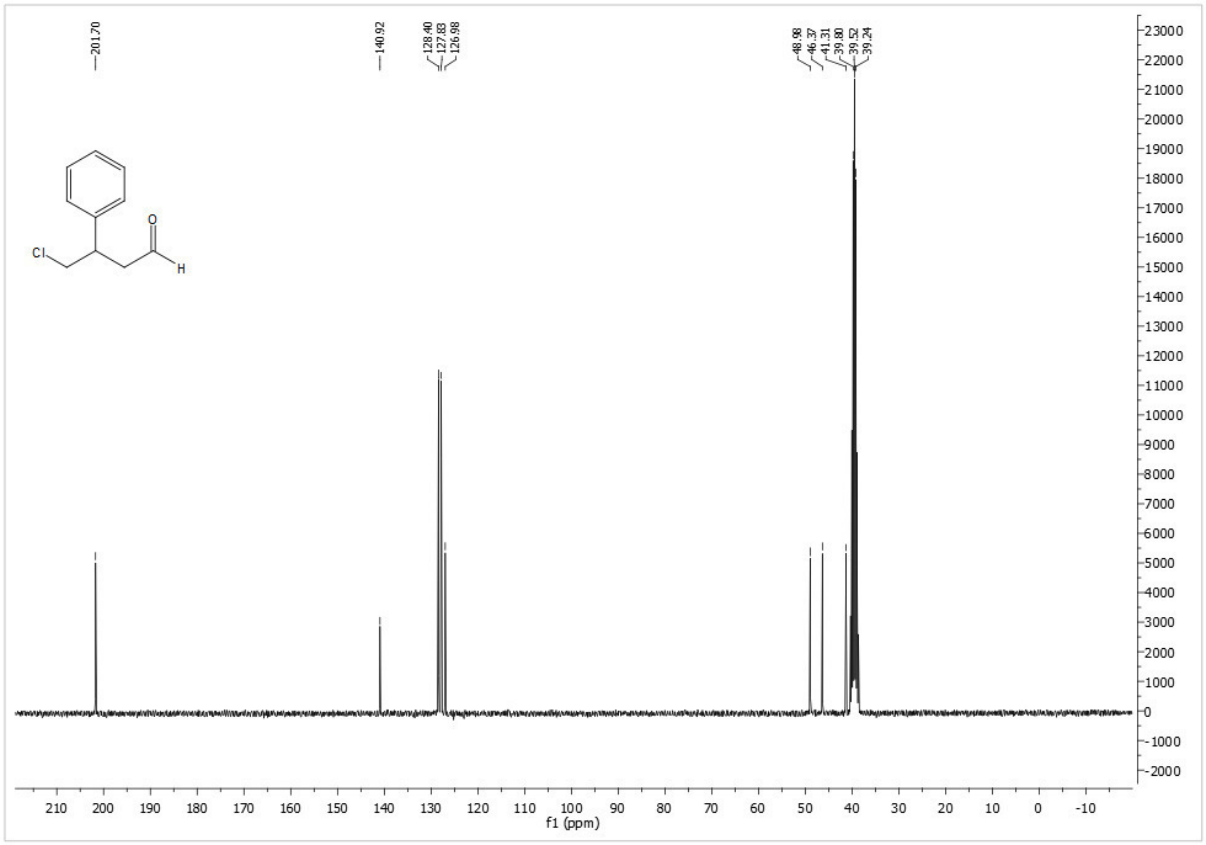

Figure 62: ^{13}C-NMR (75.53 MHz, DMSO-d_6) of compound **113**.

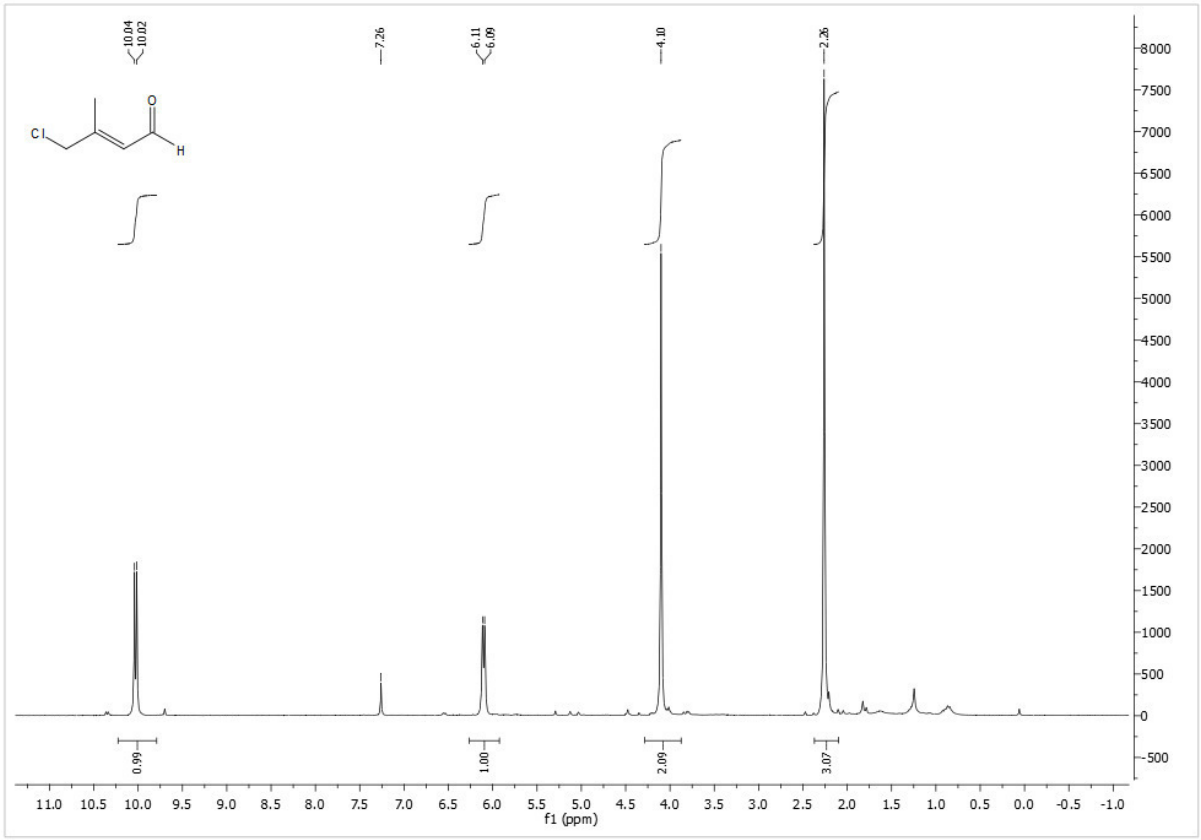

Figure 63: ^{1}H-NMR (300.36 MHz, $CDCl_3$) of compound **27**.

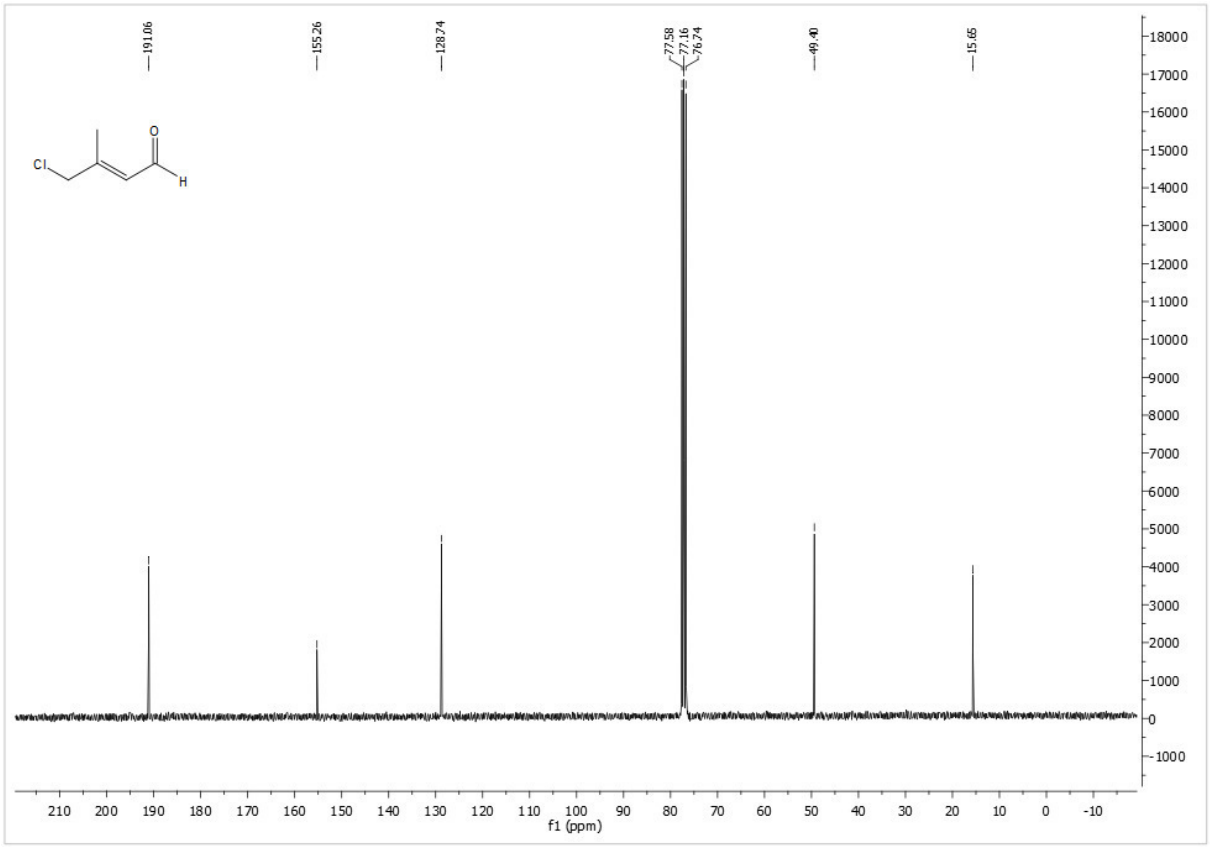

Figure 64: ^{13}C-NMR (75.53 MHz, $CDCl_3$) of compound **27**.

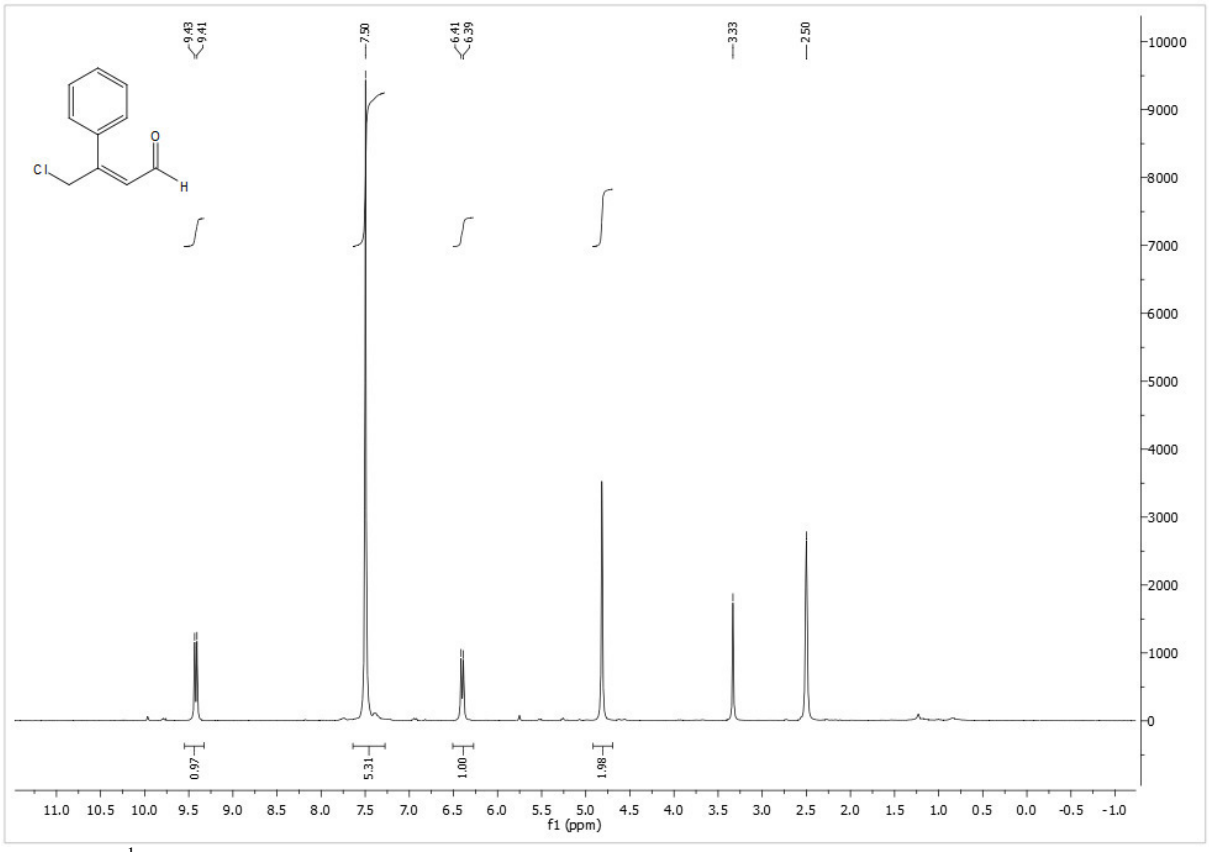

Figure 65: ^{1}H-NMR (300.36 MHz, DMSO-d_6) of compound **31**.

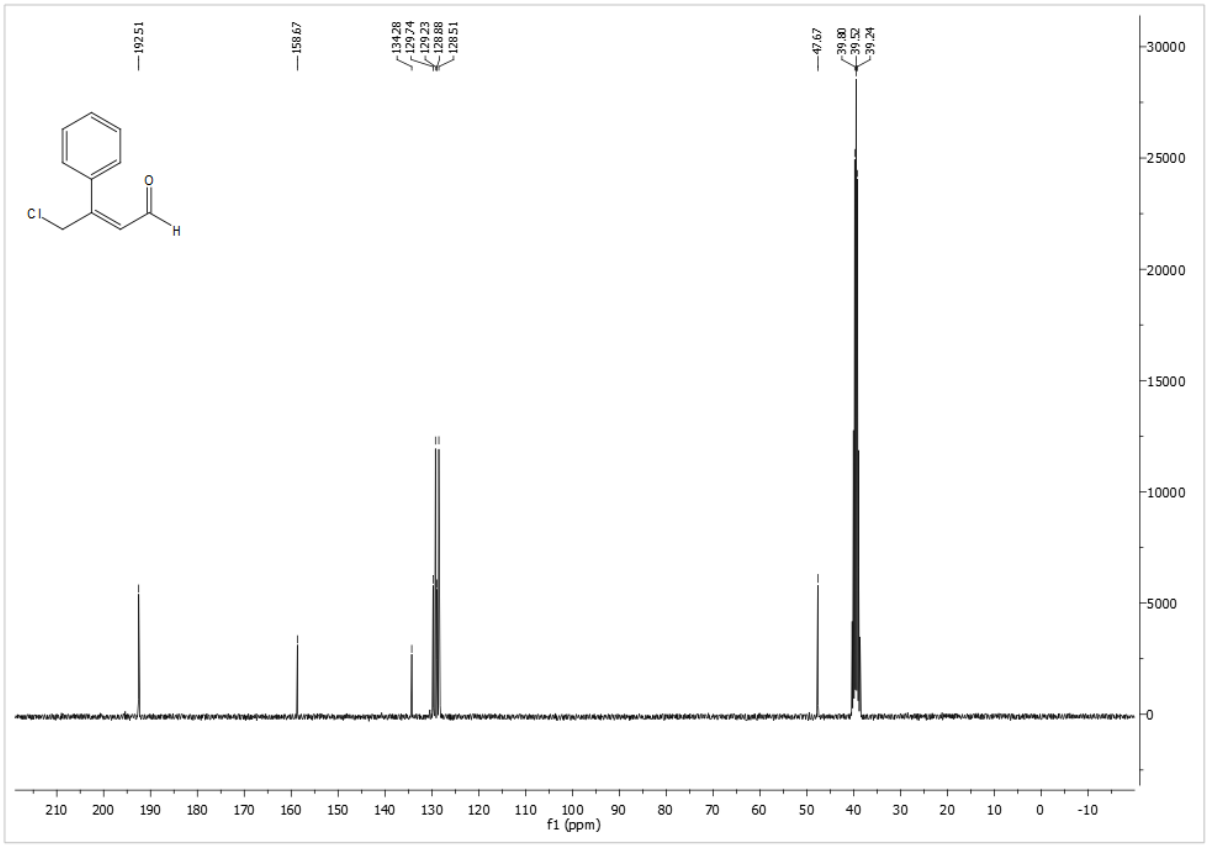

Figure 66: ^{13}C-NMR (75.53 MHz, DMSO-d_6) of compound **31**.

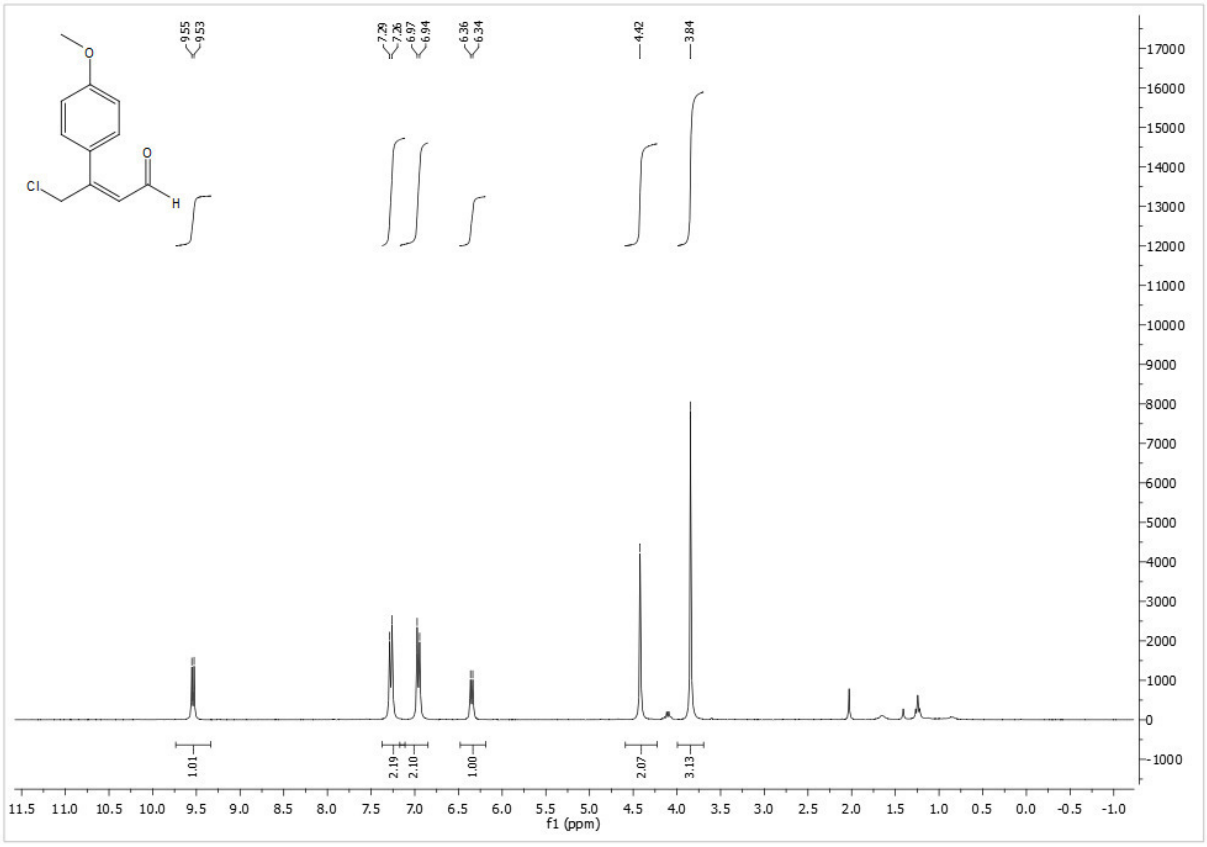

Figure 67: ^{1}H-NMR (300.36 MHz, $CDCl_3$) of compound **33**.

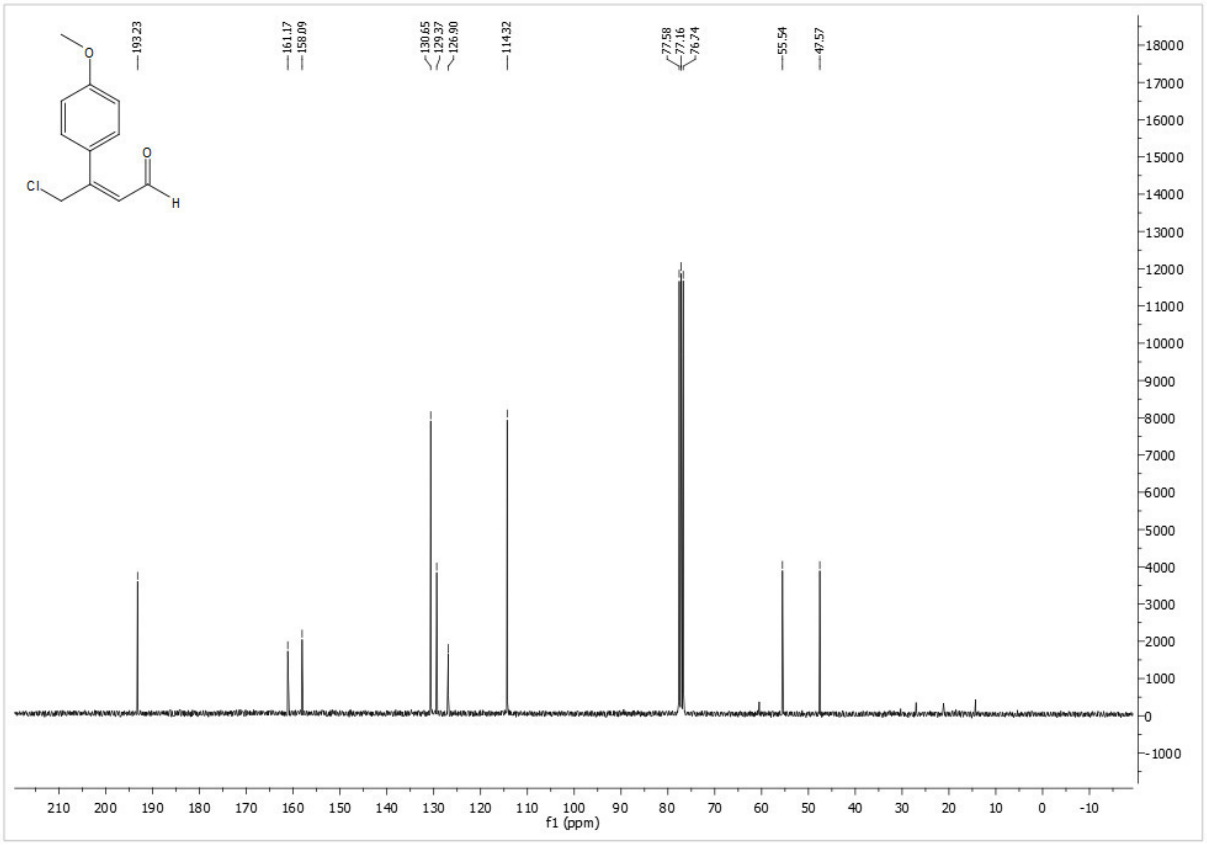

Figure 68: ^{13}C-NMR (75.53 MHz, $CDCl_3$) of compound **33**.

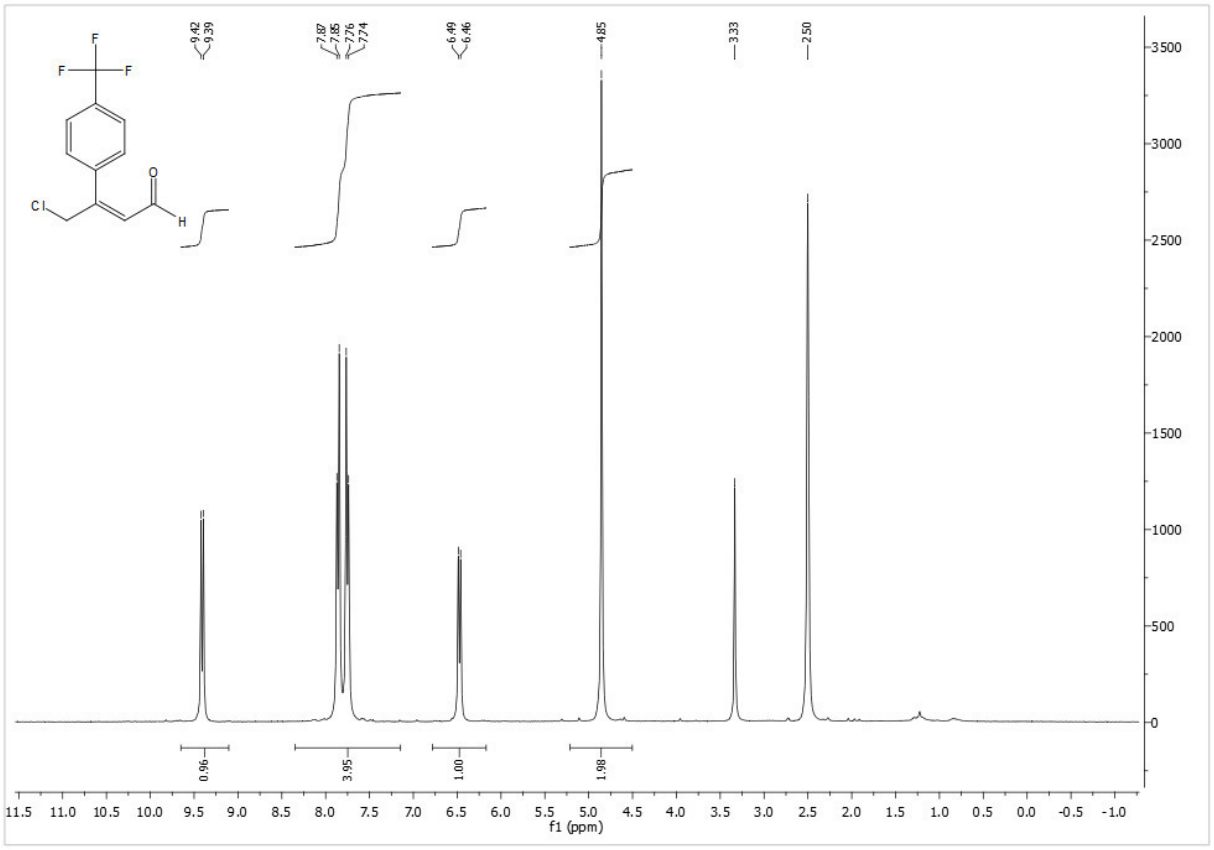

Figure 69: ^{1}H-NMR (300.36 MHz, DMSO-d_6) of compound **34**.

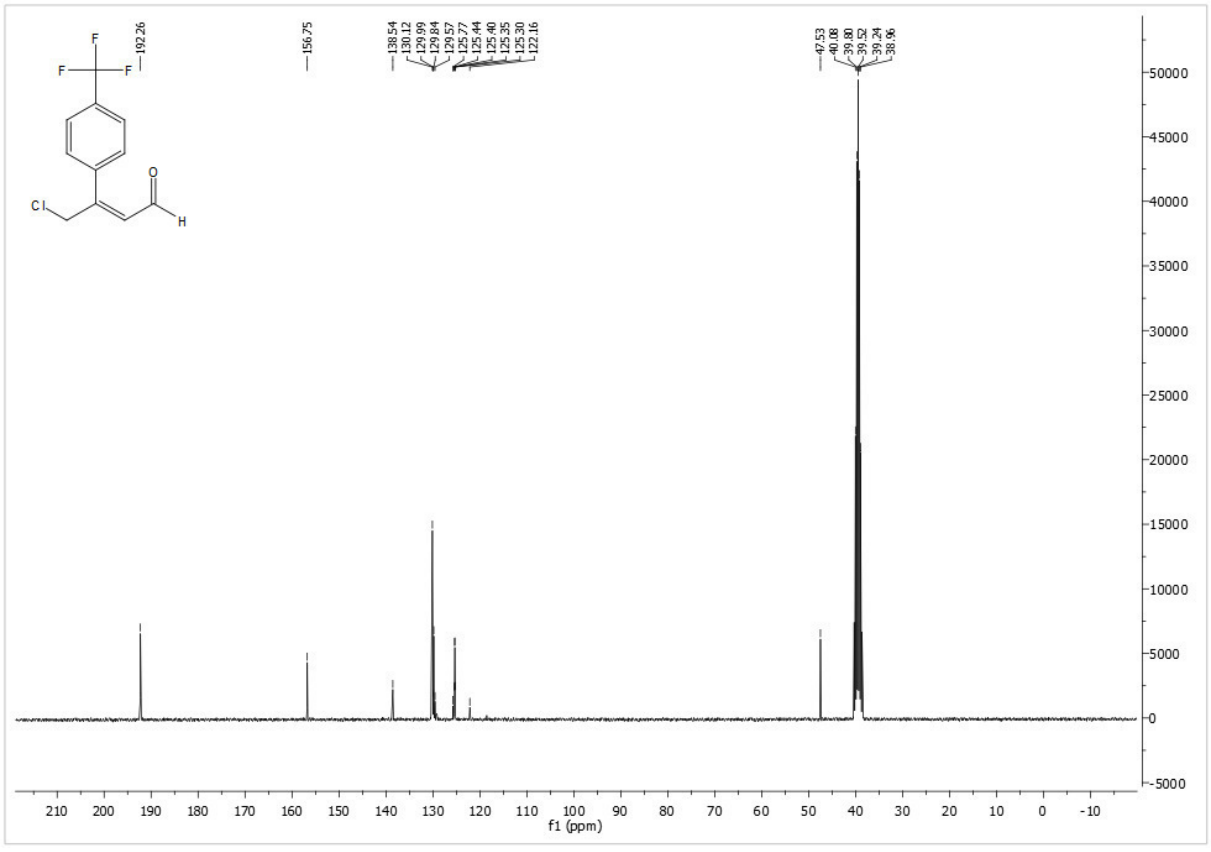

Figure 70: ^{13}C-NMR (75.53 MHz, DMSO-d_6) of compound **31**.